Polymer Injectivity

Experimental Studies of Flow in Porous Media for EOR Polymers

Badar Al Shakry

Thesis for the degree of Philosophiae Doctor (PhD)
University of Bergen, Norway
2021

UNIVERSITY OF BERGEN

Polymer Injectivity

Experimental Studies of Flow in Porous Media for EOR Polymers

Badar Al Shakry

Thesis for the degree of Philosophiae Doctor (PhD)
at the University of Bergen

Date of defense: 12.02.2021

Year: 2021

Title: Polymer Injectivity

Name: Badar Al Shakry

Print: Skipnes Kommunikasjon / University of Bergen

Preface

This thesis is submitted to the Department of Chemistry at the University of Bergen for the degree of Philosophiae Doctor (PhD).

The presented research in this thesis was experimental studies of polymer flow in porous media. The research was performed at the Center of Integrated Petroleum Research (CIPR). After CIPR period came to an end, the laboratories were administrated by Uni Research, now Uni Research has been merged into the Norwegian Research Center AS (NORCE).

This thesis was supervised by three supervisors:

- Main supervisor: Prof. Arne Skauge (Professor at University of Bergen).
- Co-supervisor: Dr. Tormod Skauge (Senior researcher at Energy Research Norway AS).
- Co-supervisor: Dr. Behruz Shaker Shiran (Senior researcher at NORCE).

This dissertation is an article-based thesis that is structured into two main parts. The first part (Chapter 1 to 4) provides literature review and background of polymer transport in porous media. The second part of the thesis synopsizes and discusses the main results that are obtained from the attached published papers (I to V).

شركة تنمية نفط عمان
Petroleum Development Oman

Acknowledgment

First and foremost, I want to acknowledge and express my gratitude to my supervisors: Prof. Arne Skauge, Dr. Tormod Skauge, and Dr. Behruz Shaker Shiran for their excellent supervision, encouragement, support, guidance, and insightful discussion during the whole course of this study. I appreciate the weekly meetings, feedback, and thorough review of this thesis and the manuscripts. Special thanks goes to Prof. Arne Skauge for his tremendous help, especially at the last phase of my PhD study. Without his support, this thesis would not have been compiled in the current form.

My acknowledgments is also extended to NORCE Energy members who I have socialized with, namely: Abduljelil Kedir, Jonas Solbakken and Nematollah Zamani. Additionally, I am thankful to my fellow PhD students: Abdul Majid Murad, Jørgen Gausdal Jacobsen and Mohamed Alzaabi. Special thanks is given to Abdul Majid Murad for proofreading and friendship.

I would also like to extend my acknowledgments to the Petroleum Development Oman company (PDO) for providing me with this valuable opportunity and the scholarship to carry out my studies abroad (master and PhD). Special thanks goes to the Learning and Development team. Additionally, Mr. Hamed Al-Hadhrami is greatly acknowledged for his assistance as a focal point of contact between PDO and me all through my study.

Finally, I would like to thank my family, especially my wife for her patience and endless support during my studies. I appreciate her encouragement to complete this journey. I am also grateful for my sons Zakaria and Mohammed, and looking forward to spending more time with them.

Abstract

Despite the maturity of the polymer flooding process that is applied in enhanced oil recovery (EOR) technologies, the core of the process, which is the flow of the polymer in porous media, is poorly understood. The types of most applied polymers in EOR are partially hydrolyzed polymers (HPAM), which exhibit non-Newtonian flow behavior. That the changes of polymer flow properties with flow velocity are a challenge for the description of the polymer flood process since the velocity changes from ultra-high near the injection well to very low further into the reservoir. At high velocities, the polymer behaves as a shear thickening fluid, i.e., the viscosity increases with velocity. This limits the injectivity of the polymer.

High flow rates in porous media impose a high shear on the polymer, which may lead to mechanical degradation. The shear degradation can be both beneficial and detrimental to the polymer flooding process. It is beneficial in the way that it reduces the viscoelasticity of the polymer, and this property is the prime factor for the reduced injectivity. However, it may be detrimental if there is a corresponding loss of shear viscosity, which is the most important factor for oil mobilization deep in the reservoir. The objective of this thesis is to improve the characterization of flow in porous media by mechanically degraded polymer solutions at high and low flow velocities with the aim to find an optimum between improved injectivity and loss of viscosity.

The thesis characterized polymer flow in porous media by performing core flood experiments at different conditions. These conditions were: different degrees of mechanical degradation, variation of polymer molecular weight and concentrations, and variation in porous media properties, i.e., permeability and wettability. The results show that there was an optimal degree of pre-degradation of the HPAM polymer, which reduced the viscoelasticity to significantly improve injectivity and, at the same time, only leads to a small reduction in viscosity. This suggests that mild pre-degradation can be used to improve polymer flood design in field applications. It was also shown

that mechanical degradation increased with propagation distance in the porous media. This is contrary to the more common belief that mechanical degradation occurs only at the point of highest shear, but not after subsequent exposure to lower shear. Another key finding is that the presence of oil in the pores greatly reduces the shear thickening, suggesting the injectivity is underestimated in core flood experiments with only water present.

List of Publications

Paper-I:

Al-Shakry, B.; Skauge, T.; Shaker Shiran, B.; Skauge, A. Impact of Mechanical Degradation on Polymer Injectivity in Porous Media. Polymers 2018, 10, 742. DOI: 10.3390/polym10070742

Paper-II:

Al-Shakry, B.; Skauge, T.; Shaker Shiran, B.; Skauge, A. Polymer Injectivity: Investigation of Mechanical Degradation of Enhanced Oil Recovery Polymers Using In-Situ Rheology. Energies 2019, 12, 49. DOI: 10.3390/en12010049

Paper-III:

Al-Shakry, B.; Shaker Shiran, B.; Skauge, T.; Skauge, A., 2019. "Polymer Injectivity: Influence of Permeability in the Flow of EOR Polymers in Porous Media" Presented at the SPE Europec featured at 81st EAGE Conference and Exhibition London, England, UK, 3-6 June. SPE-195495-MS. DOI: 10.2118/195495-MS.

Paper-IV:

Al-Shakry, B.; Shaker Shiran, B.; Skauge, T.; Skauge, A., 2018. "Enhanced Oil Recovery by Polymer Flooding: Optimizing Polymer Injectivity" Presented at the SPE Kingdom of Saudi Arabia Annual Technical Symposium and Exhibition, Dammam, Saudi Arabia, 23– 26 April. SPE-192437-MS. DOI: 10.2118/192437-MS.

Paper-V:

Skauge, A.; Zamani, N.; Gausdal Jacobsen, J.; Shaker Shiran, B.; **Al-Shakry, B.**; Skauge, T. Polymer Flow in Porous Media: Relevance to Enhanced Oil Recovery. Colloids Interfaces2018, 2, 27. DOI: 10.3390/colloids2030027

Table of Contents

List of Figures

List of Tables

Chapter 1. Introduction

1.1. Global Energy Demand

Fossil fuels such as oil, gas, and coal have been used as a primary source of energy for more than 100 years. They are used for heating, lighting, transportations, generating electricity, and manufacturing of petrochemicals. According to 2018 Shell's sustainability report [1] and Organization of the Petroleum Exporting Countries (OPEC) [2] oil is the dominating source of energy. Today, with other energy resources that shape the so-called "energy mix" received from natural gas, coal, biomass, nuclear, and renewables, oil has the largest share of 32 % of global energy demand. Given that, the development of other resources such as renewables is challenging. OPEC predicts that oil will lead the world energy with the largest share in the "energy mix" for the coming decades. Given that our world's population is expanding year by year, which is approximated to rise by 1.6 billion between 2017 and 2040 to reach 9.2 billion in 2040. This expansion of the world's population is likely to push for more demand for energy in the future. The primary energy demand expected to grow by 91 million barrels of oil equivalent a day (mboe/d) with 1.2 % annual growth to reach 365 mboe/d in 2040, over the forecast period 2015–2040. By 2040, oil demand expected to reach 111.7 million barrels per day. Given that, this energy demand has not fully been met yet at which still some parts of the world see energy poverty. For example, almost a billion people lack access to basic needs (electricity, medicines, cooking, etc.) [2].

In order to meet energy demand, it requires to increase oil reserves that can be accomplished by discovering new oil fields or extending the production of existing oil fields through technology development [3]. The discoveries of new oil fields tends to decline in number in recent years [4,5]. Therefore, developing the current oil fields by applying technologies such as enhanced oil recovery (EOR) is a great strategy to produce more oil. Utilizing the current infrastructure of oilfields to extend field life is

a key strategy for enhanced oil recovery (EOR). The deployment of EOR technology helps to gain more oil at a shorter time span.

1.2. Enhanced Oil Recovery

Various techniques are available to extract and boost oil production from the reservoir, as presented in Figure 1-1. The oil production process can be chronologically classified into three separate stages: primary, secondary, and tertiary recovery processes that are applied one after another based on their economic limits. These oil recovery processes are defined as follows [3,6]:

- Primary recovery: Initially, when an oilfield is set into production, oil is recovered naturally through pressure depletion by utilizing reservoir energy, i.e., expansion and compaction drive mechanisms. This process also is known as recovery without injection [7]. However, the utilization of natural reservoir resources or deployment of an artificial lift system is poor, and the oil recovery is relatively low (less than 30 %).

- Secondary recovery: injection of water or gas to extend oil production by repressurizing the reservoir. Water flooding is the most common secondary recovery method. A substantial amount of oil unreached by water flooding and left in the reservoir, which becomes a target for tertiary recovery processes.

- Tertiary recovery: injection of external energy resources that are not present in the reservoir to displace the oil left by primary and secondary methods. Tertiary recovery is also addressed as an EOR process.

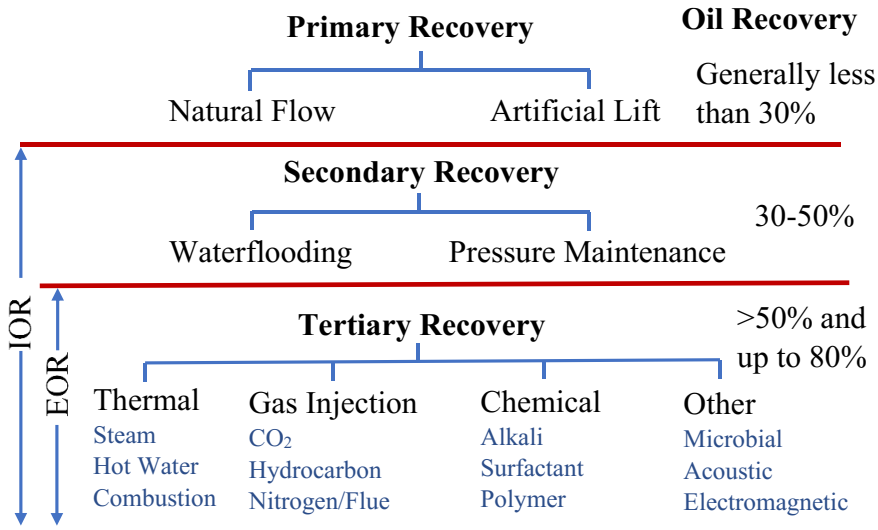

Figure 1-1 Oil recovery methods reprinted from [8].

The average oil recovery factor after waterflooding is relatively low and estimated 35 % [3]. This indicates that an enormous amount of oil is left in the reservoir, which becomes a motivation for the EOR process. Any success to recover part of this remained oil is deemed to be beneficial. For example, the increase of oil recovery factor by 10 % or from 35–45 % produces 1 trillion barrel of oil [9].

EOR technology aims to gain additional oil beyond the primary and secondary recovery process by enhanced sweeping. In some cases, EOR methods are intended to reduce residual oil saturation [10]. EOR technology is part of a broader well know process called “Improved Oil Recovery-IOR”. IOR constitutes all oil recovery processes except the primary method. It also involves other strategies used for reservoir development such as infill drilling, advance drilling and well technologies, reservoir management and control, etc. [4,11]. Both considerations of IOR with EOR may contribute to a high oil recovery factor [12].

EOR refers to all the processes except plain water or gas flood in which external energy resources are supplied to a reservoir to establish the required pressure gradient,

alter rock wettability and permeability, and modify fluids properties and interfacial tension (IFT) that facilitate the oil mobility and displacement from injection to producing well in a controllable manner [13]. EOR technology involves the most well-known commercial recovery processes as given in these reviews [4,14,15] :

- Thermal methods (TEOR): increase reservoir temperature to significantly reduce oil viscosity by introducing thermal energy to the reservoir. This includes steam injection, hot water injection, and in-situ combustion. Recent reviews on TEOR are given elsewhere [16,17]

- Gas methods (GEOR): injection of natural gas, carbon dioxide (CO_2), or nitrogen (N_2) to displace the oil. Others also term miscible GEOR as a solvent method [18].

- Chemical methods (CEOR): injection of water-based chemicals to improve oil displacement. CEOR includes polymer flooding, surfactant flooding, and alkaline surfactant polymer flooding. Polymer flooding is the most common CEOR. A recent review of CEOR is given elsewhere [19].

Besides the main EOR methods given above, other EOR processes are still unproven or under research progress, such as Microbial, hybrid EOR, etc.[18]. It depends on field development, and in most cases, EOR is recommenced to be initiated at the early maturity of the field. The variety of EOR techniques is due to the possibility of applying one technology in favor of others. For some reason, for instance, when thermal processes cannot be used because of their limitations, chemical EOR processes can be the option.

1.3. Polymer Flooding

Within CEOR processes, polymer flooding is one of the most technically proven and widely implemented technology for more than 50 years. It is deemed as a mature technology. It has shown its success in both sandstone and carbonate reservoirs [4,20]. Its main objective is to accelerate and optimize oil production by counteracting viscous fingering, thereby improve mobility ratio and, subsequently, oil sweep efficiency [3,21]. The process becomes viable for reservoirs with high mobility ratios or high permeability variations (heterogeneous reservoir) [22]. Polymer flooding aims to increase the oil recovery factor by 5–20 % over waterflood [18,23]. Its concept focuses on controlling the viscosity of injected water that was first patented in 1944 [24]. Then Pye [25] and Sandiford [26] experimentally showed the addition of a few ppm of water-soluble polymers to injected water would improve the mobility ratio compared to regular waterflood. Similar to other chemical EOR methods, polymer flooding is driven by oil prices. The process drew attention in the late 70s and 80s because of favorable oil prices [21]. Due to this, the process redeveloped and more extensive research studies were performed to address several aspects related to polymer flow behavior [27,28], retention [29-31], mechanical degradation [32-38], viscoelasticity [39,40], modeling [41,42], and different types of polymers [43]. The polymer flooding process is comprehensively documented by Sorbie [21], Sheng [44] and most recently by Thomas [45]. The timeline of the process is shown in Figure 1-2.

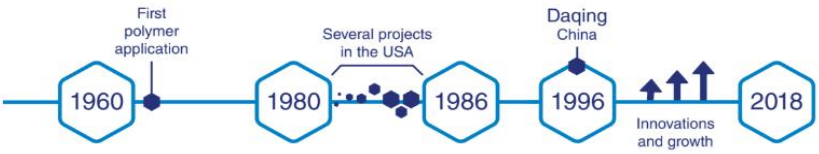

Figure 1-2 Evolution of polymer flooding process [45].

Polymer flooding showed successful experiences in different oil fields worldwide. Recently, there have been more than 800 polymer flooding projects carried

out around the world [46]. Daqing oilfield in China is the largest commercial polymer flooding project. Pelican lake in Canada is an example of polymer flooding in heavy oil. Also, Dalia in Angola is another example of polymer flooding applied offshore. Marmul in Oman and Tambaredjo in Suriname are other examples of large-scale polymer flood projects, to mention but a few [47,48].

One of the main technical challenges in polymer flooding is that its applicability at high temperature (HT), high salinity (HS), high shear reservoir conditions. According to the review by Manrique et al. [47], polymer injectivity is one of the main concerns that remains highly uncertain and implicates the proper design of the process. A well-designed polymer flooding process may give a significant increase in oil recovery and may outcompete other EOR processes at the right conditions. It is one of the most cost-efficient EOR methods [48-50]. Hence, polymer injectivity plays a significant role in the success of the process.

1.3.1. Polymer flooding mechanisms

Due to the Newtonian nature of the injected water in waterflooding and in the cases where there is a high viscosity contrast between oil and water, oil displacement is inefficient. This leaves a substantial amount of oil unrecovered. This large amount of oil can be categorized into residual and bypassed oil. Residual oil refers to immobilized or trapped oil after waterflood due to capillary forces that are dominated by the interfacial tension (IFT) between water and oil. Bypassed oil refers to unreached oil by waterflood due to viscous fingering and reservoir heterogeneity (poor mobility) [51]. The overall displacement efficiency is a function of microscopic (residual oil) and macroscopic (bypassed oil) sweep efficiency that discussed thoroughly elsewhere [6]. Polymer flooding is also known as mobility control process. The mobility control process refers to any process in which the relative mobility rates between injected and displaced fluid is modified [6]. Recall that, polymer flooding is a process in which water-soluble polymers are added into injected water to increase its viscosity and

thereby reduce its relative permeability. The polymer can be continuously injected into the reservoir or injected in concentrated form (slug injection).

Needham and Doe [52] suggested three main mechanisms that are attributed to efficient oil recovery gained by polymer flooding, which they are due to decreasing water/oil mobility ratio, increasing the fractional flow of oil, or conformance control. Mobility ratio (M) is the ratio prior to water breakthrough [53] or in other words the ratio that relates mobility of displacing fluid (water) to the mobility of displaced fluid (oil) as expressed below:

$$M = \frac{\mu_o \, k_w}{\mu_w \, k_o} \qquad \text{Equation 1}$$

Where μ_w and μ_o are the viscosity of water and oil, k_w and k_o are relative permeability of water and oil, respectively.

Increasing the viscosity of water by addition of polymer would decrease the viscosity contrast between oil and water $\frac{\mu_o}{\mu_w}$ and may decrease relative permeability to water due to polymer retention. Hence, a lower mobility ratio and therefore a better sweep efficiency can be achieved. Reducing the water/oil mobility ratio will improve the fractional flow of oil (f_o) that is defined by Buckley–Leveret theory of immiscible displacement as follows:

$$f_o = \frac{1}{1+M} \qquad \text{Equation 2}$$

Mobility ratio plays an important role in sweep efficiency as exemplified in Figure 1-3. A reduction in M will reduce viscous fingering or Saffman–Taylor instability [48]. For instance, when $M \leq 1$ the oil zone is completely swept by water, which is referred to as a piston-like displacement, and results in a “favorable” mobility ratio. However, when $M > 1$ some large portion of oil is unwept due to viscous fingering and early water breakthrough. For higher M, more oil is bypassed due to sever

channeling/fingering. The reduction of M will increase the fractional flow of oil. This may lead to more rapid production of oil and a delay of the water breakthrough. For fields with high mobility ratio, it may often be beneficial to initiate polymer flooding early and maybe even as a secondary flood [54]. Moreover, other studies, e.g. [55], supported early polymer injection specifically close to water breakthrough due to the possibility that the polymer will invade high permeable zones first and thereby improve conformance. The effectiveness of polymer flooding on reducing residual oil saturation or improving microscopic displacement efficiency is very limited and has been debated in the literature [56-59]. This will be elucidated further in the next chapters.

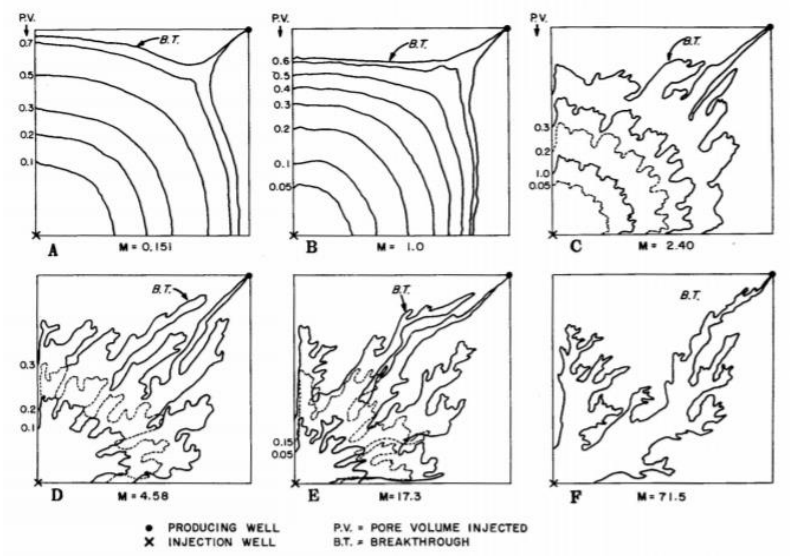

Figure 1-3 Areal sweep efficiency patterns by polymer flooding at different mobility ratios [60].

1.3.2. Types of polymers used in polymer flooding

Generally, two types of water-soluble polymers are applied in polymer flooding process: biopolymers such as xanthan and synthetic polymers such as partially

hydrolyzed polyacrylamide [21,43]. The molecular structures of these polymers are provided in Figure 1-4.

Biopolymers:

Xanthan is the most common biopolymer that is used in polymer flooding. It is a polysaccharide polymer that is produced by the bacterial fermentation process [61]. Its backbone made of glucose like monomers, and it has a helical semi-rigid molecular structure that imposes stiffness on its molecule [21,52]. This polymer is available with different molecular weights 1–15 MDa for EOR purposes [44]. The rigid molecular structure of xanthan facilitates its stability at high shear high salinity conditions. These features also facilitate its handling process in field applications. However, in freshwater, the viscosifying power of biopolymers is lower than synthetic polymers [52]. One of the major limitations of xanthan is biodegradation in the near-wellbore area, which causes loss of viscosity. Another limitation is poor filterability which can cause formation plugging, although it should be noted that the filterability has improved significantly in recent years [53]. Additionally, its thermal stability is weak at a temperature higher than 93 ℃ [52].

Synthetic polymers:

Hydrolyzed polyacrylamide (HPAM) is the most common synthetic polymer in general and most widely applied in EOR applications [21,46,62]. Hydrolyzed polyamide is a copolymer that is produced by polymerization of acrylamide and acrylic acid. This polymer has been partially hydrolyzed with the degree of hydrolysis of 15-35 % to impart a negative charge along its backbone that improves its viscosity in water and reduces its adsorption [44]. Typically, this polymer is available with a wide range of molecular weights up to 35 MDa in a liquid emulsion or solid powder forms [63]. Its performance is dominated by its molecular weight and degree of hydrolysis [52]

that plays a significant role in adsorption, shear, and thermal stability that will be discussed further with other aspects in the next chapters. Unlike xanthan, HPAM polymer has a flexible random coil structure and is very susceptible to shear degradation. It is a polyelectrolyte and sensitive to the harsh environments, such as high temperature or high salinity conditions. HPAM is a viscoelastic polymer [38]. On the other hand, synthetic polymers are more favorable compared to biopolymers because of their industrial availability, physicochemical properties, relatively lower cost, and successful records at large commercial projects [23,64,65].

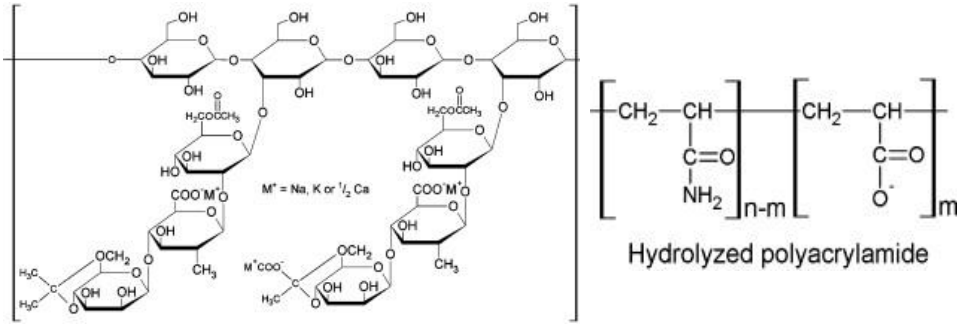

a) Xanthan b) HPAM

Figure 1-4 Molecular structure of xanthan and hydrolyzed polyacrylamide polymer (HPAM) [61].

1.3.3. Polymer flooding design

Figure 1-5 displays a workflow for designing a polymer flooding project that was suggested by Ferreira and Moreno [66]. It is a generic workflow that shows the designing process of polymer flooding, which has four stages: screening, laboratory, simulation, and field implementation. Most of the screening criteria fall into reservoir characteristics such as lithology (mostly sandstone), permeability (> 50 mD), porosity, oil viscosity (< 150 cP), temperature (< 93 °C) and salinity (< 50 000 ppm TDS) [67]. These screening criteria have been updated and expanded as the technology develops [23]. Today, polymer flooding is applied in up to 10 000 cP oil reservoirs [68] at

temperatures up to 120 °C and in salinities up to ~200 000 ppm TDS [69]. However, such screening criteria are not enough for determining the suitability of the polymer flooding process and are limited for the initial evaluation of a possible polymer flood project. Specific field polymer application requires laboratory studies to be conducted in order to evaluate other criteria that are more field-specific, such as injectivity, degradation, propagation profile, and retention. Lake et al. [18] suggested that laboratory studies are imperative, albeit the small scale applied in the lab. For instance, when the evaluation shows a failure of the process at laboratory-scale, it may also mean that the process would fail at a larger scale (field-scale). In addition, laboratory experiments provide inputs for simulation and other decisions.

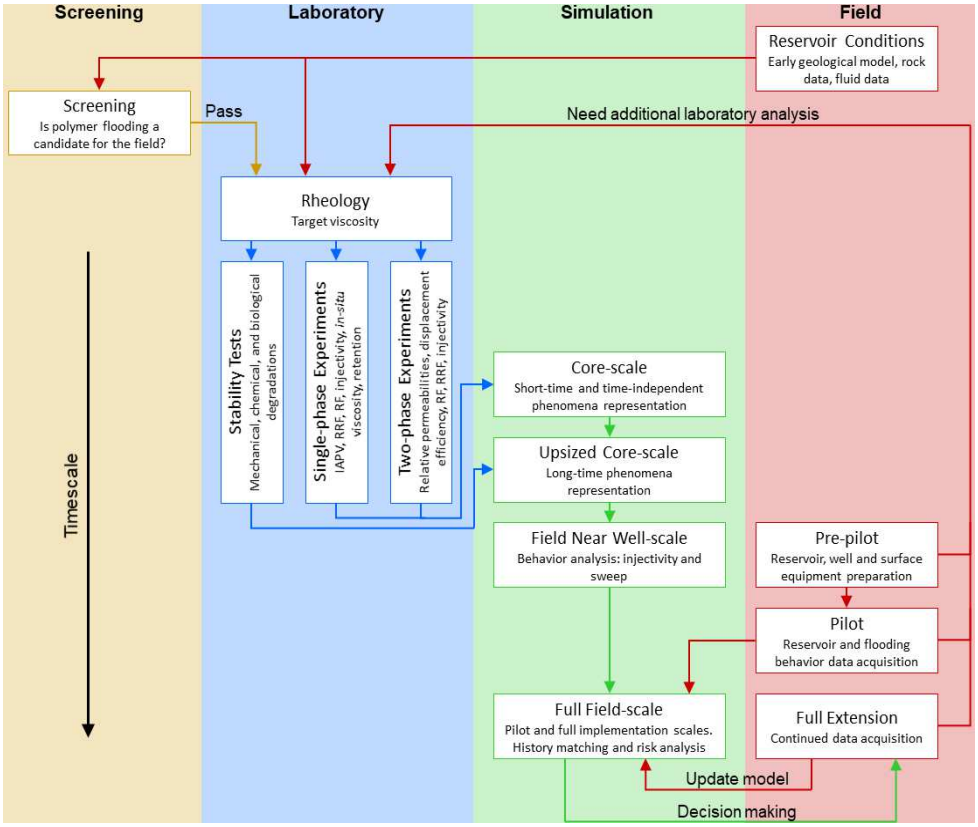

Figure 1-5 Flowchart for designing polymer flooding project [66].

1.4. Thesis Objectives

Injectivity and shear stability of HPAM polymers are among the top issues that limit the success of the process and restrict potential applications of HPAM polymers. Despite the industrial popularity of HPAM polymers as viscosifying agents for polymer flooding and other applications, their flow behavior in porous media is poorly understood. Hence, their injectivity is poorly predicted. Understanding the rheological properties of the polymer is not limited to injectivity studies but also may provide guidelines to optimize the whole process. HPAM polymers characterized by viscoelastic nature and highly susceptible to mechanical degradation [21]. In some cases, HPAM may lose more than half of its designed viscosity due to mechanical degradation [70].

In order to accelerate oil production by polymer flooding, the polymer has to provide sufficient viscosity and be able to maintain its designed viscosity during the whole course of injection. Moreover, the polymer should be capable of being injected at high flow rates. Maintaining high injection rates is desirable in order to improve the oil recovery efficiency and net present value (NPV) [44]. The near-wellbore region will impose mechanical degradation on the polymer solution, and it is of high interest to determine the in-situ viscosity of the polymer after passing through the high shear region. In addition, the impact of pre-degrading the polymer in order to reduce the near-well induced degradation is investigated.

This thesis is confined to study HPAM injectivity and rheology in porous media. For this purpose, oil recovery by polymer flooding is not included. The thesis aims to add more insights into HPAM in-situ rheology to improve polymer flooding design with respect to shear stability, reservoir viscosity and consequently, prediction of injectivity.

The thesis was experimentally carried out at core-scale to meet the following objectives:

- To investigate and analyze the flow of HPAM polymers in linear cores that were chosen to be representative of polymer flow behavior in the reservoir. In-situ rheology provides a deeper understanding of polymer flow in porous media and is supported by bulk rheology studies.

- To optimize polymer injectivity by investigating the factors that dominate polymer flow in porous media, including reservoir and polymer physicochemical properties. This consists of the following sub-objectives:

    - Studying the influence of polymer molecular weight and concentration on polymer in-situ rheology.

    - Evaluating the impact of mechanical degradation by comparing in-situ viscosity for polymers with different pre-conditioning. Pre-conditioning refers to pretreatment processes performed on polymer solution before injection via exposing polymer solution to different extent of shearing. The pretreatment process consisted of pre-filtering, re-injection, and pre-shearing processes.

    - Investigating the influence of oil saturation on polymer in-situ rheology.

    - Studying the influence of rock permeability and wettability on polymer flow in porous media.

Objectives accomplishment

In order to accomplish the objectives addressed above, the following experimental design was followed:

- Single-phase experiments were performed with different molecular weights and concentrations. The polymer solution was pretreated at different conditions prior to injection.

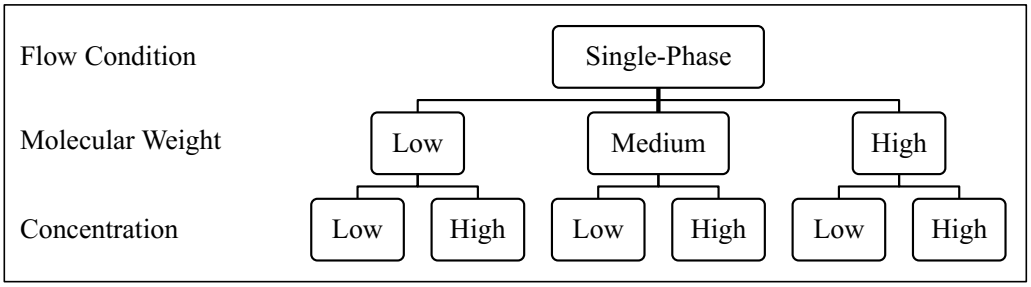

Figure 1-6 Layout for single-phase experiments.

- Two-phase experiments were performed at different wettability conditions using two different polymers with low and high molecular weight. The polymer solutions were pretreated differently to assess the impact of preshearing on polymer injectivity.

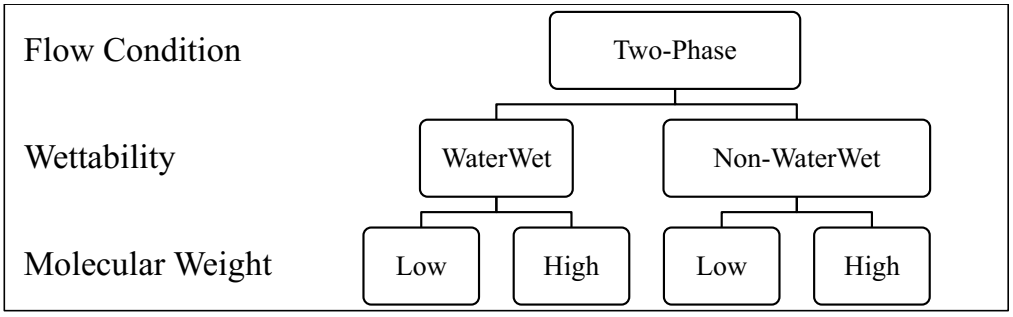

Figure 1-7 Layout for two-phase experiments

1.5. Thesis Outline

The study of polymer flow in porous media is a complex task and requires different ways of investigation. In this thesis, polymer rheology was studied based on analyses of shear viscosity along with in-situ rheology measurements. The investigations consisted of analyzing the flow behavior of polymer with and without the presence of oil in linear cores using different types of rock with different polymers. The thesis chapters are organized as follows:

- Chapter 2: briefly presents HPAM polymer rheological behavior, including physicochemical factors that affect HPAM bulk viscosity such as shear rate, molecular weight, concentration, salinity, degree of hydrolysis, pH, and temperature.

- Chapter 3: describes polymer flow in porous media. It starts by introducing the reader to some basic reservoir engineering definitions. It briefly describes the flow of HPAM in porous media with relative theories and other flow phenomena such as polymer retention and degradation.

- Chapter 4: extends the literature review with the focus on polymer injectivity and mechanical degradation.

- Chapter 5: summarizes and discusses the main results of the thesis.

- Chapter 6: concludes the thesis and provides recommendations for future studies.

Chapter 2. Polymer Rheological Behavior

Rheology is the science, a section of physics, that deals with deformation and flow of materials, both solids and liquids, especially the non-Newtonian flow of liquids and the plastic flow of solids [71]. The term rheology was created in 1920 by Eugene C. Bingham, a professor at Lafayette College in the US, in collaboration with his colleague, Markus Reiner [72]. Rheology deals with stresses and strains of materials. Each material, particularly fluids, has its own behavior to respond to the applied force. Viscosity is the most important rheological property. Based on the viscosity behavior and kinematic history, fluids are classified into two main categories which they are: Newtonian and non-Newtonian fluids.

Polymers, which are our fluids of interest herein, are known as complex fluids [73], and their rheology is both experimentally and theoretically challenging to understand despite their rich literature [74]. On the other hand, their distinctive rheology is the point of interest for EOR applications [6]. The most interesting rheological properties related to EOR polymers are their viscosity and viscoelasticity. Here in this chapter, we discuss the bulk rheology, mainly polymer viscosity.

2.1. Newtonian and non-Newtonian Fluids

Newtonian fluids are fluids whose viscosity is independent of the applied shear rate and possess zero normal stresses differences [75]. Water is the most common example of Newtonian fluids. However, any fluids whose viscosity shows dependency on shear rate are non-Newtonian and, hence, they are classified as non-Newtonian fluids. In addition to shear rate dependence, some non-Newtonian fluids have shear history dependence (time dependence). Hence, Non-Newtonian fluids are further subdivided in accordance to their dependence on shear rate and shear history. This encompasses shear-thinning (pseudoplastic), shear-thickening (dilatant), viscoelastic

fluids, etc. For example, other fluids such as thixotropic and rheopectic fluids can be referred to as time-dependent fluids, whereas pseudoplastic and dilatant fluids are deemed as time-independent fluids [75,76]. The increase of viscosity upon shearing is referred to as shear-thickening behavior that contrasts with shear-thinning behavior. Viscoelastic fluids are the kind of fluids that possess the dual nature of viscous fluid and elastic solid behaviors that depends on applied sort of deformations.

Non-Newtonian fluids generally have relatively larger molecules (macromolecules) compared to Newtonian fluids that typically have small molecules that are likely to be less deformed or oriented by the flow. This may explain the invariable viscosity of Newtonian fluids upon shearing (see Figure 2-1). Other features that differentiate non-Newtonian fluids such as polymer solutions from Newtonian fluids, e.g., water are [74]:

- The polymer solution has a very high average molecular weight (Mw).

- The polymer solution constitutes of various size of molecules with a different molecular weight that yields a wide molecular weight distribution (MWD).

- The polymer coils can adopt various configurations in response to the flow. For instance, the configuration of polymer molecules at rest is not similar to that during the flow when the polymer solution exhibits shear-thinning or thickening behavior.

- Polymer solutions at high flow velocities may develop a temporary entanglement network at which the rate of entanglement is higher than the rate of disentanglement. This leads to shear-thickening behavior.

These non-Newtonian characteristics play an important role in the response of polymer to the exposed type of flow, such as in porous media that accommodates a combination of shear and extensional flow.

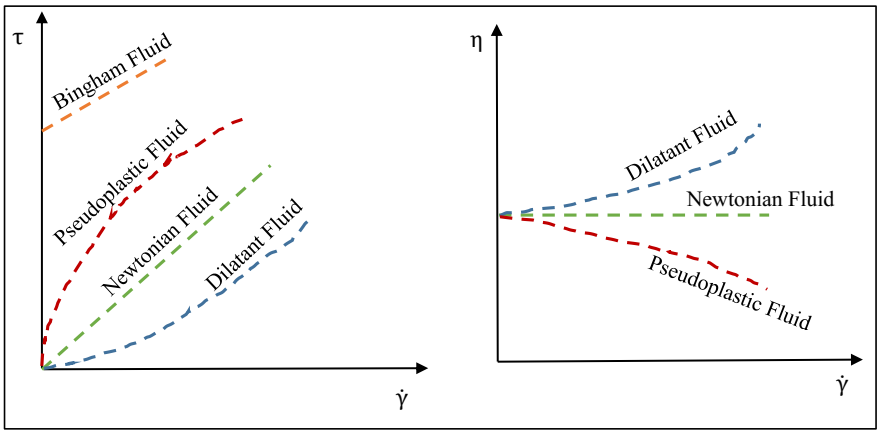

Figure 2-1 Shear stress/strain and shear viscosity of different types of fluid reprinted from [21] and [77].

2.2. Viscosity

Viscosity expresses the fluid's resistance to flow [73]. For Newtonian fluids, the relationship between shear stress (τ) and shear rate ($\dot{\gamma}$) is linear and fairly straightforward for incompressible fluid with a proportionality constant that is the viscosity(η):

$$\tau = \eta \dot{\gamma} \qquad \text{Equation 3}$$

The above equation is known as the Newtonian law of viscosity. However, for non-Newtonian fluid, the relationship between τ and $\dot{\gamma}$ is non-linear and can be expressed as follows:

$$\tau = K \dot{\gamma}^{n} \qquad \text{Equation 4}$$

For instance, for shear-thinning fluids, viscosity can be empirically expressed by the power-law model (Ostwald-deWaele) as following:

$$\eta = K\,\dot{\gamma}^{n-1}$$ Equation 5

where, K and n are power-law constants representing flow consistency and behavior indices, respectively. Correlations for power-law constants K and n are given in the literature [78-80]. The η is known as dynamic, shear or bulk viscosity. The SI unit for viscosity is Pa.s. Also, Poise is a common industrial unit for viscosity, at which 1 cP is equivalent to 1 mPa.s.

The knowledge of the rheological behavior of polymer (e.g., viscosity) is crucial for meeting polymer flooding objective, which is improving the mobility ratio. Also, the viscosity of polymer solutions is an important parameter because of its convenience of measurements at the laboratory; that is why it is widely used as screening or characterizing index for polymer flooding applications [45].

2.3. Factors Influencing HPAM Viscosity

HPAM viscosity is influenced by a multitude of variables such as shear rate, polymer molecular weight, concentration, salinity, degree of hydrolysis, solution pH, and temperature.

2.3.1. Shear rate

The viscosity profile of HPAM polymer solutions is exemplified in Figure 2-2. At low shear rates, polymer solution viscosity is constant exhibiting Newtonian behavior. As the shear rate increases, the viscosity progressively decreases upon increasing shear rate, which indicates shear-thinning behavior mainly due to the disentanglement of the molecules. Ultimately, at high shear rates, polymer molecules become fully disentangled and aligned with the flow, that is, the viscosity is constant at its minimum, hence, polymer exhibiting a second Newtonian behavior [81,82]. The

extent of each flow regime is strongly dependent on polymer physicochemical properties basically Mw and concentration in addition to the type and properties of the solvent including salinity and total dissolved solids (TDS) at a given temperature [83].

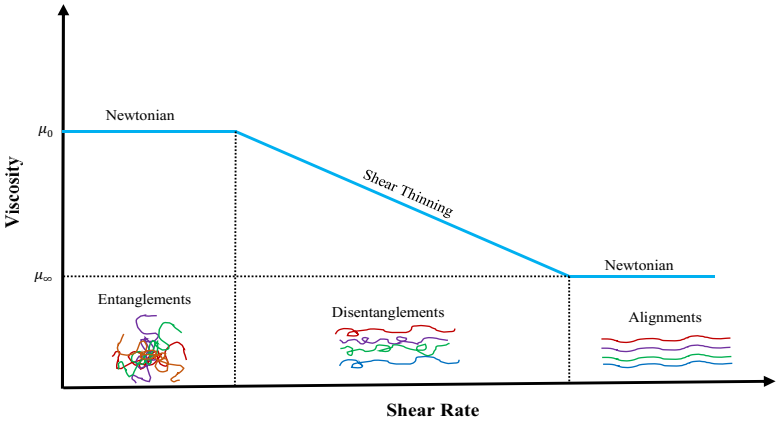

Figure 2-2 Polymer viscosity versus shear rate.

2.3.2. Molecular weight

HPAM viscosity increases with increasing polymer molecular weight (Mw) for given conditions [79,84]. This implies that higher viscosity can be provided by high Mw polymer at a lower concentration. It is worth to note that HPAM shear viscosity is dominated by average molecular weight (Mw). HPAM polymer is known as a polydisperse polymer with wide molecular weight distribution (MWD) [21,85]. The distribution plays an important role in polymer viscoelastic properties and, subsequently, its flow behavior in porous media. The high Mw polymer possesses larger molecules with longer chains; hence, larger hydrodynamic volume. The molecular size of the polymer (coil size) should be compatible to pore throat size. A role of thumb, the polymer molecules should be 10 times smaller than pore throat size [86,87]. Therefore, polymer Mw is considered one of the important screening criteria, specifically for low permeability formations.

2.3.3. Concentration

The viscosity of HPAM increases with increasing polymer concentration [84]. Additionally, the viscosity-concentration relation depends on the structure of the polymer solution. This is illustrated in Figure 2-3. As the polymer concentration increases, the interaction between molecules increases. This can be reflected by the overlap concentration (C^*) that determines the concentration limit between dilute and semi-dilute regions [88]. Overlap concentration is a function of the size of the polymer molecule; large polymers have a lower C^*. It is also a measure of the polymer chain expansion; the lower C^* value, the more expanded is the polymer chain. In dilute solution ($C \ll C^*$), the interaction between molecules is low at rest. The molecules start to interact and overlap with increasing the concentration beyond overlap concentration in which the phase behavior is referred to semi-dilute ($C \geqq C^*$) or concentrated regime at high polymer concentration ($C \gg C^*$) [89].

Graessley [90] classified polymer in solution into three main regions: dilute, semi-dilute, and concentrated regions. The semi-dilute and concentrated regions are subdivided further into unentangled and entangled regions. Recall that the polymer entanglement is one of the complex features that differentiate non-Newtonian fluids from water.

In polymer literature, most of the theories were built on the dilute region, however for the semi-dilute region, the more complexity involved particularly at the presence of entanglements. Here in this thesis, we are more interested in the semi-dilute region because most polymers EOR applications fall in this category.

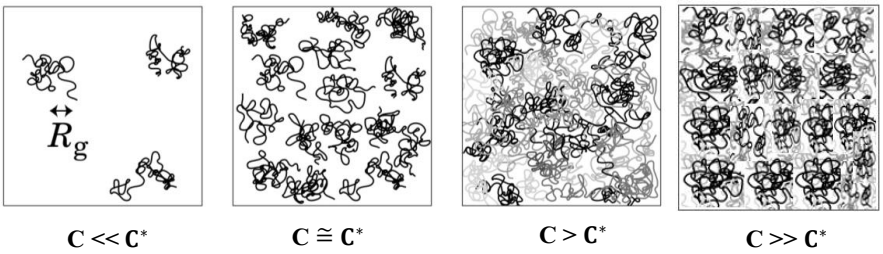

Figure 2-3 Molecules of polymer solution in different concentration regimes modified after [89].

2.3.4. Salinity

Salinity expresses the amount of dissolved solids in solution [3]. The viscosity of polymer solution depends on polymer molecular structure and hydrodynamic volume of polymer molecules [88]. However, the hydrodynamic volume of HPAM can be negatively affected by salinity and eventually impairing its coil structure. The carboxyl group is sensitive to the ionic environment and can be shielded and neutralized by salt's cations such as Na^+. Shielding electrical double layer weakens the repulsive forces among the molecules that cause the polymer coils to shrink and coil-up, thus, adapting smaller hydrodynamic volume that subsequently leads to a reduction in viscosity [80,91]. Increasing salt concentration contributes to a significant reduction in viscosity before it stabilizes and may lead to phase separation and precipitation particularly at the presence of hard cations such as Ca^{2+} and Mg^{2+} [92-94]. Precipitation of polymer molecules such as gel-formation may cause pore plugging when HPAM polymer is transported into porous media [95].

2.3.5. Degree of hydrolysis

The degree of hydrolysis usually refers to the mole fraction of carboxylate groups [96]. The hydrolysis process involves the conversion of the amid groups to

carboxyl groups that results in negative charges on the HPAM backbone (see Figure 2-4). It is an important parameter that influences polymer rheological properties. Generally speaking, it is impossible to commercially produce pure PAM polymer without being hydrolyzed to some extent [6]. HPAM polymer is partially hydrolyzed in an effort to optimize its flow characteristics such as retention, viscosity, and water stability [3]. HPAM polymers can be obtained by reacting acrylamide and sodium acrylate, which industrially can be performed in two processes either through post-hydrolysis or copolymerization process [84]. The density of negative charge increases with the increase of the degree of hydrolysis; hence the viscosity increases. However, the distribution of charges is also an important factor, and it depends on the polymer synthesis process [97]. The two manufacturing processes create a polymer product with similar Mw and degree of hydrolysis but with different charge distributions. For instance, the charge distribution of the post-hydrolysed polymer is relatively wider than that of copolymerized polymer, which means some polymer chains have less evenly distributed charge compared to others within the same product [95]. This is of particular importance to polymer viscosity and its response to the ionic environment especially at the presence of divalent ions.

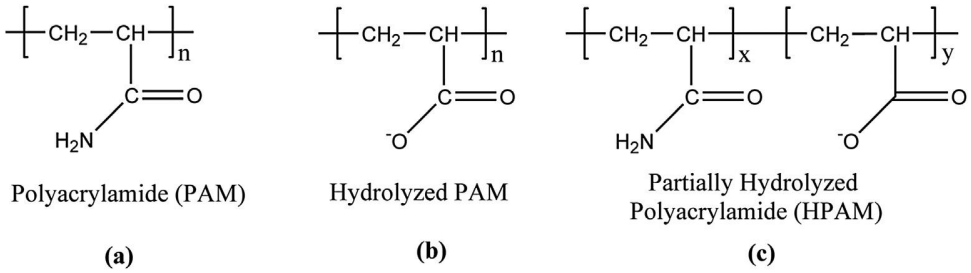

Figure 2-4 Molecular structure of hydrolyzed, partially hydrolyzed and unhydrolyzed polyacrylamide [98].

2.3.6. pH

The typical pH range for oilfield water is 7.5–9.5 [21]. HPAM viscosity strongly depends on pH in a similar manner as salinity, which controls its coiling mechanisms [99]. Recall that, when PAM polymer is partially hydrolyzed to become negatively charged polymer, its backbone consists of amino and carboxyl groups. The carboxyl group is more sensitive to pH. At low pH value, the high concentration of H^+ present in the solution neutralizes the carboxyl group. This neutralization reduces the electrostatic repulsion between the molecules, subsequently reducing the viscosity. On the other hand, at high pH value, the presence of the negatively charged of OH^- in the solution promotes electrostatic repulsion between the molecules which increases the viscosity [100]. Polymer viscosity becomes more vulnerable to pH effects in soft water [21]. The reduction of pH in low salinity solution reduces polymer chain expansion and hence leads to lower viscosity.

2.3.7. Temperature

The viscosity of HPAM highly depends on temperature and decreases sharply with increasing temperature. This elucidates that HPAM polymer has thermo-thinning behavior [101]. This is attributed to the increase of the kinetic motion of HPAM molecules with the increase of temperature. It is thereby reducing the polymer chains' entanglements and stabilizing hydrogen bonds. This results in decreasing the solution viscosity [102].

Chapter 3. Polymer Flow Aspects in Porous Media

Polymer flooding process involves injecting the polymer solution into the oil reservoirs. This process is not straightforward as most of EOR polymers (e.g., HPAM polymers) are sensitive to shear [21]. The flow of polymer in porous media is very complicated as the flow rate changes from high to low as the polymer advances from the wellbore to deep in the reservoir. Also, the variation of the pore cross-sectional area (pores and throats) within the porous media induces local expansion and contraction that impacts polymer rheology. In particular, HPAM polymers exhibit different flow that is experimentally observable but theoretically is challenging to be interpreted. Polymer flow in porous media is influenced by porous media characteristics, among other polymer physicochemical properties.

Porous media is defined as any material or structure that contains spaces or pores [103]. Usually, porous media can be envisaged as an interconnected and tortuous three-dimensional network of capillaries with different sizes and shapes that create a complex structure. The flow in porous media has a widespread application, and it has been an important field of study in different subjects for decades. For instance, in hydrology, the movement of water into the earth through sand matrices is a clear example of flow through porous media. In chemical engineering, the flow in porous media can be important in technologies such as in chromatography and gel permeation chromatography which depend on fluid diffusions and flow through porous media. Moreover, in petroleum engineering, the flow in porous media is crucial for oil and gas recoveries [103].

Some characteristics of porous media that are relevant for this study are briefly defined as follows:

- Porosity (ϕ) represents the rock capability to contain fluids. Its expressed as the volume fraction of the voids or pores (V_p) to the total or bulk volume (V_b) of the rock matrix which is mathematically given as follows:

$$\phi = \frac{V_p}{V_b} \qquad \text{Equation 6}$$

- Permeability (K) is another important parameter that describes the rock's ability to transport a fluid. Darcy's law is used to measure rock permeability as given below:

$$K = \frac{Q.\eta.L}{\Delta P.A} \qquad \text{Equation 7}$$

where, in case of core flood, Q is the volumetric injection rate ($^{m^3}/_{s}$), η is the fluid viscosity (Pa.s), ΔP is pressure drop over the core (Pa), A is the normal cross-sectional area of the core (m^2), and L is the core length (m). The SI unit for permeability is m^2. Darcy is also a common industrial unit for permeability in which 1 Darcy equals to 0.987 μm^2.

- Wettability expresses the distribution of fluid phases in porous media as a result of the interaction between the fluids and rock surfaces. Given that, pores usually contain water and/or oil/gas. The wetting state is referred to as which fluid (water or oil/gas) phase is more attracted onto the rock surface. For example, when the rock surface is surrounded by water in which the water is strongly attracted to the rock surface at the presence of oil, the wetting state is known as water-wet (Figure 3-1). Oil-wet refers to the state when the rock surface is covered by oil. Also, the intermediate wetting state refers to the wettability state when both fluid phases are likely to adhere to the rock surface [6].

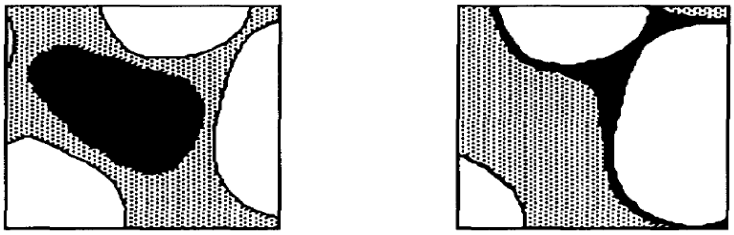

Water-wet Oil-wet

Figure 3-1 Illustrations of oil distribution in water-wet and oil-wet porous media [104].

The following parameters are related to the flow of polymer in porous media [21] :

- Resistance Factor (RF) is defined as the mobility of water to that of polymer flow in porous media which can mathematically be presented as a pressure ratio that relates pressure drop of polymer ($\Delta P_{polymer}$) to that of water injection (ΔP_{water}) before the polymer sees the porous media:

$$RF = \frac{\Delta P_{polymer}}{\Delta P_{water}} \quad \text{Equation 8}$$

Thus, apparent viscosity in porous media is related to RF as follows:

$$\eta_{app} = K \frac{A}{Q} \frac{\Delta P_{polymer}}{L} = \eta_w . RF \quad \text{Equation 9}$$

In case water viscosity is $\eta_w = 1$ cP, the apparent viscosity will be equal to RF, η_{app} = RF.

- Residual resistance factor (RRF) relates the mobility of water before and after the polymer injected into the porous media. It expresses the change in water permeability before and after polymer sees the porous media:

$$RRF = \frac{K_{wi}}{K_{wf}} = \frac{\Delta P_{water\ after\ polymer}}{\Delta P_{water\ before\ polymer}} \quad \text{Equation 10}$$

Both the in-situ parameters RF and RRF are not expected to be lower than unity [33]. Studies [105-107] used the term 'RF/RRF' for referring to polymer in-situ viscosity.

- The reservoir shear rate is one of the most difficult in-situ parameters to be accurately measured due to the complex nature of the porous media. It should account for shear and elongational strains that are present in porous media [108]. Hence the reservoir shear rate ($\dot{\gamma}$) is estimated as follows:

$$\dot{\gamma} = \alpha \frac{4\, v_D}{\sqrt{8\, K\phi}} \qquad \text{Equation 11}$$

where α is the shape factor that is assumed 2.5 for sandstones. v_D is Darcy velocity ($v_D = \frac{Q}{A}$) which should not be confused with interstitial velocity v, ($v = \frac{v_D}{\phi}$) [21,109].

3.1. HPAM Flow in Porous Media

The flow of HPAM polymer in porous media is exemplified in Figure 3-2 that may exhibit a variety of flow such as Newtonian, shear-thinning, shear-thickening, and mechanical degradation. The evolution of these flow regimes is a function of shear rate in accordance to the polymer transport from the wellbore to far deep in the reservoir. It can be seen that HPAM polymer has a similar flow to bulk rheology before the second critical shear rate. These low shear rates are analogous to polymer flow deep in the reservoir due to the availability of larger areas for flood front to propagate [110]. The first critical shear rate indicates the onset of shear-thinning. After the second critical shear rate in which the flow becomes extensional dominated, shear-thickening and mechanical degradation phenomena may be observed at high flow rates. These high shear rates are representative of polymer flow at the wellbore region.

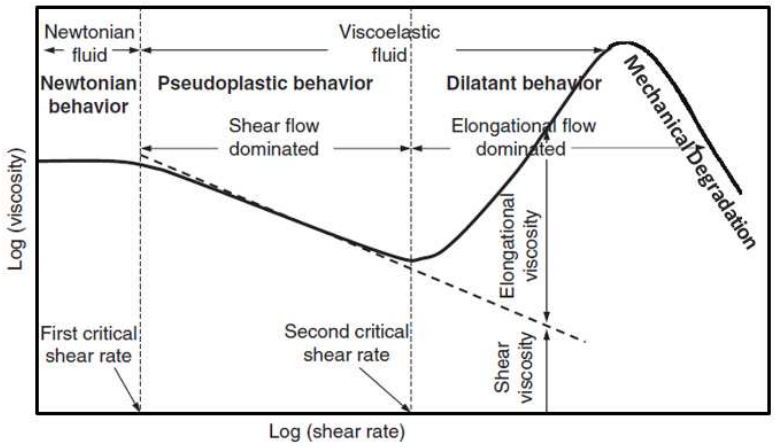

Figure 3-2 HPAM flow behaviors in porous media such as oil reservoirs formation modified from [44].

3.1.1. HPAM viscoelastic behavior

The viscoelastic behavior of HPAM polymer is described in the literature with different acronyms such as shear-thickening, rheo-thickening [57], dilatant, or pseudo-dilatant behavior. In this study, we have interchangeably used shear-thickening and apparent shear-thickening behavior to refer to the increase of viscosity over the injection rate. Shear-thickening behavior is ascribed to polymer viscoelasticity and is a characteristic of polymer flow in porous media because it is not observed in bulk rheology measurements [6]. It is also not observed for non-viscoelastic polymers such as xanthan which exhibits shear-thinning behavior in porous media similarly to its bulk rheology [21,111-116].

The literature contains two main theories that interpret the origin of shear-thickening behavior for HPAM polymers as a consequence of extensional flow, namely: coil-stretch transition and transient network theory. These theories were extensively reviewed by Nguyen and Kausch [117] and briefly given here.

- **Coil-stretch transition theory**

Coil-stretch theory attributes shear-thickening behavior to extensional viscosity that develops when polymer coils are stretched by the flow. According to this theory, polymer coils may be suddenly stretched when the strain rate is sufficiently high and exceeds a critical rate that is related to the inverse relaxation time [21,118,119]. Coil-stretch theory has been invoked to explain the observed shear-thickening behavior in a wide range of studies from different research schools, e.g., [32,120-125].

- **Transient network theory**

Transient network theory ascribes shear-thickening behavior to the extensional viscosity that arises from the formation of transient network among the polymer molecules. The theory stresses that the increase in flow resistance of semi-dilute polymers is due to the molecular interaction, such as the formation of entanglements at high flow rates. This occurs after the critical strain rate at which the entanglement time becomes smaller than the disentanglement time of the network [36]. According to this theory, the formation of a transient network has relatively more dependence on polymer concentration, and it occurs at a lower strain rate for concentrated solutions [126]. Fewer studies implied the transient network theory compared to the other theory on the interpretation of the apparent shear-thickening behavior, e.g., [127,128].

In accordance with coil-stretch transition theory, shear-thickening behavior occurs when polymer chains have insufficient time to align themselves with the flow. In other words, it develops when polymer chains resist the change in the direction of the flow due to consecutive contraction-expansion and/or porous media tortuosity [22]. This chain expansion/stretch develops normal stresses on polymer chains, which correlates with extensional viscosity. Given that, extensional viscosity is the ratio of normal stress to the elastic or elongational strain [21]. The successive expansion-contraction flow mechanism that results during polymer circulation in pore-throat at the different cross-sectional area through its flow in porous media is very crucial for

observing the shear-thickening behavior at a sufficiently high flow rate [129]. HPAM is a viscoelastic polymer with a flexible coil structure that possesses long chains with a high polydispersity index. In that, porous media accommodates both types of flow, which are shear and extensional [76]. Thus, when HPAM is transported in porous media, its molecules expand and contract consecutively. This involves coil-stretch transitions at high rates. This occurs at a critical shear rate that is related to Deborah number (De). De provides a relationship between the polymer relaxation time (τ_r) to porous media characteristic time (τ_c) that is equivalent to the inverse of porous media shear rate ($\dot{\gamma}$) [130]:

$$De = \frac{\tau_r}{\tau_c} = \dot{\gamma}\,\tau_r \qquad \text{Equation 12}$$

Studies, e.g., [109] reported that at De = 0.22 is adequate for the occurrence of shear-thickening behavior, and the viscoelastic effect becomes dominant at high De.

3.1.2. HPAM shear-thickening behavior and its relevance to EOR

HPAM shear-thickening behavior is essential for maximizing oil recovery. Hence understanding its flow in porous media is crucial for EOR applications. Studies, e.g., Vik et al. [114] demonstrated that the injection of HPAM successfully alleviated the viscous fingering observed by a shear-thinning polymer such as xanthan on displacing 500 cP viscous oil. The study was performed on Bentheimer rock, and the displacement was visualized by an X-ray scanner. The authors attributed the improvement of oil displacement and delay of polymer breakthrough during HPAM injection to the enhanced front stability during polymer flood. The improved front stability was ascribed to HPAM viscoelasticity, e.g., shear-thickening behavior. Their study also pointed out the advantage of avoiding mechanical degradation to preserve the viscoelastic nature of the polymer over the course of polymer injection.

Although HPAM viscoelasticity is beneficial or EOR purposes, however, it may impede its application in some reservoir conditions. For instance, the high pressure-buildup due to shear-thickening behavior may cause injectivity problems [116]. Some other issues and flow phenomena, such as retention and mechanical degradation, may also be related to polymer viscoelasticity. These will be discussed in detail at the end of this chapter.

3.1.3. Analytical models

The evaluation and prediction of HPAM polymer injectivity are challenging and still elusive. Current analytical models in the literature that try to predict HPAM flow behavior in porous media benefit extensively from experimental inputs. Some of the most common analytical models are given in this section. The derivations of these models were given in detail in the references thereafter. According to these models, the apparent viscosity of HPAM polymer depends on the shear (η_{sh}) and extensional (η_{ex}) viscosity as follows:

$$\eta_{app} = \eta_{sh} + \eta_{ex} \qquad \text{Equation 13}$$

The literature contains several models that may be used for predicting shear viscosity; some of them are compiled in Table 1.

Table 1 Flow models for polymer shear viscosity [76].

Model	Formula	Description
Power Law	$\eta = K\,\dot{\gamma}^{n-1}$	η is the viscosity, $\dot{\gamma}$ is the shear rate, K is the consistency index, n is the power-law index
Ellis	$\eta = \frac{\eta_0}{1 + \left(\frac{\tau}{\tau_{1/2}}\right)^{\frac{1-n}{n}}}$	η_0 is zero shear viscosity, τ is shear stress. $\tau_{1/2}$ is effective shear stress at $\eta = \frac{\eta_0}{2}$.
Carreau-Yasuda	$\eta = \eta_\infty + \frac{\eta_0 - \eta_\infty}{[1 + (\dot{\gamma}\lambda)^2]^{\frac{1-n}{2}}}$	η_∞ is the infinite shear viscosity λ is fluid relaxation constant or characteristic time that represents the onset of shear-thinning at λ^{-1}

One of the common viscoelastic models was given by Delshad et al. [130], which is also known as a unified viscosity model (UVM). UVM accounts for the viscosity over a broader range of shear rates, including shear-thickening part compared to the given shear models in Table 1. UVM is mathematically represented as follows:

$$\eta_{app} = \eta_{\infty} + (\eta_0 - \eta_{\infty})[1 + (\lambda\gamma_{eff})^2]^{\frac{(n-1)}{2}} + \eta_{max}[1 - \exp(-\lambda_2\tau_r{\gamma_{eff}}^{n_2-1})] \quad \text{Equation 14}$$

where, γ_{eff} is the effective shear rate in porous media, η_{max} is the maximum viscosity of the shear-thickening behavior at high shear rates which is a function of polymer concentration and salinity. The constants λ_2 and n_2 are empirically measured from experiments. The determination of these parameters requires the experimental observation of shear-thickening behavior through core flood experiments. The constant τ_r represents extensional polymer relaxation time. The model implies the Carreau-Yasuda equation for η_{sh} and relates η_{ex} to Deborah number in a similar approach given by earlier viscoelastic models [131,132]. UVM matched well with experimental pressure data from core experiments presented in the references [110,133]. In a similar approach, Azad and Trivedi [110] recently developed the so-called Azad-Trivedi Viscoelastic Model (AT-VEM) in an effort to avoid the in-situ measurements for η_{ex} required for UVM. Instead, AT-VEM utilizes external measurements for extensional parameters mentioned above, such as polymer relaxation time, τ_r, maximum shear-thickening viscosity, η_{max} and shear-thickening index, n_2. Both models UVM and AT-VEM do not consider the polymer mechanical degradation that may occur at high flow rates.

In a similar approach to UVM, another viscoelastic model is given by Stavland et al. [109] that covers the apparent viscosity in shear and extensional dominated flow with the consideration of polymer mechanical degradation at high shear rates (see Figure 3-3:

$$\eta_{app} = \eta_{\infty} + [(\eta_0 - \eta_{\infty})\,(1 + \lambda\dot{\gamma})^n + \lambda_2\dot{\gamma}^m]\,.\,[1 + (\lambda_3\dot{\gamma})^4]^{\frac{j}{4}} \quad \text{Equation 15}$$

where, the first part of the equation above represents a modified Carreau-Yasuda model, the middle term $\lambda_2\dot{\gamma}^m$ refers to the extensional viscosity η_{ex} and the last part refers to the polymer mechanical degradation. The time constants λ_2 and λ_3 represent the onset of shear-thickening at ${\lambda_2}^{-1}$ and mechanical degradation at ${\lambda_3}^{-1}$, respectively. The parameters j and m are empirical constants where m corresponds to the slope of shear-thickening. This model, unlike to UVM, does not require experimental data for determining extensional viscosity; however, it still requires experimental data to obtain input parameters for the mechanical degradation part. This model was unable to perfectly match core pressure data in a two-phase flow where polymer flows in the porous media at residual oil saturation [134].

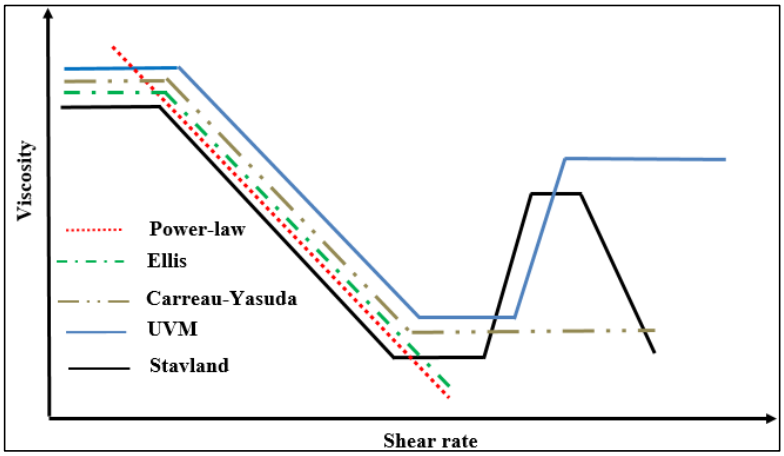

Figure 3-3 Schematic illustration of different HPAM viscosity models reprinted from [135].

3.2. Polymer Retention

Polymer retention is one of the critical parameters that determines the applicability of polymer flooding project. A polymer solution with lower retention values gives better sweep efficiency [52]. Polymer retention refers to any mechanism

that isolates polymer molecules from the bulk solution during its transport through porous media. These mechanisms, which are illustrated in Figure 3-4, are: adsorption, mechanical entrapment, and hydrodynamic retention [21]. Polymer retention reduces polymer concentration, and thus it reduces its viscosity or induces permeability reduction that impairs well injectivity. If retention is high, polymer flooding may not accelerate oil production and strongly risks its economic feasibility. According to Manichand and Seright [136], polymer retention may be considered low if the retention value is < 10 μg/g and high if the retention value is > 200 μg/g. Additional polymer required to be injected to meet the designed propagation distance in the reservoir to overcome polymer loss by retention. Polymer retention by adsorption is considered as an irreversible process [6,137].

Polymer retention depends on the physicochemical properties of polymer solutions such as polymer type, molecular structure, Mw, concentration, and degree of hydrolysis. Also, it depends on the solvent properties such as salinity, type of TDS, and pH of a solution. Moreover, it depends on porous media properties such as permeability, type of rock, and surface charge. It also depends on the presence of oil and wettability of porous media. The influence of these factors on polymer retention has been discussed in detail by Manichand and Seright [136]. Recent reviews on polymer retention have been published by Al-Hajri et al. [138] and Liu et al. [139].

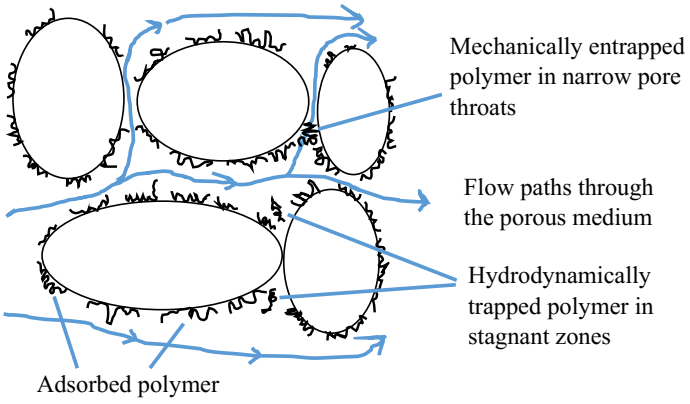

Figure 3-4 Schematic representation of polymer retention mechanisms in porous media reprinted from [21].

- **Adsorption**

When polymer solution flows in porous media, the molecules will electrostatically interact and adsorb on the rock surface. Polymer adsorption is ascribed to van der Waal's forces and hydrogen bonding between the polymer molecules and the rock surface. The extent of adsorption depends on the available surface area for polymer molecules to adsorb on [21]. It also depends on reservoir formation; for instance, polymer adsorption is higher in carbonates compared to sandstones due to the presence of divalent ions such as calcium, which is the main constituent of carbonate rocks [140,141]. Polymer adsorption is one of the most dominant retention mechanisms [21,142].

- **Mechanical entrapment**

Mechanical entrapment or straining is another retention mechanism in which polymer molecules entrapped in narrow channels. This occurs when polymer molecules are relatively larger than the flow channel (pore throat). Mechanical entrapment is more pronounced at the wellbore area, and it exponentially reduces deep in the reservoir. Mechanical entrapment may cause pore-clogging [143].

Mechanical entrapment, as a retention mechanism, should not be confused with inaccessible pore volume (IPV), which is widely mentioned in literature along with retention. IPV is not a retention mechanism, but it is a measure of available pore volume for the polymer to be accessed, and it helps to better quantify polymer retention if it is truly measured [107,144,145].

- **Hydrodynamic retention**

Hydrodynamic retention is a flow rate-dependent retention mechanism. This occurs when the flow rate is altered. For instance, some of the polymer molecules spread out from the main flow due to the sudden increase of the flow rate, and they are entrapped by corner or dead ends. This results in a concentration difference between the polymer solution that lays in stagnant areas and the polymer solution that flows in the mainstream [143]. This retention mechanism has relatively insignificant impact on polymer retention and hence slightly influences polymer in-situ rheology, e.g., RF and RRF [144,146].

3.3. Polymer Degradation

Polymer degradation refers to any process that causes the polymer solution to lose its viscosity due to the disruption of its molecular structure. This involves chain scission, reduction of molecular weight and distribution, and eventually reduction of its viscosity. There are different processes that may lead to polymer degradation, namely: biological, chemical, and mechanical degradation processes [21]. These degradation processes are briefly defined as follows:

- **Biological degradation**

Polymer biodegradation occurs by a microbial attack such as bacteria. Biopolymers such as xanthan are more vulnerable to this type of degradation. On the other hand, HPAM polymers are known for their strong biological stability against bacteria compared to xanthan. Some microorganisms may still utilize HPAM as a source of nutrition if they are present in the reservoir [95]. Biodegradation has an

inconsiderable impact on HPAM viscosity when reservoir temperature is high, or biocides are used [21].

- **Chemical degradation**

Chemical degradation of HPAM polymers occurs due to the presence of oxygen with cations such as Fe^{2+} that initiate depolymerization or non-neutral pH environment that escalates the hydrolysis [95]. This is in accordance with Sorbie [21], who also classified HPAM chemical degradation into two main processes considering the timescale: oxidative attack as a short-term process and hydrolysis attack as a long-term process. The former process causes chain scission and lowering molecular weight and eventually reducing its viscosity at the existence of free radicals such as oxygen. The latter influences polymer thickening properties that leads to higher adsorption at the presence of salts, and at sever conditions, hydrolysis may lead to phase separation and precipitation [95]. Chemical degradation processes are also driven by temperature; thus, high temperature escalates HPAM chemical degradation [6]. High temperature and non-neutral pH escalate hydrolysis as well, which also is referred to as 'thermal degradation' [84]. Reported studies by Seright and Skjevrak [147] show that HPAM may lose more than half of its viscosity due to chemical degradation. However, HPAM is relatively stable at low temperature < 50 °C even with the presence of oxygen but not cations such as Fe^{2+} [147]. This elucidates that chemical degradation may not be a critical issue for HPAM in the absence of iron or oxygen.

- **Mechanical degradation**

Mechanical degradation, which is also known as shear degradation, is related to mechanical stresses that rapture polymer molecular structure and subsequently reduce its viscosity. Mechanical stresses on HPAM polymers are developed at high flow rate regions such as dissolution facilities, valves, chokes, wellbore, etc. [63,84]. Studies,

e.g., Zaitoun et al. [70] reported that mechanical degradation might cause HPAM to lose more than half of its viscosity. It is a detrimental factor for the polymer project design and may be avoided by understanding polymer rheology and its flow behavior in porous media. HPAM mechanical degradation is one of the main topics of this thesis and will be elucidated further in the next chapter.

Besides the negative impact of the aforementioned degradation mechanisms on polymer viscosity, they may act otherwise as main working principles that are used for processing produced water (disposal approach) for polymer flooding process. These mechanisms are out of the thesis's scopes and briefly discussed elsewhere [84,148-150].

Chapter 4. Polymer Injectivity and Mechanical Degradation

4.1. Polymer Injectivity

During the polymer injection process, different issues such as pressure build-up, fracturing, polymer retention and mechanical degradation may exist in accordance with typical wellbore conditions. Recently Manrique et al. [47] provided a comprehensive review covering more than 15 past-reviews of polymer flooding between 1978 and 2016, including polymer projects at commercial and pilot scales. According to their review, the majority of the failure of polymer flooding projects owing to poor polymer injectivity.

Generally, injectivity is more considered as a qualitative term in the petroleum literature, and polymer injectivity is a measure of flowability and how seamlessly a polymer solution can be delivered into the reservoir [151]. It expresses the change of injection rate during polymer injection or water injection after polymer flood process. Over a 20 % reduction in the polymer injection rate was observed in some field polymer injectivity tests reported by Torrealba and Hoteit [152]. Injectivity might vary between the injection wells. Therefore, injectivity assessment is crucial for the polymer flooding process, and it is a determining factor for the success of the operation. Poor injectivity may restrict the application of polymer flood projects more than the cost of their chemicals does, particularly for heavy oilfields [153].

The ideal characteristic of EOR polymer is shear-thinning behavior that provides lower viscosity with lower pressure-gradient at high shear rates in order to achieve high injection rates [130]. However, in real applications of HPAM polymers, this may not be the case; instead, shear-thickening behavior may dominate the flow near the wellbore area which imposes limitations to achieve the designed injection rates and results in poor injectivity. The injectivity loss in polymer flooding is mainly due to

polymer viscoelasticity and retention. It also emerges from other factors such as reservoir properties, injection strategies, matrix injection, fracturing, degradation, well spacing and design, etc. Thomas [45] presented different scenarios that may help to diagnose the causes of polymer injectivity loss, including rheology and mechanical degradation. Likewise, Seright et al. [116] investigated the impact of polymer rheology, mechanical degradation, and filtration on polymer injectivity.

Good polymer injectivity is one of the important requirements for polymer flooding process. In field applications, polymer injection wells are scattered, and there is some residence time (typically in years) for the polymer to transport from injection to production wells. This increases the risks of polymer degradation due to different types of aforementioned degradation mechanisms in Chapter 3. Moreover, the faster injection rate slows heat transfer and delays viscosity reduction of the polymer solution. Given that the formation temperature increases with depth, polymer viscosity decreases during the injection from the viscosity-temperature effect compared to the top-side viscosity. The slow injection of the polymer allows the temperature of the polymer bulk solution to increase. This significantly reduces polymer solution viscosity. This demands for increased injection flow rate in order to avoid significant heat transfer from the formation into a polymer solution and therefore reduce thermal degradation of the polymer [152,154].

In some field cases, polymer injectivity is reported to be more successful and better than the designed one. This may be attributed either to the mechanical degradation that causes the loss of polymer viscosity or injection under fracture conditions [155,156]. The high-pressure gradient near-wellbore area caused by HPAM shear-thickening behavior is able to induce fractures if the pressure exceeds formation-parting pressure (FPP). Fractures induction expands the flow area and increases the absolute permeability, especially for unconsolidated sands [157]. However, such unintended fractures may become out of control and cause channeling that leads to loss of the expensive polymer solution into the formation, which could deteriorate the oil recovery process. Despite that, studies e.g. [116], recommended polymer injection at

or above FPP, and in cases where microfractures are present, they would be beneficial for attaining good polymer injectivity.

Injectivity of an injection well (I) is defined as the ratio of injection rate (Q) over the pressure drop (ΔP), i.e., $I = \frac{Q}{\Delta P}$ [3]. Step-rate or pressure fall-off (PFO) injectivity tests are common field practices to assess polymer injectivity. The filtration ratio test is also a common laboratory method used to assess polymer injectivity. Nevertheless, it still does not represent a precise figure of polymer behavior at different flow regimes. Hence core studies are more representative of field-scale application. Resistance factor (RF), which has been stated earlier in Chapter 3 can be used as an injectivity indicator because it relates the injectivity of water to that of polymer in terms of pressure gradient [3].

4.2. Mechanical Degradation

Mechanical degradation of EOR polymers has been presented in the literature for more than 40 years and is reviewed by Caulfield et al. [158]. However, it remains as one of the complex subjects to understand for successful polymer flooding project design and implementation. In the polymer flooding process, the injection of HPAM into the reservoir involves the exposure of the polymer solution to high shear rates, especially in the wellbore area. Given that HPAM polymers are shear sensitive; thereby, they are amenable to mechanical degradation upon exposure to high shear rates [21,32]. As a consequence of polymer mechanical degradation, the polymer solution may lose more than half of its original viscosity that deteriorates and reduces its expected performance in sweeping the oil. Recall that high polymer viscosity is a requirement to achieve a better and favorable mobility ratio. Additionally, HPAM may significantly lose its viscoelastic features because of mechanical degradation. Studies reported that the degraded polymer solution has less front stability and lower sweep efficiency compared to undegraded polymer solution [114,159].

According to Sorbie [21], mechanical degradation is a short-term attack process on the polymer molecular structure that should be taken into consideration, particularly at the presence of high shear rates, formations with low permeability, and polymer injection with long residence time in the reservoir. At high flow rates in porous media, which are corresponding to the shear rates beyond the critical shear rate, polymer molecules are fully stretched. This can evolve into the breakage of polymer molecules into fragments if the shear rates are adequate to induce chain scission due to the development of strong normal stresses. The breakage of polymer molecules is likely to occur in the middle of the chain close to the center. Longer chains such as the macromolecules are more vulnerable to shear rates and are easily degraded. Therefore, mechanical degradation of polymer solution reduces its average Mw and distribution. It alters the distribution to a greater extent than average Mw [85]. Also, it affects the polymer microstructure, hydrodynamic volume, and eventually reduces its viscosity [160].

Ghosh et al. [161] reported in their experiments, using dynamic light scattering (DLS), that degraded 8 MDa HPAM polymer had narrower MWD compared to the undegraded solution, as shown in Figure 4-1. This is consistent with other studies, e.g. [33], in which they evaluated the impact of mechanical degradation on MWD using Gel permeation liquid chromatography (GPC).

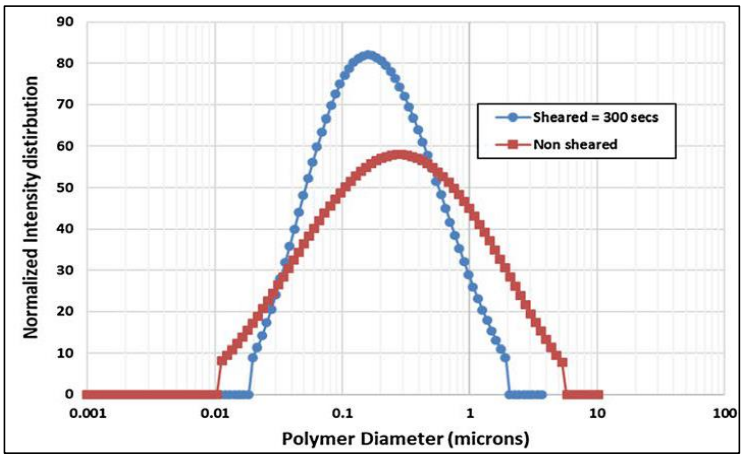

Figure 4-1 Molecular weight distribution of degraded versus undegraded 8 MDa HPAM polymer [161].

Polymer mechanical degradation depends on polymer physicochemical properties and porous media properties. For instance, it is reported that mechanical degradation increases with the increase of molecular weight [32,34,109,162]. However, it has less dependency on polymer concentration, but it may decrease with the increase of polymer concentration in the concentrated regime [34]. Also, mechanical degradation of polymer is more pronounced in formations with lower permeability [32].

The impact of salinity and TDS on polymer mechanical degradation is debated in the literature. For example, earlier studies by Maerker [32] reported that HPAM mechanical degradation increased with the increase of solution's salinity. Another hypothesis suggests that, at the presence of salts, HPAM possesses compact conformation with lower coil dimensions; hence, forming strong entanglements and aggregates, which are more persistent to be deformed upon the exposed shear rates [163]. A recent study was given by Ferreira and Moreno [164] investigated the mechanical degradation of modified HPAM at the presence of iron. Their study revealed that when the polymer solution has already chemically degraded, it becomes more shear stable and less mechanically degraded. This may be because the degraded polymer solution has already possessed lower Mw and MWD.

Some studies attributed polymer mechanical degradation to the degradation of polymer in the entrance of porous media before the polymer solution contacts the reservoir [32,37,109,119,165]. This corresponds mainly to a distance of few millimeters at the wellbore matrix that accommodates high flow velocities. However, other studies reported that polymer mechanical degradation depends on residence time [166]. For instance, Åsen et al. [162] performed experimental studies to investigate the mechanical degradation over the traveled distance in porous media that was equivalent to approximately 20 m by recycling the polymer solution into segmented 30 cm linear Bentheimer core. Their study showed that mechanical degradation was a function of core length and increased with increasing traveled distance in the linear cores. Although their conclusion was not strong and they claimed that this finding might not be realistic at field scale in which the polymer flow is more dominated by radial flow, rather than linear flow in the cores. Other studies also observed the increase of polymer mechanical degradation by increasing the exposure time to shear [123]. The investigation of the occurrence of the so-called successive mechanical degradation is part of the scope of this thesis.

4.3. Improving HPAM Shear Stability

There are different approaches presented in the literature in an effort to improve HPAM shear stability. One of these approaches is related to polymer screening and its compatibility with the field environment. Polymer type, its physicochemical properties and chemical structure are important parameters for such screening process. For instance, using low Mw polymer in designing polymer flooding operations would improve the shear stability of polymer solution [58]. On the other hand, obtaining designed viscosity target for polymer solution requires a large amount of low molecular weight polymer, which may economically not feasible for large field-scale polymer flood applications.

Another approach for improving shear stability of polymer solution is concerning the field practices and well development. This includes fracture induction, increase the number of injection wells, adopt horizontal wells, or perform well treatments. The introduction of fracture, for instance, a fracture of 15 m length, reduces the wellbore shear rate significantly and could save the polymer flooding project by the enhancement in injectivity and reduction of mechanical degradation [109,167]. The increase in the number of injection wells reduces the well spacing and the requirement for injection at a high rate per well. Horizontal wells are preferred for polymer injection due to low shear rates. Hence, horizontal wells can accommodate viscous polymer solutions up to 5000 cP compared to vertical wells that can accommodate polymer solutions with a viscosity up to 100 cP [168]. Besides, the flow regimes may be different; radial flow is dominant around the vertical wells while the linear flow is more dominant in horizontal wells, both at matrix injection [45]. However, this may not be deemed as a feasible approach for all field applications, as polymer flooding process is mainly applied in existing oilfields that have already been designed for the type of wells, the number of wells, well spacing, etc.

Incorporating some other additives such as ATBS (Acrylamido tertiary butyl sulfonate) to polyacrylamide polymer may improve its shear stability, [69,107,109,169,170]. Likewise, incorporating thiourea or alcohol may also improve the chemical and thermal stability of polymer [45]. Moreover, modifying or treating the salinity and quality (hardness) of the makeup-water would affect the shear stability of polymer solution [171]. Other HPAM derivatives [43] and engineered modified polymers such as thermally triggered polymers [172] may have better shear stability. Some studies reported that chemically degrading polymer solutions in upfront may result in better shear stability polymer solutions [164].

Another approach is pre-treatment of HPAM polymers by exposing to a certain extent of mechanical degradation that is equivalent to wellbore shear conditions. This process is also known as preshearing process. The concept may additionally infer reinjection of the polymer that has already seen porous media (e.g., reusing the injected

polymer). Also, it entails polymer filtration and removal of microgel or aggregates. This approach is also suggested by polymer manufacturers (e.g., SNF) and has already shown its success in field applications. Field tests, for instance, injectivity tests performed in West Coyote oilfield, demonstrated significant improvement in injectivity of presheared polymer solution. The polymer was presheared at approx. 10 bar using a needle valve that reduced the polymer viscosity by 20 %. Laboratory studies, e.g., [156] confirmed similar findings in that presheared polymer had better injectivity due to weak shear-thickening behavior in porous media. Dupas et al. [156] used a capillary device developed by API to partially degrade HPAM polymers to different extents. They ascribed the enhancement in injectivity or the reduction of shear-thickening to the reduction of polymer extensional viscosity. The reduction of polymer extensional viscosity was attributed to the shearing of polymer macromolecules at the high-end of its MWD, as illustrated in Figure 4-2.

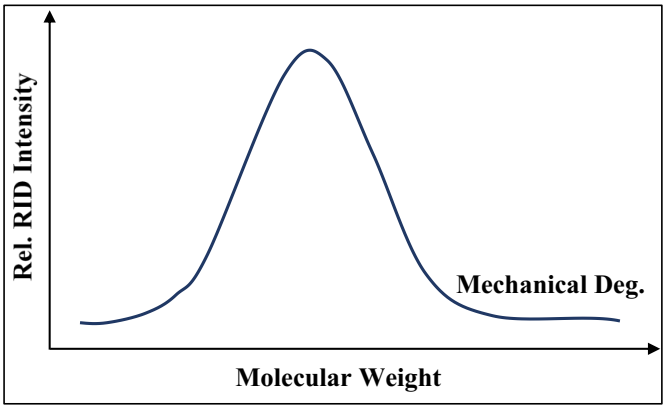

Figure 4-2 Schematic illustration of preshearing mechanism modified from [173].

Chapter 5. Main Results and Discussion

This chapter summarizes the main results that are obtained from this study and synthesizes the main achievements from Paper I to V. The results were based on experimental studies of different HPAM polymers that were characterized by bulk rheology using a rotational rheometer. Their flow properties in porous media were investigated by calculating in-situ rheology. The porous media was a natural outcrop rock of linear cores from Berea and Bentheimer sandstone. These outcrop cores are considered as standard cores that represented rock in homogenous oil reservoirs. Some of the cores were conditioned to be non-water wet by aging with crude oil.

In the first study (Paper-I), the impact of mechanical degradation on HPAM flow properties and rheology was experimentally investigated on a large scale of 5–10 cm porous media. Experimental procedures were established to measure HPAM in-situ viscosity. This involved polymer pretreatment in short cores at different levels of filtration: prefiltering and preshearing. Also, reinjection or circulation of prefiltered polymer solution that had already seen porous media at high flow rates. Some other experimental parameters were investigated, such as rate effect (hysteresis) and tapering (gradual reduction in polymer concentration). This paper also identified the impact of using backpressure regulator during in-situ measurements. Most importantly, this paper addressed reproducibility of the results. Polymer in-situ viscosity was correlated with bulk viscosity. One of the key results of this paper was the observation of polymer successive mechanical degradation. The results will be discussed later in this chapter.

In the second paper (Paper-II), the investigation of the impact of mechanical degradation on HPAM rheology was extended to various polymers at different concentrations. This involved semi-dilute and concentrated polymer solutions. Note that, Paper-II, in concept, was an extension of Paper-I. In this paper, we extended the discussion of polymer flow in porous media and permeability reduction due to polymer injection.

In the third study (Paper-III), the influence of the permeability of the porous media on HPAM rheology was investigated. This consisted of the investigation of HPAM flow in Berea and Bentheimer cores with different permeabilities. High polymer retention was identified in terms of residual resistance factor (RRF) as the dominant factor that negatively affected polymer injectivity in low permeability cores.

In the fourth paper (Paper-IV), the study of polymer flow in porous media was integrated into a two-phase water - oil system. The objective of the paper was to investigate the influence of the presence of the oil phase on polymer in-situ rheology and injectivity. The experiments were performed at a stable remaining oil saturation, S_{or}, and in porous media with different wettability conditions. The experiments were repeated to check the reproducibility of these results. The results suggested better polymer injectivity in presence of oil.

In the fifth paper (Paper-V), polymer injectivity was related to polymer in-situ rheology. The paper provided an overview of polymer flow in porous media, including extensive discussion on in-situ viscosity measurements by different models, e.g., capillary bundle model and pore network modeling. Moreover, the paper covers simulation and experimental aspects of polymer flow in porous media such as rate effect, flow geometry, and presence of oil. The paper utilized the STARS CMG simulator for history matching in the numerical part, and analysis of linear and radial geometries of Bentheimer outcrop rock as porous media for the experimental part. This study found better polymer injectivity in the presence of oil in both flow geometries (linear and radial). The study suggested additional mechanisms may contribute to the prediction of polymer injectivity in radial geometry such as unsteady-state pressure gradient, memory effect to the polymer viscoelasticity, and mechanical degradation that control the injectivity in linear cores. Note that my contribution to this paper was related to linear core flood experiments.

The summary of the results will be organized according to the following topics:

5.1. Influence of Polymer Mechanical Degradation

As stated above in Paper-I, we have established an experimental design to investigate the impact of mechanical degradation on HPAM flow behavior in porous media. This consisted of polymer preconditioning by exposing the polymer solution to different extents of shearing before measuring polymer in-situ rheology. These conditions aimed to simulate the actual field flow of polymer from the wellbore to deep in the reservoir from the linear core experiments. Prefiltering and preshearing processes were performed in short cores (L = 5cm) by injecting the polymer solution at low and high flow rates, respectively. Prefiltering was performed to remove insoluble polymer particles and aggregates in solution. This was applied by injecting the polymer solution at a low flow rate (Q = 0.5 cc/min) with less than 500 mbar pressure drop to avoid mechanical degradation. Preshearing was performed at a high injection rate and high-pressure drop to filter out and shear high Mw species in the polymer solution. Reinjection was performed by exposing the prefiltered polymer solution to a high shear rate in the long core (L = 10cm) to investigate the influence of exposure time to high shear on mechanical degradation. Hypothetically, preshearing and reinjection processes may impose the same extent of mechanical degradation according to the hypothesis that mechanical degradation is confined to the entry of the porous media [37,70,119,123].

The impact of mechanical degradation could be seen on the reduction of polymer viscoelastic behavior such as the shift of onset of shear-thickening to higher flow velocities and reduction of the degree of shear-thickening behavior. Thus, lower resistance factors. Given that these shear-thickening parameters are strongly dependent on polymer macromolecules and their chain length [122]. The reduction of shear-thickening upon shearing is ascribed to the reduction of polymer Mw and MWD as a result of molecular rapturing by the extensional stresses [32,33,42,70,85,128,174-176]. This was also experimentally observed on the shift of the resistance factor of degraded high Mw polymer solution to that of undegraded lower Mw polymer (Paper-I and II). Thereby lower pressure drop for degraded polymer solution.

The impact of mechanical degradation was relatively lower on shear viscosity compared to that of polymer viscoelasticity (see Figure 5-1). As seen, shearing the polymer solution at the onset of shear-thickening was insufficient to induce mechanical degradation for the given polymer and given porous media. Unlike Mansour et al. [124] they reported that mechanical degradation occurred in the shear-thinning region before the onset of shear-thickening. In our study, there is no alteration on RF curve of the degraded solution close to the onset of shear-thickening (prefiltered) to that of undegraded solution (fresh solution). This is in agreement with that extensional thickening is required to initiate polymer degradation [128,166]. Thereby filtration (Q $\leq$ 0.5 cc/min, $v_D \leq 0.6$ m/day) has no impact on polymer in-situ rheology compared to preshearing. However, the effect of preshearing on polymer in-situ viscosity depends on the extent of mechanical degradation. For example, preshearing at typical wellbore velocities (Q = 15 cc/min, $v_D = 19.4$ m/day) is sufficient to reduce polymer shear-thickening features while maintaining its in-situ viscosity similar to that of prefiltered solution at low flow rates. Despite this, the bulk rheology for prefiltered and presheared polymer are similar, which is direct evidence that bulk rheology alone (shear viscosity) cannot be used to predict polymer in-situ rheology.

However, if the polymer solution is exposed to high extent of mechanical degradation, it causes a significant reduction in polymer viscoelastic properties including polymer in-situ and shear viscosity as represented in Figure 5-1. For instance, degraded solutions at high rates (Q = 110 cc/min, $v_D = 141.2$ m/day) possessed a lower shear viscosity with a wider Newtonian plateau and weaker shear-thinning behavior. This suggested that degraded solution had a shorter characteristic time when assuming the inverse of polymer characteristic time is equivalent to the onset of shear-thinning, see Figure 5-1b. The measurements of polymer characteristic time and particularly zero shear viscosity are challenging by using the available apparatus in this study. Apparently, there is a trend which can be inferred for the degraded solution at a high flow rate (presheared at Q = 110 cc/min). Degradation of 16 % results in significant loss of polymer in-situ viscosity (> 50 %) at low flow rates and considerable

loss of polymer shear-thickening parameters. Similar observations reported elsewhere [116,156].

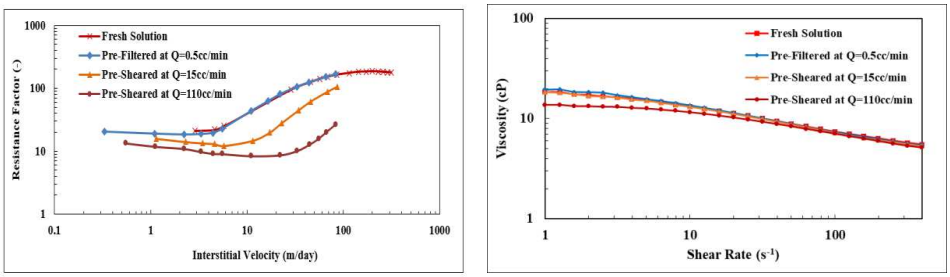

a) In-situ rheology b) Bulk rheology

Figure 5-1 Impact of different extents of mechanical degradation on HPAM in-situ and bulk rheology (Mw = 12 MDa, C = 1000 ppm). Core data were given in Paper-I.

As stated earlier, previous studies on HPAM mechanical degradation attributed its occurrence to the entrance of the porous media. According to Jouenne et al. [165], polymer mechanical degradation approached steady-state condition after the polymer solution was exposed to the point of highest strain which was proposed to occur within the first 6 mm of the porous media. However, the data presented in Paper-I for high Mw polymer showed that reinjected solution experienced additional degradation to that of presheared solution in the short core (Figure 5-2). As shown, the RF of the reinjected solution is lower than that of presheared solution. This suggests that the high Mw species propagated further into porous media and were not limited or retained by the sandface as proposed by Seright et al. [116]. This demonstrated that the high Mw polymer experienced successive degradation as it was reinjected into porous media. Suggesting equilibrium molecular weight was not satisfied [177]. This undermines the assumption given above in which the total polymer mechanical degradation is achieved at the highest point of shear that is confined within the sandface (a few millimeters of the porous media). A similar observation was also made for other polymers reported in Paper-II. Hence, the extent of mechanical degradation may also depend on the characteristic length, exposure time and the number of passes to the point of highest shear beyond physiochemical properties of the polymer solution. Other studies, e.g.

[123,162,178], also support the observation regarding successive mechanical degradation.

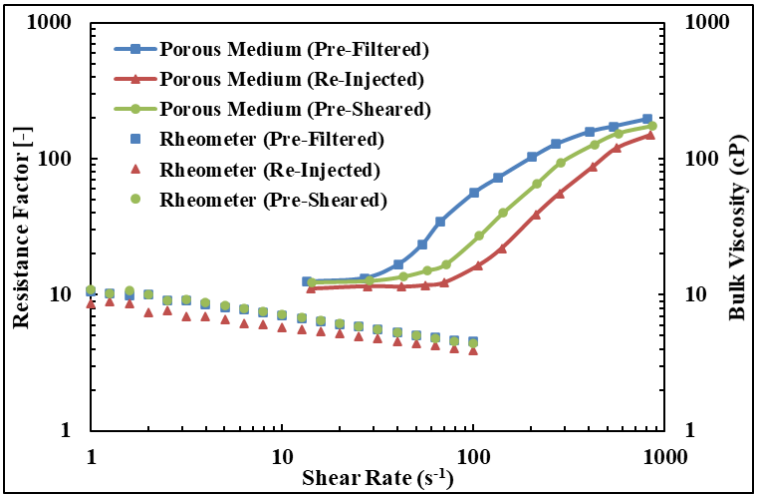

Figure 5-2 Bulk and in-situ rheology of polymer solution (Mw = 18 MDa, C = 500 ppm) modified from (Paper-I).

5.2. Influence of Polymer Mw and Concentration

In Paper-II, we have highlighted the influence of polymer molecular weight (Mw) and concentration on its in-situ flow behavior and mechanical degradation. The polymer solutions reported in paper-II were semi-dilute and were classified into two subcategories: unentangled and entangled (concentrated). Here, untangled does not mean dilute solution, but it is referred to as a relatively lower degree of entanglement in comparison with that in concentrated solutions within the semi-dilute region. Apparently, the flow behaviors of these polymers were different, even though they are all semi-dilute solutions. This suggests that the degree of entanglement (phase conformations) has its significance in defining polymer flow in porous media.

Figure 5-3 displays a remarkable variation of the resistance factor as a function of polymer Mw and concentration. The flow of unentangled polymer solutions (low

concentration) can be described as shear-thickening and near-Newtonian flow behaviors corresponding to high and low flow velocities, respectively. These observations are concordant with the previous studies reported in the literature, e.g., [42,85,116]. Polymer molecular weight was the dominant factor that influenced their in-situ flow characteristics. For instance, the highest molecular weight polymer (Mw = 18 MDa) had the strongest shear-thickening behavior that can be elucidated from the early onset and higher slop of shear-thickening. Also, the resistance factors at reservoir velocities were two times higher for relatively high Mw polymer solution (Mw = 12 MDa) to that of low Mw polymer (Mw = 8 MDa) for a given polymer concentration of 1000 ppm. According to Paper-II, mechanical degradation increased with the increase of polymer Mw for unentangled solutions which was in line with Martin [34]. The high Mw polymer experienced mechanical degradation of approx. 22 %.

The in-situ behavior of entangled polymer solutions, a polymer in concentration ($C \gg C^*$), was dominated by shear viscosity that dampens their viscoelastic features (see Figure 5-3 polymers with Mw=8 and 12 MDa at concentrations of 4000 and 3000 ppm, respectively). This demonstrated that the contribution of shear viscosity was higher than extensional viscosity. Given that, apparent polymer viscosity as illustrated here by resistance factor was a combination of shear and extensional viscosities [21]. Hence, concentrated solutions exhibited lower viscoelastic features, e.g., shear-thickening behavior. The reduction of polymer shear-thickening behavior with the increase in polymer shear viscosity was in line with other studies, e.g., [168]. However, when the molecular weight increased (see Mw = 12 MDa), viscoelastic features become stronger (e.g., shear-thickening). This was also confirmed by high Mw polymer (Mw = 18 MDa, C = 1000 ppm) in which its flow behavior was similar to that of unentangled semi-dilute polymers. This again demonstrates the influence of polymer Mw on extensional viscosity. It was also observed that, the mechanical degradation was lower for concentrated solution. This may be ascribed to the reduced vulnerability of stretching in concentrated solution when the molecules move in bundles [177]. Thus, lower stretching yields lower extensional viscosity and subsequently, lower mechanical

degradation. This is in agreement with Skauge et al. [106] in which concentrated solutions were more tolerant to mechanical degradation.

Another critical observation was the shear-thinning behavior in porous media of the concentrated solutions with the high shear viscosity (e.g., polymers Mw = 8 and 12 MDa at concentrations of 4000 and 3000 ppm, respectively). Shear-thinning behavior was not observed for unentangled solutions in porous media, even in low permeability as reported in Paper-III or at the presence of residual oil as in Paper-IV. However, as the polymer concentration is increased, shear-thinning behavior can be gradually recovered. The increase of polymer concentration increases the entanglements and the hydrodynamic interactions among the molecules that facilitate their orientation and alignment to the shear rates [179]. This possibly explains the observation of shear-thinning behavior in porous media for concentrated solutions. However, the existence of shear-thinning behavior in porous media for filtered HPAM polymers was debated by Seright et al. [116]. They attributed the occurrence of HPAM shear-thinning behavior to the presence of microgels. However, the observed shear-thinning behavior in our study was preserved by the concentrated solutions, even if the solution was exposed to degradation (presheared or reinjected). This is clear evidence of the existence of shear-thinning behavior in porous media for concentrated solutions, even if the solutions are microgel-free. Other studies, e.g. [180,181], also reported the observation of shear-thinning behavior for HPAM in porous media. The shear-thinning here at low shear rates should be differentiated from the shear-thinning upon mechanical degradation observed at high rates (e.g., see the in-situ flow behavior of fresh solution displayed in Figure 5-1). Therefore, the study in Paper-II demonstrated the four flow behaviors that HPAM may exhibit in porous media [109]: Newtonian, shear-thinning, shear-thickening and mechanical degradation.

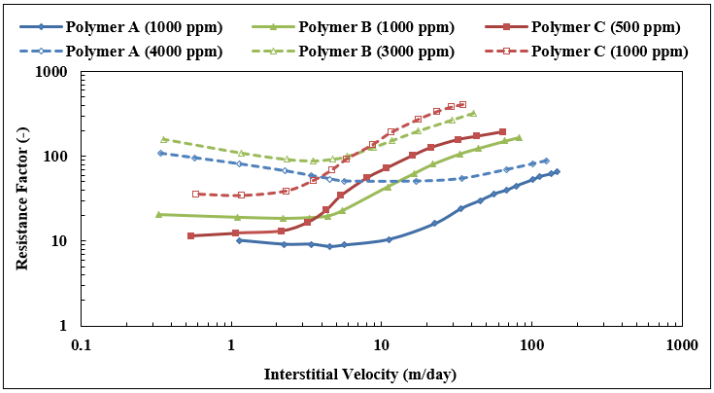

Figure 5-3 Resistance factors of different polymer solutions. Mw of polymer solutions A, B and C were 8, 12 and 18 MDa, respectively. (Paper-II)

One of the important viscoelastic features is the onset of shear-thickening. As depicted in Figure 5-3, the onset of shear-thickening occurred earlier for polymer solution with high Mw. Hence, it is as a function of polymer Mw and it inversely correlates with the increase of polymer Mw [181,182]. However, the onset of shear-thickening appeared to have less dependency on polymer concentration, as shown in Figure 5-4a. The resistance factors increased with the increase of polymer concentration, particularly at low flow velocities [74] that attributed to the increase of shear viscosity, as shown in Figure 5-4b. As one can see the overlap of RF curves of polymer solutions with a concentration of 1500 and 1000 ppm at high flow rates, despite the difference in concentrations, indicates the influence of polymer elastic properties that highly depends on polymer Mw. This was identically applied for polymer solutions with a concentration of 750 and 500 ppm. The core data for the in-situ experiments in Figure 5-4 are compiled in Table 2.

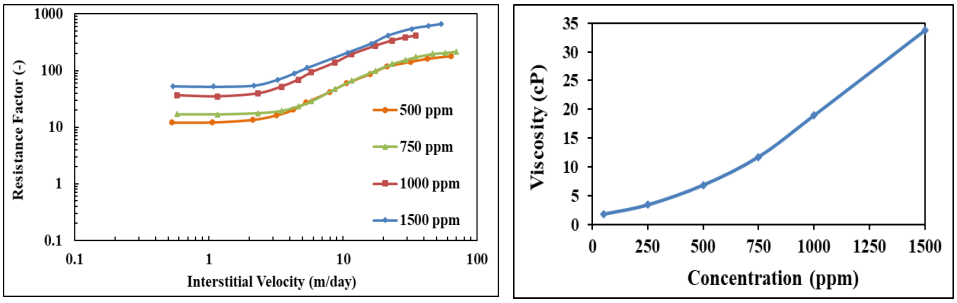

a) In-situ rheology b) Bulk rheology

Figure 5-4 In-situ and bulk rheology of prefiltered polymer solution (Mw = 18 MDa) with different concentrations. Note that some data were presented in Paper-V.

Table 2 Core and polymer solution properties (Mw = 18 MDa).

Concentration (ppm)	L (cm)	D (cm)	ϕ (-)	K_{wi} (Darcy)	K_{wf} (Darcy)	RRF (-)	η_i (cP)	η_e (cP)
500	9.54	3.77	0.24	2.48	1.35	1.8	6.81	6.62
750	9.84	3.78	0.22	2.11	0.61	3.5	11.74	10.41
1000	10.04	3.78	0.22	2.12	0.23	9.3	18.95	17.98
1500	4.89	3.79	0.24	1.99	0.32	6.3	33.76	32.87

It is worth emphasizing that concentrated solutions may not always be a feasible choice to provide high viscosity, especially for high Mw polymers, despite the better tolerance for mechanical degradation, as reported in Paper-II. For instance, according to Paper-II, the increase in polymer concentration enhanced the shear stability and reduced the mechanical degradation as seen for high Mw polymer solution (Mw =18 MDa, concentrations of 500 and then 1000 ppm). Utilizing high Mw polymer with high concentration results in high polymer retention, which is not quantified from bulk rheology. Figure 5-5 displays the in-situ rheology of high Mw polymer (Mw = 18MDa) at different concentrations by using the term 'RF/RRF' as a description of polymer in-situ viscosity. We have not considered the term 'RF/RRF' elsewhere in Paper-I and -II due to the complexity of measuring true 'RRF' that may exacerbate our analysis. Coincidently, in Figure 5-5, the in-situ viscosity of 1500 ppm was very close to that of 500 ppm for the same polymer. This is ascribed to the high retention of 1500 ppm as seen from the RRF of 6.3 to 1.8 for the 500 ppm solution.

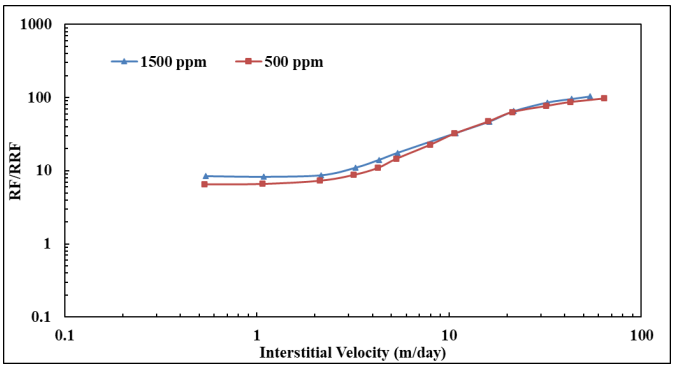

Figure 5-5 RF/RRF of prefiltered high molecular weight polymer solution (Mw = 18 MDa) at different concentrations. Core data were given in Table 2.

5.3. Influence of Permeability

The goal of Paper-III was to evaluate the impact of formation permeability on polymer flow and subsequently its injectivity. This was achieved by studying flow of different polymers in rocks with different permeabilities. Figure 5-6 shows the in-situ and effluent viscosity data of high molecular weight polymer solution (Mw = 18 MDa, C = 500 ppm) that was injected in Berea and Bentheimer cores. The permeability of the Berea, Bentheimer1 and Bentheimer2 cores were 0.1, 1.3 and 2.6 Darcy, respectively. The polymer solutions exhibited similar flow behaviors such as near-Newtonian at low velocities and shear-thickening at high velocities in Berea and Bentheimer cores. Shear-thinning behavior was not observed here, even at low permeability. This supports the conclusion of Paper-II in which shear-thinning behavior was not observable in porous media for unentangled semi-dilute polymers. This was also consistent with the earlier studies reported by Seright et al. [116]. It is interesting to see the overlap of resistance factors at high rates which indicates the dominance of elasticity for high Mw polymer as a polymer property irrespective of porous media characteristics (permeability).

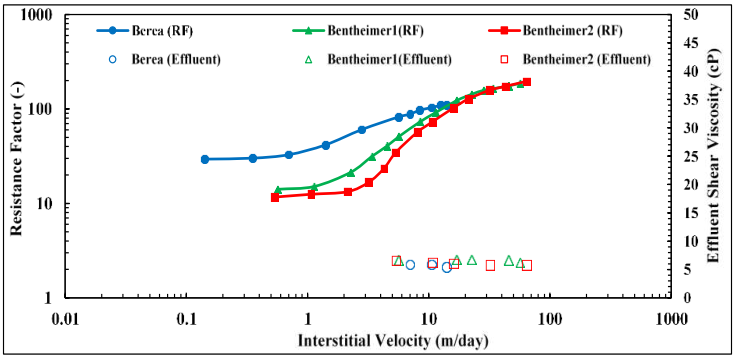

Figure 5-6 HPAM flow in porous media with different permeabilities. Polymer (Mw = 18 MDa, C = 500 ppm) Paper-III [183].

Another observation from Figure 5-6 was the high resistance factors observed in Berea core, which could be attributed to the high retention that is seen from high RRF. RRF was 10.0, 3.0 and 1.8 corresponding to Berea, Bentheimer1 and Bentheimer2 cores, respectively. RRF increased with the decrease of permeability, which implies an inverse relation between RRF and permeability [59,109]. Additionally, the shear-thickening behavior and mechanical degradation occurred at lower velocities in low permeability cores. The extent of these flow behavior correlates with permeability. For instance, the extent of shear-thickening (slope) decreased with the permeability decreases despite the early onset of shear-thickening in low preamble cores. The shift of the onset of shear-thickening to lower velocities with the decrease in permeability was in line with other studies, e.g., [40,42]. The differences in the shear-thickening behavior in Berea verses Bentheimer were possibly due to the variation of contraction ratio as Berea is characterized with small pores. Chauveteau et al. [125] found a similar trend, in which shear-thickening behavior occurred at the earlier onset but with a lower degree in porous media with low contraction ratio that resulted in lower maximum RF. Polymer mechanical degradation increased as permeability decreased. This inverse proportionally of polymer mechanical degradation against permeability was possibly due to the increase of normal stresses in low permeable porous media at a given strain rate [32,184]. Preshearing becomes an essential process for the injection of high molecular weight polymer into low permeability formation.

5.4. Influence of the Oil Presence

In Paper IV, we found that the presence of oil was one of the key factors that influence the prediction of polymer injectivity. Indeed, the presence of another phase, which here is the oil, reduces the available effective pore volume for polymer molecules to transport. As we stated in Chapter 3, the presence and distribution of the oil phase in porous media are governed by wettability. The oil phase may be present in porous media as oil droplets that are surrounded by water in water-wet media or as oil films in oil-wet media. The literature contains few studies regarding the influence of oil phase on polymer injectivity.

Presumably, when the residual oil is present as oil droplets such as in water-wet condition, the oil droplets may provide additional surfaces for the polymer to adsorb in addition to the rock surfaces. This is in contrast to the oil-wet condition where the oil films partially cover the rock surface and reduce the available surface for the polymer to adsorb [104]. Although adsorption measurements have not been performed in our study, the adsorption and mechanical entrapment are the most important retention mechanisms that are relevant for the evaluation of polymer flow both in water-wet and oil-wet conditions. Other scenarios, including the slip effect, are discussed in Paper-V.

The in-situ rheology data for the two-phase system were performed at stable saturation conditions, as presented in Paper-IV. Stable saturation condition is one of the challenges encountered in two-phase flow experiments, particularly for polymer in-situ rheology, as found in other experimental studies, e.g., [168,185]. In our experiments, the cores were flooded by water then by polymer to unexpectedly high flow rates to ensure no more oil is produced during in-situ rheology measurements. Moreover, loop injection from lowest to highest injection rates and vice versa was performed during polymer in-situ measurements to monitor if any oil is produced that may change the state of saturation.

Figure 5-7 depicts the flow of high Mw polymer that was injected in Bentheimer cores with and without oil present at different wettability. It is clear that the trend but not the extent of the resistance factor in the two-phase flow condition was concordant with that in single-phase flow (oil-free cores). The two in-situ flow behavior (shear-thickening and near-Newtonian) were observed in porous media with and without the presence of oil for unentangled semi-dilute polymer solutions. In the presence of oil, the polymer solution exhibited lower resistance factors. The onset of shear-thickening seems independent of porous media wettability. For instance, the onset of shear-thickening was 2.5, 2.6 and 2.1 m/day for prefiltered solution injected in single-phase and two-phase (water-wet and non-water wet, see Figure 5-7). However, the degree and magnitude of shear-thickening behavior were reduced by the presence of oil and were considerably reduced in non-water wet condition. It might be argued that the resistance factors applied in two-phase experiments are incomparable with that in a single-phase experiment due to the pressure data during water injection that were used for calculating RF were not at similar initial conditions. The resistance factors applied in two-phase experiments were hinged to pressure data corresponding to the water flow based on relative permeabilities after polymer flooding instead of absolute permeability. Thus, it decouples the permeability reduction caused by the polymer (retention). Hence, it was lower. This contradicts the measurements of the resistance factor applied in single-phase experiments that consider permeability reduction (retention) as the resistance factor was based on pressure data of polymer to water flow before the polymer contacts the porous media. The apparent viscosity for prefiltered solutions in aged cores (non-water wet) was lower compared to unaged (water-wet cores). This justifies the above argument because the resistance factor of both solutions was defined in a similar way and suggested positive impact of wettability on polymer apparent viscosity. The lower apparent viscosity in non-water wet core indicated better polymer injectivity. This is analogous to the other observation made with the same polymer investigated in radial geometry (Paper-V) which is in agreement with other studies in the literature [134,168]. The enhancement of polymer injectivity in non-water wet condition is ascribed to the lower retention [104,134,185].

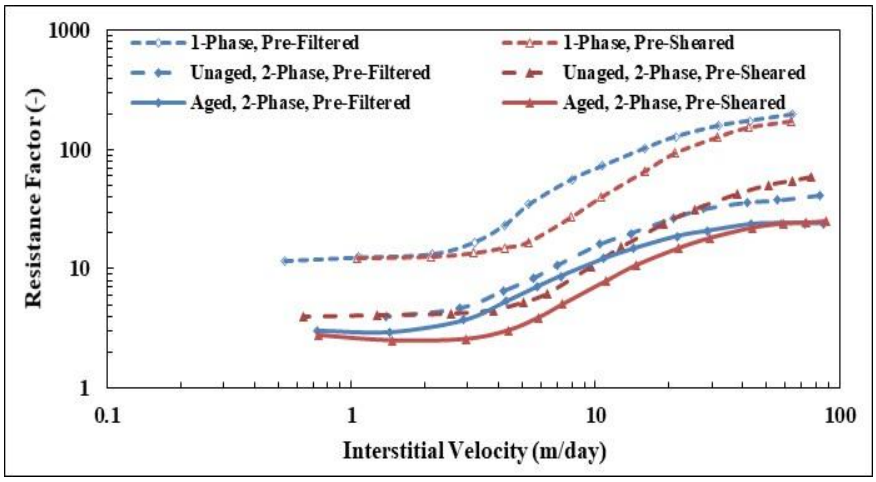

Figure 5-7 Impact of the presence of oil and wettability on the flow of HPAM polymer (Mw = 18 MDa, C = 500 ppm) [186].

As seen in Figure 5-7, the shear-thickening behavior was translated to higher velocities for the presheared polymer solution; consequently, its magnitude and slope were lower than the corresponding prefiltered solution while its in-situ viscosity was maintained. The presheared polymer solution in the aged core exhibited lower resistance factors to the presheared solution that was injected into the unaged core even though both cores had almost similar effective pore volume as both polymers were injected at similar residual oil saturation (22 %). This suggests that non-water condition is favorable for polymer injectivity.

5.5. Permeability Reduction

Permeability reduction by polymer flooding may provide a synergetic effect on improving mobility ratio without the requirement for high viscosity, especially when reservoir heterogeneity is high (better conformance) [59,187]. However, the high pressure that associates polymer injection, but not the shear-thickening behavior could be partially imposed by permeability reduction caused by polymer retention that adversely impacts polymer injectivity. We limit the discussion here to the impact of

permeability reduction on polymer injectivity. Residual resistance factor (RRF) measurements quantify permeability reduction by polymer flooding and hence qualify polymer retention. Hence, RRF measurements are crucial for polymer injectivity in which lower polymer retention is favorable for EOR applications. Additionally, polymer post flush is a vital process, especially when utilizing slug injection strategies in a polymer flooding process at which RRF should be as low as possible. RRF measurements are also important when it comes to determining what other EOR options to be implemented to recover the remaining oil after polymer flooding [188].

In our study, we found that the measurements of RRF depend on fluid exchange process (tapering). In Paper-I, we found that tapering significantly reduced RRF to reasonable values close to 2. This was only valid for highly permeable rock, i.g., Bentheimer but not Berea (Paper-III). Note that, tapering utilized the same polymer solution used in the main experiment for in-situ measurements with lower concentrations. In Paper-II, we found that RRF was a function of polymer Mw and concentration. We found the lowest Mw polymer had the lowest RRF of 1.6 that caused permeability reduction of approximately 38 %. Opposite, high RRF was observed for concentrated high Mw polymers. It also increased with decreasing permeability (Paper-III). High RRF (e.g., RRF>3) may not be feasible for mobility control EOR applications.

RRF was not significantly affected by the preshearing process for the unentangled semi-dilute polymer solutions exposed to wellbore mechanical degradation. However, slightly lower RRF values were found for extensively presheared solutions at high shear rates (Paper-I). This was in agreement with [156] in which permeability reduction by polymer was not affected by mechanical degradation. However, the RRF of concentrated solutions were relatively more reduced by preshearing process.

5.6. Other Experimental Observations

5.6.1. Ageing

HPAM polymers are known for their excellent stability for years in the absence of oxygen or iron. For instance, Shahin and Thigpen [189] reported that HPAM maintained its viscosity over two years in field pilot polymer injectivity test in white castle oilfield in the USA using 500 ppm of medium Mw HPAM dissolved in 1 % brine. Likewise, Seright et al. [94] reported that HPAM maintained half of its original viscosity for more than eight years at 100 °C at the absence of oxygen and divalent cations. This indicates good longevity of HPAM polymers. This also suggests that HPAM can be used in field applications without the need for stabilizers [168]. Following these aforementioned studies, the viscosity data presented in Figure 5-8 show good stability of HPAM polymers that were incubated at 5 °C inside a fridge over ten months. The solutions were contained no iron and their good stability is attributed to the low temperature, which slows the hydrolysis process despite the presence of oxygen. Bear in mind that, in our experiments, the polymer solutions were used within two weeks of preparation.

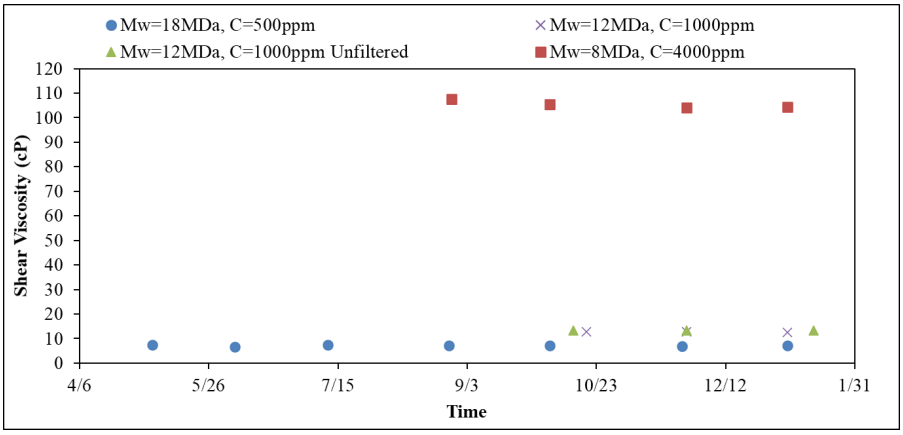

Figure 5-8 Time (month/day) effect on prefiltered HPAM bulk viscosity.

5.6.2. Backpressure regulator

We performed a detailed study to investigate the impact of backpressure (BP) regulator on polymer bulk and in-situ rheology, considering different polymers with different concentrations at different BP values. The bulk viscosity of the polymer solution was measured before and after the polymer solutions passed backpressure regulated at the same flow rate (Q = 50 cc/min), as shown in Figure 5-9. The polymer with high Mw experienced significant degradation, especially at a lower concentration. On the other hand, concentrated polymer solutions showed lower degradation (see Table 3). This indicates that the backpressure regulator caused severe degradation even when it was regulated at low pressure. As expected, the backpressure device induced more degradation when it was regulated at high pressure (30 bar) see Table 4. Also, more degradation was observed when increasing the injection rate. For instance, the degradation of polymer solution (Mw = 12 MDa, C = 1000 ppm) at flow rate Q = 15 cc/min was 24.8 % (Paper-I) which increased to 28.9 % when it was injected at Q = 50 cc/min (Table 3).

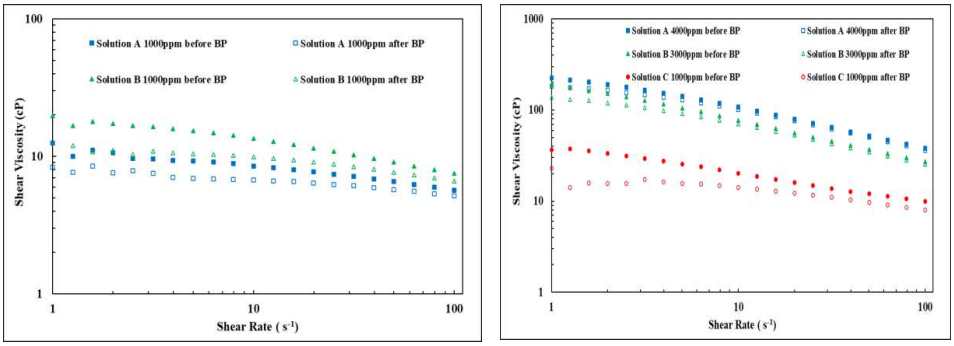

a) Semi-dilute Polymer Solutions (Unentangled)

b) Concentrated Polymer Solutions (Entangled)

Figure 5-9 backpressure effects on polymer viscosity injected at high flow rate Q = 50 cc/min through 7 bar backpressure regulator. Different polymer concentrations with different Mw: Polymer A = 8 MDa , Polymer B = 12 MDa and Polymer C = 18 MDa.

Table 3 HPAM viscosity and degradation data by backpressure (BP) regulator. Shear viscosity referred to viscosity at shear rate 10 s^{-1}. BP was set at 7 bar, and the polymer solutions were injected at the same flow rate Q = 50 cc/min.

Solution	**A (Mw = 8 MDa)**				**B (Mw = 12 MDa)**				**C (Mw = 18 MDa)**	
C (ppm)	1000		4000		1000		3000		1000	
Viscosity (cP)	Before BP	After BP	Before BP	After BP	Before BP	After BP	Before BP	After BP	Before BP	After BP
	8.50	6.72	107.50	101.00	13.53	9.92	77.58	70.78	20.30	14.14
Deg (%)	23.87		6.11		28.94		8.88		31.98	

Table 4 HPAM viscosity and degradation data by backpressure(BP) regulator. Shear viscosity referred to viscosity at shear rate 10 s^{-1}. BP was regulated at 30 bar, and the polymer solutions were injected at the same flow rate Q = 50 cc/min.

Solution	**B (Mw = 12 MDa)**		**C (Mw = 18 MDa)**	
C (ppm)	3000		1000	
Viscosity (cP)	Before BP	After BP	Before BP	After BP
	77.58	37.43	20.30	5.74
Deg (%)	52.46		75.58	

5.6.3. Injection hysteresis

The purpose of performing loop injection such as injecting the polymer from highest to lowest flow rates and vice versa was to investigate if there was any injection hysteresis in adopting radial flow scheme into linear geometry, e.g., linear cores (Paper-I). Moreover, the injection from highest to lowest flow rates is analogous to the radial distance of polymer flow from the wellbore (injector) to deep in the reservoir. In comparison, increasing flow rate is also representative of polymer flow from reservoir to wellbore near the producer. The latter may not be crucial because the pressure drop is declining near the producer and is not correctly represented here by the injection from lowest to highest flow rates in the linear cores. Hence, we focused on the polymer flow near the injector by incorporating the injection scheme of highest to lowest flow rates. Recall that, hydrodynamic retention is the most relevant aspect here as it is a rate dependant mechanism and may impact polymer in-situ rheology. However, we have not performed concentration measurements to measure hydrodynamic retention. Additionally, loop injection is beneficial for ensuring the saturation condition was maintained during the in-situ measurements in two-phase experiments.

Figure 5-10 represents the hysteresis effect on resistance factors for two prefiltered polymer solutions that were injected in cores saturated with oil. There is no injection hysteresis for low Mw polymer solution (Mw = 8 MDa) and for high polymer solution (Mw = 18 MDa) at high and low velocities. This indicated that there was no change in saturation conditions as there was no oil produced. However, hysteresis in injection scheme can be seen at the mid-range of flow velocities during the injection of high Mw polymer solutions. This is maybe attributed to increase of the injection flow rate that causes hydrodynamic retention. The observation is confirmed from effluent data given in Figure 5-11, in which lower viscosities were observed for the injection of low to high flow rates of high Mw polymer, while not for low Mw polymer solution. This is different from other studies, e.g., [34,190] that reported the injection sequence has no effect on polymer in-situ rheology.

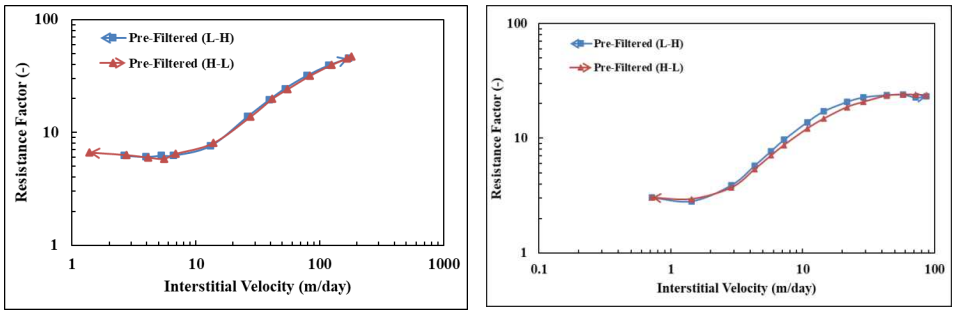

a) Mw = 8 MDa, C = 1000 ppm b) Mw = 18 MDa, C = 500 ppm

Figure 5-10 Hysteresis effect on polymer flow in porous media. The polymers are given in Paper-IV as Polymer A(Mw = 8 MDa) and B(M w= 18 MDa). Both polymers were prefiltered, and polymer A injected in Unaged core (U1) where Polymer B injected in Aged Core (A1).

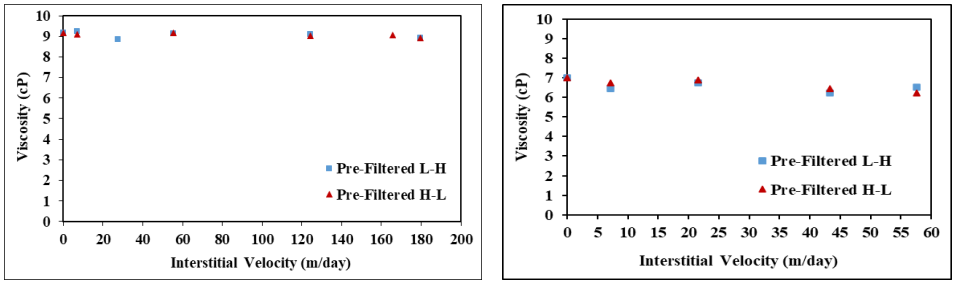

a) Mw = 8 MDa, C = 1000 ppm b) Mw = 18 MDa, C = 500 ppm

Figure 5-11 Effluent data for low and high Mw polymer solutions injected at different injection schemes. The polymers are given in Paper-IV as Polymer A(Mw = 8 MDa) and B(Mw = 18 MDa). Both polymers were prefiltered, and polymer A injected in Unaged core (U1) where Polymer B injected in Aged Core (A1).

Chapter 6. Conclusions and Recommendations

6.1. Conclusions

There are some crucial aspects to consider for better prediction of polymer injectivity. The rheology and viscoelasticity of HPAM polymer have a prominent role on the injectivity behavior. In-situ flow such as performed in cores in this study, allows the observation of polymer flow behaviors that are not seen in bulk rheology. Hence, in-situ rheology can be more representative of actual polymer flow in real field applications that aids to appropriately define its utility more than bulk rheology does. If the polymer solution is not a gel or gel-like, shear-thickening behavior may dominate the polymer flow in high shear rates areas such as those present in the wellbore region and may influence the polymer injection. Therefore, analysis of the shear-thickening should be considered for better prediction of polymer injectivity in terms of pressure build-up, especially at matrix injection. The assumption of constant polymer viscosity (Newtonian) or reduction (shear-thinning behavior) in that region may yield erroneous prediction (overestimation) of polymer injectivity.

In a good agreement with other studies in the literature, HPAM is a shear-sensitive polymer. This facilitates the filtration process in a way that does not require extensive filtration which is applied for biopolymers to remove polymer microgels and aggregates. On the other hand, this may also be considered as weak shear stability if it is not controlled, particularly at wellbore area that accommodates high velocities which are sufficient to induce polymer mechanical degradation. HPAM shear stability was evaluated by bulk and in-situ rheology. Different shear conditions were evaluated, which includes: prefiltering, reinjection and preshearing. The study reveals that these processes reduced HPAM viscoelasticity while not its in-situ viscosity. This suggests that HPAM in-situ viscosity deep in the reservoir has less influence by polymer viscoelasticity. That is in sharp contrast to the wellbore area, where polymer viscoelasticity may lead to high injection pressures and degradation may occur.

The following points conclude the linear core studies presented in the papers I-V:

- Successive (progressive) mechanical degradation was observed for the high molecular weight polymer. It hampers the prediction of polymer injectivity. This also indicates that the porous media characteristic length impacts polymer degradation.

- Polymer Mw and concentration have been identified as the main factors that influence its flow behavior in porous media. These factors appear to be more important with regard to injectivity than porous media properties such as permeability, oil saturation and wettability.
    - The influence of polymer Mw and distribution can be seen on the strong viscoelastic properties of the polymer, e.g., shear-thickening behavior and mechanical degradation.
    - The influence of concentration can be seen on the viscous properties of the polymer, such as shear viscosity and shear-thinning behavior.

- Porous media properties such as permeability and wettability affect the polymer apparent viscosity without changing its flow behavior. For instance, shear-thinning behavior was not observed with permeability variation nor with wettability alteration for unentangled semi-dilute polymers.
    - Polymer apparent viscosity increases as permeability decreases.
    - Polymer apparent viscosity decreases at the presence of oil and considerably decreases in non-water wet condition.

- The onset of polymer viscoelastic behavior is found to be strongly linked to polymer type (Mw) while its degree varies with Mw, concentration and porous media properties.

  - The onset of shear-thickening is inversely correlated with polymer molecular weight and porous media permeability.
  - The onset of shear-thickening is independent of polymer concentration for unentangled semi-dilute polymers. Also, it is independent of the presence of oil and porous media wettability.
  - The degree and magnitude of shear-thickening increase with the increase of polymer Mw and concentration and decrease as permeability decreases. A lower degree of shear-thickening was found at the presence of oil.

- Permeability reduction was observed after polymer injection, which was quantified by the residual resistance factor (RRF):
  - High permeability reduction (high RRF) was found in polymer injection of high Mw polymer, particularly in low permeability.
  - RRF is inversely proportional with formation permeability.
  - Representable RRF measurements can be achieved for Bentheimer but not Berea by tapering without the need for a large amount of chase-water.

- Polymer mechanical degradation is proportionally increasing with polymer Mw and flow velocity. It reduces with the increase of polymer concentration.

- Polymer injectivity can be optimized through:
  - Polymer preshearing: submitting HPAM to wellbore mechanical degradation reduces its viscoelasticity. The onset of shear-thickening for presheared polymer solution shifts to high velocities. This allows the increase in injection rate without increasing the differential pressure. The presheared polymer also approaches its in-situ viscosity faster when considering radial flow.
  - Injection in oil or non-water wet zones may result in better injectivity.

Therefore, polymer injectivity benefits by mechanical degradation, and it can be optimized by the preshearing process. Nevertheless, the reduction of polymer viscoelastic properties upon shearing should not be at the expense of losing too much of its apparent viscosity. Sustainable polymer in-situ viscosity is a requirement for successful polymer flooding project. Hence, the improvement in polymer injectivity should be weighed against the loss of polymer sweep performance in the reservoir.

6.2. Recommendations for Further Studies

The current study aimed to understand the injectivity of EOR polymers in relation to their rheological behavior, including mechanical degradation with and without the presence of oil incorporating polymer pre-treatment process. 'HPAM flow in porous media' is still a research topic. Hence, I think this study will provide insights for similar future studies dealing in general with the non-Newtonian fluids that flow in porous media and specifically with HPAM polymers and their derivatives. Additional work may be suggested for future studies:

- Using a high-pressure experimental setup would allow the injection of the polymer over a wide range of flow rates. This would enable us to obtain a full curve of polymer in-situ behavior, as shown in Figure 3-2 and subsequently extend the investigation of the impact of preshearing on the whole in-situ behavior. Observing polymer flow behavior at very high rates such as maximum apparent viscosity and shear-thinning due to mechanical degradation would help normalizing the in-situ rheology as proposed in the literature, e.g., [191].

- Extending core characterization beyond the absolute porosity and permeability to include determination of pore size distribution (e.g., using mercury porosimetry [21]) before performing polymer injection aids in core selection with similar properties (twin cores). A minor change in local rock properties may hamper the comparative analysis even if core samples appear to have identical absolute permeability and porosity.

- Other polymer in-situ flow studies, e.g., [180] revealed that there is a discrepancy between linear and radial flow geometries on assessing polymer injectivity. Recently, Garrepally et al. [191] confirmed similar observation in which the assessment of mechanical degradation may vary between the linear and radial geometry. Suggesting there is a flow geometry dependence on polymer flow in porous media. Although radial flow is complex, incorporating radial flow geometry aids to better estimate polymer injectivity and mechanical degradation.

- The current study met its objectives by adopting engineering approach to investigate the mechanical degradation of HPAM polymers in linear cores. Incorporating analytical chemistry approaches using size-exclusion chromatography techniques [81,177,192] to evaluate the impact of mechanical degradation on Mw and MWD would be beneficial for understanding polymer flow and designing better polymer with good shear stability [33]. It may also help to isolate the impact of prefiltering and preshearing on polymer MWD. Relaxation time measurements can also be beneficial for incorporating available polymer viscosity analytical models with experimental data.

- The dependence of polymer mechanical degradation on porous media characteristic length is still not defined. Hence, applying the above suggestions may aid in defining the impact of the polymer residence time on mechanical degradation. Reinjecting presheared polymer solution may envision the possible occurrence of polymer successive-mechanical degradation.

References

1. plc, R.D.S. *Sustainability Report*; 2018.
2. Countries, O.o.t.P.E. *OPEC World Oil Outlook*; 978-3-9503936-6-8; Vienna, Austria, 2018.
3. Lake, L.W. *Enhanced Oil Recovery*; Prentice Hall, Inc.: 1989.
4. Alvarado, V.; Manrique, E. Enhanced Oil Recovery: An Update Review. *Energies* **2010**, *3*, 1529-1575, doi: https://doi.org/10.3390/en3091529.
5. Babadagli, T. Philosophy of EOR *Journal of Petroleum Science and Engineering* **2020**, *188*, doi: https://doi.org/10.1016/j.petrol.2020.106930
6. Green, D.W.; Willhite, G.P. *Enhanced Oil Recovery*; Richardson, Texas, 1998; Vol. 6.
7. Muggeridge, A.; Cockin, A.; Webb, K.; Frampton, H.; Collins, I.; Moulds, T.; Salino, P. Recovery rates, enhanced oil recovery and technological limits. *Phil. Trans. R. Soc.* **2014**, *372*, doi: https://doi.org/10.1098/rsta.2012.0320.
8. Munisteri, I.; Kotenev, M. Mature Oil Fields: Preventing Decline. **2013**, *09*, 9-17, doi: https://doi.org/10.2118/0313-009-TWA.
9. Labastie, A. En Route: Increasing Recovery Factors: A Necessity. *Journal of Petroleum Technology* **2011**, *63*, 12 - 13, doi: https://doi.org/10.2118/0811-0012-JPT.
10. Thomas, S. Enhanced Oil Recovery – An Overview. *Oil & Gas Science and Technology – Rev. IFP* **2008**, *63*, doi: https://doi.org/10.2516/ogst:2007060.
11. Stosur, G.J.; Hite, J.R.; Carnahan, N.F.; Miller, K. The Alphabet Soup of IOR, EOR and AOR: Effective Communication Requires a Definition of Terms. In Proceedings of SPE International Improved Oil Recovery Conference in Asia Pacific, Kuala Lumpur, Malaysia, 20-21 October 2003, SPE-84908-MS, doi: https://doi.org/10.2118/84908-MS.
12. McCormack, M.P.; Thomas, J.M.; Mackie, K. Maximising Enhanced Oil Recovery Opportunities in UKCS Through Collaboration. In Proceedings of Abu Dhabi International Petroleum Exhibition and Conference Abu Dhabi, UAE., 10–13 November 2014, SPE-172017-MS, doi: https://doi.org/10.2118/172017-MS.
13. Sharp, J.M. The Potential Of Enhanced Oil Recovery Processes. In Proceedings of Fall Meeting of the Society of Petroleum Engineers of AIME, Dallas, Texas, 28 September-1 October 1975, SPE-5557-MS, doi: https://doi.org/10.2118/5557-MS.
14. Nwidee, L.N.; Theophilus, S.; Barifcani, A.; Sarmadivaleh, M.; Iglauer, S. EOR Processes, Opportunities and Technological Advancements. *INTECH* **2016**, doi: https://doi.org/10.5772/64828.
15. Mogensen, K.; Masalmeh, S. A review of EOR techniques for carbonate reservoirs in challenging geological settings. *Journal of Petroleum Science and Engineering* **2020**, doi: https://doi.org/10.1016/j.petrol.2020.107889.
16. Ameli, F.; Alashkar, A.; Hemmati-Sarapardeh, A. Thermal Recovery Processes. In *Fundamentals of Enhanced Oil and Gas Recovery from Conventional and Unconventional Reservoirs*, Elsevier Science: 2018.
17. Mokheimer, E.M.A.; Hamdy, M.; Abubakar, Z.; Shakeel, M.R.; Habib, M.A.; Mahmoud, M. A Comprehensive Review of Thermal Enhanced Oil Recovery: Techniques Evaluation. *Journal of Energy Resources Technology* **2019**, *141*, doi: https://doi.org/10.1115/1.4041096.
18. Lake, L.W.; Schmidt, R.L.; Venuto, P.B. A Niche for Enhanced Oil Recovery in the 1990s. *Oilfield Review*, 1992; Vol. 4, pp 55-61.
19. Gbadamosi, A.O.; Junin, R.; Manan, M.A.; Agi, A.; Yusuff, A.S. An overview of chemical enhanced oil recovery: recent advances and prospects. *Int. Nano. Lett.* **2019**, *9*, 1-32, doi: https://doi.org/10.1007/s40089-019-0272-8.
20. Xu, Z.; Li, S.; Li, B.; Chen, D.; Liu, Z.; Li, Z. A review of development methods and EOR technologies for carbonate reservoirs. *Pet. Sci.* **2020**, doi: https://doi.org/10.1007/s12182-020-00467-5.
21. Sorbie, K.S. *Polymer-Improved Oil Recovery* Blackie and Son Ltd: Glasgow, U.K., 1991.
22. Gangoli, N.; Thodos, G. Enhanced Oil-Recovery Techniques-State-Of-The-Art Review. *J Can Petrol Technol* **1977**, *16*, doi: https://doi.org/10.2118/77-04-01.

23. Rellegadla, S.; Prajapat, G.; Agrawal, A. Polymers for enhanced oil recovery: fundamentals and selection criteria. *Appl. Microbiol. Biotechnol.* **2017**, *101*, 4387–4402, doi: https://doi.org/10.1007/s00253-017-8307-4.
24. Detling, K.D. Process of recovering oil from oil sands. 1944.
25. Pye, D.J. Improved Secondary Recovery by Control of Water Mobility. *Journal of Petroleum Technology* **1964**, *16*, 911-916, doi: https://doi.org/10.2118/845-PA.
26. Sandiford, B.B. Laboratory and Field Studies of Water Floods Using Polymer Solutions to Increase Oil Recoveries. *Journal of Petroleum Technology* **1964**, *16*, doi: https://doi.org/10.2118/844-PA.
27. Nouri, H.H.; Root, P.J. A Study of Polymer Solution Rheology, Flow Behavior, and Oil Displacement Processes. In Proceedings of 46th Annual Fall Meeting of the Society of Petroleum Engineers of AIME, New Orleans, Louisiana, 3-6 October 1971, doi: https://doi.org/10.2118/3523-MS.
28. Mungan, N. Shear Viscosities of Ionic Polyacrylamide Solutions. *Society of Petroleum Engineers Journal* **1972**, *12*, 469 - 473, doi: https://doi.org/10.2118/3521-PA.
29. Szabo, M.T. Molecular and Microscopic Interpretation of the Flow of Hydrolyzed Polyacrylamide Solution Through Porous Media. In Proceedings of 47th Annual Fall Meeting of the Society of Petroleum Engineers of AIME, San Antonio, Texas, 8-11 October 1972, SPE-4028-MS, doi: https://doi.org/10.2118/4028-MS.
30. Chauveteau, G.; Kohler, N. Polymer Flooding: The Essential Elements for Laboratory Evaluation. In Proceedings of SPE Improved Oil Recovery Symposium, Tulsa, Oklahoma, USA, 22-24 April 1974, SPE-4745-MS, doi: https://doi.org/10.2118/4745-MS.
31. Chauveteau, G.; Kohler, N. Influence of Microgels in Polysaccharide Solutions on Their Flow Behavior Through Porous Media. *Society of Petroleum Engineers Journal* **1984**, *24*, 361-368, doi: https://doi.org/10.2118/9295-PA.
32. Maerker, J.M. Shear Degradation of Partially Hydrolyzed Polyacrylamide Solutions. *Society of Petroleum Engineers Journal* **1975**, *15*, 311-322, doi: https://doi.org/10.2118/5101-PA.
33. Seright, R.S.; Maerker, J.M.; Holzwarth, G. Mechanical Degradation of Polyacrylamides Induced by Flow through Porous-Media. *ACS Polymer Preprints*, 1981; Vol. 22, pp 30-33.
34. Martin, F.D. Mechanical Degradation of Polyacrylamide Solutions in Core Plugs From Several Carbonate Reservoirs. *SPE Formation Evaluation* **1986**, *1*, 139-150, doi: https://doi.org/10.2118/12651-PA.
35. Morris, C.W.; Jackson, K.M. Mechanical Degradation of Poly-Acrylamide Solutions in Porous Media. In Proceedings of SPE Symposium on Improved Methods of Oil Recovery, Tulsa, Oklahoma, USA, 16-17 April 1978, SPE-7064-MS, doi: https://doi.org/10.2118/7064-MS.
36. Odell, J.A.; Muller, A.J.; Keller, A. Non-Newtonian Behavior of Hydrolyzed Polyacrylamide in Strong Elongational Flows - a Transient Network Approach. *Polymer* **1988**, *29*, 1179-1190, doi: https://doi.org/10.1016/0032-3861(88)90042-0.
37. Seright, R.S. The Effects of Mechanical Degradation and Viscoelastic Behavoir on Injectivity of Polyacrylamide Solutions. *Society of Petroleum Engineers Journal* **1983**, *23*, 475-485, doi: https://doi.org/10.2118/9297-PA.
38. Juarez-Morejon, J.L.; Bertin, H.; Omari, A.; Hamon, G.; Cottin, C.; Morel, D.; Romero, C.; Bourdarot, G. A New Approach to Polymer Flooding: Impact of the Early Polymer Injection and Wettability on Final Oil Recovery. *SPE Journal* **2019**, *24*, 129 - 139, doi: https://doi.org/10.2118/190817-PA.
39. Gogarty, W.B.; Levy, G.L. Viscoelastic Effects in Polymer Flow Through Porous Media. In Proceedings of 47th Annual Fall Meeting of the Society of Petroleum Engineers of AIME, San Antonio, Texas, 8-11 October 1972, SPE-4025-MS, doi: https://doi.org/10.2118/4025-MS.
40. Han, X.; Wang, W.; Xu, Y. The Viscoelastic Behavior of HPAM Solutions in Porous Media and It's Effects on Displacement Efficiency. In Proceedings of International Meeting on Petroleum Engineering, Beijing, China, 14-17 November 1995, SPE-30013-MS, doi: https://doi.org/10.2118/30013-MS.

41. Sorbie, K.S.; Roberts, L.J. A Model for Calculating Polymer Injectivity Including the Effects of Shear Degradation. In Proceedings of SPE Enhanced Oil Recovery Symposium, Tulsa, Oklahoma, 15-18 April 1984, SPE-12654-MS, doi: https://doi.org/10.2118/12654-MS.
42. Heemskerk, J.; Rosmalen, R.; Janssen-van, R.; Holtslag, R.J.; Teeuw, D. Quantification of Viscoelastic Effects of Polyacrylamide Solutions. In Proceedings of SPE Enhanced Oil Recovery Symposium, Tulsa, Oklahoma, 15-18 April 1984, SPE-12652-MS, doi: https://doi.org/10.2118/12652-MS.
43. Scott, A.J.; Romero-Zerón, L.; Penlidis, A. Evaluation of Polymeric Materials for Chemical Enhanced Oil Recovery. *Processes* **2020**, *8*, doi: https://doi.org/10.3390/pr8030361.
44. Sheng, J. *Modern Chemical Enhanced Oil Recovery: Theory and Practice*; Gulf Professional Pub.: USA, 2010.
45. Thomas, A. *Essentials of Polymer Flooding Technique*; John Wiley & Sons: 2019.
46. Saleh, L.; Wei, M.; Zhang, Y.; Bai, B. Data Analysis for Polymer Flooding That Is Based on a Comprehensive Database. *SPE Reservoir Evaluation & Engineering* **2017**, *20*, 876 - 893, doi: https://doi.org/10.2118/169093-PA.
47. Manrique, E.; Ahmadi, M.; Samani, S. Historical and recent observations in polymer floods: an update review. *C.T.F Cienc. Tecnol. Futuro* **2017**, *6*, 17-48, doi: https://doi.org/10.29047/01225383.72.
48. Yegin, C.; Jia, B.; Zhang, M.; Suhag, A.; Ranjith, R.; Balaji, K.; Peksaglam, Z.; Thanon, D.; Putra, D.; Wijaya, Z., et al. Next-Generation Supramolecular Assemblies as Displacement Fluids in EOR. In Proceedings of SPE Europec featured at 79th EAGE Conference and Exhibition Paris, France, 12–15 June 2017, SPE-185789-MS, doi: https://doi.org/10.2118/185789-MS.
49. Poulsen, A.; Shook, G.M.; Jackson, A.; Ruby, N.; Charvin, K.; Dwarakanath, V.; Thach, S.; Ellis, M. Results of the UK Captain Field Interwell EOR Pilot. In Proceedings of SPE Improved Oil Recovery Conference Tulsa, Oklahoma, USA, 14-18 April 2018, SPE-190175-MS, doi: https://doi.org/10.2118/190175-MS.
50. Delamaide, E. Comparison of Steam and Polymer Injection for the Recovery of Heavy Oil. In Proceedings of SPE Western Regional Meeting, Bakersfield, California, USA, 23-27 April 2017, SPE-185728-MS, doi: https://doi.org/10.2118/185728-MS.
51. Azad, M.S.; Trivedi, J.J. Quantification of the Viscoelastic Effects During Polymer Flooding: A Critical Review. *SPE Journal* **2019**, *24*, doi: https://doi.org/10.2118/195687-PA.
52. Needham, R.B.; Doe, P.H. Polymer Flooding Review. *Journal of Petroleum Technology* **1987**, *39*, 1503-1507, doi: https://doi.org/10.2118/17140-PA.
53. Chang, H.L. Polymer Flooding Technology Yesterday, Today, and Tomorrow. *Journal of Petroleum Technology* **1978**, *30*, 1113-1128, doi: https://doi.org/10.2118/7043-PA.
54. Skauge, A.; Shaker Shiran, B.; Ormehaug, P.A.; Carreras, E.S.; Klimenko, A.; Levitt, D. X-Ray CT Investigation of Displacement Mechanisms for Heavy Oil Recovery by Low Concentration HPAM Polymers. In Proceedings of SPE Improved Oil Recovery Conference, Tulsa, Oklahoma, USA, 31 August - 4 September 2020, SPE-200461-MS, doi: https://doi.org/10.2118/200461-MS.
55. Shi, L.; Zhu, S.; Guo, Z.; Zhao, W.; Xue, X.; Wang, X.; Ye, Z. Experimental Study on the Effect of Polymer Injection Timing on Oil Displacement in Porous Media. *Processes* **2020**, *8*, 93, doi: https://doi.org/10.3390/pr8010093.
56. Jin, J.; Qi, P.; Mohanty, K.; Balhoff, M. Experimental Investigation of the Effect of Polymer Viscoelasticity on Residual Saturation of Low Viscosity Oils. In Proceedings of PE Improved Oil Recovery Conference, Tulsa, OK, USA, 31 August – 4 September 2020, SPE-200414-MS, doi: https://doi.org/10.2118/200414-MS.
57. Azad, M.S.; Trivedi, J.J. Extensional Effects during Viscoelastic Polymer Flooding: Understanding Unresolved Challenges. *SPE Journal* **2020**, doi: https://doi.org/10.2118/201112-PA.
58. Azad, M.S.; Trivedi, J.J. Does Polymer's Viscoelasticity Influence Heavy-Oil Sweep Efficiency and Injectivity at 1 ft/D? *SPE Reservoir Evaluation & Engineering* **2020**, *23*, doi: https://doi.org/10.2118/193771-PA.

59. Seright, R.S. How Much Polymer Should Be Injected During a Polymer Flood? *SPE Journal* **2017**, *22*, 1 - 18, doi: https://doi.org/10.2118/179543-PA.
60. Habermann, B. The Efficiency of Miscible Displacement As A Function of Mobility Ratio. *Transactions of the AIME* **1960**, *219*, doi: https://doi.org/10.2118/1540-G.
61. Wever, D.A.Z.; Picchionia, F.; Broekhuisa, A.A. Polymers for enhanced oil recovery: A paradigm for structure–property relationship in aqueous solution. *Progress in Polymer Science* **2011**, *36*, 1558– 1628, doi: https://doi.org/10.1016/j.progpolymsci.2011.05.006.
62. Standnes, D.C.; Skjevrak, I. Literature review of implemented polymer field projects. *Journal of Petroleum Science and Engineering* **2014**, *122*, 761-775, doi: https://doi.org/10.1016/j.petrol.2014.08.024.
63. Flavien, G.; Christophe, R.; Lionel, L.; Antoine, T. Offshore Polymer EOR Injection Philosophies, Constrains and Solutions. In Proceedings of SPE Improved Oil Recovery Conference, Tulsa, Oklahoma, USA, 31 August - 4 September 2020, SPE-200368-MS, doi: https://doi.org/10.2118/200368-MS
64. Delamaide, E.; Moreau, P.; Tabary, R. A New Approach for Offshore Chemical Enhanced Oil Recovery. In Proceedings of Offshore Technology Conference Houston, Texas, USA, 4–7 May 2015, OTC-25919-MS, doi: https://doi.org/10.4043/25919-MS.
65. Morel, D.; Vert, M.; Jouenne, S.; Nahas, E. Polymer Injection in Deep Offshore Field: The Dalia Angola Case. In Proceedings of SPE Annual Technical Conference and Exhibition, Denver, Colorado, USA, 21–24 September 2008, SPE-116672-MS, doi: https://doi.org/10.2118/116672-MS.
66. Ferreira, V.; Moreno, R. Workflow for Oil Recovery Design by Polymer Flooding. In Proceedings of ASME 2018 37th International Conference on Ocean, Offshore and Arctic Engineering, Madrid, Spain, June 17-22, 2018 2018, OMAE2018-78359, doi: https://doi.org/10.1115/OMAE2018-78359.
67. Sheng, J.J.; Leonhardt, B.; Azri, N. Status of Polymer-Flooding Technology. *J Can Petrol Technol* **2015**, *54*, 116-126, doi: https://doi.org/10.2118/174541-PA.
68. Delamaide, E. Exploring the Upper Limit of Oil Viscosity for Polymer Flood in Heavy Oil. In Proceedings of SPE Improved Oil Recovery Conference, Tulsa, Oklahoma, USA, 14-18 April 2018, SPE-190180-MS, doi: https://doi.org/10.2118/190180-MS.
69. Masalmeh, S.; AlSumaiti, A.; Gaillard, N.; Daguerre, F.; Skauge, T.; Skuage, A. Extending Polymer Flooding Towards High-Temperature and High-Salinity Carbonate Reservoirs. In Proceedings of Abu Dhabi International Petroleum Exhibition & Conference Abu Dhabi, UAE, 11-14 November 2019, SPE-197647-MS, doi: https://doi.org/10.2118/197647-MS.
70. Zaitoun, A.; Makakou, P.; Blin, N.; Al-Maamari, R.S.; Al-Hashmi, A.R.; Abdel-Goad, M.; Al-Sharji, H.H. Shear Stability of EOR Polymers. *Spe Journal* **2012**, *17*, 335-339, doi: https://doi.org/10.2118/141113-Pa.
71. De Vicente, J. *RHEOLOGY*; InTech: Rijeka, Croatia, 2012.
72. Osswald, T.A.; Rudolph, N. *Polymer Rheology: Fundamentals and Applications*; Carl Hanser Verlag GmbH & Company KG: USA, 2014.
73. Bird, R.B.; Stewart, W.E.; Lightfoot, E.N. *Transport Phenomena*; John Wiley & Sons, Inc.: USA, 2002.
74. Grigorescu, G.; Kulicke, W.-M. Prediction of Viscoelastic Properteis and Shear Stability of Polymers in Solution. In *Advances in Polymer Science*, Springer-Verlag Berlin Heidelberg: Berlin, 2000; Vol. 152.
75. Deshpande, A.P.; Krishnan, J.M.; Kumar, S. *Rheology of Complex Fluids*; Springer: 2010.
76. Sochi, T. Flow of Non-Newtonian Fluids in Porous Media. *Journal of Polymer Science Part B-Polymer Physics* **2010**, *48*, 2437-2467, doi: https://doi.org/10.1002/polb.22144.
77. Polymer Properties Database. Availabe online: http://polymerdatabase.com/polymer%20physics/Viscosity2.html (accessed on 6/6/2018).
78. Gao, C. Empirical correlations for viscosity of partially hydrolyzed Polyacrylamide. *Journal of Petroleum Exploration and Production Technology* **2013**, *4*, 209–213, doi: https://doi.org/10.1007/s13202-013-0064-z.
79. Hashmet, M.R.; Onur, M.; Tan, I.M. Empirical Correlations for Viscosity of Polyacrylamide Solutions with the Effects of Concentration, Molecular Weight and Degree of Hydrolysis of

Polymer. *Journal of Applied Sciences* **2014**, *14*, 1000-1007, doi: https://doi.org/10.3923/jas.2014.1000.1007.
80. Hashmet, M.R.; Onur, M.; Tan, I.M. Empirical Correlations for Viscosity of Polyacrylamide Solutions with the Effects of Salinity and Hardness. *Journal of Dispersion Science and Technology* **2014**, *35*, 510-517, doi: https://doi.org/10.1080/01932691.2013.797908.
81. Chauveteau, G. Fundamental Criteria in Polymer Flow Through Porous Media And Their Importance in the Performance Differences of Mobility-Control Buffers. In *Water-Soluble Polymers*, Advances in Chemistry: 1986; Vol. 213, pp. 227-267.
82. He, X.; Xue, F.; Chen, Q.; Huang, G.; Zhang, R. Macromolecular motions and hydrodynamic radius variation in dilute solutions under shear action. *Polym. Int.* **2015**, *64*, 766-772, doi: https://doi.org/10.1002/pi.4850.
83. Tapias, F.A.; Lizcano, J.C.; Lopes, R.B. Effects of salts and temperature on rheological and viscoelastic behavior of low molecular weight HPAM solutions. *Revista Fuentes: El reventón energético* **2018**, *16*, 19-35, doi: https://doi.org/10.18273/revfue.v16n1-2018002.
84. Thomas, A.; Gaillard, N.; Favero, C. Some Key Features to Consider When Studying Acrylamide-Based Polymers for Chemical Enhanced Oil Recovery. *Oil Gas Sci. Technol.* **2013**, *67*, 887-902, doi: https://doi.org/10.2516/ogst2012065.
85. Noïk, C.; Delaplace, P.; Muller, G. Physico-Chemical Characteristics of Polyacrylamide Solutions after Mechanical Degradation through a Porous Medium. In Proceedings of SPE International Symposium on Oilfield Chemistry, San Antonio, Texas, 14-17 February 1995, SPE-28954-MS, doi: https://doi.org/10.2118/28954-MS.
86. Jolma, I.W.; Strand, D.; Stavland, A.; Fjelde, I.; Hatzignatiou, D. When Size Matters - Polymer Injectivity in Chalk Matrix. In Proceedings of 9th European Symposium on Improved Oil Recovery, Stavanger, Norway, 24-27 April 2017, doi: https://doi.org/10.3997/2214-4609.201700362
87. Yiqiang, L.; Junxin, G.; Dandan, Y.; Junjian, L.; Hualong, L. Study on the Matching Relationship between Polymer Hydrodynamic Characteristic Size and Pore Throat Radius of Target Block S Based on the Microporous Membrane Filtration Method. *Journal of Chemistry* **2014**, doi: https://doi.org/10.1155/2014/569126.
88. Ferguson, J.; Walters, K.; Wolff, C. Shear and extensional flow of polyacrylamide solutions. *Rheol. Acta* **1990**, *29*, 571-579, doi: https://doi.org/10.1007/BF01329303.
89. Teraoka, I. *Polymer Solutions: An Introduction to Physical Properties*; John Wiley & Sons, Inc.: Brooklyn, New York, 2002.
90. Graessley, W.W. Polymer chain dimensions and the dependence of viscoelastic properties on concentration, molecular weight and solvent power. *POLYMER* **1980**, *21*, doi: https://doi.org/10.1016/0032-3861(80)90266-9.
91. Cai, S.; Zhao, H.; Li, T.; He, X.; Wang, X.; Rodriguesc, A.M.; Zhang, R. Influence of molecular interplay on the HPAM/UR rheological properties in an aqueous solution. *RSC Advances* **2017**, *7*, 37055–37064, doi: https://doi.org/10.1039/c7ra05263d.
92. Ryles, R.G. Chemical Stability Limits of Water-Soluble Polymers Used in Oil Recovery Processes. *SPE Reserv. Eng.* **1988**, *3*, 23-34, doi: https://doi.org/10.2118/13585-PA.
93. Akbari, S.; Mahmood, S.M.; Tan, I.M.; Ghaedi, H.; Ling, O.L. Assessment of Polyacrylamide Based Co-Polymers Enhanced by Functional Group Modifications with Regards to Salinity and Hardness. *polymers* **2017**, *9*, doi: https://doi.org/10.3390/polym9120647.
94. Seright, R.S.; Campbell, A.R.; Mozley, P.S. Stability of Partially Hydrolyzed Polyacrylamides at Elevated Temperatures in the Absence of Divalent Cations. *SPE Journal* **2010**, *15*, doi: https://doi.org/10.2118/121460-PA.
95. Raffa, P.; Druetta, P. *Chemical Enhanced Oil Recovery: Advances in Polymer Flooding and Nanotechnology*; Walter de Gruyter GmbH & Co KG: 2019; pp. 185.
96. Lewandowska, K. Comparative studies of rheological properties of polyacrylamide and partially hydrolyzed polyacrylamide solutions. *Journal of Applied Polymer Science* **2007**, *103*, 2235-2241, doi: https://doi.org/10.1002/app.25247.

97. Spildo, K.; Sæ, E.I.Ø. Effect of Charge Distribution on the Viscosity and Viscoelastic Properties of Partially Hydrolyzed Polyacrylamide. *Energy & Fuels* **2015**, *29*, 5609–5617, doi: https://doi.org/10.1021/acs.energyfuels.5b01066.
98. Ma, Q.; Shuler, P.J.; Aften, C.W.; Tang, Y. Theoretical studies of hydrolysis and stability of polyacrylamide polymers. *Polymer Degradation and Stability* **2015**, *121*, 69-77, doi: https://doi.org/10.1016/j.polymdegradstab.2015.08.012.
99. Choi, S.K.; Sharma, M.M.; Bryant, S.; Huh, C. pH-Sensitive Polymers for Novel Conformance-Control and Polymer-Flood Applications. *SPE Reservoir Evaluation & Engineering* **2010**, *13*, 926-939, doi: https://doi.org/10.2118/121686-PA.
100. Dang, T.Q.C.; Chen, Z.; Nguyen, T.B.N.; Bae, W. Rheological Modeling and Numerical Simulation of HPAM Polymer Viscosity in Porous Media. *Energy Sources, Part A: Recovery, Utilization, and Environmental Effects* **2015**, *37*, 2189-2197, doi: https://doi.org/10.1080/15567036.2011.624156.
101. Liang, K.; Han, P.; Chen, Q.; Su, X.; Feng, Y. Comparative Study on Enhancing Oil Recovery under High Temperature and High Salinity: Polysaccharides Versus Synthetic Polymer. *ACS Omega* **2019**, *4*, 10620-10628, doi: https://doi.org/10.1021/acsomega.9b00717.
102. Wu, G.; Yu, L.; Jiang, X. Synthesis and properties of an acrylamide- based polymer for enhanced oil recovery: A preliminary study. *Advances in Polymer Technology* **2018**, doi: https://doi.org/10.1002/adv.21949.
103. Dullien, F. *Porous Media Fluid Transport and Pore Structure*; Elsevier Science: 2012.
104. Broseta, D.; Medjahed, F.; Lecourtier, J.; Robin, M. Polymer Adsorption/Retention in Porous Media: Effects of Core Wettability and Residual Oil. *SPE Advanced Technology Series* **1995**, *3*, doi: https://doi.org/10.2118/24149-PA.
105. Muhammed, F.; Dean, E.; Pitts, M.; Wyatt, K.; Kozlowicz, B.; Khambete, M.; Jensen, T.; Sumner, E.; Ray, C. Scleroglucan Polymer Injectivity Test Results in the Adena Oilfield. In Proceedings of SPE Improved Oil Recovery Conference, Tulsa, OK, USA, 18 – 22 April 2020, SPE-200309-MS, doi: https://doi.org/10.2118/200309-MS.
106. Skauge, T.; Kvilhaug, O.A.; Skauge, A. Influence of Polymer Structural conformation and Phase Behavoir on In-Situ Viscosity. In Proceedings of IOR 2015 – 18th European Symposium on Improved Oil Recovery, Dresden, Germany, 14-16 April 2015, Th B04, doi: https://doi.org/10.3997/2214-4609.201412154.
107. Alfazazi, U.; Thomas, N.C.; Alameri, W.; Al-Shalabi, E.W. Experimental investigation of polymer injectivity and retention under harsh carbonate reservoir conditions. *J. Pet. Sci. Eng.* **2020**, *192*, 107262, doi: https://doi.org/10.1016/j.petrol.2020.107262.
108. Hoagland, D.A.; Prud'homme, R.K. Hydrodynamic Chromatography as a Probe of Polymer Dynamics during Flow through Porous Media. *Macromolecules* **1989**, *22*, 775-781, doi: https://doi.org/10.1021/ma00192a044.
109. Stavland, A.; Jonsbraten, H.; Lohne, A.; Moen, A.; Giske, N.H. Polymer Flooding - Flow Properties in Porous Media versus Rheological Parameters. In Proceedings of SPE EUROPEC/EAGE Annual Conference and Exhibition, Barcelona, Spain, 14-17 June 2010, SPE-131103-MS, doi: https://doi.org/10.2118/131103-MS.
110. Azad, M.S.; Trivedi, J.J. Novel viscoelastic model for predicting the synthetic polymer's viscoelastic behavior in porous media using direct extensional rheological measurements. *Fuel* **2019**, *235*, 218-226, doi: https://doi.org/10.1016/j.fuel.2018.06.030.
111. Elhossary, D.A.; Alameri, W.; Al-Shalabi, E.W. Experimental Investigation of Biopolymer Rheology and Injectivity in Carbonates. In Proceedings of Offshore Technology Conference, Houston, Texas, USA, 4-7 May 2020, OTC-30680-MS, doi: https://doi.org/10.4043/30680-MS.
112. Clarke, A.; Howe, A.M.; Mitchell, J.; Staniland, J.; Hawkes, L.A. How Viscoelastic Polymer Flooding Enhances Displacement Efficiency. *SPE Journal* **2016**, *21*, 675 - 687, doi: https://doi.org/10.2118/174654-PA.
113. Teeuw, D.; Hesselink, F.T. Power-Law Flow And Hydrodynamic Behaviour Of Biopolymer Solutions In Porous Media. In Proceedings of SPE Oilfield and Geothermal Chemistry

Symposium, Stanford, California, 28-30 May 1980, SPE-8982-MS, doi: https://doi.org/10.2118/8982-MS.
114. Vik, B.; Kedir, A.; Kippe, V.; Sandengen, K.; Skauge, T.; Solbakken, J.; Zhu, D. Viscous Oil Recovery by Polymer Injection; Impact of In-Situ Polymer Rheology on Water Front Stabilization. In Proceedings of SPE Europec featured at 80th EAGE Conference and Exhibition, Copenhagen, Denmark, 11-14 June 2018, SPE-190866-MS, doi: https://doi.org/10.2118/190866-MS.
115. Fletcher, A.J.P.; Flew, S.R.G.; Lamb, S.P.; Lund, T.; Bjornestad, E. Measurements of Polysaccharide Polymer Properties in Porous Media. In Proceedings of SPE International Symposium on Oilfield Chemistry, California, 20-22 February 1991, SPE-21018-MS, doi: https://doi.org/10.2118/21018-MS.
116. Seright, R.S.; Seheult, M.; Talashek, T. Injectivity Characteristics of EOR Polymers. *SPE Reservoir Evaluation & Engineering* **2009**, *12*, 783-792, doi: https://doi.org/10.2118/115142-PA.
117. Nguyen, T.Q.; Kausch, H.-H. *Flexible Polymer Chains in Elongational Flow: Theory and Experiment* 1999.
118. De Gennes, P.G. Coil-stretch transition of dilute flexible polymers under ultrahigh velocity gradients. *The Journal of Chemical Physics* **1974**, *60*, 5030, doi: https://doi.org/10.1063/1.1681018.
119. Chauveteau, G. Molecular Interperation of Several Different Properties of Flow of Coiled Polymer Solutions Through Porous Media in Oil Recovery Conditions. In Proceedings of SPE Annual Technical Conference and Exhibition, San Antonio, Texas, USA, 4-7 October 1981, SPE-10060-MS, doi: https://doi.org/10.2118/10060-MS.
120. Haas, R.; Durst, F. Viscoelastic flow of dilute polymer solutions in regularly packed beds. *Rheologica Acta* **1982**, *21*, 566-571, doi: https://doi.org/10.1007/978-3-662-12809-1_57.
121. Moan, M.; Magueur, A. Transient extensional viscosity of dilute flexible polymer solutions. *Journal of Non-Newtonian Fluid Mechanics* **1988**, *30*, 343-354, doi: https://doi.org/10.1016/0377-0257(88)85033-X.
122. Kulicke, W.M.; Haas, R. Flow behavior of dilute polyacrylamide solutions through porous media. 1. Influence of chain length, concentration, and thermodynamic quality of the solvent. *Ind. Eng. Chem.* **1984**, *23*, 308–315, doi: https://doi.org/10.1021/i100015a008.
123. Al Hashmi, A.R.; Al Maamari, R.S.; Al Shabib, I.S.; Masnsoor, A.M.; Zaitoun, A.; Al Sharji, H.H. Rheology and mechanical degradation of high-molecular-weight partially hydrolzed polyacrylamide during flow through capillaries. *Journal of Petroleum Scinece and Engineering* **2013**, *105*, 100-106, doi: https://doi.org/10.1016/j.petrol.2013.03.021.
124. Mansour, A.M.; Al-Maarnari, R.S.; Al-Hashmi, A.S.; Zaitoun, A.; Al-Sharji, H. In-situ rheology and mechanical degradation of EOR polyacrylamide solutions under moderate shear rates. *Journal of Petroleum Science and Engineering* **2014**, *115*, 57-65, doi: https://doi.org/10.1016/j.petrol.2014.02.009.
125. Chauveteau, G.; Moan, M.; Magueur, A. Thickening behaviour of dilute polymer solutions in non-inertial elongational flows. *Journal of Non-Newtonian Fluid Mechanics* **1984**, *16*, 315-327, doi: https://doi.org/10.1016/0377-0257(84)85017-X.
126. Rodriguez, S.; Romero, C.; Sargenti, M.L.; Muller, A.J.; Saez, A.E.; Odell, J.A. Flow of Polymer-Solutions through Porous-Media. *Journal of Non-Newtonian Fluid Mechanics* **1993**, *49*, 63-85, doi: https://doi.org/Doi 10.1016/0377-0257(93)85023-4.
127. Martins Afonso, M.; Vincenzi, D. Nonlinear elastic polymers in random flow. *J. Fluid Mech.* **2005**, *540*, 99-108, doi: https://doi.org/10.1017/S0022112005005951.
128. Muller, A.J.; Odell, J.A.; Carrington, S. Degradation of Semidilute Polymer-Solutions in Elongational Flows. *Polymer* **1992**, *33*, 2598-2604, doi: https://doi.org/10.1016/0032-3861(92)91143-P.
129. Galindo-Rosales, F.J.; Campo-Deaño, L.; Pinho, F.T.; van Bokhorst, E.; Hamersma, P.J.; Oliveira, M.S.N.; Alves, M.A. Microfluidic systems for the analysis of viscoelastic fluid flow phenomena in porous media. *Microfluid Nanofluid* **2012**, *12*, 485–498, doi: https://doi.org/10.1007/s10404-011-0890-6.

130. Delshad, M.; Kim, D.H.; Magbagbeola, O.A.; Huh, C.; Pope, G.A.; Tarahhom, F. Mechanistic Interpretation and Utilization of Viscoelastic Behavior of Polymer Solutions for Improved Polymer-Flood Efficiency. In Proceedings of SPE Symposium on Improved Oil Recovery, Tulsa, Oklahoma, USA, 20-23 April 2008, SPE-113620-MS, doi: https://doi.org/10.2118/113620-MS.
131. Masuda, Y.; Tang, K.-C.; Miyazawa, M.; Tanaka, S. 1D Simulation of Polymer Flooding Including the Viscoelastic Effect of Polymer Solution. *SPE Reservoir Engineering.* **1992**, *7*, 247 - 252, doi: https://doi.org/10.2118/19499-PA.
132. Hirasaki, G.J.; Pope, G.A. Analysis of Factors Influencing Mobility and Adsorption in the Flow of Polymer Solution Through Porous Media. *Society of Petroleum Engineers Journal* **1974**, *14*, 337-346, doi: https://doi.org/10.2118/4026-PA.
133. Lotfollahi, M.; Farajzadeh, R.; Delshad, M.; Al-Abri, A.; Wassing, B.M.; Al-Mjeni, R.; Awan, K.; Bedrikovetsky, P. Mechanistic Simulation of Polymer Injectivity in Field Tests. *SPE Journal* **2016**, doi: https://doi.org/10.2118/174665-PA.
134. Hatzignatiou, D.; Moradi, H.; Stavland, A. Polymer flow through water- and oil-wet porous media. *Journal of Hydrodynamics* **2015**, *27*, 748-762, doi: https://doi.org/10.1016/S1001-6058(15)60537-6.
135. Skauge, T.; Kvilhaug, O.A.; Skauge, A. *Pore-scale phenomena in polymer frontal displacement*; UP 003/2012; 2012; p 72.
136. Manichand, R.N.; Seright, R.S. Field vs. Laboratory Polymer-Retention Values for a Polymer Flood in the Tambaredjo Field. *SPE Reservoir Evaluation & Engineering* **2014**, *17*, 314 - 325, doi: https://doi.org/10.2118/169027-PA.
137. Zaitoun, A.; Kohler, N. Two-Phase Flow Through Porous Media: Effect of an Adsorbed Polymer Layer. In Proceedings of SPE Annual Technical Conference and Exhibition, Houston, Texas, 2-5 October 1988, SPE-18085-MS, doi: https://doi.org/10.2118/18085-MS.
138. Al-Hajri, S.; Mahmood, S.M.; Abdulelah, H.; Akbari, S. An Overview on Polymer Retention in Porous Media. *energies* **2018**, *11*, doi: https://doi.org/10.3390/en11102751.
139. Liu, Y.; Wu, X.; Zhai, X.; Shi, G.; Ye, Y.; Li, S.; Xiao, P. The research status and summary of adsorption and retention mechanism of polymer. In Proceedings of IOP Conf. Series: Materials Science and Engineering, Hangzhou, China, 18-20 April 2020, doi: https://doi.org/10.1088/1757-899X/892/1/012023.
140. Kamal, M.S.; Sultan, A.S.; Al-Mubaiyedh, U.A.; Hussein, I.A. Review on Polymer Flooding: Rheology, Adsorption, Stability, and Field Applications of Various Polymer Systems. *Polymer Reviews* **2015**, *55*, 491-530, doi: https://doi.org/10.1080/15583724.2014.982821.
141. Hashmet, M.R.; AlSumaiti, A.M.; Qaiser, Y.; AlAmeri, W.S. Laboratory Investigation and Simulation Modeling of Polymer Flooding in High-Temperature, High-Salinity Carbonate Reservoirs. *Energy & Fuels* **2017**, *31*, 13454−13465, doi: https://doi.org/10.1021/acs.energyfuels.7b02704.
142. Ferreira, V.H.S.; Moreno, R.B.Z.L. Polyacrylamide Adsorption and Readsorption in Sandstone Porous Media. *SPE Journal* **2020**, *25*, doi: https://doi.org/10.2118/199352-PA.
143. Sugar, A.; Serag, M.F.; Torrealba, V.A.; Buttner, U.; Habuchi, S.; Hoteit, H. Visualization of Polymer Retention Mechanisms in Porous Media Using Microfluidics. In Proceedings of SPE Europec featured at 82nd EAGE Conference and Exhibition, Amsterdam, The Netherlands, 8-11 December 2020, SPE-200557-MS, doi: https://doi.org/10.2118/200557-MS.
144. Wang, D.; Li, C.; Seright, R.S. Laboratory Evaluation of Polymer Retention in a Heavy Oil Sand for a Polymer Flooding Application on Alaska's North Slope. *SPE Journal* **2020**, doi: https://doi.org/10.2118/200428-PA.
145. Akbari, S.; Mahmood, S.M.; Nasr, N.H.; Al-Hajri, S.; Sabet, M. A critical review of concept and methods related to accessible pore volume during polymer-enhanced oil recovery. *J. Pet. Sci. Eng.* **2019**, *182*, doi: https://doi.org/10.1016/j.petrol.2019.106263.
146. Zhang, G.; Seright, R.S. Hydrodynamic Retention and Rheology of EOR Polymers in Porous Media. In Proceedings of SPE International Symposium on Oilfield Chemistry, Woodlands, Texas , USA, 13-15 April 2015, SPE-173728-MS, doi: https://doi.org/10.2118/173728-MS.

147. Seright, R.S.; Skjevrak, I. Effect of Dissolved Iron and Oxygen on Stability of Hydrolyzed Polyacrylamide Polymers. *SPE Journal* **2015**, *20*, doi: https://doi.org/10.2118/169030-PA.
148. Chen, R.; Qi, M.; Zhang, G.; Yi , C. Comparative experiments on polymer degradation technique of produced water of polymer flooding oilfield. In Proceedings of IOP Conf. Series: Earth and Environmental Science, 2018, doi: https://doi.org/10.1088/1755-1315/113/1/012208.
149. Xiong, B.; Loss, R.D.; Shields, D.; Pawlik, T.; Hochreiter, R.; Zydney, A.L.; Kumar, M. Polyacrylamide degradation and its implications in environmental systems. *NPJ Clean Water* **2018**, doi: https://doi.org/10.1038/s41545-018-0016-8.
150. Opsahl, E.; Kommedal, R.K. Literature Review: Environmental Considerations in Polymer Flooding with Synthetic Polymers on the Norwegian Continental Shelf. In Proceedings of IOR 2017 - 19th European Symposium on Improved Oil Recovery, Apr 2017 2017, doi: https://doi.org/10.3997/2214-4609.201700478.
151. Shuler, P.J.; Kuehne, D.L.; Uhl, J.T.; Walkup Jr., G.W. Improving Polymer lnjectivity at West Coyote Field, California. *SPE Reservoir Engineering.* **1987**, *2*, 271 - 280, doi: https://doi.org/10.2118/13603-PA.
152. Torrealba, V.A.; Hoteit, H. Improved polymer flooding injectivity and displacement by considering compositionally-tuned slugs. *J. Pet. Sci. Eng.* **2019**, *178*, 14-26, doi: https://doi.org/10.1016/j.petrol.2019.03.019.
153. Seright, R.S. Potential for Polymer Flooding Reservoirs With Viscous Oils. *SPE Reservoir Evaluation & Engineering* **2010**, *13*, doi: https://doi.org/10.2118/129899-PA.
154. Zhang, Y.; Wang, J.; Jia, P.; Liu, X.; Zhang, X.; Liu, C.; Bai, X. Viscosity Loss and Hydraulic Pressure Drop on Multilayer Separate Polymer Injection in Concentric Dual-Tubing. *Energies* **2020**, *13*, 1637, doi: https://doi.org/10.3390/en13071637.
155. De Simoni, M.; Boccuni, F.; Sambiase, M.; Spagnuolo, M.; Albertini, M.; Tiani, A.; Masserano, F. Polymer Injectivity Analysis and Subsurface Polymer Behavior Evaluation. In Proceedings of SPE EOR Conference at Oil and Gas West Asia, Muscat, Oman, 26-28 March, 2018 2018, SPE-190383-MS, doi: https://doi.org/10.2118/190383-MS.
156. Dupas, A.; Henaut, I.; Rousseau, D.; Poulian, P.; Tabary, R.; Argillier, J.-F.; Aubry, T. Impact of Polymer Mechanical Degradation on Shear and Extensional Viscosities: Toward Better Injectivity Forecasts in Polymer Flooding Operations. In Proceedings of SPE International Symposium on Oilfield Chemistry, The Woodlands,Texas, USA, 8–10 April 2013, SPE-164083-MS, doi: https://doi.org/10.2118/164083-MS.
157. Zhou, J.; Dong, Y.; Pater, C.J.; Zitha, P.L.J. Experimental Study of the Impact of Shear Dilation and Fracture Behavior during Polymer Injection for Heavy Oil Recovery in Unconsolidated Reservoirs. In Proceedings of Canadian Unconventional Resources & International Petroleum Conference, Calgary, Alberta, Canada., 19–21 October 2010, SPE-137656-MS, doi: https://doi.org/10.2118/137656-MS.
158. Caulfield, M.J.; Qiao, G.G.; Solomon, D.H. Some Aspects of the Properties and Degradation of Polyacrylamides. *Chem. Rev.* **2002**, *102*, 3067–3084, doi: https://doi.org/10.1021/cr010439p.
159. Zampieri, M.F.; Quispe, C.C.; Moreno, R.B.Z.L. Model upsizing for integrated evaluation of polymer degradation and polymer flooding lab data. *Journal of Petroleum Science and Engineering* **2019**, *176*, 735-744, doi: https://doi.org/10.1016/j.petrol.2019.01.047.
160. Shi, L.; Zhu, S.; Ye, Z.; Xue, X.; Liu, C.; Lan, X. Effect of microscopic aggregation behavior on polymer shear resistance. *J. Appl. Polym. Sci.* **2019**, *137*, 48670, doi: https://doi.org/10.1002/app.48670.
161. Ghosh, P.; Zepeda, A.; Bernal, G.; Mohanty, K.K. Transport of Associative Polymers in Low-Permeability Carbonates. *Transp Porous Med* **2020**, *133*, 251–270, doi: https://doi.org/10.1007/s11242-020-01422-z.
162. Åsen, S.M.; Stavland, A.; Strand, D.; Hiorth, A. An Experimental Investigation of Polymer Mechanical Degradation at cm and m Scale. *SPE Journal* **2019**, *24*, 1,700 - 701,713, doi: https://doi.org/10.2118/190225-PA.

163. Dupuis, D.; Lewandowski, F.Y.; Steiert, P.; Wolff, C. Shear thickening and time-dependent phenomena: the case of polyacrylamide solutions. *Journal of Non-Newtonian Fluid Mechanics* **1994**, *54*, 11-32, doi: https://doi.org/10.1016/0377-0257(94)80013-8.
164. Ferreira, V.H.S.; Moreno, R.B.Z.L. Polyacrylamide Mechanical Degradation and Stability in the Presence of Iron. In Proceedings of Offshore Technology Conference, Rio de Janeiro, Brazil, 24-26 October 2017, OTC-27953-MS, doi: https://doi.org/10.4043/27953-MS.
165. Jouenne, S.; Chakibi, H.; Levitt, D. Polymer Stability After Successive Mechanical-Degradation Events. *SPE Journal* **2018**, *23*, 18-33, doi: https://doi.org/10.2118/186103-PA.
166. Müller, A.J.; Patruyo, L.G.; Montano, W.; Roversi-M, D.; Moreno, R.; Ramírez, N.E.; Sáez, A.E. Mechanical Degradation of Polymers in Flows Through Porous Media: Effect of Flow Path Length and Particle Size. *Applied Mechanics Reviews* **1997**, *50*, S149-S155, doi: https://doi.org/10.1115/1.3101827.
167. Rubalcava, D.; Al-Azri, N. Results & Interpretation of a High Viscous Polymer Injection Test in a South Oman Heavy Oil Field. In Proceedings of SPE EOR Conference at Oil and Gas West Asia, Muscat, Oman, 21–23 March 2016, SPE-179814-MS, doi: https://doi.org/10.2118/179814-MS.
168. Al-Maamari, R.S.; Al-Hashmi, A.; Al-Azri, N.; Al-Riyami, O.; Al-Mjeni, R.; Dupuis, G.; Zaitoun, A. Laboratory Support of Heavy-Oil Polymer Flood Project. In Proceedings of SPE EOR Conference at Oil and Gas West Asia, Muscat, Oman 21-23 March 2016, SPE-179823-MS, doi: https://doi.org/10.2118/179823-MS.
169. Jouenne, S. Polymer flooding in high temperature, high salinity conditions: Selection of polymer type and polymer chemistry, thermal stability. *Journal of Petroleum Science and Engineering* **2020**, *195*, 107545, doi: https://doi.org/10.1016/j.petrol.2020.107545.
170. Skauge, T.; Ormehaug, P.A.; AlSumaiti, A.; Masalmeh, S.; Skauge, A. Polymer Stability At Harsh Temperature And Salinity Conditions. In Proceedings of SPE Conference at Oman Petroleum & Energy Show, 13 - 15 September 2021, SPE-200176-MS, doi: https://doi.org/10.2118/200176-MS.
171. Divers, T.; Gaillard, N.; Bataille, S.; A., T.; Favéro, C. Successful Polymer Selection for CEOR: Brine Hardness and Mechanical Degradation Considerations. In Proceedings of SPE Oil and Gas India Conference and Exhibition, Mumbai, India, 4–6 April 2017, SPE-185418-MS, doi: https://doi.org/10.2118/185418-MS.
172. Rashid, B.; Stapley, J.; Clifford, P.; Chappell, D.; Kiani, M.; Andrews, W.J.; Hart, E.C. Successful Field Trial of a Novel, Reservoir-Triggered Polymer: Results, Interpretation and Simulation. In Proceedings of SPE Improved Oil Recovery Conference Tulsa, Oklahoma, USA, 14-18 April 2018, SPE-190159-MS, doi: https://doi.org/10.2118/190159-MS.
173. Glasbergen, G.; Wever, D.; Keijzer, E.; Farajzadeh, R. Injectivity Loss in Polymer Floods: Causes, Preventions and Mitigations. In Proceedings of SPE Kuwait Oil & Gas Show and Conference, Mishref, Kuwait, 11–14 October 2015, SPE-175383-MS, doi: https://doi.org/10.2118/175383-MS.
174. Culter, J.D.; Mayhan, K.G.; Patterson, G.K.; Sarmasti, A.A.; Zakin, J.L. Entrance Effects on Capillary Degradation of Dilute Polystrene Solutions. *Journal of Applied Polymer Science* **1972**, *16*, doi: https://doi.org/10.1002/app.1972.070161227.
175. Puls, C.; Clemens, T.; Sledz, C.; Kadnar, R.; Gumpenberger, T. Mechanical Degradation of Polymers During Injection, Reservoir Propagation and Production - Field Test Results 8 TH Reservoir, Austria. In Proceedings of SPE Europec featured at 78th EAGE, Vienna, Austria, 30 May – 2 June 2016, SPE-180144-MS, doi: https://doi.org/10.2118/180144-MS.
176. Moan, M.; Omari, A. Molecular analysis of the mechanical degradation of polymer solution through a porous medium. *Polymer Degradation and Stability* **1992**, *35*, 277-281, doi: https://doi.org/10.1016/0141-3910(92)90036-5.
177. Yu, J.F.S.; Zakin, J.L.; Patterson, G.K. Mechanical degradation of high molecular weight polymers in dilute solution. *Journal of Applied Polymer Science* **1979**, *23*, 2493-2512, doi: https://doi.org/10.1002/app.1979.070230826.
178. Wei, B.; Romero-Zerón, L.; Rodrigue, D. Mechanical Properties and Flow Behavior of Polymers for Enhanced Oil Recovery. *Journal of Macromolecular Science, Part B: Physics* **2014**, *53*, 625–644, doi: https://doi.org/10.1080/00222348.2013.857546.

179. Lecourtier, J.; Chauveteau, G. Propagation of Polymer Slugs Through Porous Media. In Proceedings of SPE Annual Technical Conference and Exhibition, Houston, Texas, 16-19 September 1984, SPE-13034-MS, doi: https://doi.org/10.2118/13034-MS.
180. Skauge, T.; Skauge, A.; Salmo, I.C.; Ormehaug, P.A.; Al-Azri, N.; Wassing, L.M.; Glasbergen, G.; Van Wunnik, J.N.; Masalmeh, S.K. Radial and Linear Polymer Flow - Influence on Injectivity. In Proceedings of SPE Improved Oil Recovery Conference, Tulsa, Oklahoma, USA., 11–13 April 2016, SPE-179694-MS, doi: https://doi.org/10.2118/179694-MS.
181. Howe, A.M.; Clarke, A.; Giernalczyk, D. Flow of concentrated viscoelastic polymer solutions in porous media: effect of MW and concentration on elastic turbulence onset in various geometries. *Soft Matter* **2015**, *11*, 6419-6431, doi: https://doi.org/10.1039/c5sm01042j.
182. Gramain, P.; Myard, P. Elongational Deformation by Shear Flow of Flexible Polymers Adsorbed in Porous Media. *Macromolecules* **1980**, *14*, 180-184, doi: https://doi.org/10.1021/ma50002a037.
183. Al-Shakry, B.; Shaker Shiran, B.; Skauge, T.; Skauge, A. Polymer Injectivity: Influence of Permeability in the Flow of EOR Polymers in Porous Media. In Proceedings of SPE Europec featured at 81st EAGE Conference and Exhibition London, England, UK, 3-6 June 2019, SPE-195495-MS, doi: https://doi.org/10.2118/195495-MS.
184. Southwick, J.G.; Manke, C.W. Molecular Degradation, Injectivity, and Elastic Properties of Polymer Solutions. *SPE Reserv. Eng.* **1988**, *3*, 1,193 - 191,201, doi: https://doi.org/10.2118/15652-PA.
185. Wever, D.A.Z.; Bartlema, H.; ten Berge, A.B.G.M.; Al-Mjeni, R.; Glasbergen, G. The Effect of the Presence of Oil on Polymer Retention in Porous Media from Clastic Reservoirs in the Sultanate of Oman. In Proceedings of SPE EOR Conference at Oil and Gas West Asia, Muscat, Oman, 26-28 March 2018, SPE-190430-MS, doi: https://doi.org/10.2118/190430-MS.
186. Al-Shakry, B.; Shiran, B.S.; Skauge, T.; Skauge, A. Enhanced Oil Recovery by Polymer Flooding: Optimizing Polymer Injectivity. In Proceedings of SPE Kingdom of Saudi Arabia Annual Technical Symposium and Exhibition, Dammam, Saudi Arabia, 23– 26 April 2018, SPE-192437-MS, doi: https://doi.org/10.2118/192437-MS.
187. Zhu, S.; Shi, L.; Wang, X.; Liu, C.; Xue, X.; Ye, Z. Investigation into mobility control mechanisms by polymer flooding in offshore high-permeable heavy oil reservoir. *Energy Sources, Part A* **2020**, doi: https://doi.org/10.1080/15567036.2020.1797941.
188. Li, K.; Cheng, C.; Liu, C.; Jia, L. Enhanced oil recovery after polymer flooding by wettability alteration to gas wetness using numerical simulation. *Oil & Gas Science and Technology - Rev. IFP Energies nouvelles* **2018**, *73*, doi: https://doi.org/10.2516/ogst/2018029.
189. Shahin, G.T.; Thigpen, D.R. Injecting Polyacrylamide Into Gulf Coast Sands: The White Castle Q Sand Polymer-Injectivity Test. *SPE Reservoir Engineering.* **1996**, *11*, doi: https://doi.org/10.2118/24119-PA.
190. Ferreira, V.H.d.S. Key parameters on the flow of polymer solutions through porous medium : experimental and modeling studies. Universidade Estadual de Campinas, 2019.
191. Garrepally, S.; Jouenne, S.; Leuqeux, F.; Olmsted, P.D. Polymer Flooding - Towards a Better Control of Polymer Mechanical Degradation at the Near Wellbore. In Proceedings of SPE Improved Oil Recovery Conference, Tulsa, Oklahoma, USA, 31 August - 4 September 2020, SPE-200373-MS, doi: https://doi.org/10.2118/200373-MS.
192. Xiong, B.; Purswani, P.; Pawlik, T.; Samineni, L.; Karpyn, Z.T.; Zydney, A.L.; Kumar, M. Mechanical degradation of polyacrylamide at ultra high deformation rates during hydraulic fracturing. *Environ. Sci.: Water Res.* **2020**, *6*, 166–172, doi: https://doi.org/10.1039/c9ew00530g.

Publications

Paper-I:

Impact of Mechanical Degradation on Polymer Injectivity in Porous Media

polymers

MDPI

Article

Impact of Mechanical Degradation on Polymer Injectivity in Porous Media

Badar Al-Shakry [1,2,*], Tormod Skauge [3,†], Behruz Shaker Shiran [2] and Arne Skauge [1,3,†]

1 Department of Chemistry, University of Bergen, Allegaten 41, Bergen 5007, Norway; Arne.Skauge@uib.no
2 Uni Research CIPR, Allegaten 41, Bergen 5007, Norway; Behruz.Shaker@uni.no
3 Energy Research Norway, Allegaten 41, Bergen 5007, Norway; Tormod.Skauge@energyresearch.no
* Correspondence: Badar.Al-Shakry@uni.no; Tel.: +47-5558-3672
† These authors contributed equally to this work.

Received: 21 May 2018; Accepted: 3 July 2018; Published: 5 July 2018

Abstract: Polymer flooding is an established enhanced oil recovery (EOR) method; still, many aspects of polymer flooding are not well understood. This study investigates the influence of mechanical degradation on flow properties of polymers in porous media. Mechanical degradation due to high shear forces may occur in the injection well and at the entrance to the porous media. The polymers that give high viscosity yields at a sustainable economic cost are typically large, MW > 10 MDa, and have wide molecular weight distributions. Both MW and the distributions are altered by mechanical degradation, leading to changes in the flow rheology of the polymer. The polymer solutions were subjected to different degrees of pre-shearing and pre-filtering before injected into Bentheimer outcrop sandstone cores. Rheology studies of injected and produced polymer solutions were performed and interpreted together with in situ rheology data. The core floods showed a predominant shear thickening behavior at high flow velocities, which is due to successive contraction/expansion flow in pores. When pre-sheared, shear thickening was reduced but with no significant reduction in in situ viscosity at lower flow rates. This may be explained by reduction in the extensional viscosity. Furthermore, the results show that successive degradation occurred which suggests that the assumption of the highest point of shear that determines mechanical degradation in a porous media does not hold for all field relevant conditions.

Keywords: HPAM polymer; rheology; viscosity; injectivity; mechanical degradation; polymer flooding

1. Introduction

Among several processes which are applied to increase oil recovery, polymer flooding has been widely implemented as a mobility control technique in tertiary enhanced oil recovery (EOR) [1]. The most basic method of recovering oil from a reservoir is by pressure depletion [2]. The pressure difference between the oil reservoir and the surface will lead to production of oil until the reservoir pressure becomes too low for production. Reservoir utilization is poor, typically 95%–80% of the oil remains in the ground, and the energy costs of demobilizing the oil field and remobilizing at a new site is relatively high. The energy recovery is improved by injecting water or gas into the reservoir to maintain pressure. This reduces the remaining oil to 80%–40%. Still, in most cases, there is more oil left in the reservoir than produced at the end of the economic lifetime of the oil field. So-called tertiary methods are used to reduce the remaining oil down to 60%–30% of the initial volume. This includes injection of fluids or gases not naturally present in the reservoir [2]. The purpose of polymer flooding is to improve the sweep efficiency compared to waterflooding by the addition of water-soluble polymer to viscosify the injected fluid. The increase in fluid viscosity results in improved

macroscopic displacement of oil by reducing the mobility ratio between the water and the oil phase (injected fluid mobility vs. displaced fluid mobility), which reduces frontal instability. It may also increase microscopic displacement since the viscous force which mobilizes trapped oil droplet may overcome the capillary forces preventing the oil droplets from being mobilized [2,3]. Commonly, two types of polymers have been utilized in EOR applications: synthetic polymers, primarily partially hydrolyzed polyacrylamide (HPAM), and biopolymers, mainly xanthan. Both polymers are used as viscosifying agents [4]. Wang, et al. [5] reported the success of polymer flooding in increasing oil recovery factor of Daqing oil field in China. Among many other successful field polymer flooding projects reported by Standnes and Skjevrak [6], HPAM is the most commonly used EOR polymer.

HPAM transported in oil reservoirs will experience different flow velocities due to high flow rates at the injector and also due to local pore size variations. This results in expansion and contraction of polymer flow inside the porous media. It would accordingly exhibit different flow regimes with respect to shear rates. These different flow regimes have been widely discussed previously, e.g., by Chauveteau [7], Southwick and Manke [8], Stavland, et al. [9], Zamani, et al. [10], and Skauge, et al. [11]. Due to its viscoelastic nature, its in situ viscosity is a contribution of viscous and elastic properties, e.g., shear and extensional viscosity, respectively [12].

In a pure shear flow such as the flow in viscometer, HPAM exhibits shear thinning behavior that can be described by a power law equation [13]. Shear thinning behavior is an ideal injectivity characteristic of EOR polymers, where viscosity decreases with the increase in shear rate. High flow velocities are inherent in wellbore areas [14]. They cause an increase in polymer apparent viscosity in porous medium (shear thickening) in contrast to dominant bulk thinning behavior measured in a viscometer. In a porous medium, at low flow velocities, shear viscosity is dominant while the flow is dominated by extensional viscosity at high velocities [15]. During the extensional flow, polymer coils experience high extensional stresses that induce flow resistance which gives the substantial rise on apparent viscosity [16,17]. This is theoretically interpreted by coil transition theory [7]; however, this theory has been debated subsequently by transient network theory, which explains the origin of shear thickening regarding disentanglement timescale [18,19]. Regardless of the theoretical interpretations of shear thickening, it has been experimentally observed even at very low concentrations of HPAM, see, e.g., [20–23]. It increases linearly with the flow velocity after the onset of shear thickening [24]. The onset of shear thickening has been given high attention in literature; even more than the effect of the magnitude of shear thickening on viscosity [22]. The onset of shear thickening is a function of many parameters, such as polymer molecular weight, concentration, degree of hydrolysis, salinity, temperature and rock permeability [9,15,23,25].

In conjunction with shear thickening at high flow velocities discussed above, HPAM solution is also prone to mechanical degradation [3,26]. Mechanical degradation of polymer can be described as an irreversible process that leads to the breakage of polymer molecules due to high mechanical stresses induced by high flow velocities or elongational deformations [16,26–28]. The breakage of polymer chain induces a significant loss on polymer viscosity. Consequently, it reduces its displacement efficiency [28]. Mechanical degradation is a function of flow velocity, pore geometry, pore tortuosity, polymer-fluid and polymer-rock interactions and physicochemical properties of the polymer. It would be high for high flow rate, high molecular weight polymer, high brine salinity and low formation permeability [26,29]. Claims have been made that mechanical degradation occurs at the entry point of the sand face and therefore is independent of path length [7,28,30,31].

Polymer injectivity is strongly bound with its rheology [11,30]. For instance, shear thickening behavior limits polymer injectivity through associative pressure build-up that might cause wellbore fracturing or polymer mechanical degradation. In cases where fracturing or fracture growth occurs due to polymer injection, it might spoil the economy of polymer flooding project due to early breakthrough and loss of polymer sweep efficiency [32]. However, in cases where mechanical degradation occurs, it can alter polymer rheological properties and cause loss in viscosity. Both fracturing and polymer mechanical degradation make the pre-assessment of polymer injectivity challengeable.

HPAM mechanical degradation could be minimized if the polymer is submitted for a certain amount of mechanical degradation prior injection into reservoir [2,3,16]. This approach is well-known as the polymer pre-shearing process. This was discussed in Seright, et al. [33], in which mechanical degradation of HPAM solution occurs at the high end of polymer molecular weight distribution (MWD), as shown in Figure 1. This is because high molecular weight molecules have large size, which could offer more resistance to flow. Therefore, large elongational stresses causing breakdown of molecules resulting in degradation. During the pre-shearing process, high molecular weight species will break down into some combination of lower molecular weight fragments, leading to a new MWD. The new MWD of degraded polymer translated into lower MWD. Hence, HPAM viscoelastic properties that depend on high molecular weight species are more affected compared to shear viscosity that depends on average molecular weight which relatively less altered by pre-shearing process [26]. Moreover, the pre-shearing process results in better filterability [34] by removing polymer aggregates or micro gel that responsible for pore blockage. This eliminates the high apparent resistance factors that may appear at low flow rates cause injectivity issues [29]. Chain scission mechanisms associated with polymer degradation or shearing were extensively discussed by Odell, et al. [35] and Muller, et al. [36]. The amount of pre-shearing should be optimized to avoid the loss of polymer viscosity and improve its injectivity characteristics [37].

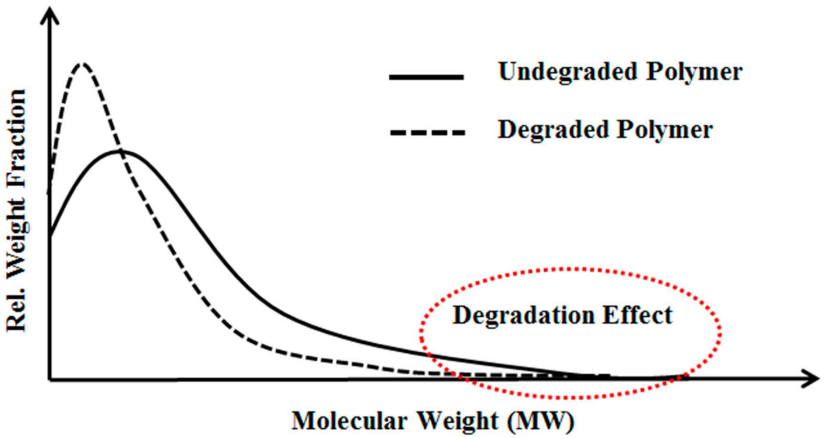

Figure 1. Schematic illustration of the effect of mechanical degradation on polymer molecular weight distribution (MWD) based on the observations reported by Seright, et al. [33]. The peak of the degraded solution shifts to a lower molecular weight. MWD was reduced for the degraded solution.

To represent the flow of polymer near wellbore areas and as it advances within the reservoir using linear cores is challenging due to different states of velocity regimes. For example, unsteady state flow conditions are present at wellbore areas, while a steady state condition is applied in the lab for core flood studies. The experimental design of core flood has to consider filtration and degradation effects on polymers, as reported by some earlier studies, e.g., Martin [38,39]. The effect of the prefiltering process in which the polymer subjected to low flow rate before injection has an insignificant impact on polymer in situ viscosity [40]. This is also observed in the experimental study performed by Skauge, et al. [23]. They investigated the role of polymer phase behavior on in situ viscosity, in which they found the molecular weight of polymer is the key factor dominating in situ rheology of semi-dilute polymers. Jouenne, et al. [41] performed degradation studies using a blender, capillaries and porous media. The kinetics of degradation fit a master curve as a function of normalized time, regardless of the media in which the degradation occurred. Moreover, the polymer will not be further degraded beyond the point of highest strain which determined the steady state value of degradation. Until the

steady state was reached, degradation increased with the number of passes of the point of highest strain. This was reached at less than 6 mm in synthetic porous media.

The present work aims to study the influence of mechanical degradation on HPAM rheology at a larger scale, at 5–10 cm of propagation. This was performed by flooding polymer through porous media and analyzing the injected and eluted samples. For this purpose, highly permeable outcrop rock (Bentheimer cores) was used. The experiments were carried out at room temperature using two types of semi-dilute HPAM polymers dissolved in brines with a given salinity. The polymers were pre-treated by prefiltering or pre-shearing through porous media prior to injection in order to represent the filtration and shearing processes induced on the polymer by the porous media in a field case. In such a field case, the polymer might be sheared near the injection well, where high flow velocities are achieved. High molecular weight fractions may be filtered by retention mechanisms as it propagates through the porous media at either high (near-well) or low velocity (deeper in the reservoir). Propagation effects were evaluated by re-injecting polymer that had already experienced high shear to evaluate if further mechanical degradation would occur at the same flow velocities (and thereby same shear rates). Results from this study reveal that pre-shearing at high flow rates (representative of near wellbore areas) has a larger impact than prefiltration. One consequence of this is that mechanical degradation due to high shear may improve injectivity without significantly reducing polymer in situ viscosity at (lower) reservoir flow rates. Another key observation is that polymer degradation occurs successively for high MW polymer. This indicates that it is not only the molecular weight and point of highest strain that determine the degree of degradation but also the exposure time and number of exposures to high strain. These are important aspects to implement in polymer flood design.

2. Materials and Methods

2.1. Polymer Preparation

Hydrolyzed polyacrylamide (HPAM) polymers with a 30% degree of hydrolysis were used for this study with different molecular weights and concentrations, as shown in Table 1. It is well-known that HPAM polymers have a broad spectrum of molecular weight distribution (e.g., Polydispersity Index > 1) [3,42]. These polymers on average contain 90% active material, as reported from the supplier. They were obtained as white granular powders from SNF Floerger, France. The polymer solutions were prepared by dissolving these polymers into 1 wt % NaCl brine. Initially, approximately 5000 ppm stock solution was carefully prepared and then diluted into the required concentrations. The preparation of stock solution was achieved by adding 3.0 g of polymer powder slowly into the shoulder of the vortex of 540.0 g brine while maintaining vigorous stirring using a magnetic stirrer until the vortex disappeared. Then, the stirring speed was decreased to 150 rpm and the polymer solution was left under slow mixing overnight. The prepared solution was kept at 5 °C inside a fridge and was used within two weeks of preparation.

The polymers were previously used in a different study and at the given concentrations and brine salinity, both polymers solutions A and B were within the semi-dilute region, see Skauge, et al. [23].

Table 1. Physicochemical properties of polymers.

Solution	Polymer (Flopaam) Type	Molecular Weight (10^6 g/mol = MDa)	Polymer Concentration (mg/L = ppm)	Viscosity (mPa.s)
A	3630 s	18	500	7.45
B	3430 s	12	1000	13.54

2.2. Brine

Brine solution containing 1 wt % NaCl was prepared by dissolving NaCl powder obtained from Sigma-Aldrich (Munich, Germany) into deionized water. Then the solution was filtered by using a 0.45 μm cellulose nitrate filter. The filtered brine was used in the preparation of polymer solutions and measurement of core petrophysical properties (e.g., porosity and permeability).

2.3. Porous Medium

Cylindrical cores of Bentheimer sandstone were used as porous medium with an average length and diameter of 10 and 3.8 cm, respectively. Also, short Bentheimer cores of 5 cm length were used for prefiltering and pre-shearing processes. Bentheimer sandstone is considered to be homogenous since it mainly contains quartz mineral [43]. The average core porosity and permeability for the 16 cores investigated were found to be 23% ± 1% and 2.4 ± 0.2 Darcy, respectively. The short cores were not measured directly, but were assumed to be within the range of the long cores reported in Table 2 and Tables 4–7.

2.4. Rheology

Shear viscosity for polymer solutions was measured at 22 °C by using a Kinexus Pro (Malvern, UK) rheometer. Two types of geometries were used: cone-plate geometry (CP 2/50) with 2° inclination and 50 mm diameter in titanium was used for solutions with viscosity greater than 10 mPa.s, while a double gap geometry (DG 25) with 25 mm diameter was used for solutions with viscosity less than 10 mPa.s.

2.5. Core Flooding

The core flooding experiments were carried out under room temperature (22 °C). Figure 2 illustrates the experimental set-up which consists of dual piston Quizix pump, transfer cylinder, core holder, backpressure regulator and effluent collector, which were mounted in series. Differential pressure transducers with maximum range of 5 and 30 bar were mounted between the inlet and outlet of the core holder to monitor pressure drop across the core during injection. The backpressure regulator was mounted at the outlet of the core to apply a pressure of 5 bar to dissolve any air that maybe found within porous medium before flooding. The backpressure regulator was removed during polymer injection to avoid polymer degradation.

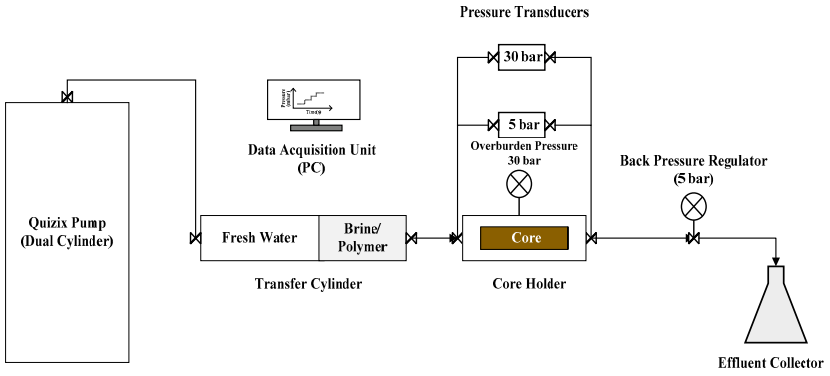

Figure 2. Schematic diagram of the core flooding apparatus.

Before injecting polymer solution into the cores for in situ rheology, the polymer solutions were pretreated differently as illustrated in Figure 3. Polymer pretreatment methods are described below:

- Step I, **pre-filtering** the polymer solution through short cores (L = 5 cm) at low flow rate (Q = 0.5 cc/min, v_D = 0.6 m/day). The pre-filtered polymer solution will be then injected into longer core (L = 10 cm) for in situ rheology measurements. This step was carried out to avoid any microgel in the solution and filter out any possible large MW species. This step represents industrialized polymers which are used in field applications. It is also considered as a baseline for comparison with polymer solutions which were treated differently based on Steps II and III.
- Step II, **re-injecting** the effluent that was collected from Step I through a long core (L = 10 cm) at highest flow rate (e.g., the highest flow rate was achieved when the difference between overburden pressure and pump pressure is 10 bar). This injection rate was (Q = 12.0 and 15.0 cc/min, v_D = 15.5 and 19.3 m/day) for Solutions A and B, respectively. This step was carried out to investigate the effect of core length on the extent of degradation mechanisms as the degradation performed on long core compared to short core in Step III. Also, re-injected solution represents the flow of industrial polymer (prefiltered polymer) deep in reservoir that has already experienced filtration and degradation effects.
- Step III, **pre-shearing** the polymer solutions through short cores (L = 5 cm) at the highest flow rate obtained from Step II. Then, the pre-sheared solution is injected into a longer core (L = 10 cm) for in situ rheology measurements. In this step, large MW species in the solution are possibly filtered and mechanically sheared to lower MW species.

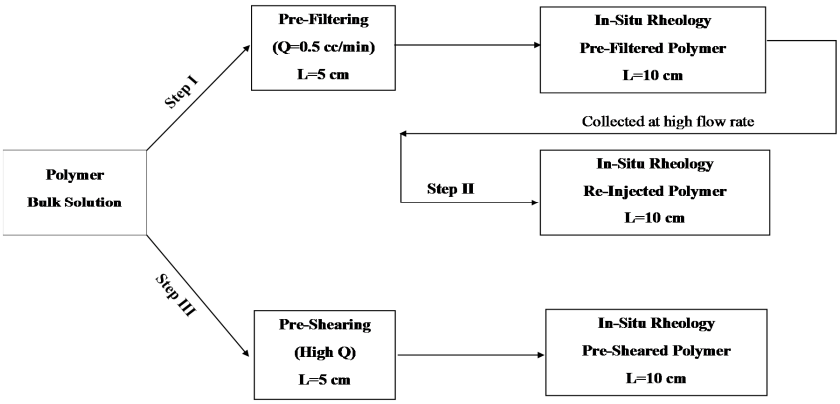

Figure 3. Flow chart of polymer pre-treatment methods and injection into porous medium.

After saturating the core plugs with brine and porosity measurements, brine was injected into the cores at different flow rates to determine the absolute permeability. Absolute permeability (K_{abs}) was obtained by Darcy's law (Equation (1)):

$$K_{abs} = \frac{Q \cdot \eta \cdot L}{\Delta P \cdot A} \quad (1)$$

where, Q is injection flow rate, η is fluid viscosity, ΔP is pressure drop across the core, L and A are core length and cross-sectional area, respectively. Note that interstitial velocity (v) was obtained from Darcy velocity (v_D), where ϕ is the porosity of porous media.

$$v = \frac{Q}{A \cdot \phi} = \frac{v_D}{\phi} \quad (2)$$

Polymer solution, after pretreatment, was injected into the core using Quizix pumps at low flow rate (Q = 0.5 cc/min, v_D = 0.6 m/day) for at least 2 PV to satisfy porous medium polymer adsorption level and achieving stable differential pressure. Then, polymer flow rate was varied in a stepwise manner from the highest to the lowest rate. Each rate step was continued until a stabilized pressure drop across the core was achieved. Resistance factor (*RF*) was calculated as following [3]:

$$RF = \frac{\Delta P_p}{\Delta P_w} \quad (3)$$

where ΔP_p is the pressure drop of polymer during polymer flow and ΔP_w is the pressure drop of brine before polymer flow in porous medium.

Samples of effluents were collected at different flow rates to measure their shear viscosity by rheometer and compared with initial solution viscosity. The following equation was used to express the change in shear viscosity by taking shear viscosity at shear rate of 10 s^{-1} [41]:

$$\text{Deg}(\%) = \frac{\eta_i - \eta_e}{\eta_{i-}\eta_w} 100\% \quad (4)$$

where, η_i is injected solution viscosity, η_e is effluent viscosity and η_w is brine viscosity which was measured to be 1.04 mPa.s.

After terminating the polymer injection, the core's permeability to brine was re-measured after injecting 5 PV of brine at high flow rates proceeded by two steps of tapering. Tapering was performed by injecting diluted effluent at low flow rate (Q = 1.0 cc/min, v_D = 1.3 m/day) with 50% and 25% of initial effluent concentration (e.g., in the case of Solution A, effluent of this polymer was collected and diluted into 250 and 125 ppm). Residual resistance factor (*RRF*), which is the permeability to brine before polymer flooding to permeability of brine after polymer flooding, was calculated using Equation (5) [44]:

$$RRF = \frac{K_{wi}}{K_{wf}} \quad (5)$$

where K_{wi} is the absolute permeability to brine before polymer flow and K_{wf} is the absolute permeability to brine after polymer flow after tapering.

3. Results and Discussion

3.1. Shear Viscosity

Shear viscosity measurements were carried out for shear rates 1–1000 s^{-1} as shown in Figure 4. Rheometer measurements were very well matching with the power law model by setting n = 0.81 and 0.72 and k = 11.49 and 25.80 for bulk Solutions A and B, respectively. Both solutions show predominantly shear thinning behavior, while Solution B shows indications of a Newtonian plateau for shear rates <2 s^{-1}. The viscosity increase observed at high shear rates is mainly due to turbulence flow caused by high rotational speed (which is also observed for brine) that causes an artifact in measurements [45]. The turbulence should not be confused with the apparent shear thickening observed in porous media flow. Shear viscosity is 7.45 and 13.54 mPa.s for bulk Solutions A and B, respectively, using the reservoir flow relevant shear rate of 10 s^{-1} as a reference.

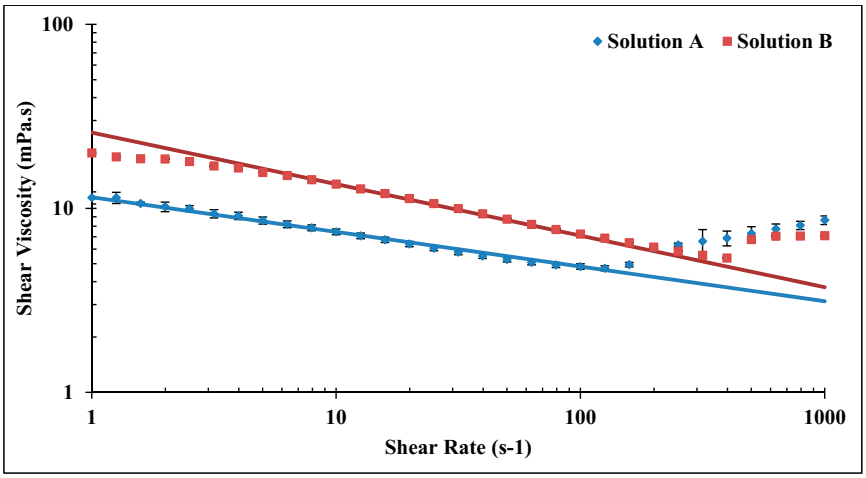

Figure 4. Shear viscosity of bulk Solutions A and B in 1 wt % NaCl at 22 °C. Solid lines represent power law model. Error bars for Solution B are smaller than the size of each point (±0.20 mPa.s).

3.2. Apparent Viscosity in Porous Medium vs. Shear Viscosity in Rheometer

In order to compare the flow of polymer in porous medium with the flow in rheometer, it is necessary to translate the flow velocity in porous medium to shear rate. Determining the exact equivalent shear rate in porous medium is not possible due to its distribution of pore size, tortuosity and complexity. The following equation is conventionally used to estimate an effective shear rate in porous medium [7]:

$$\dot{\gamma} = \alpha \frac{4v_D}{\sqrt{8K_w\phi}} \quad (6)$$

where v_D is Darcy fluid velocity, ϕ porosity, K_w absolute permeability, α shape factor, which is an empirical parameter. Here we have applied an α value of 2.5 for consolidated sandstone (Bentheimer) [3]. The apparent viscosity of polymer flowing in porous medium is represented by the resistance factor (*RF*). Given that the other factors in Equation (1) are the same, apparent viscosity equals RF × μ_w. Apparent viscosity was calculated from Equation (3) for each flow rate. The comparison of the shear viscosity from the rheometer and apparent viscosity from the porous media for Solution A is shown in Figure 5. At lower shear rates ($\dot{\gamma} < 30\ s^{-1}$), apparent viscosity approaches the upper Newtonian plateau observed from bulk flow shear viscosity. However, at moderate and high shear rates, apparent viscosity in porous medium diverges from viscosity measured in rheometer. This is clearly seen in that Newtonian and shear thickening behaviors are observed in porous medium, while shear thinning behavior is shown by rheometer. However, the two curves are not expected to show the same trend as flow in porous medium is different from shear flow in a rheometer.

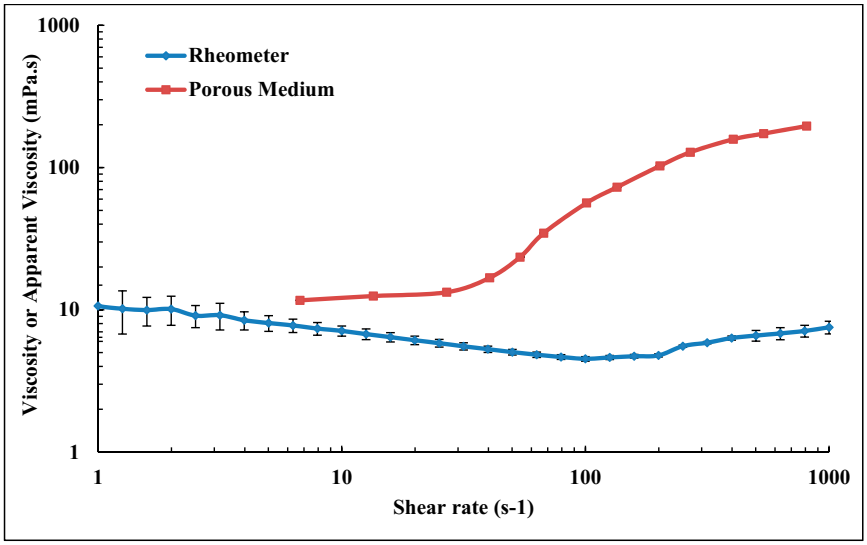

Figure 5. Viscosity of pre-filtered Solution A (Concentration = 500 ppm, MW = 18 MDa) measured in porous medium and in bulk.

3.3. Apparent Viscosity

The apparent viscosity of polymer flowing in porous medium is represented by the resistance factor (*RF*), see Figure 6. *RF* was calculated from Equation (3) for each flow rate and is plotted vs. interstitial velocity as calculated from Equation (2). Steady state conditions were achieved at each flow rate before changing to the next rate. The experiment was performed on twin plugs (see Table 2) with the same polymer. An apparent Newtonian plateau is observed at low flow velocity. Above a critical flow velocity, i.e., 3–5 m/day, shear thickening is observed. It was found that the injection scheme from lowest to highest flow rate has lower RF at higher velocities; the difference between the schemes was 23% at the highest velocity. The difference is relatively smaller at lower velocities. The pressure was stable for the highest rate for both schemes and the reason for the discrepancy is not clear. It is, however, reproducible and may be due to difference in hydrodynamic retention for a core saturated at high rate versus one saturated at a low rate. Since adsorption measurements were not performed for the two cases, no firm conclusions can be made on this matter. The injection scheme from highest to lowest flow rates was adopted for this study. This may also be more representative for flow velocities experienced in a reservoir where it is subjected to high velocities in near wellbore areas.

Table 2. Properties of cores used for hysteresis investigation of polymer injection scheme.

Injection Scheme	L (cm)	D (cm)	ϕ (-)	K_{wi} (Darcy)
Injection from lowest to highest Q	9.41	3.75	0.22	2.17
Injection from highest to lowest Q	9.44	3.78	0.22	2.18

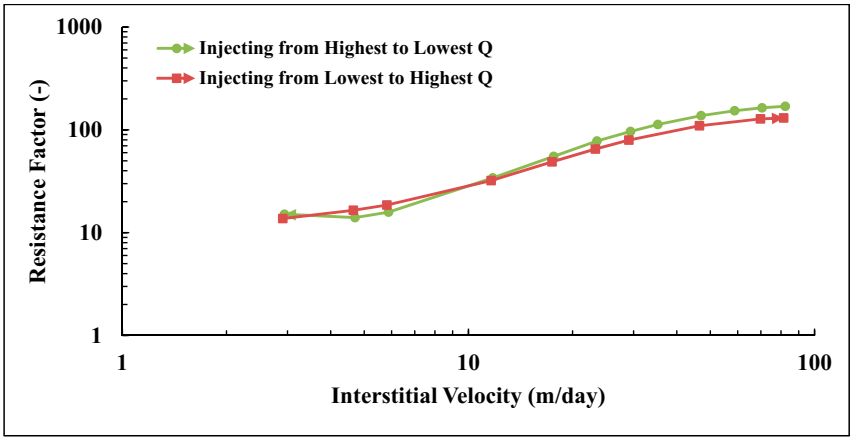

Figure 6. Resistance factor versus interstitial velocity for pre-sheared Solution A. The polymer was sheared at Q = 12 cc/min and RF measured at different injection schemes.

3.4. Backpressure Regulator Effects

Typical core flood setup consists of a backpressure regulator which is used to stabilize the pressure across the core and removes any air within the system. However, it was found that the backpressure regulator can induce a mechanical degradation of polymer, as can be seen from the reduction of shear viscosity as presented in Figure 7 and the tabulated data in Table 3. High molecular weight polymer with low concentration (Solution A) experience high degradation compared to lower molecular weight polymer (Solution B). Solution A lost more than 50% of its original viscosity after passing backpressure regulator at high flow rates. The flow rates applied for the investigation were Q = 12 and 15 cc/min for Solutions A and B, respectively. Please note that the backpressure regulator was not used during investigation of polymer in situ rheology to avoid mechanical degradation of polymer.

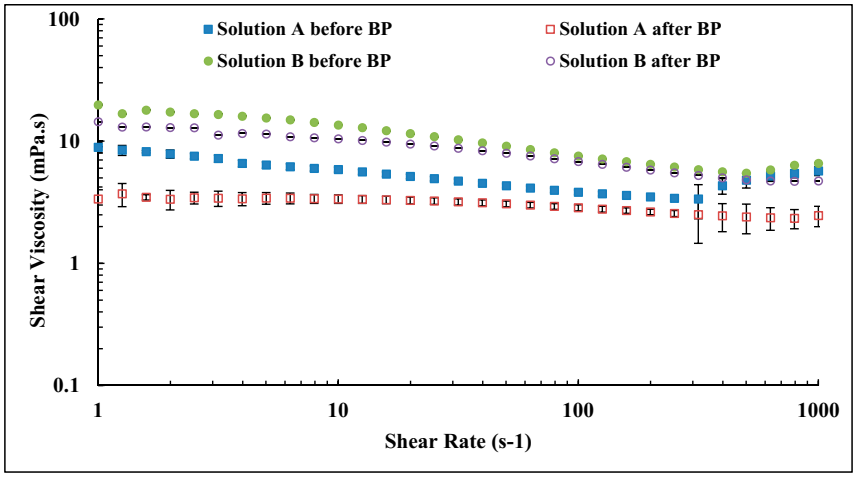

Figure 7. Shear viscosity vs. shear rate of polymers injected through backpressure regulator at high flow rates.

Table 3. Effect of backpressure regulator on shear viscosity of Solutions A and B. Shear viscosity measured at $\dot{\gamma} = 10\ s^{-1}$.

Measurements	Solution A		Solution B	
	Before BP	After BP	Before BP	After BP
Shear Viscosity (mPa.s)	5.85	3.36	13.53	10.43
Deg (%)	0.00	51.8	0.00	24.8

3.5. In Situ Viscosity of Solution A

Three core floods were performed to determine the influence of polymer pre-treatment on in situ viscosity. The three pre-treatment methods are described in Figure 3. Core data are given in Table 4. Resistance factor as a function of flow velocity for Solution A (Concentration = 500 ppm, MW = 18 MDa) is presented in Figure 8. All three core floods show apparent Newtonian behavior at low flow velocities followed by shear thickening behavior at higher flow velocities. At low flow velocities, all the solutions approach an *RF* value of ~12 regardless of their pre-treatment procedure. However, after the onset of shear thickening, the solutions show distinctly different *RF* curves. The pre-filtered solution exhibits the highest *RF* compared to the pre-sheared and reinjected solutions. The *RF* correlates to the onset of shear thickening. Pre-filtered solution has an onset of shear thickening at $v_c = 2.5$ m/day, which is lower than for pre-sheared and reinjected solutions which have $v_c = 4.0$ and 6.7 m/day, respectively. The onset of shear thickening was measured apparently from the *RF* curve that represents the point of departure from Newtonian to shear thickening behavior. The shift in the onset of shear thickening to higher velocities indicates that the polymer has experienced degradation and that the molecular weight distribution is altered [25,26].

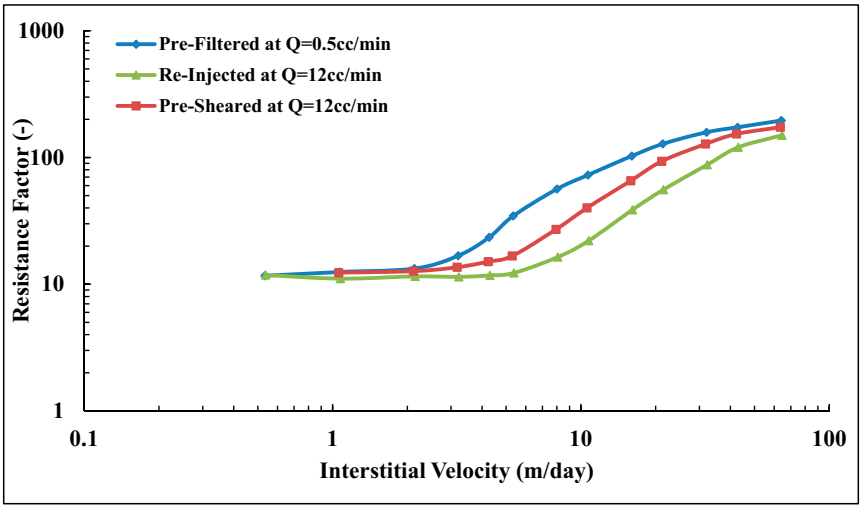

Figure 8. Resistance factor (*RF*) vs. interstitial velocity for Solution A.

Table 4. Core and solution properties for injected Solution A (Concentration = 500 ppm, MW = 18 MDa).

Exp.	L (cm)	D (cm)	ϕ (-)	K_{wi} (Darcy)	K_{wf} (Darcy)	RRF (-)	η_i (mPa.s)	η_e (mPa.s)	v_c (m/day)	m $(m/day)^{-1}$
Pre-filtered at Q = 0.5 cc/min	9.82	3.77	0.24	2.57	1.40	1.84	7.11	5.79	2.51	7.68
Re-injected at Q = 12 cc/min	9.78	3.77	0.24	2.39	1.28	1.86	5.79	-	6.71	3.00
Pre-sheared at Q = 12 cc/min	9.72	3.77	0.24	2.25	0.82	2.75	7.13	7.21	4.00	4.32

In addition to the effect on the onset of shear thickening, mechanical degradation markedly affects the degree of shear thickening. The degree of shear thickening is represented by the slope of shear thickening part of the *RF* curve, i.e., the change of RF with respect to flow velocity. The higher slope was found for pre-filtered solution, $m = 7.7\ (m/day)^{-1}$ compared to pre-sheared and reinjected solutions (m = 4.3 and 3.0 $(m/day)^{-1}$, respectively). Reinjected solution experienced further degradation when reinjected into porous media. This indicates further degradation occurred with increasing core length.

During the polymer injection, shear viscosity of effluents were measured as shown in Figure 9. The viscosity at v = 0 m/day means the injected viscosity of solution after passing pre-treatment processes (η_i). The highest flow velocity (v = 64.1 m/day) for the pre-filtered solution showed a shear degradation of 22%. However, no significant shear degradation was observed for pre-sheared solutions. The injected viscosity of the reinjected solution is lower than that of injected pre-filtered and pre-sheared solutions which could explain the lower *RF* observed in the porous medium. Still, this is not sufficient to explain the difference in *RF* curves observed for pre-sheared and pre-filtered solutions that have similar injected viscosity but show different flow behavior in the porous medium. This is further evidence that in situ viscosity cannot be predicted from bulk shear viscosity measurements, even for flooding experiments with the same polymer, concentration, brine and temperature. However, this is only true for flow velocities above the onset of shear thickening. Below, at typical reservoir flow velocities, the in situ viscosities are very similar. The pre-treatment at high shear reduces the extensional viscosity [25,26,46–48]. This confirms that the high *RF* values at high flow velocities are due to extensional viscosity that is negligible at low velocities in which shear viscosity is more dominant.

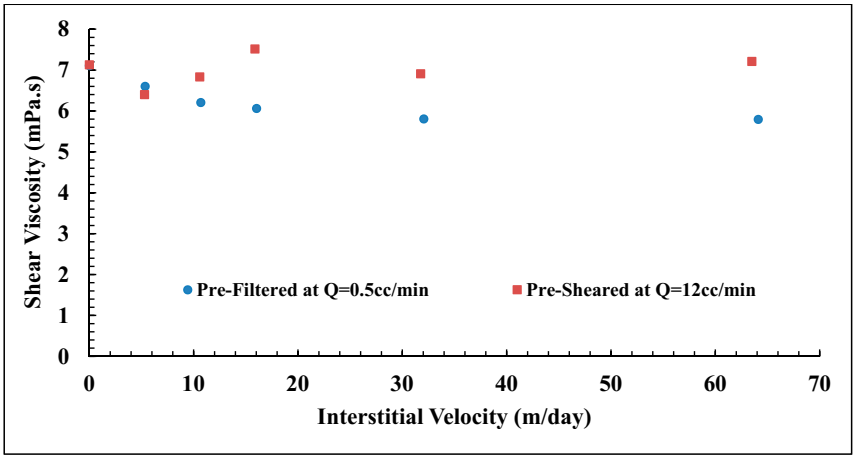

Figure 9. Effluents shear viscosity of Solution A measured at $\dot{\gamma} = 10\ s^{-1}$. Error bars are smaller than the size of each point (±0.20 mPa.s).

3.6. In Situ Viscosity of Solution B

The same procedures were applied for Solution B (Concentration = 1000 ppm, MW = 12 MDa), which has a shear viscosity of 13.54 mPa.s at 10 s^{-1}. Figure 10 shows *RF* curves for Solution B at different preparation procedures. Core data are given in Table 5. At low flow velocities, a weak shear thinning behavior was observed, which was not observed for Solution A. This is most likely because Solution B has a higher concentration than polymer A, for which the degree of entanglements is higher in Solution B. Another observation is that all three solutions approach similar *RF* values at low velocities, which shows that the degree of pre-shearing and re-injection of polymer at high rates do not significantly change the in situ viscosity at typical reservoir flow rates. This is in sharp contrast to higher flow rates, where significant differences are observed. It was found that the pre-filtered solution possesses an earlier onset of shear thickening (v_c = 4.1 m/day) compared with pre-sheared and reinjected solutions (v_c = 12.0 and 7.7 m/day; respectively). Furthermore, the degree of shear thickening was higher for pre-filtered solution, m = 3.5 $(\mathrm{m/day})^{-1}$ compared to pre-sheared and reinjected solutions (m = 1.5 and 2.3 $(\mathrm{m/day})^{-1}$, respectively).

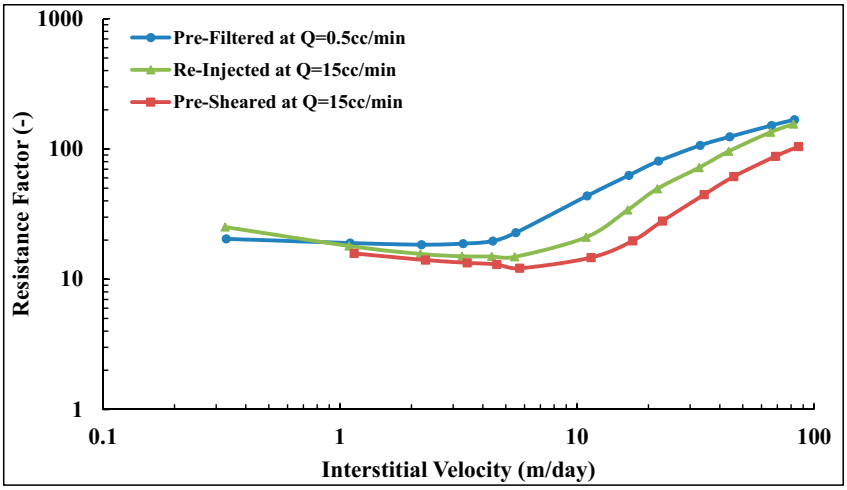

Figure 10. Resistance factor (*RF*) versus interstitial velocity for Solution B (Concentration = 1000 ppm, MW = 12 MDa).

Table 5. Core and solution properties for injected Solution B (Concentration = 1000 ppm, MW = 12 MDa).

Exp.	L (cm)	D (cm)	ϕ (-)	K_{wi} (Darcy)	K_{wf} (Darcy)	RRF (-)	η_i (mPa.s)	η_e (mPa.s)	v_c (m/day)	m $(\mathrm{m/day})^{-1}$
Pre-filtered at (Q = 0.5 cc/min)	9.82	3.79	0.23	2.16	0.96	2.24	13.57	13.31	4.06	3.50
Re-injected at (Q = 15 cc/min)	9.57	3.79	0.23	2.08	1.24	1.68	13.31	12.75	7.69	2.28
Pre-sheared at (Q = 15 cc/min)	10.27	3.77	0.23	2.80	1.54	1.82	13.10	12.75	11.99	1.46

Effluent viscosities do not show significant degradation for any of the three core floods as shown in Figure 11. This corresponds well with the *RF* curves that show similar viscosity at typical reservoir flow velocities, i.e., 0.1 to 1.0 m/day. However, the effluents collected at higher flow velocities, such as 30 to 70 m/day also show similar values, while the *RF* values are significantly different. This shows that the difference in shear thickening at high velocities is due to extensional viscosity, which is not reflected in the measurements of shear viscosity.

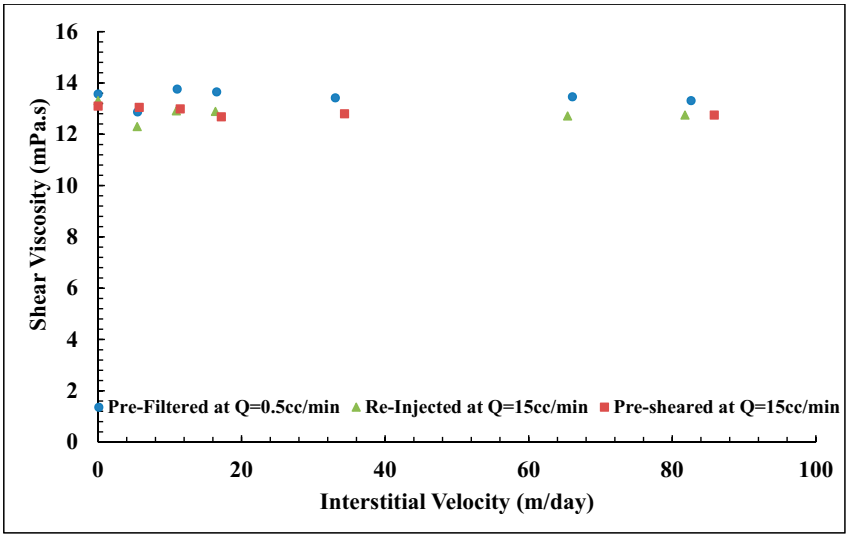

Figure 11. Effluent shear viscosity of Solution B measured at $\dot{\gamma}$ = 10 s^{-1}. Error bars are smaller than the size of each point (±0.20 mPa.s).

3.7. Influence of Degradation on Polymer Molecular Weight

Figure 12 shows the effect of pre-shearing on the onset of shear thickening for high molecular weight polymer (Solution A) to that of lower molecular weight polymer (Solution B). Shift in onset of shear thickening has been an indication of reduction of molecular weight distribution [9,23,25]. It is generally difficult to quantify the reduction of MWD due to the difficulties in determining MW of high molecular weight polymers by methods such as size exclusion chromatography (SEC) and asymmetric flow field-flow fractionation (AF4) [49–52]. To characterize the reduction by core floods would usually require a large number of core floods. In this experiment, the onset of shear thickening and the shape of the *RF* curves are similar after the onset of shear thickening for pre-sheared Solution A and pre-filtered Solution B (Figure 12). This indicates the MWD of Solution A was shifted to lower distribution similar to that of prefiltered Solution B. This supports the observation given by Puls, et al. [53], in which the pre-shearing process reduces HPAM molecular weight distribution, as they observed by using size exclusion chromatography (SEC) for determining the MW of solution.

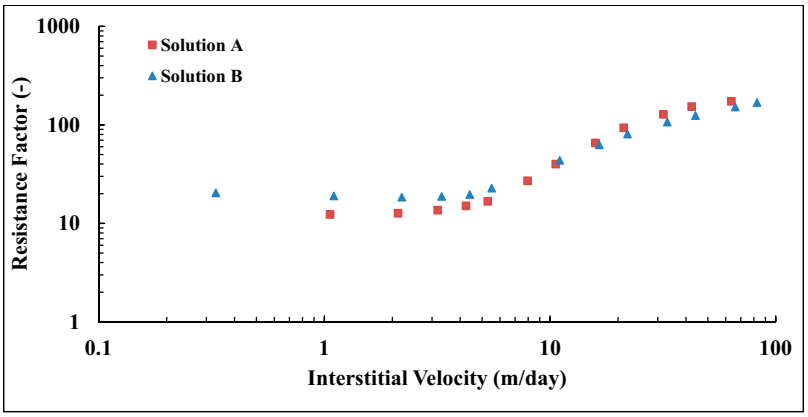

Figure 12. Influence of pre-shearing on Solution A (MW = 18 MDa) compared to pre-filtered Solution B (MW = 12 MDa).

3.8. Permeability Reduction

HPAM flowing in a porous medium will adsorb on rock surfaces and be trapped within narrow pores, resulting in polymer retention. Polymer retention consequently causes permeability reduction which can be experimentally evaluated by residual resistance factor (*RRF*). Lake [2] reported that *RRF* can be reduced if the polymer is pre-sheared before injection. *RRF* is a function of polymer molecular weight, degree of hydrolysis, flow velocity and pores structures. Other authors, such as Yerramill, et al. [54] and Morris and Jackson [46], reported that *RRF* increases with increasing polymer concentration.

RRF values obtained for Solutions A and B in this experimental study are shown in Figure 13. The *RRF* for pre-filtered Solutions A and B were 1.8 and 2.2, respectively. In this context, the difference in *RRF* is regarded as small, particularly when considering the difference in concentration and molecular weight for Solutions A and B (Concentration = 500 and 1000 ppm, MW = 18 and 12 MDa, respectively). Similarly, there were small differences in *RRF* between degraded (pre-sheared and re-injected) and non-degraded solutions (pre-filtered).

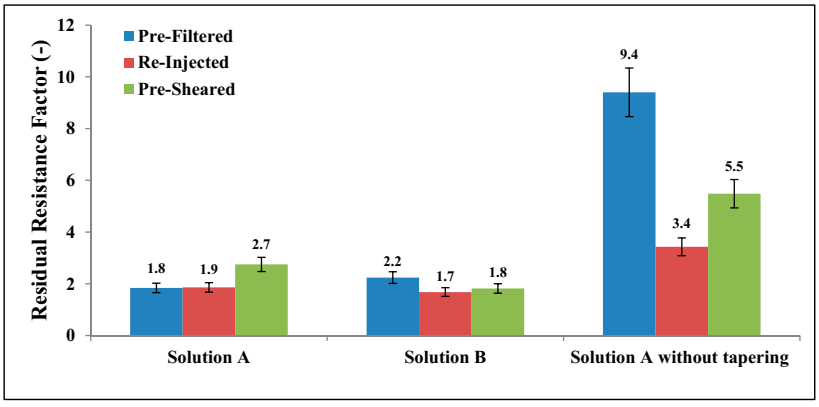

Figure 13. Residual resistance factor (*RRF*) after tapering for both solutions and without tapering for Solution A.

How to measure "true" *RRF* has been debated [55]. In this experiment, the influence of tapering on *RRF* was quantified. *RRF* values were reduced from 9.4 to 1.8 for pre-filtered Solution A before and after tapering; respectively. Recall that tapering was performed to flush out as much as possible of the retained polymer. Tapering was performed in two steps before water post-flush by injecting diluted polymer effluent with 50 and 25% of initial effluent polymer concentration. The error bars in Figure 13 are based on repeated measurements.

3.9. Reproducibility of Experiments

The shift in onset of shear thickening to higher velocities and the reduction in slope for pre-sheared and re-injected solutions are consistent with a mechanical degradation and alteration of polymer molecular weight distribution. Figure 8 shows a successive degradation of high molecular weight polymer as it is reinjected into porous media, while this is in contrast with the lower molecular weight solution shown in Figure 10. It was not clear if the polymer might be exposed to further degradation during reinjection, as reported by Sorbie and Roberts [56] and Al Hashmi, et al. [31].

To further investigate the difference on the extent of mechanical degradation found between pre-shearing and reinjection in which the core length has been varied. Similar sets of experiments were preformed, which confirm that resistance factor of prefiltered solutions for both polymers are reproducible, as shown in Figure 14. This confirms that RF is reproducible for the prefiltered solution, which indicates the cores were fairly homogenous in that they have quite similar absolute properties (e.g., porosity and permeability as shown in Table 6).

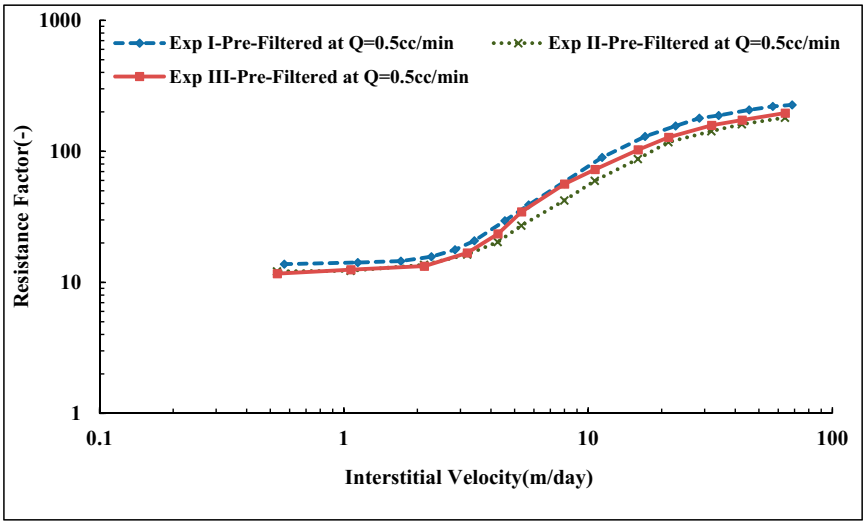

Figure 14. Reproduced resistance factor vs. interstitial velocity of pre-filtered Solution A.

Table 6. Core and solution properties for reproducibility study performed with Solution A (Concentration = 500 ppm, MW = 18 MDa).

Exp.	L (cm)	D (cm)	ϕ (-)	K_{wi} (Darcy)	K_{wf} (Darcy)	RRF (-)	η_i (mPa.s)	η_e (mPa.s)
Exp I-Pre-Filtered at Q = 0.5 cc/min	9.37	3.76	0.23	2.59	0.28	9.4	7.34	5.26
Exp I- Re-Injected at Q = 12 cc/min	9.58	3.77	0.22	2.28	0.67	3.4	5.26	4.84
Exp I- Pre-Sheared at Q = 12 cc/min	9.44	3.78	0.22	2.18	0.40	5.5	-	-
Exp II- Pre-Filtered at Q = 0.5 cc/min	9.54	3.77	0.24	2.48	1.35	1.8	6.81	6.62
Exp II- Re-Injected at Q = 12 cc/min	9.81	3.77	0.24	2.41	1.17	2.1	6.62	6.18
Exp II- Pre-Sheared at Q = 12 cc/min	9.74	3.77	0.23	2.19	0.98	2.2	4.06	4.55
Exp III- Pre-Filtered at Q = 0.5 cc/min	9.82	3.77	0.24	2.57	1.40	1.8	7.11	5.79
Exp III-Re-Injected at Q = 12 cc/min	9.78	3.77	0.24	2.39	1.28	1.9	5.79	-
Exp III-Pre-Sheared at Q = 12 cc/min	9.72	3.77	0.24	2.25	0.82	2.8	7.13	7.21
Exp IV -Pre-Sheared at Q = 12 cc/min	9.88	3.78	0.22	2.31	1.12	2.1	6.51	6.30
Exp V-Pre-Sheared at Q = 12 cc/min and Pre-Filtered at Q = 0.5 cc/min	10.00	3.79	0.22	2.72	1.15	2.4	5.93	5.37

However, some disparity was found on reproducing resistance factor of pre-sheared and reinjected solutions. It was found in some experiments that reinjected solution experienced further degradation compared to pre-sheared solution, as in Exp I and III in Figure 15. The high degradation found of reinjected solution on Exp I is attributed to the associated effect with the use of the backpressure regulator, which was not used in the rest of the experiments. The match between RF curves of pre-sheared solution in Exp II and V demonstrates that the pre-shearing process can filter and pre-shear the polymer. A disparity was found in reproducing the resistance factor of the pre-sheared solution as well. This could be expected due to the fact that pretreated polymer could experience different fields of shear rate due to different topology of the cores, regardless of the similarity between the cores' apparent petrophysical properties (see Table 6). The pre-shearing process could further or similarly degrade the polymer as the reinjection process does, and vice versa. This indicates that the core length or exposure time has an effect on the degradation mechanism, although some previous studies [41] have reported that polymer degradation has less dependency in on core length. This could be true in synthetic porous medium but not in realistic porous media such core plugs. However, the dependence of successive polymer degradation on characteristic length to approach a steady state value in a realistic porous medium is ambiguous and still not defined.

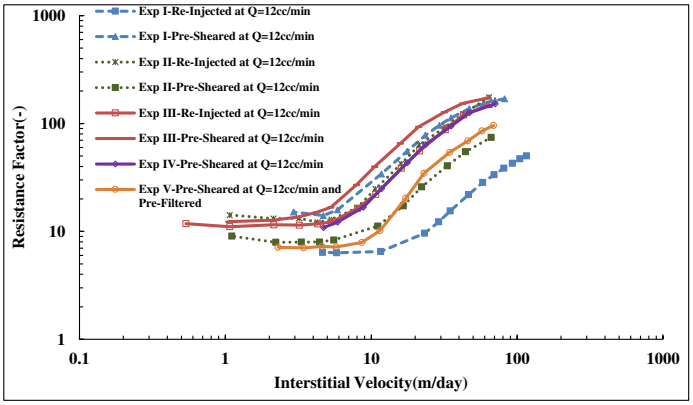

Figure 15. Reproduced resistance factor vs. interstitial velocity of pre-sheared and reinjected Solution A.

3.10. Pre-Shearing at Very High Flow Rates

The pre-shearing process described in Figure 3 was based on the highest shear rate that was achieved from the first step which was limited by experimental setup. In this experiment, the polymer (Solution A) was pre-sheared at extremely high flow rate (Q = 130 cc/min, v_D = 166.8 m/day) in a short core and its shear viscosity degraded by 32% compared to original bulk viscosity of 6.16 mPa.s. It can be seen in Figure 16 that a significant reduction in its in situ viscosity, i.e., the reduction is more than 50% compared to prefiltered and pre-sheared polymers at lower flow rate. Moreover, a significant alteration can be observed on viscoelastic properties of pre-sheared polymer at high flow rate. The onset of shear thickening is shifted to much higher velocities and the degree of shear thickening reduced significantly. Furthermore, it was found that residual resistance factor can be reduced if the polymer is submitted to high degradation as can be seen in Table 7. The core properties of prefiltered and pre-sheared polymer at Q = 12 cc/min were presented earlier in Table 4.

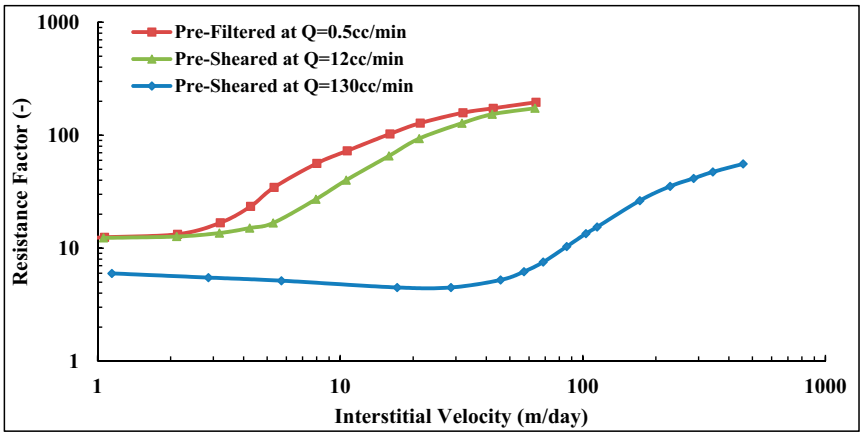

Figure 16. Resistance factor of pre-sheared Solution A at different flow rates verses prefiltered solution.

Table 7. Core and solution properties for pre-sheared Solution A and B at very high flow rates.

Exp.	L (cm)	D (cm)	ϕ (-)	K_{wi} (Darcy)	K_{wf} (Darcy)	RRF (-)	η_i (mPa.s)	η_e (mPa.s)	v_c (m/day)	m (m/day)$^{-1}$
Solution A										
Pre-sheared at Q = 130 cc/min	8.87	3.78	0.22	2.37	1.49	1.6	4.52	4.47	53.61	0.18
Solution B										
Pre-sheared at Q = 110 cc/min	9.71	3.79	0.23	1.87	1.09	1.7	11.30	11.26	33.5	0.37

Similar observations were found for Solution B with lower molecular weight that was pre-sheared at high flow rate (Q = 110 cc/min, v_D = 141.2 m/day). Please note that the flow rate applied for pre-shearing this solution was lower than Solution A due to the higher concentration of Solution B. Its shear viscosity degraded by 16% compared to the bulk viscosity of Solution B, which was 13.25 mPa.s. This results in a significant loss of its in situ viscosity, as well, compared to prefiltered and pre-sheared solutions at lower flow rates, as can be seen in Figure 17. Its viscoelastic parameters reduced, and the onset of shear thickening shifted to much higher velocities, while the degree of shear thickening is reduced. Core properties and viscoelastic parameters for prefiltered and pre-sheared Solution B at low and high flow rates are given in Tables 5 and 7, respectively.

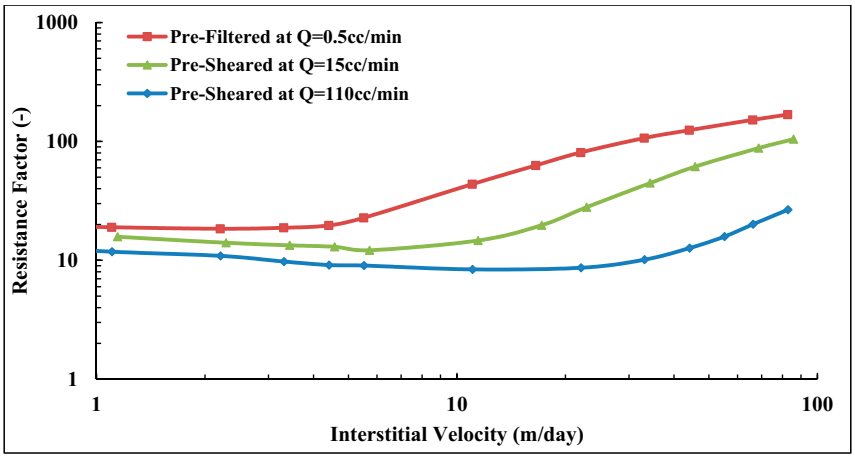

Figure 17. Resistance factor of pre-sheared Solution B at different flow rates versus prefiltered solution.

It can be also seen from Figures 16 and 17 that both solutions responded differently to the high flow rate applied for each of them. High molecular weight polymer suffers more degradation compared to lower solution as discussed earlier in this paper. Although it was pre-sheared at a lower rate compared to Solution B. Hence, the applied flow rate for the pre-shearing process has to be optimized to avoid the loss of polymer viscosity while improve its viscoelastic properties that results in better injectivity.

4. Conclusions

The influence of mechanical degradation and filtration on in situ rheology has been investigated for two HPAM polymers with different molecular weights. Three conditions were evaluated: (1) solutions filtered through a short Bentheimer core at low flow rate (prefiltering); (2) prefiltered solutions subsequently injected at high rate through a Bentheimer core (reinjected); and (3) solutions mechanically degraded through a short Bentheimer core at high flow rate (pre-shearing). The following conclusions could be made:

- At high flow velocities, similar to those experienced in the near wellbore area of an injector, polymer flow history plays a substantial role for HPAM in situ viscosity. Solutions exposed to high rates were mechanically degraded and showed delay in onset of shear thickening and reduction in apparent viscosity compared to the solutions exposed to low rates.
- All solutions, regardless of previous exposure to high or low rates, showed similar apparent viscosity and predominantly Newtonian behavior at low velocities (i.e., reservoir velocities).
- These results show that mechanical degradation is beneficial for the polymer types and concentrations investigated here since injection pressures are reduced and reservoir apparent viscosities are maintained.
- Polymer flow history (pretreatment) has little impact on residual resistance factors (*RRF*). *RRF* is found to be more influenced by fluid exchange process (tapering).
- Mechanical degradation during polymer reinjection is coupled to several parameters such as characteristics of the porous media, flow rate, geometry (inlet/outlet effect), and polymer exposure time to the porous media. Results indicate that re-exposure to the same shear conditions (same flow rate and porous media) may lead to additional mechanical degradation.
- HPAM flowing in porous medium at low velocities (e.g., reservoir velocities) show predominantly Newtonian behavior followed by shear thickening at higher flow velocities (e.g., at wellbore area). Both flow behaviors are absent in rheometer measurements that demonstrate a predominantly

shear thinning behavior at comparable flow rates. This conclusion is limited to the polymer concentration used (weak semi-dilute region).

- Initial studies show that a backpressure regulator can induce a mechanical degradation of polymer that reduces its viscoelastic properties and may lead to erroneous conclusions from laboratory experiments. All experiments reported were made without a backpressure regulator.

Author Contributions: Conceptualization, T.S. and A.S.; Formal analysis, T.S.; Methodology, B.S.S.; Supervision, A.S.; Writing—original draft, B.A.-S.; Writing—review & editing, B.A.-S., T.S., B.S.S. and A.S.

Funding: This research received no external funding.

Acknowledgments: We wish to thank Petroleum Development Oman (PDO) for providing study scholarship for Badar Al-Shakry.

Conflicts of Interest: The authors declare no conflict of interest.

Nomenclature

A	cross-sectional area (cm^2)
AF4	Asymmetrical flow field-flow fractionation
BP	backpressure
C^*	critical overlap concentration (ppm)
D	core dimeter (cm)
EOR	enhanced oil recovery
HPAM	partially hydrolyzed polyacrylamide
k	viscosity constant
K_{abs}	absolute permeability to brine (Darcy)
K_{wf}	absolute permeability to brine after polymer flow (Darcy)
K_{wi}	absolute permeability to brine before polymer flow (Darcy)
L	core length (cm)
MW	molecular weight (MDa)
MWD	molecular weight distribution, dimensionless
n	power law index, dimensionless
PV	pore volume, dimensionless
Q	flow rate (cc/min)
RF	resistance factor, dimensionless
RRF	residual resistance factor, dimensionless
SEC	size exclusion chromatography
v	interstitial velocity (m/day)
v_c	onset of shear thickening (m/day)
v_D	Darcy velocity (m/day)
ΔP_p	pressure drop during polymer flow (bar)
ΔP_w	pressure drop during water flow (bar)
η_e	effluent viscosity (mPa.s)
η_i	injected solution viscosity(mPa.s)
η_w	brine viscosity (mPa.s)
ϕ	porosity, dimensionless
$\dot{\gamma}$	shear rate (s^{-1})

References

1. Sheng, J.J.; Leonhardt, B.; Azri, N. Status of polymer-flooding technology. *J. Can. Pet. Technol.* **2015**, *54*, 116–126. [CrossRef]
2. Lake, L.W. *Enhanced Oil Recovery*; Prentice Hall, Inc.: Upper Saddle River, NJ, USA, 1989.
3. Sorbie, K.S. *Polymer-Improved Oil Recovery*; Blackie and Son Ltd.: Glasgow, UK, 1991.
4. Hill, H.J.; Brew, J.R.; Claridge, E.L.; Hite, J.R.; Pope, G.A. The behavior of polymers in porous media. In Proceedings of the SPE Improved Oil Recovery Symposium, Tulsa, OK, USA, 22–24 April 1974.

5. Wang, D.; Zhao, L.; Cheng, J.; Wu, J. Actual field data show that production costs of polymer flooding can be lower than water flooding. In Proceedings of the SPE International Improved Oil Recovery Conference in Asia Pacific, Kuala Lumpur, Malaysia, 20–21 October 2003.
6. Standnes, D.C.; Skjevrak, I. Literature review of implemented polymer field projects. *J. Pet. Sci. Eng.* **2014**, *122*, 761–775. [CrossRef]
7. Chauveteau, G. Molecular interperation of several different properties of flow of coiled polymer solutions through porous media in oil recovery conditions. In Proceedings of the SPE Annual Technical Conference and Exhibition, San Antonio, TX, USA, 4–7 October 1981.
8. Southwick, J.G.; Manke, C.W. Molecular degradation, injectivity, and elastic properties of polymer solutions. *SPE Reserv. Eng.* **1988**, *3*, 1–193. [CrossRef]
9. Stavland, A.; Jonsbraten, H.; Lohne, A.; Moen, A.; Giske, N.H. Polymer flooding-flow properties in porous media versus rheological parameters. In Proceedings of the SPE EUROPEC/EAGE Annual Conference and Exhibition, Barcelona, Spain, 14–17 June 2010.
10. Zamani, N.; Kaufmann, R.; Kosinski, P.; Skauge, A. Mechanisms of non-newtonian polymer flow through porous media using navier-stokes approach. *J. Dispers. Sci. Technol.* **2015**, *36*, 310–325. [CrossRef]
11. Skauge, T.; Skauge, A.; Salmo, I.C.; Ormehaug, P.A.; Al-Azri, N.; Wassing, L.M.; Glasbergen, G.; Van Wunnik, J.N.; Masalmeh, S.K. Radial and linear polymer flow-influence on injectivity. In Proceedings of the SPE Improved Oil Recovery Conference, Tulsa, OK, USA, 11–13 April 2016.
12. Be, M.; Hincapie, R.E.; Rock, A.; Gaol, C.L.; Tahir, M.; Ganzer, L. Comprehensive evaluation of the eor polymer viscoelastic phenomenon at low reynolds number. In Proceedings of the SPE Europec Featured at 79th EAGE Conference and Exhibition, Paris, France, 12–15 June 2017.
13. Mungan, N. Shear viscosities of ionic polyacrylamide solutions. *Soc. Pet. Eng. J.* **1972**, *12*, 469–473. [CrossRef]
14. Smith, F.W. The behavoir of partially hydrolyzed polyacrylamide solutions in porous media. *J. Pet. Technol.* **1970**, *22*, 148–156. [CrossRef]
15. Ranjbar, M.; Rupp, J.; Pusch, G.; Meyn, R. Quantification and optimization of viscoelastic effects of polymer solutions for enhanced oil recovery. In Proceedings of the SPO/DOE Eighth Symposium on Enhanced Oil Recovery, Tulsa, OK, USA, 22–24 April 1992.
16. Sheng, J. *Modern Chemical Enhanced Oil Recovery: Theory and Practice*; Gulf Professional Pub.: Houston, TX, USA, 2010.
17. Walters, K.; Jones, D.M. The extensional viscosity behavior of polymeric liquids of use in eor. In Proceedings of the SPE International Symposium on Oilfield Chemistry, Houston, TX, USA, 8–10 February 1989.
18. Rodriguez, S.; Romero, C.; Sargenti, M.L.; Muller, A.J.; Saez, A.E.; Odell, J.A. Flow of polymer-solutions through porous-media. *J. Non-Newton. Fluid* **1993**, *49*, 63–85. [CrossRef]
19. Odell, J.A.; Muller, A.J.; Keller, A. Non-newtonian behavior of hydrolyzed polyacrylamide in strong elongational flows-a transient network approach. *Polymer* **1988**, *29*, 1179–1190. [CrossRef]
20. Chauveteau, G.; Moan, M. The onset of dilatant behavior in non-inertial flow of dilute polymer-solutions through channels with varying cross-sections. *J. Phys. Lett.* **1981**, *42*, L201–L204. [CrossRef]
21. Ferguson, J.; Walters, K.; Wolff, C. Shear and extensional flow of polyacrylamide solutions. *Rheol. Acta* **1990**, *29*, 571–579. [CrossRef]
22. Flew, S.; Sellin, R.H.J. Non-newtonian flow in porous media-a laboratory study of polyacrylamide solutions. *J. Non-Newton. Fluid Mech.* **1993**, *47*, 169–210. [CrossRef]
23. Skauge, T.; Kvilhaug, O.A.; Skauge, A. Influence of polymer structural conformation and phase behavoir on in-situ viscosity. In Proceedings of the IOR 18th European Symposium on Improved Oil Recovery, Dresden, Germany, 17 April 2015.
24. Lee, J.K.; Seo, G.T. Apparent elongational viscosity of dilute polymer solutions. *Korean J. Chem. Eng.* **1996**, *13*, 554–558. [CrossRef]
25. Heemskerk, J.; Rosmalen, R.; Janssen-van, R.; Holtslag, R.J.; Teeuw, D. Quantification of viscoelastic effects of polyacrylamide solutions. In Proceedings of the SPE Enhanced Oil Recovery Symposium, Tulsa, OK, USA, 15–18 April 1984.
26. Maerker, J.M. Shear degradation of partially hydrolyzed polyacrylamide solutions. *Soc. Pet. Eng. J.* **1975**, *15*, 311–322. [CrossRef]
27. Culter, J.D.; Mayhan, K.G.; Patterson, G.K.; Sarmasti, A.A.; Zakin, J.L. Entrance effects on capillary degradation of dilute polystrene solutions. *J. Appl. Polym. Sci.* **1972**, *16*, 3381–3385. [CrossRef]

28. Zaitoun, A.; Makakou, P.; Blin, N.; Al-Maamari, R.S.; Al-Hashmi, A.R.; Abdel-Goad, M.; Al-Sharji, H.H. Shear stability of eor polymers. *SPE J.* **2012**, *17*, 335–339. [CrossRef]
29. Seright, R.S.; Fan, T.G.; Wavrik, K.; Balaban, R.D. New insights into polymer rheology in porous media. *SPE J.* **2011**, *16*, 35–42. [CrossRef]
30. Seright, R.S. The effects of mechanical degradation and viscoelastic behavoir on injectivity of polyacrylamide solutions. *Soc. Pet. Eng. J.* **1983**, *23*, 475–485. [CrossRef]
31. Al Hashmi, A.R.; Al Maamari, R.S.; Al Shabib, I.S.; Masnsoor, A.M.; Zaitoun, A.; Al Sharji, H.H. Rheology and mechanical degradation of high-molecular-weight partially hydrolzed polyacrylamide during flow through capillaries. *J. Pet. Sci. Eng.* **2013**, *105*, 100–106. [CrossRef]
32. Seright, R.S.; Seheult, M.; Talashek, T. Injectivity characteristics of eor polymers. *SPE Reserv. Eval. Eng.* **2009**, *12*, 783–792. [CrossRef]
33. Seright, R.S.; Maerker, J.M.; Holzwarth, G. Mechanical degradation of polyacrylamides induced by flow through porous-media. *ACS Polym. Prepr.* **1981**, *22*, 30–33.
34. Hincapie, R.E.; Ganzer, L. Assessment of polymer injectivity with regards to viscoelasticity: Lab evaluations towards better field operations. In Proceedings of the EUROPEC 2015, Madrid, Spain, 1–4 June 2015.
35. Odell, J.A.; Muller, A.J.; Narh, K.A.; Keller, A. Degradation of polymer-solutions in extensional flows. *Macromolecules* **1990**, *23*, 3092–3103. [CrossRef]
36. Muller, A.J.; Odell, J.A.; Carrington, S. Degradation of semidilute polymer-solutions in elongational flows. *Polymer* **1992**, *33*, 2598–2604. [CrossRef]
37. Glasbergen, G.; Wever, D.; Keijzer, E.; Farajzadeh, R. Injectivity loss in polymer floods: Causes, preventions and mitigations. In Proceedings of the SPE Kuwait Oil & Gas Show and Conference, Mishref, Kuwait, 11–14 October 2015.
38. Martin, F.D. Laboratory investigations in the use of polymers in low permeability reservoirs. In Proceedings of the 49th Annual Fall Meeting of the Society of Petroleum Engineers of AIME, Houston, TX, USA, 6–9 October 1974.
39. Martin, F.D. Mechanical degradation of polyacrylamide solutions in core plugs from several carbonate reservoirs. *SPE Form. Eval.* **1986**, *1*, 139–150. [CrossRef]
40. Gumpenberger, T.; Deckers, M.; Kornberger, M.; Clemens, T. Experiments and simulation of the near-wellbore dynamics and displacement efficiencies of polymer injection, matzen field, austria. In Proceedings of the Abu Dhabi International Petroleum Conference and Exhibition, Abu Dhabi, UAE, 11–14 November 2012.
41. Jouenne, S.; Chakibi, H.; Levitt, D. Polymer stability after successive mechanical-degradation events. *SPE J.* **2017**. [CrossRef]
42. Noïk, C.; Delaplace, P.; Muller, G. Physico-chemical characteristics of polyacrylamide solutions after mechanical degradation through a porous medium. In Proceedings of the SPE International Symposium on Oilfield Chemistry, San Antonio, TX, USA, 14–17 February 1995.
43. Skauge, A.; Ormehaug, P.A.; Gurholt, T.; Vik, B.; Bondino, I.; Hamon, G. 2-D visualisation of unstable waterflood and polymer flood for displacement of heavy oil. In Proceedings of the SPE Improved Oil Recovery Symposium, Tulsa, OK, USA, 14–18 April 2012.
44. Chauveteau, G.; Kohler, N. Polymer flooding: The essential elements for laboratory evaluation. In Proceedings of the SPE Improved Oil Recovery Symposium, Tulsa, OK, USA, 22–24 April 1974.
45. Ewoldt, R.H.; Johnston, M.T.; Caretta, L.M. Experimental challenges of shear rheology: How to avoid bad data. In *Complex Fluids in Biological Systems: Experiment, Theory, and Computation*; Springer Science+Business Media: New York, NY, USA, 2015; pp. 207–241.
46. Morris, C.W.; Jackson, K.M. Mechanical degradation of poly-acrylamide solutions in porous media. In Proceedings of the SPE Symposium on Improved Methods of Oil Recovery, Tulsa, OK, USA, 16–17 April 1978.
47. Hincapie, R.E.; Duffy, J.; O'Grady, C.; Ganzer, L. An approach to determine polymer viscoelasticity under flow through porous media by combining complementary rheological techniques. In Proceedings of the SPE Enhanced Oil Recovery Conference, Kuala Lumpur, Malaysia, 11–13 August 2015.
48. Dupas, A.; Henaut, I.; Rousseau, D.; Poulian, P.; Tabary, R.; Argillier, J.-F.; Aubry, T. Impact of polymer mechanical degradation on shear and extensional viscosities: Toward better injectivity forecasts in polymer flooding operations. In Proceedings of the SPE International Symposium on Oilfield Chemistry, The Woodlands, TX, USA, 8–10 April 2013.

49. Hunt, J.A.; Young, T.S.; Green, D.W.; Willhite, G.P. Size-exclusion chromatography in the measurement of concentration and molecular weight of some eor polymers. *SPE Reserv. Eng.* **1988**, *3*, 835–841. [CrossRef]
50. Thomas, A.; Gaillard, N.; Favero, C. Some key features to consider when studying acrylamide-based polymers for chemical enhanced oil recovery. *Oil Gas Sci. Technol.* **2013**, *67*, 887–902. [CrossRef]
51. Dalsania, Y.; Doda, A.; Trivedi, J. Characterization of ultrahigh-molecular-weight oilfield polyacrylamides under different ph environments by use of asymmetrical-flow field-flow fractionation and multiangle-light-scattering detector. *SPE J.* **2017**. [CrossRef]
52. Rodriguez, L.; Antignard, S.; Giovannetti, B.; Dupuis, G.; Gaillard, N.; Jouenne, S.; Bourdarot, G.; Morel, D.; Zaitoun, A.; Grassl, B. A new thermally stable synthetic polymer for harsh conditions of middle east reservoirs: Part ii. Nmr and size exclusion chromatography to assess chemical and structural changes during thermal stability tests. In Proceedings of the SPE Improved Oil Recovery Conference, Tulsa, OK, USA, 9–10 May 2018.
53. Puls, C.; Clemens, T.; Sledz, C.; Kadnar, R.; Gumpenberger, T. Mechanical degradation of polymers during injection, reservoir propagation and production-field test results 8 th reservoir, austria. In Proceedings of the SPE Europec Featured at 78th EAGE, Vienna, Austria, 30 May–2 June 2016.
54. Yerramill, S.S.; Zitha, P.L.J.; Yerramilli, R.C. Novel insight into polymer injectivity for polymer In Proceedings of the SPE European Formation Damage Conference and Exhibition, Noordwijk, The Netherlands, 5–7 June 2013.
55. Seright, R.S. How much polymer should be injected during a polymer flood? In Proceedings of the SPE Improved Oil Recovery Conference, Tulsa, OK, USA, 11–13 April 2016.
56. Sorbie, K.S.; Roberts, L.J. A model for calculating polymer injectivity including the effects of shear degradation. In Proceedings of the SPE Enhanced Oil Recovery Symposium, Tulsa, OK, USA, 15–18 April 1984.

Paper-II:

Polymer Injectivity: Investigation of Mechanical Degradation of Enhanced Oil Recovery Polymers Using In-Situ Rheology

energies

MDPI

Article

Polymer Injectivity: Investigation of Mechanical Degradation of Enhanced Oil Recovery Polymers Using In-Situ Rheology

Badar Al-Shakry [1,2,*], Tormod Skauge [3], Behruz Shaker Shiran [2] and Arne Skauge [1,2,3]

1 Department of Chemistry, University of Bergen, Allegaten 41, 5007 Bergen, Norway; Arne.Skauge@uib.no
2 NORCE Energy, CIPR, Nygårdsgaten 112, 5008 Bergen, Norway; besh@norceresearch.no
3 Energy Research Norway, Allegaten 41, 5007 Bergen, Norway; Tormod.Skauge@energyresearch.no
* Correspondence: Badar.Al-Shakry@uib.no; Tel.: +47-5558-3672

Received: 22 November 2018; Accepted: 19 December 2018; Published: 24 December 2018

Abstract: Water soluble polymers have attracted increasing interest in enhanced oil recovery (EOR) processes, especially polymer flooding. Despite the fact that the flow of polymer in porous medium has been a research subject for many decades with numerous publications, there are still some research areas that need progress. The prediction of polymer injectivity remains elusive. Polymers with similar shear viscosity might have different in-situ rheological behaviors and may be exposed to different degrees of mechanical degradation. Hence, determining polymer in-situ rheological behavior is of great significance for defining its utility. In this study, an investigation of rheological properties and mechanical degradation of different partially hydrolyzed polyacrylamide (HPAM) polymers was performed using Bentheimer sandstone outcrop cores. The results show that HPAM in-situ rheology is different from bulk rheology measured by a rheometer. Specifically, shear thickening behavior occurs at high rates, and near-Newtonian behavior is measured at low rates in porous media. This deviates strongly from the rheometer measurements. Polymer molecular weight and concentration influence its viscoelasticity and subsequently its flow characteristics in porous media. Exposure to mechanical degradation by flow at high rate through porous media leads to significant reduction in shear thickening and thereby improved injectivity. More importantly, the degraded polymer maintained in-situ viscosity at low flow rates indicating that improved injectivity can be achieved without compromising viscosity at reservoir flow rates. This is explained by a reduction in viscoelasticity. Mechanical degradation also leads to reduced residual resistance factor (RRF), especially for high polymer concentrations. For some of the polymer injections, successive degradation (increased degradation with transport length in porous media) was observed. The results presented here may be used to optimize polymer injectivity.

Keywords: enhanced oil recovery (EOR); polymer flooding; injectivity; rheology; viscoelasticity; non-Newtonian flow; mechanical degradation; HPAM

1. Introduction

In today's oil industry, chemical enhanced oil recovery techniques such as polymer flooding play a substantial role in promoting oil production. This is attributed to the achieved improvement on sweep efficiency that boosts oil production over conventional waterflooding. In such a process, water-soluble polymers are added to viscosify injected water in order to achieve lower viscosity contrast between injected water and displaced oil, and therefore a favorable mobility ratio [1]. Besides mobility control, high viscosity polymers are required for better conformance control relevant to heterogeneous reservoirs with high permeability variations such as the presence of thief zones [2].

There are two types of polymers suit enhanced oil recovery (EOR) applications which are: biopolymers, e.g., xanthan, and synthetic polymers, e.g., partially hydrolyzed polyacrylamide (HPAM). Regardless of the nature and differences in the molecular structure of these two polymers, polymer viscosity is the main physical property in the context of polymer flooding. Polymer viscosity depends on polymer molecular structure, molecular weight [3], polymer concentration [4], salinity [5,6], temperature [7,8], degree of hydrolysis [9], pH [10], flow model and type of forces dominating the flow [11].

While xanthan is well-known to be viscous dominated, HPAM is strongly influenced by both viscous and elastic properties [12]. It is essential to understand the significance and consequences when HPAM fluids become elastic dominated. HPAM viscoelasticity is important for many applications in the oil industry in general (e.g., drag reduction, drilling, etc.) and specifically in EOR applications such as polymer flooding [1,13–16], Low Salinity Polymer (LSP) flooding [17,18] and Alkaline-Surfactant-Polymer (ASP) flooding [19,20]. In polymer flooding, HPAM viscoelasticity is believed to contribute to higher oil recovery in general and some claim that it might reduce residual oil saturation due to promoting pulling effect mechanisms [21–24]. HPAM shear thickening behavior may, in some cases, contribute to improving front stability and oil recovery [25]. On the other hand, the significant pressure gradient associated with shear thickening phenomena can limit polymer injection, cause wellbore damage or fracturing. The influence of mechanical degradation on shear rheology will be discussed in this paper.

Polymer Injectivity and Mechanical Degradation

Polymer injectivity is a measure of how easily a polymer solution can be delivered into a reservoir formation [26]. It is also a measure of how fast polymer solution can be injected and propagate through the reservoir. It is a critical task because a decline in injectivity can turn the predicted cashflow of polymer flooding projects negatively [27,28]. This is basically due to the delay of oil production or high pumping cost. Both aforementioned polymers (xanthan and HPAM) may suffer from injectivity problems for different reasons. For instance, the presence of microgels and impurities in xanthan may limit its injectivity [29]. However, HPAM viscoelasticity and retention are the main factors that restrict its injectivity. The design of polymer flooding projects has to cover some key aspects such as reservoir formation, oil saturation, injection strategy, polymer rheology, degradation, compatibility with other chemicals, economy, etc. [30]. This paper intends to investigate some of these aspects such as the link between polymer rheology and degradation.

The theories and observations associated with the characterization of flow of biopolymers such as xanthan are typically united in that xanthan has pseudoplastic rheological behavior in porous media similar to that predicted in pure shear flow such in the rheometer [31–35]. However, the situation is more complicated for HPAM due to its viscoelastic nature and the complexity of porous media. Despite the rich literature of polymer flow in porous media, the theoretical interpretations are still conflicting on the analysis of the observed HPAM in-situ flow behaviors. HPAM polymers are well-known to have high polydispersity index [36] and possess long relaxation time. HPAM has a flexible molecular structure and highly sensitive to shear environments. When HPAM flows in porous media, it is exposed to both shear and elongational deformations as it is transported through converging-diverging (C↔D) flow channels [36,37]. This results in successive expansion and contraction (E↔C) of polymer conformation as it flows through porous media. Figure 1 illustrates a schematic representation of typical flow regions that are exhibited by HPAM with respect to shear rate. The polymer exhibits near-Newtonian behavior at which its apparent viscosity is independent of imposed shear rates ($\dot{\gamma} < \dot{\gamma}_{c1}$). As the shear rate increases further, apparent viscosity decreases and the polymer solution exhibits shear thinning behavior. During shear thinning, polymer molecules start to disentangle with increasing shear rate until approaching another Newtonian plateau at which the state of disentanglement is very high. However, above $\dot{\gamma}_{c2}$, the extensional flow becomes predominant at which polymer chains have insufficient time to recoil and align with the flow causing coil-stretch (C↔S) transition that yields in a gradual increase of apparent viscosity with shear rate. The normal

stresses that are responsible for chain stretch cause a rise in the extensional viscosity and consequently cause pressure buildup and high apparent viscosity (shear thickening behavior). If the stretch rates that are associated with shear thickening behavior are high enough, chain stretch might evolve into chain fragmentation. Chain scissions due to mechanical degradation yields in viscosity loss as can be seen at high shear rates displayed in Figure 1. These flow phenomena are detailed elsewhere [11,37–40]. The large strain forces cause large molecules to shear preferentially. Literature reviews on polymer mechanical degradation [41,42] showed that the assessment of mechanical degradation is complex, particularly in the presence of entanglements and concentrated conformational regimes. It is very important to understand how HPAM macromolecules contribute to changing its flow phenomena and increasing its apparent viscosity at high flow rates that scales several folds higher than predicted in simple shear flow such that generated by the rheometer.

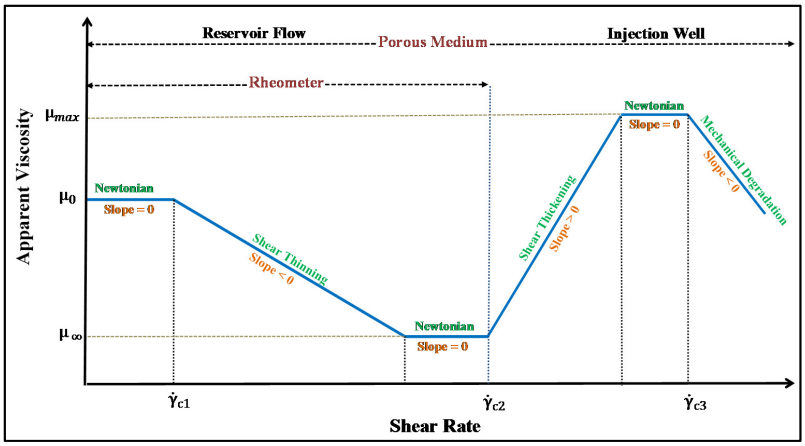

Figure 1. Schematic diagram of HPAM apparent viscosity vs shear rate.

In addition to HPAM shear stability discussed above, the dimensions and conformation of HPAM molecules strongly depend on the salt concentration and types of TDS existing in solution. HPAM is a negatively charged polymer, and therefore at the presence of salts, the repulsion forces among polymer chains decrease due to shielding negative charges which cause coiling-up phenomena [43]. In some cases, the presence of salts in high concentration might lead to phase separation (e.g., gel-formation) [44]. The reduction in viscosity due to salinity is more pronounced at the presence of divalent cations (e.g., Ca^{2+}, Mg^{2+}, etc.) compared to that of monovalent cations like Na^{+} [43].

The previous study by Skauge et al. [45] demonstrated a combination of experiments for investigating the contributions of polymer molecular weight and concentration conformational regimes to its rheological properties. The measurements included shear viscosity (rotational rheometer), dynamic viscosity (small amplitude oscillatory shear SAOS) and in-situ rheology (Bentheimer cores). The study classified the investigated polymer solutions into different conformational regimes; dilute, semi-dilute, concentrated semi-dilute and gel solutions, based on critical overlap concentration (C^*). SAOS measurements indicated whether the polymer solution is viscous or elastic dominated at a particular concentration. The initial studies showed a correlation between bulk elastic modulus G' and apparent shear thickening. The more elastic polymer exhibited higher resistance factor in porous media. The study also revealed that polymer conformation regime has a high influence on its in-situ rheological behavior. Shear viscosity data showed that mechanical degradation was high for high Mw polymer dissolved in high salinity brine. Also, mechanical degradation was lower for concentrated

solutions. Recent review with current knowledge on HPAM polymers flow in porous media concerning theoretical and experimental aspects is given by Skauge et al. [46].

One of the most critical aspects of HPAM polymer is mechanical degradation. Such an effect directly influences polymer viscosifying efficiency as well as alters its rheological properties. Both HPAM shear thickening behavior and mechanical degradation are well reported [12,47–50]. Mechanical degradation might occur along with the onset of shear thickening [51]. Onset of shear thickening has received a great attention in the literature as it is an indication of viscoelasticity in porous medium [50,52–55]. Any alteration of the molecular structure of HPAM through exposing it to shear rate above or below the onset of shear thickening may change its apparent shear thickening behavior [56]. Preshearing polymer by exposing HPAM to wellbore mechanical degradation is a suggested approach to improve its viscoelastic properties which promotes its injectivity [57]. Despite the efforts that have been made to understand and model polymer mechanical degradation, the dependence of polymer mechanical degradation on polymer Mw, MWD, concentration, and polymer transport distance in porous media requires more investigation [12,26,49].

The impact of mechanical degradation on polymer average Mw and molecular weight distribution (MWD) were examined in different studies. For example, Seright et al. [58] investigated the mechanical degradation effect on polymer Mw and MWD by using gel permeation liquid chromatography (GPC). The degraded solutions showed narrower MWD compared to that of undegraded samples. Hence, degraded polymer solution has a lower polydispersity. This concept was also confirmed by size exclusion chromatography (SEC) [59] and asymmetric flow field-flow fractionation (AF4) [30,60–62]. Reduction of Mw or change in MWD is the reason for the observed reduction in screen factor [12,63] that correlates with reduction of resistance factor as well.

Noïk et al. [36] investigated the effect of Mw, concentration and different types of solvents on the mechanical degradation of HPAM in short glass cylinders packed with sand particles. The high Mw polymers were subjected to wellbore mechanical degradation through successive reinjection into porous media. Reinjection process represents the evolution of degradation as a function of residence time or the length of porous media. Degradation was assessed by observing the change in intrinsic viscosity of solutions before and after degradation. They found that the degree of degradation is independent of concentration for dilute solutions and was only dependent on Mw. However, for concentrated solutions, the degradation increases with concentration and has less dependency on average Mw.

Several studies attributed HPAM mechanical degradation to the polymer degradation in sandface, and therefore, understated the effect of polymer residence time or transported distance in porous media [12,38,49,64,65]. For example, Maerker [12] attributed mechanical degradation to the first 0.5 inch of porous media while Warner [64] attributed it to the first inch of unperforated wellbore based on studies performed in Berea rock. Müller et al. [51] reported that the mechanical degradation of HPAM polymers increased with travel distance and progressively degraded until reached an asymptotic value that depends on the stretch rate which related to Reynold's number. A recent study given by Jouenne et al. [66] highlighted the observation of mechanical degradation at entry face and limited it for the first 6mm of porous media based on studies performed in a ceramic disk. However, Al-Shakry et al. [67] conducted experimental studies using HPAM polymers that showed high Mw polymer underwent successive degradation as reinjected into the porous media. This suggests that the degree of degradation may depend on exposure time and number of exposures to high strain beside polymer Mw and concentration. The findings were also in line with Åsen et al. [68]. The dependence of mechanical degradation on travelled distance in porous media has a significant practical consequences specifically when considering the effect on large scale medium such as field conditions. These observations were also supported by other studies based on analyzing shear viscosity data alone [69–71].

Despite the current efforts made both experimentally and theoretically to clarify the problem of mechanical degradation, the current understanding is not complete, and further analyses are required.

This paper extends our previous work [67] that provides a basis for this study on experimental investigation of the impact of mechanical degradation on polymer in-situ rheology. This work extends the analyses to address the influence of polymer physicochemical properties, particularly molecular weight and concentration on polymer mechanical degradation and its in-situ behavior. Particular attention was given for the impact of preconditioning the polymer solution prior to injection into the porous media on polymer in-situ rheology. The study was performed in a realistic porous medium using high preamble linear Bentheimer core plugs. The results from this paper give an insight into in-situ rheological behavior of commercial HPAM polymers, which may be beneficial in polymer screening and designing of polymer flooding EOR operations. The results from this study may also serve as useful input for simulation models.

2. Material and Methods

2.1. Synthetic Brine

Synthetic brine of 1wt.% NaCl was prepared and filtered through a 0.45 µm cellulose nitrate filter. The brine composite (NaCl powder) was obtained from Sigma-Aldrich (Munich, Germany). The prepared filtered brine was employed in the preparation of bulk polymer solutions, core saturation and permeability measurements.

2.2. Polymer Preparation

Three types of partially hydrolyzed polyacrylamide (HPAM) with 30% degree of hydrolysis were employed in this study with different concentrations as shown in Table 1. These polymers are Flopaam 3330 s, 3430 s and 3630 s which are donated as polymer A, B and C, respectively. These polymers were received in powder form from SNF Floerger. Each polymer was prepared with low and high concentration within semi-dilute region to provide a low and high degree of entanglements, respectively. The selected concentration for each polymer was based on overlap concentration (C^*) determined in earlier studies performed by Skauge et al. [45].

The polymer stock solution of 5000 ppm was prepared by gradually dissolving 3.0 g of polymer powder into the vortex of 1 wt.%NaCl brine under vigorous stirring until the vortex became invisible. The polymer solution was left under slow mixing at a stirring speed of 150 rpm for at least 24 h before dilution into required concentration. The polymer was thoroughly sealed during the preparation. The prepared aqueous polymer solution was incubated at 5 °C inside a fridge and used within two weeks of preparation to avoid any chance of chemical degradation.

Table 1. Molecular weights and concentrations of polymers.

Polymer	Polymer (Flopaam) Type	Molecular Weight (10^6 g/mol = MDa)	Polymer Concentration (mg/L = ppm)
A	3330 s	8	1000 4000
B	3430 s	12	1000 3000
C	3630 s	18	500 1000

2.3. Shear Viscosity Measurements

Shear viscosity measurements were carried out at room temperature (22 °C) by using a Kinexus Pro Rheometer (Malvern, UK). The rheometer is equipped with different geometries which make the measurements more accurate and convenient to conduct based on fluid types and viscosity. Hence, double-gap geometry was used during the measurements of viscosities lower than 10 cP and cone-plate

geometry was used for measuring viscosities higher than 10 cP. The viscosity measurements were fitted by power law model given below:

$$\eta = K\dot{\gamma}^{n-1} \quad (1)$$

where, η is shear viscosity (cP), $\dot{\gamma}$ is shear rate (s^{-1}), K is the consistency index ($cP.s^{(n-1)}$) and n is the flow behavior index (dimensionless).

2.4. Porous Medium

The experiments were conducted in linear Bentheimer outcrop cores with an average length and diameter of 10 cm and 3.8 cm, respectively. Similar cores of Bentheimer with shorter length of 5 cm were also used for prefiltering and preshearing processes. Details of each core are given in results and discussion section.

2.5. Experimental Procedures

The experimental setup displayed in Figure 2 mainly consists of Quizix-QX dual piston pump, transfer cylinder, core holder, pressure transducers, back pressure regulator and effluent collector. Note that, backpressure regulator was used during permeability measurements to dissolve any air in the setup and it was removed during polymer injection to avoid polymer degradation.

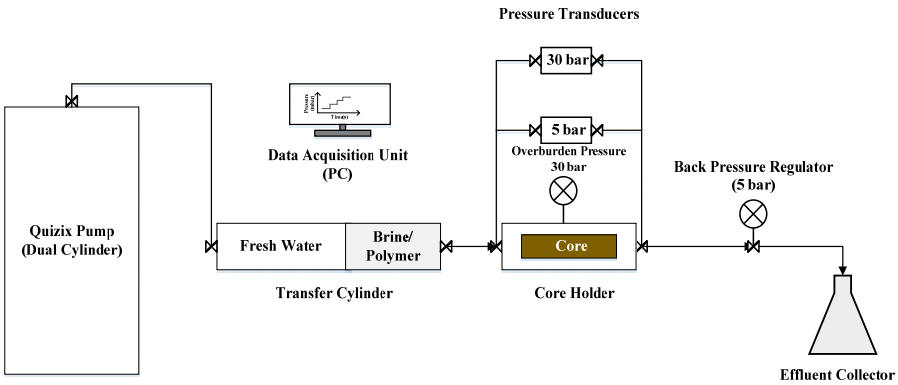

Figure 2. Schematic diagram of core flooding apparatus used for in-situ rheology experiments.

Core flood experiments were conducted at room temperature (22 °C) and consisted of three stages as detailed in the previous study [67]. The core flood procedure was performed as follows:

2.5.1. Brine Pre-Flush

Before injecting the brine, the core plugs were vacuumed and saturated with brine for at least two days to ensure achieving ionic equilibrium between the core plug and brine followed by porosity measurements. Then, the core plug was mounted in the core holder and brine was injected at various flow rates to measure absolute permeability (K_{abs}) which was calculated according to Darcy's law (Equation (2)):

$$K_{abs} = \frac{Q \times \eta \times L}{\Delta P \times A} \quad (2)$$

where, Q is injection flow rate, η is fluid viscosity, ΔP is pressure drop across the core, L and A are core length and cross-sectional area, respectively. By considering Darcy velocity (v_D) which is also

known as superficial flow velocity as Q/A, the average or interstitial velocity (v) is given in Equation (3), where ϕ is the porosity of porous media:

$$v = \frac{v_D}{\phi} \tag{3}$$

Darcy velocity v_D was also applied to calculate reservoir shear rate $\dot{\gamma}$. A conventional formula was used to estimate reservoir formation shear rate [65]:

$$\dot{\gamma} = \alpha \frac{4\, v_D}{\sqrt{8\, K_{abs}\, \phi}} \tag{4}$$

where, α is formation shape factor which is assumed 2.5 for Bentheimer sandstone [1,38].

2.5.2. Polymer Injection

The investigated polymers were pretreated first before injection into the main cores. Pretreatment processes consisted of prefiltering, reinjecting and preshearing as illustrated in Figure 3. Pre-filtering and preshearing processes were performed on short cores (L = 5 cm) at low and high flow rates, respectively. Reinjected polymer has been prefiltered first in short core then sheared at high flow rate in long core (L = 10 cm). The flow rate used in prefiltering process was (Q = 0.5 cc/min, v_D = 0.6 m/day) whereas the flow rates applied in preshearing and reinjecting are given in Table 2. Recall that the purpose of prefiltering was to remove any microgel in the solution and filter out any possible large Mw species. This step represents available commercial polymers that are utilized in field applications. Prefiltered polymer solutions also serve as a baseline for comparison with presheared and reinjected solutions. Preshearing was carried out to induce partial degradation in which large Mw species in the solution are likely filtered and mechanically degraded to lower Mw species. While reinjection was designed to evaluate the evolution of polymer degradation with respect to the residence time of polymer solution, core characteristic length, number of passes and multi entry effects.

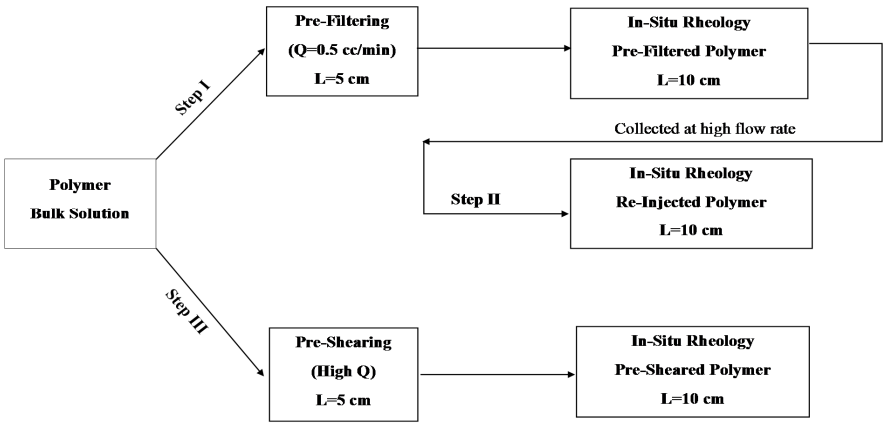

Figure 3. Polymer pretreatment processes.

Table 2. Applied flow rates for presheared and reinjected polymer solutions.

Polymer	A		B		C	
Concentration (ppm)	1000	4000	1000	3000	500	1000
Q (cc/min)	26	22	15	7	12	6
v_D (m/day)	33.5	28.4	19.4	9.0	15.5	7.7

Pretreated polymer solution was injected into the main core at low flow rate (Q = 0.5 cc/min, $v_D = 0.6$ m/day) for at least 2 PV. This was performed to satisfy polymer adsorption level in the core and achieving steady-state condition (stable differential pressure over time). Then, the injection flow rate was increased gradually to achieve highest flow rate given in Table 2 and then decreased in a stepwise manner from highest to lowest flow rate. The polymer injection over wide flow rates was performed to simulate the velocities that are anticipated near wellbore region and deep in the reservoir. Resistance factor (RF) was calculated as follows [72]:

$$RF = \frac{\Delta P_p}{\Delta P_w} \quad (5)$$

where, ΔP_p is the pressure drop of the polymer during polymer flow and ΔP_w is the pressure drop of the brine before polymer flow in the porous medium.

After injecting for at least 1 PV for each step rate and steady-state condition was achieved, effluent samples of were collected at different flow rates and their shear viscosity was measured by the rheometer. The following equation was used to express the change in shear viscosity (mechanical degradation) [66]:

$$Deg(\%) = \frac{\eta_i - \eta_e}{\eta_{i-}\ \eta_w} \times 100 \quad (6)$$

where, η_i is injected solution viscosity, η_e is effluent viscosity and η_w is brine viscosity which was measured to be 1.04 cP. The viscosity data used in this equation were measured at the shear rate of 10 s^{-1}.

2.5.3. Brine Post-Flush

After terminating the polymer injection, tapering was performed by injecting 5 PV of diluted polymer effluent with 50 and 25% of initial effluent concentration. During tapering the injection of the diluted polymer was performed at low flow rate (Q = 1.0 cc/min, $v_D = 1.3$ m/day) for 1 PV then gradually increased to higher flow rates. After tapering with polymer, brine was injected at low flow rate (Q = 0.5 cc/min, $v_D = 0.6$ m/day) for 1 PV then the injection rate was increased in a stepwise manner. The final permeability to brine was measured after flushing 5 PV of brine at high rates proceeded by two steps of tapering. Tapering was performed in an effort to approach 'true' residual resistance factor (RRF) which was calculated using Equation (7) [72]:

$$RRF = \frac{K_{wi}}{K_{wf}} \quad (7)$$

where, K_{wi} and K_{wf} are the absolute permeability's to brine before and after polymer flow in porous media, respectively. These values were calculated by using Equation (2).

3. Results and Discussion

3.1. Shear Viscosity

The bulk shear viscosity of polymer solutions was measured in the rheometer at a wide range of shear rates as shown in Figure 4. At the mid-range of shear rates, all the solutions exhibited a predominant shear thinning behavior. The measurements were showed a good fit to the power law model (Equation (1)) using the fitting parameters given in Table 3. Concentrated solutions showed a higher slope of shear thinning behavior compared to the solutions with lower concentration as seen in Figure 4. Accordingly, the flow behavior index n decreases as polymer concentration increases (see Table 3) and vice versa for the consistency index K. This is due to the high degree of entanglements present in concentrated solutions. Hence polymer molecules are more sensitive to imposed shear rate that reduces the degree of entanglements resulting in lower viscosity with increasing flow rates [73].

Shear viscosity increases with increasing polymer molecular weight or concentration. For a given polymer concentration of 1000 ppm, the shear viscosity of polymer A, B and C were 8.4, 13.6 and 19.0 cP, respectively, measured at $\dot{\gamma}$ = 10 s^{-1}. We are using a shear rate of 10 s^{-1} in this study as a reference of reservoir relevant shear rate. The increase of viscosity with Mw is ascribed to increase in hydrodynamic volume and charge density per molecule. On the other hand, the increase of viscosity with respect to concentration is ascribed to the increase of the number of molecules that increases the interaction and repulsion forces among negatively charged polymer molecules [6].

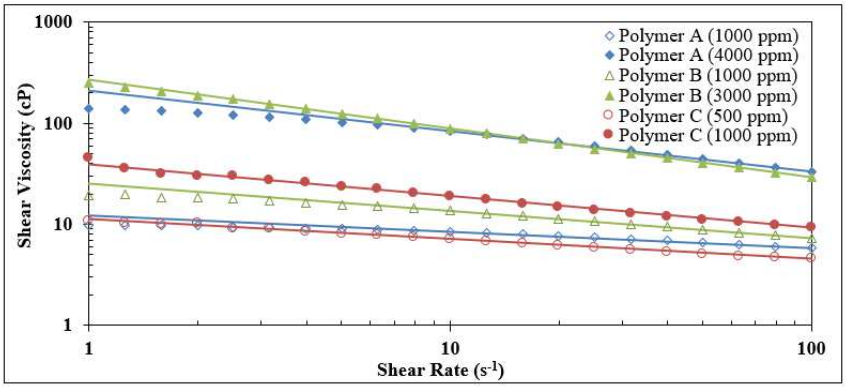

Figure 4. Shear viscosity of prefiltered bulk solutions A, B and C in 1 wt. % NaCl at 22 °C. Solid lines represent the power law model.

Table 3. Power law fitting parameters K, n and coefficient of determination R^2.

Polymer	A		B		C	
Concentration (ppm)	1000	4000	1000	3000	500	1000
K ($cP.s^{(n-1)}$)	12.30	207.98	25.17	268.52	11.17	38.99
n	0.84	0.60	0.73	0.52	0.80	0.69
R^2	0.93	0.95	0.97	1.00	0.99	0.98

3.2. In-Situ Polymer Rheology

3.2.1. Apparent Viscosity in Porous Medium vs Bulk Viscosity in Rheometer

In this study, polymer apparent viscosity in the porous medium is represented by resistance factor (RF) as a function of interstitial velocity. However, translating polymer flow velocity in porous medium to shear rate is required to correlate flow velocity in porous medium with the shear rate in rheometer. Determining the shear rate in porous medium is challenging due to many factors such as wide pore size distributions, tortuosity and complexity of porous media. A conventional formula given in Equation (4) was used to estimate reservoir formation shear rate. Figure 5 shows the viscosity profiles of polymer B (3000 ppm) in porous medium versus bulk shear viscosity in the rheometer. Resistance factor and apparent viscosity profiles of polymer in porous media were consistent. The polymer exhibited a predominantly shear thinning behavior in rheometer while it exhibited different flow behaviors in porous media. At shear rates $\dot{\gamma}$ < 30 s^{-1}, the polymer exhibited shear thinning behavior in porous media while shear thickening behavior was observed at shear rates $\dot{\gamma}$ > 52 s^{-1}. A near-Newtonian behavior was observed during the transition between shear thinning to shear thickening behaviors. Both in-situ behaviors (near-Newtonian and shear thickening) in porous medium were not predicted by shear rheology. This is expected due to the different nature of flow exists in porous medium which is not purely shear flow as in rheometer [37].

Figure 5 shows bulk shear viscosity decreased while the apparent viscosity increased. For example, at $\dot{\gamma} \approx 400\ s^{-1}$, bulk shear viscosity was 16.7 cP while apparent viscosity was ~300 cP which is more than 10 times higher than bulk shear viscosity. This indicates the contribution of extensional viscosity to apparent viscosity at high flow rates. Polymer apparent viscosity is a combination of shear and extensional viscosity of viscoelastic polymers [1].

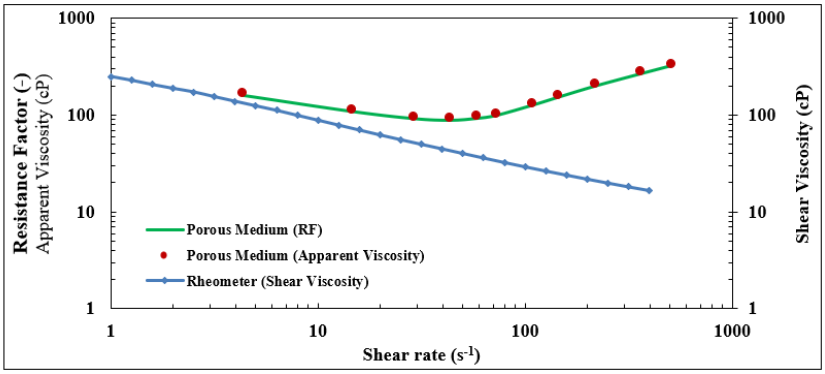

Figure 5. Viscosity profiles of prefiltered Polymer B (3000 ppm) as measured in the porous medium and in bulk.

3.2.2. Flow of Semi-Dilute Polymer Solutions

Figure 6 depicts the resistance factor of polymer A, B and C versus interstitial velocity. The concentration of polymer A and B was 1000 ppm while for polymer C was 500 ppm. Shear viscosity data of prefiltered solutions A, B and C were 8.4, 13.5 and 7.1 cP, respectively, as tabulated in Table 4. At low velocities all the polymers exhibited near-Newtonian behavior followed by shear thickening at high velocities. This represents the general behavior of polymer flow in porous medium for semi-dilute solutions. Similar observations have been reported elsewhere [11,12,49,50,74]. The RF curves are strongly dependent on polymer molecular weight. For example, RF at reservoir velocities of polymer A was 2 times lower than that of polymer B which was ~ 18.4. Similarly, shear thickening behavior was more dramatic for polymer C with high Mw. This could be observed from the earlier onset of shear thickening for polymer C (v_c = 2.5 m/day) to that of polymers B and A (v_c = 4.1 and 7.0 m/day, respectively). Moreover, the stronger viscoelastic properties of high Mw polymer C can be observed from the slope of apparent shear thickening 7.7 $(m/day)^{-1}$ compared to 3.5 and 0.5 $(m/day)^{-1}$ for polymer B and A, respectively. This yields higher RF values for polymer C (RF ~196) at high flow rate compared to that of lower Mw polymers.

It is worth noting that effluents shear viscosity of prefiltered solutions for polymers A and B did not show significant mechanical degradation at the investigated flow velocities. However, prefiltered polymer C showed degradation at high velocities (Deg = 21.7%). This could be the reason for lower RF values for reinjected polymer C in Figure 6c.

Reinjection process was carried out to simulate the polymer flow deep in the reservoir (radially distant from the wellbore). This process also demonstrates the effect of exposure time at high shear on polymer degradation. In this process, the polymer solution passed two cores at different flow rates before measuring in-situ rheology in the main core. The first core (5 cm length) was used for the pre-filtering process at low flow rate (Q = 0.5 cc/min), while the second core (10 cm length) was used as shearing media. Hence, this process differs from the presheared polymer process in which the polymer solution was sheared in a short core and at high flow velocity before the measurement of in-situ rheology in the main core (see Figure 3 for details). Therefore, the results will be compared with preshearing process. Pretreatment methods (reinjection and preshearing) caused a reduction

of RF values at high velocities while RF values were similar to prefiltered solution at low velocities. This could be clearly seen from the shift of the onset to higher velocities and reduction on the degree of shear thickening. In Figure 6a, RF profile of reinjected polymer A indicates more degradation occurred compared to presheared solution. This is analogous to the observation shown in Figure 6c for polymer C at low concentration. This confirms the occurrence of successive degradation as the polymer was reinjected in porous media which is inline with some other studies [68,75]. However, this was not observed for polymer B. The successive polymer degradation observed in this study in contrast to the current understanding of mechanical degradation which is mainly confined to sand face degradation and is believed to be independent of travelled distance in porous media [38,49,66].

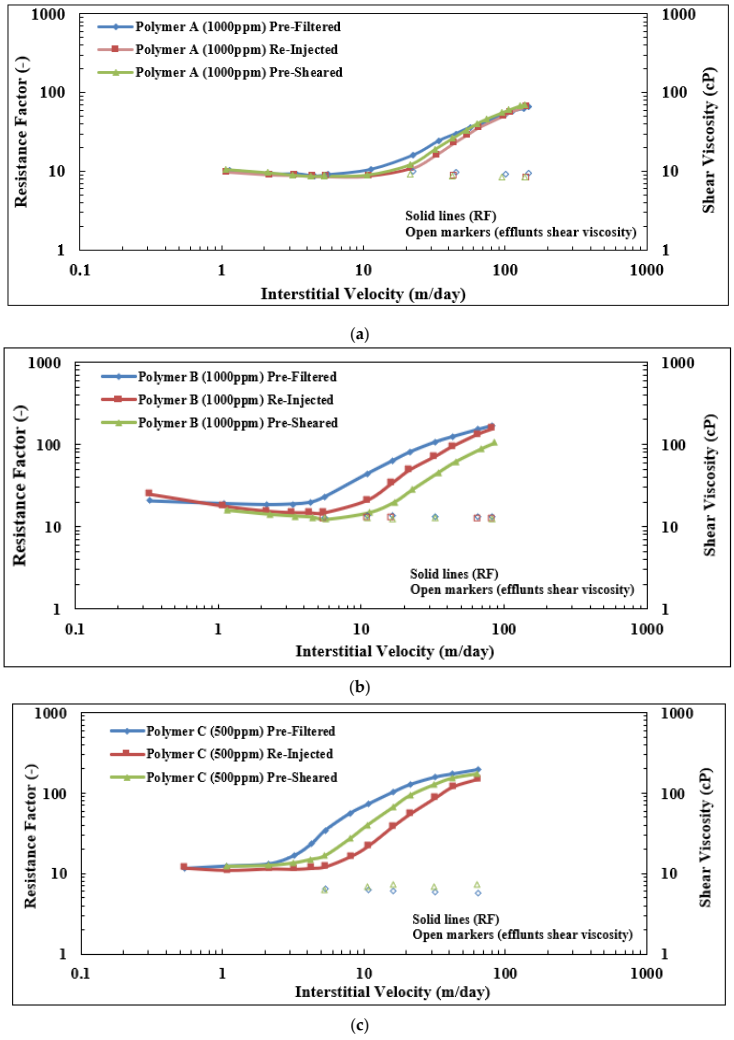

Figure 6. Resistance factor versus interstitial velocity for semi-dilute polymers A, B and C. Open markers indicate effluent shear viscosity for the given velocity measured at $\dot{\gamma} = 10\ s^{-1}$. (**a**) Polymer A (Mw ≈ 8 MDa, Concentration = 1000 ppm); (**b**) Polymer B (Mw ≈ 12 MDa, Concentration = 1000 ppm); (**c**) Polymer C (Mw ≈ 18 MDa, Concentration = 500 ppm).

The difference between shear viscosity of effluents and resistance factor values at low velocities was different depending on polymer type. This indicates that the difference in polymer retention correlates with the increase of polymer molecular weight. That is, the difference between RF values and effluent viscosity at similar velocities increases with the increase of polymer molecular weight. For instance, Newtonian RF values were ~9, 18, 12 with bulk shear viscosity of 8.4, 13.5 and 7.1 cP for prefiltered polymers A, B and C, respectively.

Table 4. Cores and viscoelastic properties of semi-dilute polymers at concentration of 1000 ppm for polymers A and B, and 500 ppm for polymer C.

Experiment	L (cm)	D (cm)	ϕ (-)	K_{wi} (Darcy)	K_{wf} (Darcy)	RRF (-)	η_i (cP)	η_e (cP)	v_c (m/day)	m $(m/day)^{-1}$
Polymer A Pre-Filtered	9.28	3.79	0.23	1.81	1.12	1.61	8.44	8.19	6.98	0.54
Polymer A Re-Injected	9.74	3.79	0.23	2.26	1.16	1.95	8.19	8.28	16.92	0.53
Polymer A Pre-Sheared	10.22	3.77	0.24	2.40	1.48	1.62	8.52	8.42	15.79	0.66
Polymer B Pre-Filtered	9.82	3.79	0.23	2.16	0.96	2.24	13.57	13.31	4.06	3.50
Polymer B Re-Injected	9.57	3.79	0.23	2.08	1.24	1.68	13.31	12.75	7.69	2.28
Polymer B Pre-Sheared	10.27	3.77	0.23	2.80	1.54	1.82	13.54	12.75	11.99	1.46
Polymer C Pre-Filtered	9.82	3.77	0.24	2.57	1.40	1.84	7.11	5.79	2.51	7.68
Polymer C Re-Injected	9.78	3.77	0.24	2.39	1.28	1.86	5.79	-	6.71	3.00
Polymer C Pre-Sheared	9.72	3.77	0.24	2.25	0.82	2.75	7.13	7.21	4.00	4.32

3.2.3. Flow of Concentrated Polymer Solutions

The behavior of concentrated polymer solutions ($C >> C^*$) in porous media seems to be dominated by shear viscosity that overrides their elastic properties. In such solutions, the interaction between polymer molecules is dominant and polymer chains are entangled [11]. Figure 7 shows apparent shear thinning, near-Newtonian and shear thickening behaviors which become very important flow aspects for high concentrated polymer solutions with high shear viscosity. For instance, Figure 7a depicts the flow of polymer A at concentration of 4000 ppm in porous media, in particular parlance, it exhibits pseudo-gel behavior. As this figure shows for prefiltered polymer A, at high velocities ($v > 31.0$ m/day) weak shear thickening behavior is observed with slight increase in RF values compared to near-Newtonian plateau at flow velocities $5.7 < v < 31.0$ m/day. RF values corresponding to shear thickening behavior are lower than shear viscosity. This suggests that the contribution of extensional viscosity is lower than that of shear viscosity which dominates the polymer flow behavior. Below $v < 5.7$ m/day, the RF values increase with decreasing flow velocity indicating strong shear thinning behavior. Similar trend was observed for relatively higher Mw polymer B except that the shear thickening becomes stronger (see Figure 7b). This confirms that the concentration or in other words, solution conformational regime, has an obvious influence on polymer in-situ rheology. However, concentrated high Mw polymer C (Figure 7c) exhibits near-Newtonian behavior at lower shear rates that are analogous to semi-dilute polymers discussed earlier without the presence of shear thinning behavior. This could be ascribed to lower shear viscosity of polymer C at 1000 ppm compared to the other two polymers A and B. Higher molecular weight polymers possess higher RF at high velocity than the low Mw polymers with higher concentration. This also indicates the contribution of higher elastic properties such as elastic viscosity compared to that of lower Mw solutions.

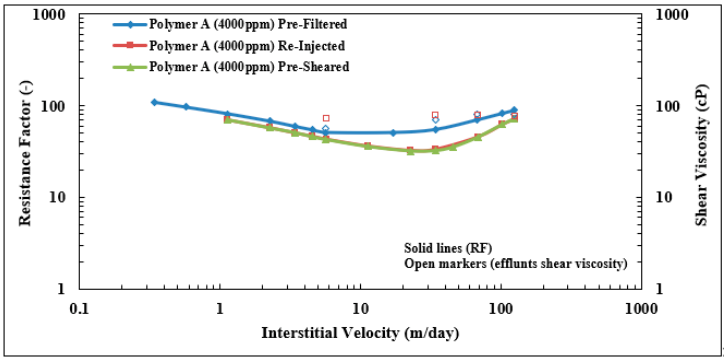

(**a**)

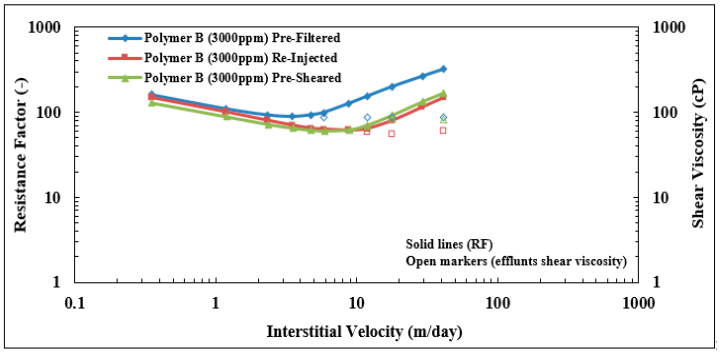

(**b**)

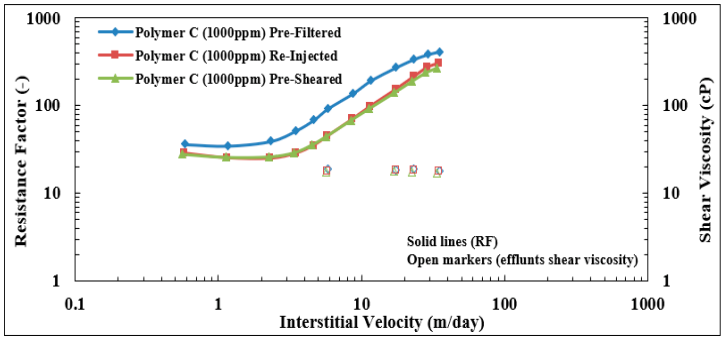

(**c**)

Figure 7. Resistance factor versus interstitial velocity for concentrated polymers A B and C at concentration of 4000 3000 and 1000 ppm, respectively. Open markers indicate effluent shear viscosity for the given velocity measured at $\dot{\gamma} = 10\ s^{-1}$. (**a**) Polymer A (Mw ≈ 8 MDa, Concentration = 4000 ppm); (**b**) Polymer B (Mw ≈ 12 MDa, Concentration = 3000 ppm); (**c**) Polymer C (Mw ≈ 18 MDa, Concentration = 1000 ppm).

The existence of shear thinning in porous media is conditional and argued by Seright et al. [76] at which they attribute shear thinning to the presence of micro-gels in polymer solution. However, the results in Figure 7 show a contradictory observation and confirm the existence of shear thinning

phenomena for concentrated solution in porous media even if the polymer has been pre-filtered or presheared (microgel-free).

Exposing the polymer to wellbore mechanical degradation alters its viscoelastic behavior through the shift of Newtonian plateau and onset of shear thickening to higher velocities as is seen in Figure 7 for both reinjected and presheared solutions A and B. However, insignificant alteration occurs on shear thinning part. Effluent viscosity of reinjected solution B suffers more degradation compared to presheared sample which could be due to attachment of backpressure device that might induce additional degradation to polymer solution [67]. RF curves of degraded solutions C (reinjected and presheared) are coincident which indicates that the solution tolerates wellbore mechanical degradation compared to semi-dilute solution with same polymer C discussed above (see Figure 6c). However, the RF curves of degraded solution C were lower than prefiltered solution which could be due to filtration effect and also lower RRF (see Table 5).

Table 5. Cores and viscoelastic properties of concentrated polymers A, B and C at concentration of 4000, 3000 and 1000 ppm, respectively.

Experiment	L (cm)	D (cm)	ϕ (-)	K_{wi} (Darcy)	K_{wf} (Darcy)	RRF (-)	η_i (cP)	η_e (cP)	v_c (m/day)	m $(m/day)^{-1}$
Polymer A Pre-Filtered	9.69	3.77	0.23	2.75	1.48	1.86	83.02	79.31	31.00	0.37
Polymer A Re-Injected	10.05	3.74	0.23	2.53	1.58	1.60	79.31	76.74	43.00	0.43
Polymer A Pre-Sheared	9.95	3.77	0.23	2.50	1.84	1.36	77.91	-	42.00	0.45
Polymer B Pre-Filtered	9.85	3.79	0.22	2.40	0.73	3.31	88.76	85.90	4.37	8.45
Polymer B Re-Injected	9.52	3.78	0.22	2.64	1.04	2.53	85.90	66.12	11.21	2.96
Polymer B Pre-Sheared	9.93	3.78	0.22	2.35	0.85	2.77	83.79	80.79	9.08	3.59
Polymer C Pre-Filtered	10.04	3.78	0.22	2.12	0.23	9.27	18.95	17.98	2.31	16.07
Polymer C Re-Injected	9.81	3.78	0.22	2.01	0.33	6.09	17.98	17.46	3.78	9.71
Polymer C Pre-Sheared	9.68	3.78	0.23	2.37	0.80	2.96	17.86	17.14	3.40	8.47

3.2.4. Onset and Slope of Shear Thickening Behavior

Figure 8 presents the resistance factor change for prefiltered polymers A, B and C at different concentrations. As this figure shows, RF is influenced by both polymer molecular weight and concentration. That is, RF gains strength with increasing Mw and concentration. This is inline with the increase in shear viscosity shown in Figure 4 where shear viscosity increases with increase in Mw and concentration. However, the impact of Mw and concentration on RF values in the porous media is a function of velocity. RF is dominated by molecular weight at high velocities to a greater extent than concentration and vice versa at low velocities below the onset of shear thickening. For instance, RF curves of polymer A converge to similar values at high velocities regardless of the significant difference in concentration while the concentration differentiates the RF at low velocities. This indicates the contribution of both shear and elastic viscosity in polymer flow through porous media, although shear viscosity reaches its minimum at high velocities [74]. The degree and magnitude of shear thickening increase with the increase in molecular weight and concentration. This highlights the influence of shear and elastic viscosities on the slope of apparent shear thickening [37].

The onset of shear thickening and the flow behavior of polymer are more important than the extensional magnitude itself in determining the suitability of polymer for EOR applications [77]. Hence, onset of shear thickening has received extensive attention in the literature [50,52,53,78]. Figure 8 shows polymer molecular weight has an obvious influence on the onset of shear thickening. A solution with higher molecular weight experiences earlier onset of shear thickening. With increasing polymer Mw, the apparent shear thickening increases, conversely, the onset of shear thickening shifts to lower velocities [79].

Moreover, Figure 8 shows that onset of shear thickening is independent of polymer concentration. This observation excludes 4000 ppm polymer A which exhibits a gel-like behavior and yields shift of the onset to higher velocities. This confirms that the conformational state of polymer solution has more influence on the onset of shear thickening compared to the concentration value itself. This could be one of the reasons that cause a controversial observations in the literature regarding the correlation

between the onset and polymer concentration. For example, Chauveteau and Moan [52] reported the onset of shear thickening decreases with increasing polymer concentration for investigated wide concentration range (21–1360 ppm). However, a close look on the reported data, we could see the onset was almost similar for a specific concentration range (e.g., 170–680 ppm). This again indicates the conformational state influences the onset of shear thickening. For instance, within a semi-dilute regime, the onset of shear thickening decreases with molecular weight increases regardless of concentration [79,80]. The apparent viscosity from the resistance factor gradually increases as polymer concentration increases [81].

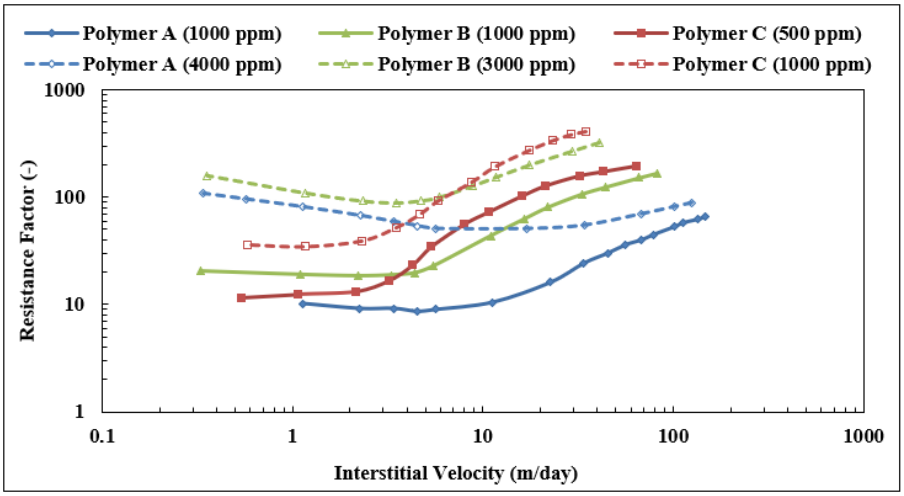

Figure 8. Resistance factor versus interstitial velocity for prefiltered polymers A, B and C at different concentrations.

3.3. Polymer Mechanical Degradation

The presented results showed the impact of wellbore mechanical degradation on both bulk shear viscosity and in-situ rheology. Despite the insignificant impact of mechanical degradation on shear viscosity of effluents, a considerable alteration of in-situ rheology behavior occurred. The significant alteration was found with reduction of apparent shear thickening behavior by shifting its onset to higher velocity and reduction of the slope while maintaining in-situ viscosity. The amount of alteration was influenced by polymer conformational regime. For instance, the change of the onset of shear thickening by comparing presheared solution A with a prefiltered sample was 126.2% at concentration of 1000 ppm, while this percentage drops to 35.5% when polymer concentration increases to 4000 ppm. This is also valid for polymers B and C. This elucidates that increasing polymer concentration is beneficial for polymer shear stability [36,82]. However, the impact of mechanical degradation on the slope of shear thickening was independent of polymer conformation regime (concentration). For example, the change of the slope of shear thickening of presheared solution B compared to prefiltered sample was 58.6% at concentration of 1000 ppm while it was 57.5% when polymer concentration increased to 3000 ppm. Similar observations were found for the other two polymers. This indicates that the impact of wellbore mechanical degradation on shifting onset of shear thickening to higher velocities was lower for concentrated solutions compared to that of semi-dilute polymer solutions. The change in the slope of shear thickening due to mechanical degradation seems independent of concentration.

3.3.1. Influence of Mechanical Degradation on In-Situ Rheology

Figure 9 compares the impact of mechanical degradation on the reduction of RF values of high Mw polymers B and C to RF of prefiltered polymer A which has relatively lower Mw. Recall from the discussion above, polymer Mw is a dominating factor on the polymer flow behavior after onset of shear thickening for semi-dilute polymers. Reduction of slope and shift of onset of shear thickening to higher velocities is an indication of a reduction of polymer MWD [50]. For example, the degree was reduced and onset of shear thickening of high Mw Polymer C (Mw ≈ 18 MDa) shifted to higher velocities due to preshearing. Therefore, RF curve similar to that of lower Mw prefiltered Polymer B (Mw ≈ 12 MDa) was achieved. A similar observation was found for presheared polymer B where preshearing resulted in shifting RF values closer to RF of prefiltered polymer A (Mw ≈ 8 MDa). This was also observed for concentrated solutions as shown on the right Figure 9.

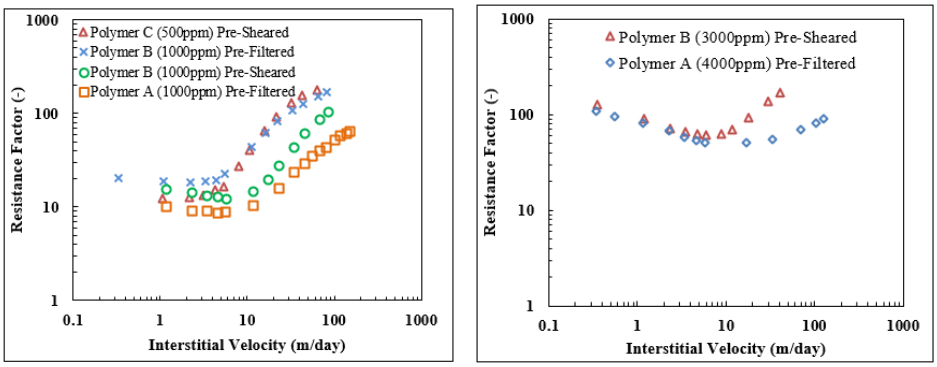

(**a**) (**b**)

Figure 9. Influence of preshearing on degrading the resistance factor of high Mw polymers to that of lower Mw prefiltered solutions. (**a**) Semi-dilute polymer solutions; (**b**) Concentrated polymer solutions.

3.3.2. Mechanical Degradation at Elevated Velocities

Figure 10 displays the effect of mechanical degradation on shear viscosity of effluent polymer solutions at a broad range of shear rates. These experiments were designed to compare the degradation effect in different polymers which have been exposed to comparable shear rate. It is clear that polymer C with high Mw experienced more shear degradation at similar injection rate applied for all solutions. For instance, degradation at Q = 90 cc/min was 4.0%, 12.0%, 20.0% for polymers A, B and C, respectively.

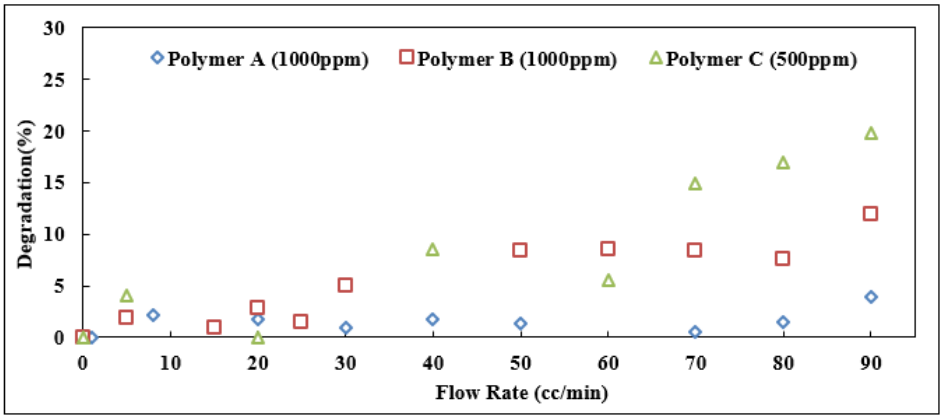

Figure 10. Shear degradation at elevated velocities for polymer A, B and C.

Figure 11 shows the in-situ flow of polymer B that has been presheared at different flow rates. Fresh (undegraded) solution is the same solution described in Figure 10 that has a shear viscosity of 13.3 cP and was injected into short Bentheimer core at various injection rates. It can be seen that the RF profile of fresh solution is identical to RF profile of prefiltered solution at similar velocities. This indicates that prefiltering at low flow rates (Q $\leq$ 0.5 cc/min, $v_D \leq$ 0.6 m/day) will not alter RF values. However, increasing preshearing rate to (Q = 15 cc/min, v_D = 19.4 m/day) will significantly alter viscoelastic properties such as the onset and degree of shear thickening, while not significantly affecting in-situ viscosity and bulk shear viscosity. However, preshearing the polymer at very high injection rate (Q = 110 cc/min, v_D = 141.2 m/day) causes a shear degradation of 16% and a considerable reduction (> 50%) on in-situ viscosity by comparing its Newtonian plateau that was observed in porous media with prefiltered solution. The reduction of polymer viscoelastic properties such as the onset and degree of shear thickening is extremely high. The maximum RF value of presheared solution at Q = 110 m/day was 26.6 which is more than 6 times lower than that of prefiltered solution at comparable velocity. Additionally, RRF of presheared solution at Q = 110 cc/min was reduced to 1.7 compared to 1.8 and 2.2 for presheared solution at Q = 15 cc/min and prefiltered solution at Q = 0.5 cc/min, respectively.

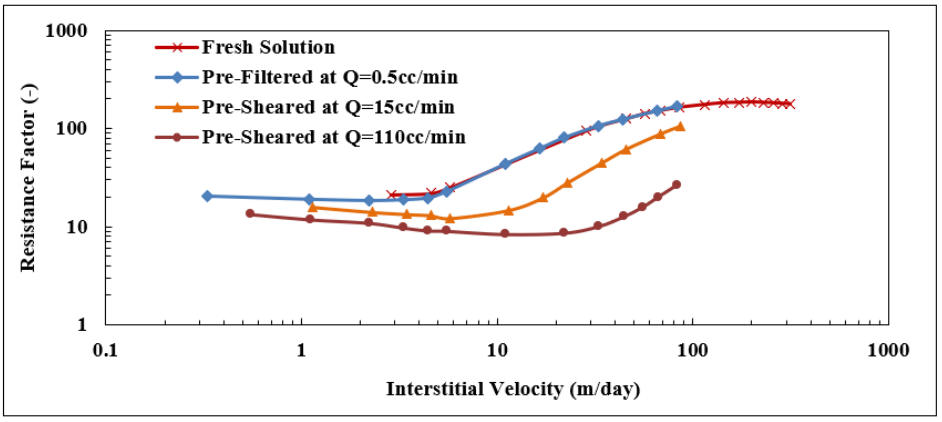

Figure 11. Resistance factor versus interstitial velocity for polymer B presheared at different flow rates.

3.4. Permeability Reduction

Polymer retention in porous media has similar importance to its viscoelasticity (discussed above) on the sweep efficiency and injectivity. It is a determining parameter in screening EOR polymers. When HPAM is transported in porous media, it tends to adsorb on rock surfaces and may trap within small pores resulting in polymer retention. Polymer retention reflects different mechanisms such as adsorption, straining (mechanical entrapment) and hydrodynamic retention (rate effect) [72,83]. As a consequence of polymer retention, permeability reduction occurs. Experimentally, permeability reduction can be evaluated by residual resistance factor (RRF) [57].

RRF is a measure of the extent of permeability reduction of porous media due to polymer injection. RRF correlates directly with the permeability of the porous media and the molecular weight of polymer. Therefore, higher RRF values may result from polymer flooding in low permeability reservoirs using high molecular weight polymers. Generally, for homogeneous porous media with lower contrast in permeability of different zones or layers, the intention is to obtain lower RRF values (RRF $\leq$ 2) while keeping RF values higher possible at reservoir velocities [84]. This is to increase the sweep efficiency of polymer flooding process by reducing the mobility ratio of displacing and displaced fluids. However, higher RRF values can be beneficial where the porous media is heterogeneous with significant contrast in permeability of different layers. In such cases, higher RRF values could result in better conformance control and thereby improved sweep efficiency through flow diversion into un-swept regions.

Figure 12 depicts RRF values measured for prefiltered polymers A, B and C at different concentrations. It can be seen that concentrated polymers have higher RRF compared to solutions with lower concentration. Furthermore, RRF appears to be significantly dependent on polymer Mw to a greater extent than concentration. This could be elucidated by looking at a similar polymer concentration of 1000 ppm, we can see RRF for polymers A, B and C were 1.6, 2.2 and 9.3 respectively. This emphasizes the increase of RRF with Mw [79].

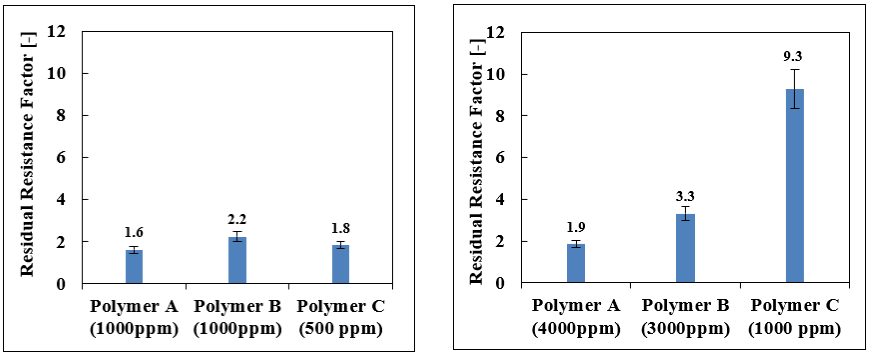

Figure 12. Residual resistance factor (RRF) of prefiltered polymers A, B and C. (**a**) Semi-dilute polymer solutions; (**b**) Concentrated polymer solutions.

Figure 13 displays the impact of polymer pretreatment (prefiltering, reinjecting and preshearing) on RRF values. Presented RRF values are quite scattered. This could be due to challenges on measuring 'true' RRF which has been debated in the literature [84]. One reason could be due to experimental artifacts ascribed to the amount of brine and strategies applied during brine post-flush such as tapering [67]. Another reason could be due to unapproachable steady-state condition during the injection of brine alone after polymer flooding to satisfy Darcy's Law conditions in Equation (2). This is suggested due to the viscoelasticity of retained molecules [85]. However, in some cases, the impact of mechanical degradation on RRF was not significant. This might be due to the reason that high molecular species tend to adsorb first as the polymer transports in porous media. High molecular

species could also be found in degraded solutions if degradation is not significant which may be enough to form a similar adsorbed layer of non-degraded solutions [70]. Measuring 'true' RRF is an essential task that would certainly improve the estimation of effective polymer viscosity in porous media by using the term RF/RRF.

However, the general trend from the data presented in Figure 13 shows that pretreatment of polymer solutions prior to injection into the porous media results in a reduction in RRF values. That is, RRF values of prefiltered solutions are generally higher than RRF of presheared and reinjected solutions.

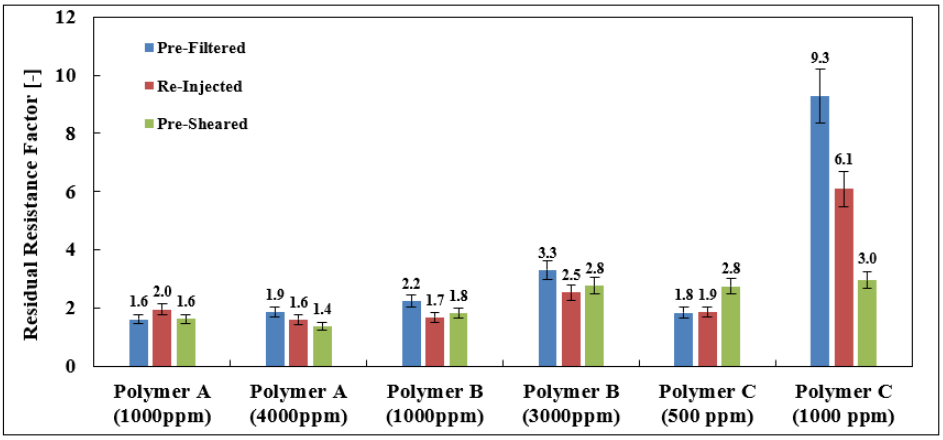

Figure 13. Residual resistance factor (RRF) of polymers A, B and C at different concentrations.

3.5. Polymer Injectivity

As stated before, polymer injectivity is a measure of how efficiently polymer solution can be delivered into reservoir matrix. The shear viscosity measurement alone cannot predict injectability of polymer solutions, as it does not reflect the existence of all flow regimes during polymer flow in porous media. Besides other factors, matrix fracturing is one major concern in polymer flooding projects that restricts polymer injection. Injection under matrix condition that may evolve into fracture formation is only a function of injection pressure, irrespective of polymer bulk viscosity [86]. This means fracture initiation is more attributed to polymer viscoelasticity, particularly shear thickening behavior that yields significant pressure build-up. Therefore, polymer injectivity could be inferred from RF and RRF measurements. The pressure gradient associated with high RF values that are found at wellbore region reduces polymer injectivity. Additionally, the decline in polymer injectivity might occur when retention is high as reflected by high RRF in this study (e.g., RRF > 3 is not recommended for EOR applications). Shear thickening may be dampened for each polymer either by increasing the polymer concentration or mechanically degrading the polymer solution before the injection. From economical perspective, the former requires increasing the dosage of polymer which subsequently demands high cost. It may also yield in high RRF. Whereas the latter relates to polymer type more specifically polymer Mw at which the cost of the manufacturing process of low and high Mw polymer is quite similar [87]. The loss of shear viscosity within 20–30% due to preshearing could be tolerated economically and cause a significant reduction in extensional viscosity that results in a reduction of resistance factor [71]. Additionally, preshearing could also be beneficial, so that high molecular species are sheared and avoided. These species are mainly responsible for wellbore plugging problems that result in permeability reduction. This may increase the shear rates at wellbore area that promotes pressure build-up and eventually mechanically degrade the polymer solution. This suggests

preshearing high Mw polymer solution is a favorable strategy to optimize its injectivity which is consistent with other studies [88].

4. Conclusions

Series of core flood experiments have been performed to investigate in-situ behavior of partially hydrolyzed polyacrylamide polymers (HPAM) in porous media. The influence of HPAM molecular weight and concentration on polymer in-situ rheology has been investigated. Additionally, the impact of mechanical degradation on polymer rheological behavior has been studied. Based on the results, polymer injectivity can be optimized. More specifically, the following conclusions could be made:

- In-situ rheological behavior of HPAM in porous media is different from bulk rheology observed in the rheometer.
    - Shear thickening behavior was observed at high velocities representative of those present in the near wellbore region. Near-Newtonian behavior was observed at low velocities representative of those present deep in the reservoir.
    - The degree and magnitude of shear thickening increased for higher polymer Mw and concentration.
    - Shear thinning behavior at low velocities was observed for concentrated solutions while not for semi-dilute solutions.
- Exposing HPAM solutions to mechanical degradation through preshearing process prior to injection facilitates its flow in porous media and enhances its injectivity. This is ascribed to a reduction in viscoelastic properties.
    - Onset of shear thickening shifted to higher velocities.
    - The magnitude and the degree of shear thickening behavior were reduced while in-situ viscosity at low flow rates was maintained.
- RRF appears to be dominated by molecular weight and concentration.
    - High RRF found for high molecular weight polymers with high concentration.
    - Degraded solutions have lower RRF values specifically for concentrated solutions of high Mw polymers. This effect was more pronounced when polymer solution was degraded at very high velocities.
- Improvement (reduction) in polymer viscoelastic properties and RRF through preshearing process can optimize polymer injectivity.

Author Contributions: Conceptualization, T.S. and A.S.; Formal analysis, B.A.-S., T.S., B.S.S. and A.S.; Investigation, B.A.-S.; Methodology, B.A.-S., and B.S.S.; Project administration, A.S.; Supervision, T.S., B.S.S. and A.S.; Writing—original draft, B.A.-S.; Writing—review & editing, T.S., B.S.S. and A.S.

Funding: This research received no external funding.

Acknowledgments: We wish to thank Energi Simulation, Canada and the PETROMAKS 2 program at Norwegian Research Council for financial support. We also acknowledge Petroleum Development Oman (PDO) for providing study scholarship for Badar Al-Shakry.

Conflicts of Interest: The authors declare no conflict of interest.

Nomenclature

A = core cross-sectional area (cm^2)
AF4 = Asymmetrical flow field-flow fractionation
ASP = Alkaline Surfactant Polymer
C = concentration (ppm)
C^* = critical overlap concentration (ppm)
D = core dimeter (cm)
Deg = mechanical degradation (%)
EOR = enhanced oil recovery
GPC = gel permeation chromatography
HPAM = partially hydrolyzed polyacrylamide
K = flow consistency index ($cP.s^{(n-1)}$)
K_{abs} = absolute permeability (Darcy)
K_{wf} = absolute permeability after polymer flow (Darcy)
K_{wi} = absolute permeability before polymer flow (Darcy)
L = core length (cm)
LSP = Low Salinity Polymer
Mw = molecular weight (MDa)
MWD = molecular weight distribution, dimensionless
n = flow behavior index, dimensionless
PV = pore volume, dimensionless
Q = injection flow rate (cc/min)
R^2 = coefficient of determination, dimensionless
RF = resistance factor, dimensionless
RRF = residual resistance factor, dimensionless
SAOS = small-amplitude oscillatory shear
SEC = size exclusion chromatography
TDS = total dissolved solids
v = interstitial velocity (m/day)
v_c = onset of shear thickening (m/day)
v_D = Darcy or Superficial velocity (m/day)
ΔP_p = pressure drop during polymer flow (bar)
ΔP_w = pressure drop during water flow (bar)
η_e = effluent viscosity (cP)
η_i = injected solution viscosity(cP)
η_w = brine viscosity (cP)
ϕ = porosity, dimensionless
$\dot{\gamma}$ = shear rate (s^{-1})

References

1. Sorbie, K.S. *Polymer-Improved Oil Recovery*; Blackie and Son Ltd.: Glasgow, UK, 1991. [CrossRef]
2. Al Baqlani, S.; Singh, S.K.; Glasbergen, G.; van Elk, H. Polymer distribution concepts for large scale polymer floods in the sultanate of oman: Simplicity or flexibility? In Proceedings of the SPE EOR Conference at Oil and Gas West Asia, Muscat, Oman, 26–28 March 2018. [CrossRef]
3. Wilton, R.R.; Torabi, F. Rheological assessment of the elasticity of polymers for enhanced heavy oil recovery. In Proceedings of the SPE Heavy Oil Conference-Canada, Calgary, AB, Canada, 11–13 June 2013. [CrossRef]
4. Szabo, M.T. Molecular and microscopic interpretation of the flow of hydrolyzed polyacrylamide solution through porous media. In Proceedings of the Fall Meeting of the Society of Petroleum Engineers of AIME, San Antonio, TX, USA, 8–11 October 1972. [CrossRef]
5. Gao, C. Empirical correlations for viscosity of partially hydrolyzed polyacrylamide. *J. Pet. Explor. Prod. Technol.* **2013**, *4*, 209–213. [CrossRef]

6. Hashmet, M.R.; Onur, M.; Tan, I.M. Empirical correlations for viscosity of polyacrylamide solutions with the effects of concentration, molecular weight and degree of hydrolysis of polymer. *J. Appl. Sci.* **2014**, *14*, 1000–1007. [CrossRef]
7. Gao, C. Viscosity of partially hydrolyzed polyacrylamide under shearing and heat. *J. Pet. Explor. Prod. Technol.* **2013**, *3*, 203–206. [CrossRef]
8. De Morais, S.C.; Cardoso, O.R.; de Carvalho Balaban, R. Thermal stability of water-soluble polymers in solution. *J. Mol. Liq.* **2018**, *265*, 818–823. [CrossRef]
9. Lewandowska, K. Comparative studies of rheological properties of polyacrylamide and partially hydrolyzed polyacrylamide solutions. *J. Appl. Polym. Sci.* **2007**, *103*, 2235–2241. [CrossRef]
10. Choi, S.K.; Sharma, M.M.; Bryant, S.; Huh, C. Ph-sensitive polymers for novel conformance-control and polymer-flood applications. *SPE Reserv. Eval. Eng.* **2010**, *13*, 926–939. [CrossRef]
11. Skauge, T.; Skauge, A.; Salmo, I.C.; Ormehaug, P.A.; Al-Azri, N.; Wassing, L.M.; Glasbergen, G.; Van Wunnik, J.N.; Masalmeh, S.K. Radial and linear polymer flow—Influence on injectivity. In Proceedings of the SPE Improved Oil Recovery Conference, Tulsa, OK, USA, 11–13 April 2016. [CrossRef]
12. Maerker, J.M. Shear degradation of partially hydrolyzed polyacrylamide solutions. *Soc. Pet. Eng. J.* **1975**, *15*, 311–322. [CrossRef]
13. Chang, H.L. Polymer flooding technology yesterday, today, and tomorrow. *J. Pet. Technol.* **1978**, *30*, 1113–1128. [CrossRef]
14. Needham, R.B.; Doe, P.H. Polymer flooding review. *J. Pet. Technol.* **1987**, *39*, 1503–1507. [CrossRef]
15. Standnes, D.C.; Skjevrak, I. Literature review of implemented polymer field projects. *J. Pet. Sci. Eng.* **2014**, *122*, 761–775. [CrossRef]
16. Sheng, J.J.; Leonhardt, B.; Azri, N. Status of polymer-flooding technology. *J. Can. Pet. Technol.* **2015**, *54*, 116–126. [CrossRef]
17. Skauge, A.; Shiran, B.S. Low salinity polymer flooding. In Proceedings of the IOR 2013—17th European Symposium on Improved Oil Recovery, St. Petersburg, Russia, 16–18 April 2013. [CrossRef]
18. Unsal, E.; Ten Berge, A.B.G.M.; Wever, D.A.Z. Low salinity polymer flooding: Lower polymer retention and improved injectivity. *J. Pet. Sci. Eng.* **2017**, *163*, 671–682. [CrossRef]
19. Zhu, Y.; Hou, Q.; Jian, G.; Ma, D.; Wang, Z. Current development and application of chemical combination flooding technique. *Pet. Explor. Dev.* **2013**, *40*, 96–103. [CrossRef]
20. Sheng, J.J. A comprehensive review of alkaline–surfactant–polymer (asp) flooding. *Asian-Pac. J. Chem. Eng.* **2014**, *9*, 471–489. [CrossRef]
21. Huh, C.; Pope, G.A. Residual oil saturation from polymer floods: Laboratory measurements and theoretical interpretation. In Proceedings of the SPE Symposium on Improved Oil Recovery, Tulsa, OK, USA, 20–23 April 2008. [CrossRef]
22. Xie, C.; Lv, W.; Wang, M. Shear-thinning or shear-thickening fluid for better eor?—A direct pore-scale study. *J. Pet. Sci. Eng.* **2017**, *161*, 683–691. [CrossRef]
23. Erincik, M.Z.; Qi, P.; Balhoff, M.T.; Pope, G.A. New method to reduce residual oil saturation by polymer flooding. *SPE J.* **2018**, *23*. [CrossRef]
24. Fan, J.C.; Wang, F.C.; Chen, J.; Zhu, Y.B.; Lu, D.T.; Liu, H.; Wu, H.A. Molecular mechanism of viscoelastic polymer enhanced oil recovery in nanopores. *R. Soc. Open Sci.* **2018**, *5*, 180076. [CrossRef]
25. Vik, B.; Kedir, A.; Kippe, V.; Sandengen, K.; Skauge, T.; Solbakken, J.; Zhu, D. Viscous oil recovery by polymer injection; impact of in-situ polymer rheology on water front stabilization. In Proceedings of the SPE Europec Featured at 80th EAGE Conference and Exhibition, Copenhagen, Denmark, 11–14 June 2018. [CrossRef]
26. Sorbie, K.S.; Roberts, L.J. A model for calculating polymer injectivity including the effects of shear degradation. In Proceedings of the SPE Enhanced Oil Recovery Symposium, Tulsa, OK, USA, 15–18 April 1984. [CrossRef]
27. Milton, H.W.; Argabright, P.A.; Gogarty, W.B. Eor prospect evaluation using field manufactured polymer. In Proceedings of the SPE California Regional Meeting, Ventura, CA, USA, 23–25 March 1983. [CrossRef]
28. Sieberer, M.; Clemens, T.; Peisker, J.; Ofori, S. Polymer flood field implementation—Pattern configuration and horizontal versus vertical wells. In Proceedings of the SPE Improved Oil Recovery Conference, Tulsa, OK, USA, 14–18 April 2018. [CrossRef]
29. Chauveteau, G.; Kohler, N. Influence of microgels in polysaccharide solutions on their flow behavior through porous media. *Soc. Pet. Eng. J.* **1984**, *24*, 361–368. [CrossRef]

30. Thomas, A.; Gaillard, N.; Favero, C. Some key features to consider when studying acrylamide-based polymers for chemical enhanced oil recovery. *Oil Gas Sci. Technol.* **2013**, *67*, 887–902. [CrossRef]
31. Teeuw, D.; Hesselink, F.T. Power-law flow and hydrodynamic behaviour of biopolymer solutions in porous media. In Proceedings of the SPE Oilfield and Geothermal Chemistry Symposium, Stanford, CA, USA, 28–30 May 1980. [CrossRef]
32. Chauveteau, G.; Zaitoun, A. Basic rheological behavior of xanthan polysaccharide solutions in porous media: Effects of pore size and polymer concentration. In *Enhanced Oil Recovery*; Fayers, F.J., Ed.; Elsevier: Amstrdam, The Netherlands, 1981.
33. Morris, E.R.; Cutler, A.N.; Ross-Murphy, S.B.; Rees, D.A.; Price, J. Concentration and shear rate dependence of viscosity in random coil polysaccharide solutions. *Carbohydr. Polym.* **1981**, *1*, 5–21. [CrossRef]
34. Cannella, W.J.; Huh, C.; Seright, R.S. Prediction of xanthan rheology in porous media. In Proceedings of the SPE Annual Technical Conference and Exhibition, Houston, TX, USA, 2–5 October 1988. [CrossRef]
35. González, J.M.; Müller, A.J.; Torres, M.F.; Sáez, A.E. The role of shear and elongation in the flow of solutions of semi-flexible polymers through porous media. *Rheol. Acta* **2005**, *44*, 396–405. [CrossRef]
36. Noïk, C.; Delaplace, P.; Muller, G. Physico-chemical characteristics of polyacrylamide solutions after mechanical degradation through a porous medium. In Proceedings of the SPE International Symposium on Oilfield Chemistry, San Antonio, TX, USA, 14–17 February 1995. [CrossRef]
37. Southwick, J.G.; Manke, C.W. Molecular degradation, injectivity, and elastic properties of polymer solutions. *SPE Reserv. Eng.* **1988**, *3*, 193–201. [CrossRef]
38. Stavland, A.; Jonsbraten, H.; Lohne, A.; Moen, A.; Giske, N.H. Polymer flooding—Flow properties in porous media versus rheological parameters. In Proceedings of the SPE EUROPEC/EAGE Annual Conference and Exhibition, Barcelona, Spain, 14–17 June 2010. [CrossRef]
39. Wevera, D.A.Z.; Picchionia, F.; Broekhuisa, A.A. Polymers for enhanced oil recovery: A paradigm for structure–property relationship in aqueous solution. *Prog. Polym. Sci.* **2011**, *36*, 1558–1628. [CrossRef]
40. Zamani, N.; Kaufmann, R.; Kosinski, P.; Skauge, A. Mechanisms of non-newtonian polymer flow through porous media using navier-stokes approach. *J. Dispers. Sci. Technol.* **2015**, *36*, 310–325. [CrossRef]
41. Knight, J. *Mechanical Shear Degradation of Polymers in Solution: A Review*; Royal Aircraft Establishment: London, UK, 1976.
42. Caulfield, M.J.; Qiao, G.G.; Solomon, D.H. Some aspects of the properties and degradation of polyacrylamides. *Chem. Rev.* **2002**, *102*, 3067–3084. [CrossRef] [PubMed]
43. Hashmet, M.R.; Onur, M.; Tan, I.M. Empirical correlations for viscosity of polyacrylamide solutions with the effects of salinity and hardness. *J. Dispers. Sci. Technol.* **2014**, *35*, 510–517. [CrossRef]
44. Ryles, R.G. Chemical stability limits of water-soluble polymers used in oil recovery processes. *SPE Reserv. Eng.* **1988**, *3*, 23–34. [CrossRef]
45. Skauge, T.; Kvilhaug, O.A.; Skauge, A. Influence of polymer structural conformation and phase behavoir on in-situ viscosity. In Proceedings of the IOR 2015—18th European Symposium on Improved Oil Recovery, Dresden, Germany, 14–16 April 2015. [CrossRef]
46. Skauge, A.; Zamani, N.; Jacobsen, J.G.; Shiran, B.S.; Al-Shakry, B.; Skauge, T. Polymer flow in porous media: Relevance to enhanced oil recovery. *Colloids Interfaces* **2018**, *2*, 27. [CrossRef]
47. Hill, H.J.; Brew, J.R.; Claridge, E.L.; Hite, J.R.; Pope, G.A. The behavior of polymers in porous media. In Proceedings of the SPE Improved Oil Recovery Symposium, Tulsa, OK, USA, 22–24 April 1974. [CrossRef]
48. Hirasaki, G.J.; Pope, G.A. Analysis of factors influencing mobility and adsorption in the flow of polymer solution through porous media. *Soc. Pet. Eng. J.* **1974**, *14*, 337–346. [CrossRef]
49. Seright, R.S. The effects of mechanical degradation and viscoelastic behavoir on injectivity of polyacrylamide solutions. *Soc. Pet. Eng. J.* **1983**, *23*, 475–485. [CrossRef]
50. Heemskerk, J.; Rosmalen, R.; Janssen-van, R.; Holtslag, R.J.; Teeuw, D. Quantification of viscoelastic effects of polyacrylamide solutions. In Proceedings of the SPE Enhanced Oil Recovery Symposium, Tulsa, OK, USA, 15–18 April 1984. [CrossRef]
51. Muller, A.J.; Patruyo, L.G.; Montano, W.; Roversi-M, D.; Moreno, R.; Ramírez, N.E.; Sáez, A.E. Mechanical degradation of polymers in flows through porous media: Effect of flow path length and particle size. *Appl. Mech. Rev.* **1997**, *50*, S149–S155. [CrossRef]
52. Chauveteau, G.; Moan, M. The onset of dilatant behavior in non-inertial flow of dilute polymer-solutions through channels with varying cross-sections. *J. Phys. Lett.* **1981**, *42*, L201–L204. [CrossRef]

53. Zamani, N.; Bondino, I.; Kaufmann, R.; Skauge, A. Effect of porous media properties on the onset of polymer extensional viscosity. *J. Pet. Sci. Eng.* **2015**, *133*, 483–495. [CrossRef]
54. Rock, A.; Hincapie, R.E.; Wegner, J.; Födisch, H.; Ganzer, L. Pore-scale visualization of oil recovery by viscoelastic flow instabilities during polymer eor. In Proceedings of the 19th European Symposium on Improved Oil Recovery, Stavanger, Norway, 24–27 April 2017. [CrossRef]
55. Kawale, D.; Marques, E.; Zitha, P.L.J.; Kreutzer, M.T.; Rossena, W.R.; Boukany, P.E. Elastic instabilities during the flow of hydrolyzed polyacrylamide solution in porous media: Effect of pore-shape and salt. *Soft Matter* **2017**, *13*, 765–775. [CrossRef]
56. Hu, Y.; Wang, S.Q.; Jamieson, A.M. Rheological and rheooptical studies of shear-thickening polyacrylamide solutions. *Macromolecules* **1995**, *28*, 1847–1853. [CrossRef]
57. Lake, L.W. *Enhanced Oil Recovery*; Prentice Hall, Inc.: Upper Saddle River, NJ, USA, 1989.
58. Seright, R.S.; Maerker, J.M.; Holzwarth, G. Mechanical degradation of polyacrylamides induced by flow through porous-media. *ACS Polym. Prepr.* **1981**, *22*, 30–33.
59. Puls, C.; Clemens, T.; Sledz, C.; Kadnar, R.; Gumpenberger, T. Mechanical degradation of polymers during injection, reservoir propagation and production—Field test results 8 th reservoir, austria. In Proceedings of the SPE Europec Featured at 78th EAGE, Vienna, Austria, 30 May–2 June 2016. [CrossRef]
60. Hunt, J.A.; Young, T.S.; Green, D.W.; Willhite, G.P. Size-exclusion chromatography in the measurement of concentration and molecular weight of some eor polymers. *SPE Reserv. Eng.* **1988**, *3*, 835–841. [CrossRef]
61. Dalsania, Y.; Doda, A.; Trivedi, J. Characterization of ultrahigh-molecular-weight oilfield polyacrylamides under different ph environments by use of asymmetrical-flow field-flow fractionation and multiangle-light-scattering detector. *SPE J.* **2018**, *23*, 48–65. [CrossRef]
62. Rodriguez, L.; Antignard, S.; Giovannetti, B.; Dupuis, G.; Gaillard, N.; Jouenne, S.; Bourdarot, G.; Morel, D.; Zaitoun, A.; Grassl, B. A new thermally stable synthetic polymer for harsh conditions of middle east reservoirs: Part ii. Nmr and size exclusion chromatography to assess chemical and structural changes during thermal stability tests. In Proceedings of the SPE Improved Oil Recovery Conference, Tulsa, OK, USA, 14–18 April 2018. [CrossRef]
63. Foshee, W.C.; Jennings, R.R.; West, T.J. Preperation and testing of partially hydrolyzed polyacrlamide solutions. In Proceedings of the SPE Annual Fall Technical Conference and Exhibition, New Orleans, LA, USA, 3–6 October 1976. [CrossRef]
64. Warner, H.R. *Analysis of Mechanical Degradation Data on Partially Hydrolyzed Polyacrylamide Solutions*; Society of Petroleum Engineers: Richardson, TX, USA, 1976.
65. Chauveteau, G. Molecular interperation of several different properties of flow of coiled polymer solutions through porous media in oil recovery conditions. In Proceedings of the SPE Annual Technical Conference and Exhibition, San Antonio, TX, USA, 4–7 October 1981. [CrossRef]
66. Jouenne, S.; Chakibi, H.; Levitt, D. Polymer stability after successive mechanical-degradation events. *SPE J.* **2018**, *23*, 18–33. [CrossRef]
67. Al-Shakry, B.; Skauge, T.; Shiran, B.S.; Skauge, A. Impact of mechanical degradation on polymer injectivity in porous media. *Polymers* **2018**, *10*, 742. [CrossRef]
68. Åsen, S.M.; Stavland, A.; Strand, D.; Hiorth, A. An experimental investigation of polymer mechanical degradation at cm and m scale. In Proceedings of the SPE Improved Oil Recovery Conference, Tulsa, OK, USA, 14–18 April 2018. [CrossRef]
69. Al Hashmi, A.R.; Al Maamari, R.S.; Al Shabib, I.S.; Masnsoor, A.M.; Zaitoun, A.; Al Sharji, H.H. Rheology and mechanical degradation of high-molecular-weight partially hydrolzed polyacrylamide during flow through capillaries. *J. Pet. Sci. Eng.* **2013**, *105*, 100–106. [CrossRef]
70. Dupas, A.; Henaut, I.; Rousseau, D.; Poulian, P.; Tabary, R.; Argillier, J.-F.; Aubry, T. Impact of polymer mechanical degradation on shear and extensional viscosities: Toward better injectivity forecasts in polymer flooding operations. In Proceedings of the SPE International Symposium on Oilfield Chemistry, The Woodlands, TX, USA, 8–10 April 2013. [CrossRef]
71. Zaitoun, A.; Makakou, P.; Blin, N.; Al-Maamari, R.S.; Al-Hashmi, A.R.; Abdel-Goad, M.; Al-Sharji, H.H. Shear stability of eor polymers. *SPE J.* **2012**, *17*, 335–339. [CrossRef]
72. Chauveteau, G.; Kohler, N. Polymer flooding: The essential elements for laboratory evaluation. In Proceedings of the SPE Improved Oil Recovery Symposium, Tulsa, OK, USA, 22–24 April 1974. [CrossRef]

73. GRAESSLEY, W.W. *The Entanglement Concept in Polymer Rheology*; Springer: Berlin/Heidelberg, Germany, 1974.
74. Kulicke, W.M.; Haas, R. Flow behavior of dilute polyacrylamide solutions through porous media. 1. Influence of chain length, concentration, and thermodynamic quality of the solvent. *Ind. Eng. Chem. Fundam.* **1984**, *23*, 308–315. [CrossRef]
75. Mansour, A.M.; Al-Maarnari, R.S.; Al-Hashmi, A.S.; Zaitoun, A.; Al-Sharji, H. In-situ rheology and mechanical degradation of eor polyacrylamide solutions under moderate shear rates. *J. Pet. Sci. Eng.* **2014**, *115*, 57–65. [CrossRef]
76. Seright, R.S.; Seheult, M.; Talashek, T. Injectivity characteristics of eor polymers. *SPE Reserv. Eval. Eng.* **2009**, *12*, 783–792. [CrossRef]
77. Flew, S.; Sellin, R.H.J. Non-newtonian flow in porous media-a laboratory study of polyacrylamide solutions. *J. Non-Newtonian Fluid Mech.* **1993**, *47*, 169–210. [CrossRef]
78. Jouenne, S.; Heurteux, G. Flow of polymer solutions through porous media-prediction of mobility reduction from ex-situ measurements of elasticity. In Proceedings of the IOR 2017—19th European Symposium on Improved Oil Recovery, Stavanger, Norway, 24–27 April 2017. [CrossRef]
79. Gramain, P.; Myard, P. Elongational deformation by shear flow of flexible polymers adsorbed in porous media. *Macromolecules* **1980**, *14*, 180–184. [CrossRef]
80. Pelletier, E.; Viebke, C.; Meadows, J.; Williams, P.A. Dilute polyacrylamide solutions under uniaxial extensional flow. *Langmuir* **2003**, *19*, 559–565. [CrossRef]
81. Grigorescu, G.; Kulicke, W.-M. Prediction of viscoelastic properteis and shear stability of polymers in solution. In *Advances in Polymer Science*; Springer-Verlag: Berlin/Heidelberg, Germany, 2000.
82. Martin, F.D. Mechanical degradation of polyacrylamide solutions in core plugs from several carbonate reservoirs. *SPE Form. Eval.* **1986**, *1*, 139–150. [CrossRef]
83. Al-Hajri, S.; Mahmood, S.M.; Abdulelah, H.; Akbari, S. An overview on polymer retention in porous media. *Energies* **2018**, *11*, 2751. [CrossRef]
84. Seright, R.S. How much polymer should be injected during a polymer flood? *SPE J.* **2017**, *22*, 1–18. [CrossRef]
85. Han, X.-Q. *Viscoelastic Behaviour of Polymer Molecules Retained in Porous Media*; Society of Petroleum Engineers: Richardson, TX, USA, 1990.
86. Zhou, J.; Dong, Y.; Pater, C.J.; Zitha, P.L.J. Experimental study of the impact of shear dilation and fracture behavior during polymer injection for heavy oil recovery in unconsolidated reservoirs. In Proceedings of the Canadian Unconventional Resources & International Petroleum Conference, Calgary, AB, Canada, 19–21 October 2010. [CrossRef]
87. Wever, D.A.Z.; Polgar, L.M.; Stuart, M.C.A.; Picchioni, F.; Broekhuis, A.A. Polymer molecular architecture as a tool for controlling the rheological properties of aqueous polyacrylamide solutions for enhanced oil recovery. *Ind. Eng. Chem. Res.* **2013**, *52*, 16993–17005. [CrossRef]
88. Wang, D.; Xia, H.; Liu, Z.; Yang, Q. Study of the mechanism of polymer solution with visco-elastic behavior increasing microscopic oil displacement efficiency and the forming of steady "oil thread" flow channels. In Proceedings of the SPE Asia Pacific Oil and Gas Conference and Exhibition, Jakarta, Indonesia, 17–19 April 2001. [CrossRef]

Paper-V:

Polymer Flow in Porous Media: Relevance to Enhanced Oil Recovery

colloids and interfaces

MDPI

Article

Polymer Flow in Porous Media: Relevance to Enhanced Oil Recovery

Arne Skauge [1,2,*], Nematollah Zamani [3], Jørgen Gausdal Jacobsen [1,3], Behruz Shaker Shiran [3], Badar Al-Shakry [1] and Tormod Skauge [2]

[1] Department of Chemistry, University of Bergen, Allegaten 41, N-5020 Bergen, Norway; joja@norceresearch.no (J.G.J.); Badar.Al-Shakry@uni.no (B.A.-S.)
[2] Energy Research Norway, N-5020 Bergen, Norway; Tormod.Skauge@energyresearch.no
[3] Uni Research, N-5020 Bergen, Norway; Nematollah.zamani@uni.no (N.Z.); Behruz.shaker@uni.no (B.S.S.)
* Correspondence: arne.skauge@kj.uib.no; Tel.: +47-5558-3358

Received: 1 June 2018; Accepted: 3 July 2018; Published: 10 July 2018

Abstract: Polymer flooding is one of the most successful chemical EOR (enhanced oil recovery) methods, and is primarily implemented to accelerate oil production by sweep improvement. However, additional benefits have extended the utility of polymer flooding. During the last decade, it has been evaluated for use in an increasing number of fields, both offshore and onshore. This is a consequence of (1) improved polymer properties, which extend their use to HTHS (high temperature high salinity) conditions and (2) increased understanding of flow mechanisms such as those for heavy oil mobilization. A key requirement for studying polymer performance is the control and prediction of in-situ porous medium rheology. The first part of this paper reviews recent developments in polymer flow in porous medium, with a focus on polymer in-situ rheology and injectivity. The second part of this paper reports polymer flow experiments conducted using the most widely applied polymer for EOR processes, HPAM (partially hydrolyzed polyacrylamide). The experiments addressed highrate, near-wellbore behavior (radial flow), reservoir rate steady-state flow (linear flow) and the differences observed in terms of flow conditions. In addition, the impact of oil on polymer rheology was investigated and compared to single-phase polymer flow in Bentheimer sandstone rock material. Results show that the presence of oil leads to a reduction in apparent viscosity.

Keywords: EOR; polymer flooding; in-situ rheology; non-Newtonian flow in porous medium

1. Introduction

The success of polymer flooding depends on the ability of injected solutions to transport polymer molecules deep into a reservoir, thus providing enhanced mobility ratio conditions for the displacement process. In the following sections, we focus on the principal parameters that are crucial in the decision-making process for designing a satisfactory polymer flood design.

The application of polymer flooding to tertiary oil recovery may induce high injection pressures, resulting in injectivity impairment. Since the volumetric injection rate during polymer flooding is constrained by formation fracture pressure, project economics may be significantly affected. Thus, injectivity is a critical parameter and key risk factor for implementation of polymer flood projects.

A large number of injectivity studies, both theoretical and experimental, have been performed in porous media during recent decades, albeit they were mainly studies of linear cores in the absence of residual oil [1–7]. Recently, Skauge et al. [8] performed radial injectivity experiments showing significant reduction in differential pressure compared to linear core floods. This discrepancy in polymer flow in linear cores compared to that in radial disks is partly explained by the of differing pressure conditions that occur when polymer molecules are exposed to transient and semi-transient

pressure conditions in radial disks, as opposed to the steady state conditions experienced in linear core floods. In addition, they observed that the onset of apparent shear thickening occurs at significantly higher flux in radial floods. Based on these results, injectivity was suggested to be underestimated from experiments performed in linear core plugs. However, these experiments were performed in the absence of residual oil. If residual oil has a significant effect on polymer propagation in porous media, experiments performed in its absence will not be able to accurately predict polymer performance.

Experimental studies investigating the effects of residual oil on polymer propagation through porous media have been sparse, although they have generally shown decreasing levels of polymer retention in the presence of residual oil [9,10].

The polymer adsorbs to the rock surface and may also block pores due to polymer size (straining) and flow rate (hydrodynamic retention). In addition, different trapping mechanisms may take place. The polymer retention phenomena influence the flow of polymer in porous media, however, these effects are beyond the scope of this paper. The subject has been reviewed in several other books and papers, e.g., Sorbie [11] and Lake [12].

History matches performed in this study aim to highlight the injectivity of partially hydrolyzed polyacrylamides (HPAMs) in radial disks saturated with residual oil, as these conditions best mimic actual flow conditions in oil reservoirs. Results show that the presence of residual oil reduces the apparent viscosity of HPAM in flow through porous media, thus improving injectivity. These results may facilitate increased implementation of polymer EOR (enhanced oil recovery) projects, as previous projects deemed infeasible may now be economically viable.

2. Theory

2.1. In-Situ Rheology

Polymer viscosity as a function of shear rate is usually measured using a rheometer. During the measurement process, polymer solutions are exposed to different shear rates in a stepwise manner. For each shear rate, polymer viscosity is measured after steady state conditions are achieved; at this state, it is referred to as bulk viscosity. However, polymer molecules experience significantly different flow conditions in rheometers compared to porous media. In particular:

(I) unlike rheometers, porous media exhibit an inherently complex geometry;
(II) phenomena such as mechanical degradation may change rheological properties;
(III) although they only demonstrate shear thinning behavior in rheometers, polymer solutions may exhibit apparent shear thickening behavior above a certain critical flow rate;
(IV) due to the tortuosity of porous media and existence of several contraction-expansion channels, polymer solutions are exposed to a wide range of shear rates at each flow rate and where extensional viscosity becomes more dominant, resulting in significantly different rheology behavior compared to bulk flow.

To account for these contrasting flow conditions, in-situ viscosity has been suggested to describe the fluid flow behavior of polymer solutions in porous media. In-situ viscosity is a macroscopic parameter that can be calculated using Darcy's law for single-phase non-Newtonian fluids:

$$\mu_{app} = \frac{KA}{Q}\frac{\Delta P}{L} \quad (1)$$

It is generally measured in core flood experiments as a function of Darcy velocity. Comparison of in-situ and bulk rheology (Figure 1) shows vertical and horizontal shifts between viscosity curves. Vertical shifts may be due to phenomena such as mechanical degradation, while horizontal shifts are due to a conversion factor between in-situ shear rate and Darcy velocity, shown as α. The red line in Figure 1 shows an increase in apparent viscosity, which is due to polymer adsorption. The adsorbed layer of polymer reduces the effective pore size and blocks smaller pores, both leading to increased

resistance to flow e.g., as determined by an increase in pressure at a given rate compared to a non-adsorbing situation. In contrast, a reduction in pressure (and therefore, in apparent viscosity) can be observed in the presence of depleted layers (see e.g., Sorbie [11]) which leads to slip effects.

Due to the time-consuming nature of in-situ measurements, there have been several attempts to investigate in-situ rheology, both analytically and numerically. In spite of extensive studies [13–22], limited success has been achieved to reliably relate in-situ to bulk viscosity based on polymer solution and porous media properties. Most of these models were developed based on analytical solutions of non-Newtonian flow through capillary bundles, which simplifies the complex geometry of porous media.

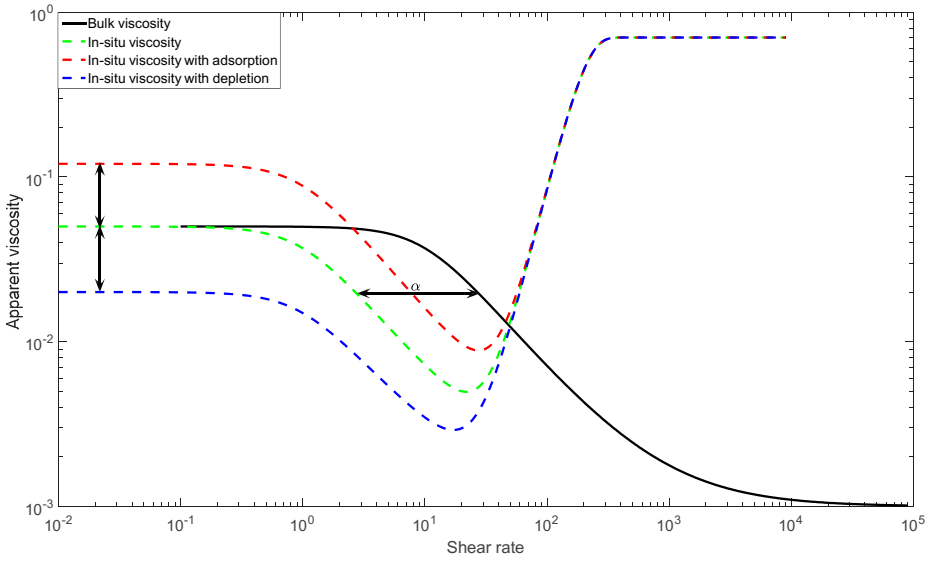

Figure 1. Schematic comparison of in-situ and bulk rheology.

In the following, the calculation procedure of in-situ viscosity is briefly explained:

1. Analytical solutions for a power-law fluid ($\mu = C\,\dot{\gamma}^{n-1}$) at a given flow rate through a capillary tube with an arbitrary radius (R) can be defined by Equation (2). By comparing Equation (2) with the Poiseuille volumetric flow rate for Newtonian fluids in a tube (Equation (3)), an apparent viscosity and shear rate can be obtained from Equations (4) and (5), respectively.
2. The analytical equation in a single tube (Equation (5)) can be extended to account for real porous media by using the capillary bundle approach [23–25]. An equivalent radius of a capillary bundle model for porous media with known porosity (ϕ), permeability (K) and tortuosity (ψ) can be obtained by Equation (6). By calculating the Darcy velocity and substituting the equivalent radius (Equation (6)) into Equation (5), the apparent shear rate as a function of Darcy velocity can be obtained by Equation (7).

$$Q = \frac{\pi n}{3n+1}\left(\frac{\Delta P}{2CL}\right)^{1/n} R^{\frac{3n+1}{n}} \tag{2}$$

$$Q = \frac{\pi}{8\mu}\frac{\Delta P}{L} R^4 \tag{3}$$

$$\mu_{eff} = C\left(\frac{3n+1}{4n}\right)\left(\frac{R\Delta P}{2CL}\right)^{\frac{n-1}{n}} \tag{4}$$

$$\mu_{app} = C\,\dot{\gamma}_{app}^{n-1} \Rightarrow \dot{\gamma}_{app} = \left(\frac{3n+1}{4n}\right)^{\frac{1}{n-1}} \left(\frac{R\Delta P}{2CL}\right)^{1/n} \tag{5}$$

$$R_{eq} = \sqrt{\frac{8K\psi}{\phi}} \tag{6}$$

$$\dot{\gamma}_{app} = 4\left(\frac{3n+1}{4n}\right)^{\frac{n}{n-1}} \frac{U}{\sqrt{8K\phi\psi}} \tag{7}$$

3. The above expressions are considered as an analytical basis for calculating apparent viscosity in porous media. Based on Equation (7), a simplified linear correlation between apparent shear rate and Darcy velocity is generally suggested, i.e., Equation (8), in which the correction factor (α) is the key factor. Some proposed equations for the correction factor are summarized in Table 1. By comparing different coefficients, different values for apparent viscosity may be obtained.

$$\dot{\gamma}_{app} = \alpha \frac{U}{\sqrt{K\phi}} \tag{8}$$

Table 1. Summary of proposed models for correction factor (α).

Model	Equation for Correction Factor (α)	Description
Analytical solution	$4\left(\frac{3n+1}{4n}\right)^{\frac{n}{n-1}}$	n is the power index in power-law region
Hirasaki and Pope [26]	$\frac{12}{\sqrt{150}}\left(\frac{3n+1}{4n}\right)^{\frac{n}{n-1}}$	n is the power index in power-law region
Cannella et al. [16]	$\frac{\beta}{\sqrt{S_w}}\left(\frac{3n+1}{n}\right)^{\frac{n}{n-1}}$	n is the power index in power-law region, S_w is water saturation, β is a constant equal to 6.

Based on the capillary bundle approach, other models were also proposed by Bird et al. [24], Christopher and Middleman [25], and Teeuw and Hesselink [15], in which the modified Blake-Kozeny model is used for power-law fluids (Equation (9)) and apparent viscosity is obtained using Equation (10).

$$U = \left(\frac{K}{\mu_{app}}\frac{\Delta P}{L}\right)^{1/n} \tag{9}$$

$$\mu_{app} = C\left(\frac{3n+1}{4n}\right)^{n}\left(\frac{K\phi}{\beta}\right)^{(1-n)/2} \tag{10}$$

Based on the discussion given by Teeuw and Hesselink [15], tortuosity has a dual effect on both shear rate and shear stress calculations. Christopher and Middleman [25] only incorporated tortuosity in shear stress calculations, while Bird et al. [24] incorporated tortuosity into the shear rate term. The various values of β chosen by different authors are summarized in Table 2.

Table 2. β values applied by different authors where ψ = 25/12.

Model	B
Bird et al. [24]	$\sqrt{2\psi}$
Christopher and Middleman [25]	$\sqrt{\frac{2}{\psi}}$
Teeuw and Hesselink [15]	$\sqrt{2}$

Hirasaki and Pope [26] conducted several core flood experiments where permeability was in the range 7–23 mD, porosity in the range 18–20% and residual oil between 20% and 32%. Based on these

experiments, they concluded that apparent viscosity could be calculated using the capillary bundle approach and Blake-Kozeny model as follows:

$$\mu_{app} = HU^{n-1} \tag{11}$$

where:

$$H = \frac{C}{12}\left(\frac{9n+3}{n}\right)^{n}(150K\phi)^{\frac{1-n}{2}} \tag{12}$$

They also included pore size distribution in their calculations:

$$\mu_{app} = \frac{C}{4}\left(\frac{1+3n}{n}\right)^{n}\frac{\int_0^\infty \sigma(R)R^2dR}{\left[\int_0^\infty \sigma(R)R^{\frac{1+n}{n}}dR\right]^{n}}\left(\frac{q}{\phi}\right)^{n-1} \tag{13}$$

Sadowski and Bird [16] used the Ellis model to obtain viscosity from the shear rate. The following equations for apparent viscosity were suggested based on the Blake-Kozeny model and capillary bundle approach:

$$\frac{1}{\mu_{eff}} = \frac{1}{\mu_0}\left(1+\frac{4}{n+3}\left[\frac{\tau_{RH}}{\tau_{1/2}}\right]^{n-1}\right) \tag{14}$$

$$\tau_{Rh} = \left(\frac{\Delta P}{L}\right)\left[\frac{D_p\phi}{6(1-\phi)}\right] \tag{15}$$

In the above expressions, μ_0, $\tau_{1/2}$ and n are Ellis model parameters that can be measured in rheometers. By applying these equations, they obtained an acceptable match between experimental and predicted results for low to medium molecular weight polymers.

In summary, none of the proposed models for non-Newtonian fluids in porous media based on the capillary bundle approach are in agreement with all experimental results. Therefore, some known limitations of the capillary bundle approach are noted as follows:

- It neglects complex features of porous media such as tortuosity and pore size distribution.
- It assumes unidirectional flow as it neglects interconnectivity between pores.
- It cannot be representative for flow in an anisotropic medium due to its assumption of unique permeability along propagation direction.
- It assumes a single radius along bundles with no variation in cross-sectional area. The contraction-expansion feature of non-Newtonian flow in porous media is of high importance, especially when studying extensional viscosity, yield stress and elasticity.
- It is generally developed based on rheological models in which analytical solutions for velocity profiles are available (e.g., power-law and Ellis model). Analytical solutions for some models (e.g., Carreau model) are quite difficult and the equation for velocity is implicit (Equation (10) for the Carreau model) and needs to be solved iteratively.

$$\frac{\partial v_z}{\partial r} = -\frac{\Delta p\, r}{2L}\left\{\mu_\infty + \frac{\mu_\infty - \mu_0}{\left[1+\left(\lambda\frac{\partial v_z}{\partial r}\right)^2\right]^{\frac{n-1}{2}}}\right\} \tag{16}$$

Duda et al. [27] studied polymer solution rheology inside porous media and reported that experimentally measured pressure drops were greater than those predicted by capillary bundle models, especially at lower values of the Carreau power index. Based on their study, a key reason for underestimating correction factors using the capillary bundle approach is the model's failure to capture either the interconnectivity of pores or non-uniform cross-sections of pore bodies and pore throats (i.e., abrupt contractions and expansions, also known as aspect ratio).

According to the aforementioned limitations of the capillary bundle approach and lack of a universally accepted equation for calculating shear rates in porous media, the application of effective medium theory was eventually suggested. This method was able to remediate certain weaknesses in capillary bundle approach, for example, by incorporating pore interconnectivity and variation in cross-sections. Canella et al. [18] extended this method to account for power-law fluids in porous media. Core floods were conducted using xanthan in the concentration range 300–1600 ppm, rock lithology (sandstone and carbonates) in the permeability range 40–800 mD and various oil residuals (0–29%). Their general assumption was that bulk rheological properties of polymer solutions obey the power-law model, and they suggested the following equation for the relation between shear rate and Darcy velocity based on effective medium theory:

$$\dot{\gamma}_{app} = \beta\left(\frac{3n+1}{4n}\right)^{\frac{n}{n-1}} \frac{q}{\sqrt{K\phi S_w}} \tag{17}$$

Canella et al. achieved a satisfactory match with their experimental results by using a constant value of 6 for β, although this value far exceeds correction factors suggested by other researchers [28–30]. Even though all published results in the literature are not covered by using this correction factor, better agreement between analytical and experimental results was obtained, such as in experiments performed by Teeuw and Hesselink [15] and Gogarty [31].

Canella et al. [18] demonstrated that apparent viscosity depends on both microscopic (connectivity, pore size distribution) and macroscopic properties (permeability, porosity) of porous media. Despite calculation improvements, neither effective medium theory nor the capillary bundle model are able to accurately estimate the correction factor. The great discrepancies in results obtained by the models described above and the wide range of correction factors suggested [17] confirm that a universally accepted model does not yet exist. Insufficiency of these models to predict in-situ viscosity may be attributed to their lack of incorporating time dependence and their use of oversimplified porous media models (e.g., capillary bundle).

To avoid over-simplification of porous media obtained by using the capillary bundle approach, pore network modelling has been suggested. In contrast to the capillary bundle approach, pore network modeling envisages porous media as interconnected bundles with idealized geometries where larger pores (pore bodies) are connected via smaller ones (pore throats). Pore network models have been used by Sorbie et al. [20] to study non-Newtonian fluids that exhibit shear thinning properties; later, several authors studied these phenomena [21,32–35]. Using network modeling, Sorbie et al. [20] showed that in connected (2D) networks of porous media, the average shear rate in the network correlates linearly with the flow rate. This result is not obvious and indeed is rather unexpected. Thus, any formula of the form of Equation (8) which is linear in U, and has a "shift factor", will do well for shear thinning fluids. The paper also shows that a similar argument holds for extensional flow where the extensional rate in the porous medium correlates linearly with flow rate (U). Lopez et al. [21] applied a pore network model to study non-Newtonian fluids using the same approach as for Newtonian fluids, except that viscosity in each bundle was not assumed to be constant and was considered as a function of pressure drop. Therefore, an iterative approach was suggested to calculate pressure drop and apparent viscosity. Although they obtained satisfactory agreement between analytical and experimental results using this approach, Balhoff and Thompson [34] stated that effects of concentration were neglected, and consequently proposed a new model based on CFD calculations to include effects of concentration in calculating conductivity of pore throats. They used pore network modeling to model shear thinning polymer flow with yield stress within a sand-pack.

Zamani et al. [35] studied the effects of rock microstructures on in-situ rheology using digital rock physics and reported that microscopic properties such as aspect ratio, coordination number and tortuosity may affect deviation of in-situ from bulk rheology.

In some experiments [23,27,31,36], in-situ rheology has been reported to deviate significantly from the behavior in bulk flow, such that in-situ rheology may not be calculated directly from bulk

rheology using the previously mentioned models. To achieve this, one may use these approaches assuming that either in-situ rheological properties are different from bulk rheological properties (e.g., Hejri et al. [36]) or that the relationship between apparent shear rate and Darcy velocity is non-linear (e.g., Gogarty [31]).

Calculation of in-situ rheology is a controversial subject. Until now, there has been no direct method to obtain it and, generally it has been measured by performing core floods. However, Skauge et al. [37] observed significantly different in-situ rheology for HPAM in linear compared to radial geometry. This discrepancy might be due to differing pressure regimes and flux conditions experienced by polymer solutions flowing through these inherently different flow geometries.

The problem with in-situ rheology calculations extends beyond finding the appropriate correction/shift factor. It also encompasses predicting the onset of extensional viscosity, which is treated as a separate subject in the following section.

2.2. Extensional Viscosity

Several experimental results show that, although polymer solutions (e.g., HPAM) only demonstrate shear thinning behavior in a rheometer, they may exhibit apparent shear thickening behavior above a critical shear rate in porous media (Figure 2) [23,27,31,36]. Generally, polymer flow in porous media may be divided into two distinct flow regimes: shear dominant and extensional dominant flow regimes. Since apparent shear thickening occurs in the extensional flow regime, it may also be referred to as extensional viscosity.

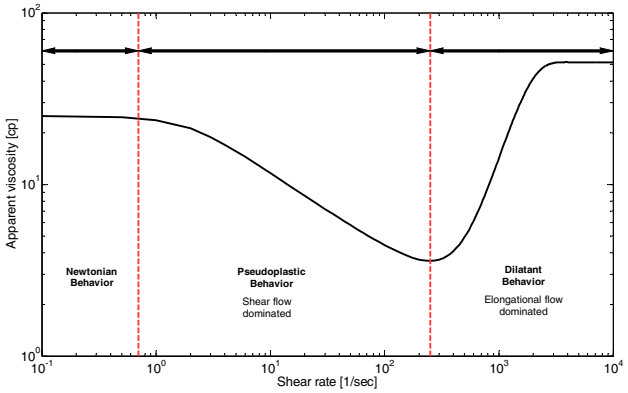

Figure 2. Schematic illustration of apparent viscosity in porous media.

Although its source is poorly understood, extensional viscosity is considered one of the principal aspects of polymer flow in porous media due to its influence on injectivity and oil mobilization. This phenomenon was suggested to be a consequence of elastic properties of polymer solutions (elongational dominated [38] or inertia-dominated flow [39]). As a result, extensional viscosity is often used interchangeably with elongational viscosity, shear thickening behavior, viscosity enhancement, dilatant behavior and viscoelasticity. Two different models are generally used to explain this phenomenon, the transient network model [40–42] and coil stretch model [43]. We adhere to the latter of these models.

Polymer molecules may be envisaged as entangled coils, and when exposed to a flow field, two forces may arise. First, an entropic force that attempts to maintain the existing polymer coil configuration. As coil entanglement increases, higher resistance to deformation is observed. Second the drag force resulting from interactions between solvent fluid and polymer molecules. When shear rate increases beyond a critical rate, molecule configurations change abruptly from coil to stretched states. Therefore,

polymer coils start to deform, resulting in anisotropy and stress differences between elongation and compression. Consequently, normal stresses and elastic properties become more dominant.

Choplin and Sabatie [40] suggested that when polymer molecules are exposed to a simple shear flow at a constant shear rate ($\dot{\gamma}$), molecules rotate at a constant angular velocity (ω) proportional to applied shear rate, and in each rotation polymer molecules are stretched and compressed. The time between each rotation can be calculated by Equation (18).

$$t = \frac{\pi}{2} k \dot{\gamma} \tag{18}$$

where k is a constant of proportionality, related to viscosity. If t is higher than the Zimm relaxation time, no dilatant behavior occurs. Consequently, the critical shear rate at the onset of dilatant behavior may be calculated based on Zimm relaxation time as follows:

$$\lambda_z = \frac{6}{\pi^2} \frac{M_w}{RT} [\mu]_0 \mu_s \tag{19}$$

$$t \leq \lambda_z, \dot{\gamma} \geq \gamma^* \overset{We = \dot{\gamma}\lambda_z}{\Rightarrow} We^* = \lambda_z * \dot{\gamma}^* = \frac{\pi}{2} k \tag{20}$$

Polymer viscosity behavior in extensional flow may be entirely different from its behavior in pure shear flow, i.e., polymer solution may show simultaneous shear thinning and extension thickening behavior. Theoretically, extensional viscosity can be calculated from Equation (21), where N_1 is normal stress difference and $\dot{\epsilon}$ is stretch rate. The relative importance of extensional viscosity and shear viscosity is defined by a dimensionless parameter known as the Trouton ratio (Equation (22)), initially proposed by Trouton [44]. For non-Newtonian fluids (especially viscoelastic fluids), Tr can reach very large values, such as 10^3 to 10^4 (i.e., when polymer solution demonstrates shear thinning and extension thickening simultaneously).

$$\mu_e = \frac{N_1}{\dot{\epsilon}} \tag{21}$$

$$Tr = \frac{\mu_e}{\mu_s} \tag{22}$$

In Figure 2, the in-situ viscosity of viscoelastic polymers is depicted in both shear and extensional flow regime. At the onset of polymer flow, the generated hydrodynamic force from fluid flow (i.e., drag force) is below the threshold value in terms of overcoming entropic forces. Therefore, polymer configuration persists in a coil shape, and viscosity remains constant and equal to the zero-shear rate viscosity (upper Newtonian plateau). As flow rate increases, polymer molecules are exposed to larger drag forces that disentangle polymer coils and aligns them along the flow direction. This coil alignment reduces resistance to flow (i.e., induces viscosity reduction) and is referred to as shear thinning. When the orientation of polymer molecules is completely aligned, they will start to stretch at increasing flow rates. A change in the deformation of polymer molecules may cause normal stress differences. At low stretch rates ($\dot{\epsilon}$), N_1 is very low and by increasing the stretch rate, N_1 dramatically increases. In other words, beyond the critical shear rate ($\dot{\gamma}_c$), instead of intramolecular interaction, intermolecular interactions will develop which generate amorphous structures much larger than average polymer chain dimensions [28,45].

Within the extensional flow regime, the apparent viscosity generally reaches a maximum value, subsequently followed by a decreasing viscosity interval. This phenomenon may be interpreted as high viscoelastic stresses causing polymer rupture and chain halving, and it has been reported as being more severe in low-permeability porous media [46]. As molecular rupture occurs, new molecular weight distributions emerge (larger molecular weight fractions are distorted) and viscosity behavior of the polymer may be governed by a new molecular weight distribution.

The onset of extensional viscosity-the transition point between shear-dominant and extensional dominant flow-depends on polymer, solvent, and porous media properties. The effects of polymer

properties on extensional viscosity can be investigated by using special rheometers that only generate pure extensional flow [47–56]. In the following, the effects of polymer, solvent and porous media properties on the onset of extensional viscosity are explained.

2.2.1. Polymer Concentration

Chauveteau [55] reported that the maximum relaxation time increases with polymer concentration, thus dilatant behavior commences at lower shear rates (Figure 3). He also included the effect of concentration in the expression for Zimm relaxation time, producing Equation (23).

$$\lambda_z = \frac{6}{\pi^2}\mu_s \frac{\mu_{ro} - 1}{C}\frac{M_w}{RT} \tag{23}$$

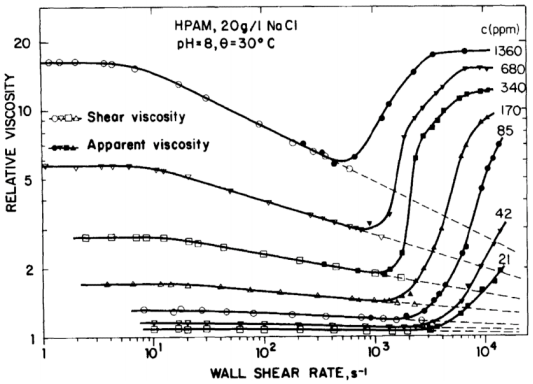

Figure 3. Effect of polymer concentration on the onset of extensional viscosity in a model with 45 successive constrictions. Reproduced with permission from [55].

The effect of concentration on extensional viscosity was also investigated by Lewandowska [56]. In contrast to Chauveteau, he reported that dilatant behavior commences at higher shear rates with increasing polymer concentration. He attributed this observation to the higher degree of entanglement as the concentration increases, thus increasing the extent of the shear thinning region.

Briscoe et al. [57] could not identify a consistent trend between polymer concentration and onset of extensional viscosity. They assumed that only a narrow region of polymer concentrations is able to generate apparent shear thickening behavior. Below a critical concentration limit, defined as the critical overlap concentration (C*), few polymer chains are able to form transient networks. At concentrations above C*, the extent of shear thinning may increase and, consequently, the onset of apparent shear thickening may be delayed. This effect was also studied by Dupuis et al. [58], where they observed that the onset of dilatant behavior decreased with polymer concentration. However, rheological behavior above the critical shear rate deviated among different concentration ranges (low: 30–60 ppm; medium: 120–240 ppm; and high: 480–960 ppm). Jiang et al. [59] also confirmed scattered data for the onset of extensional viscosity as function of polymer concentration. Clarke et al. [60] reported that the onset of extensional viscosity is independent of concentration and only depends on molecular weight.

2.2.2. Molecular Weight

The lengths of polymer chains increase with molecular weight, resulting in higher inter- and intramolecular entanglement. Thus, the extent of the shear thinning region increases and, consequently, delay the onset of dilatant behavior [56]. However, this explanation directly contradicts the expression for the Zimm relaxation time (Equation (23)), where the latter increases with molecular weight and causes critical shear rate to occur at a lower shear rate.

Jiang et al. [59] also studied the effects of molecular weight on the onset of extensional viscosity. They concluded that relaxation time increases with molecular weight, thus the onset of extensional viscosity occurs at lower shear rates. In addition, they observed that this trend was not valid above a critical molecular weight.

Clarke et al. [60] proposed the following correlation for the dependency of the onset of extensional viscosity on polymer molecular weight:

$$\lambda_{ext} \propto MW^2 C_p^0 \tag{24}$$

2.2.3. Salinity Effect

The effect of salinity on polymer rheology may be crucial in some reservoir conditions [11,61,62], and depends on polymer type. For typical EOR polymers (e.g., xanthan, HPAM, or generally non-hydrolyzed polymers), increasing salinity generally reduces coil gyration and hydrodynamic radius. Due to the repulsion between ionic groups in HPAM solutions, increasing salinity compresses the electrical double layer on molecular chains and electrostatic repulsion decreases. In the case of HPAM, the reaction mechanism varies for different metal ions i.e., either monovalent (Na^+) or divalent (Ca^{2+}) cations. In the monovalent case, it may suppress the charge effect and reduce the hydrodynamic radius. In the divalent case, reactions between cations (i.e., Ca^{2+}) can play the role of cross-linkers and influence the conformation and rheological properties of HPAM. In both cases, larger shear rates are required to uncoil polymers and the apparent shear thickening commences at larger shear rates [57,58,63].

2.2.4. Degree of Hydrolysis

When HPAM is dissolved in water, electrostatic repulsion forces cause polymer molecules to expand easily and the shear thinning region is shortened. Therefore, as the degree of hydrolysis increases, the onset of apparent shear thickening decreases [56].

2.2.5. Pressure and Temperature Effect

Although polymers are considered incompressible fluids, they do exhibit some degree of compressibility. Thus, pressure may have an impact on viscosity. By increasing pressure, the free volume between polymer molecules decreases and Brownian motion of polymer chains is inhibited, consequently resulting in viscosity increase of polymer solution. Experimental results [64] indicate that the onset of extensional viscosity decrease significantly with pressure.

The effects of temperature on polymer rheology has also been studied extensively [57,59,65,66] and results show that the critical shear rate and onset of dilatant behavior are retarded with increasing temperature. This behavior may have the following two explanations. Firstly, polymer relaxation time and solvent viscosity should both decrease with increasing temperature, based on Equation (23). Secondly, solvent quality decreases with temperature. By decreasing solvent quality, coil size is reduced, and to compensate for this reduction, a larger shear rate is needed to uncoil and elongate the polymer. Therefore, the onset of extensional viscosity occurs at higher shear rates.

2.2.6. Porous Media Properties

In addition to polymer properties, porous media may also significantly influence the generation of extensional flow, as shown by several experimental [25] and numerical studies [67]. Due to variation in cross-sectional area along its propagation path, polymer molecules are forced to accelerate and decelerate. Consequently, they will experience both stretch and shear flow in porous media, and above a critical flow rate, extensional flow will dominate shear flow.

To envisage polymer flow in porous media, the latter may be considered as a simplified contraction-expansion channel. As polymer molecules enter contractions, they will be compressed and stretched. If the flow is below a critical velocity, deformed polymer molecules have sufficient time to

return to their original state. Therefore, when polymer solutions enter subsequent contractions, no stress is stored and no additional resistance to flow is observed. However, if polymer relaxation time is high and polymer molecules are not able to return to their equilibrium state between contractions, stress will be stored and accumulated, thus resulting in steep increases in pressure drop and apparent viscosity. This phenomenon can be interpreted as a memory effect of polymer molecules.

Due to the inherent nature of porous media, polymer molecules are sheared near the wall and elongated at the flow axis. Therefore, molecular momentum is transferred by both tangential and normal stress components in porous media. Seeing that polymer molecules are able to rotate in pore space, molecules are not strained and effective viscosity is only controlled by shear. In contrast, if molecules are exposed to strain for sufficient time, molecule deformation plays a major role and effective viscosity will be defined by strain [25,67–72].

To predict the onset of extensional viscosity in porous media, the dimensionless Deborah number is defined as a ratio between the characteristic relaxation time of a fluid (θ_f) and characteristic time of porous media (θ_p), considered as the average time to travel from one pore body to another (Equation (25)). In other words, the Deborah number may be interpreted as the ratio between elastic and viscous forces. Based on this expression, the Deborah number is zero for Newtonian fluids and infinity for Hookean elastic solids.

$$N_{De} = \frac{\theta_f}{\theta_p} \tag{25}$$

Polymer solutions may have a wide range of molecular weights leading to a large number of relaxation times. Many researchers have used the longest relaxation time as representative of θ_f. However, this may cause the overestimation of Deborah numbers at the onset of extensional viscosity. Relaxation times may also be calculated from normal stress differences [73].

Some experimental observations revealed that the onset of extensional viscosity occurs when N_{De} is larger than 0.5 [74]. However, the Deborah number is not constant in different experiments and a wide range of values has been reported. Marshall and Metzner [73] reported a Deborah number of 0.1 at the onset of extensional viscosity, while Chauveteau [55] reported a relatively high Deborah number of 10. This wide range of reported Deborah numbers at the onset of extensional viscosity is due to difficulties in calculating stretch rates in porous media. To support this idea, Heemskerk et al. [75] reported that by using different polymer types in the same rock sample, critical Deborah numbers (N_{De}) were identical. However, when the same polymer was used in different rock samples, the critical N_{De} varied between 1 and 2. They concluded that measured relaxation times from experimental results can be used to practically define the onset of extensional viscosity, but they acknowledged that equations for calculating stretch rate are not able to capture the exact N_{De} at the onset of extensional viscosity. Zamani et al. [67] proposed that to obtain a more accurate estimation of the critical N_{De}, the stretch rate distribution at the pore scale is required. Metzner et al. [76] concluded that the critical Deborah number might only be used as a first estimation of the onset of extensional viscosity. In Table 3, some suggested equations for the calculation of Deborah number are summarized.

Table 3. Proposed equations for Deborah number calculation.

Model	Equation	Description
Masuda et al. [77]	$N_{De} = \theta_f \, \dot{\gamma}_{eq}$ $\dot{\gamma}_{eq} = \frac{\dot{\gamma}_c \lvert U_w \rvert}{\sqrt{k} \, k_{rw} \phi S_w}$	They used the inverse of the shear rate for θ_p. U_w is the Darcy velocity, k_{rw} is the water relative permeability, S_w is water saturation and $\dot{\gamma}_c$ is a constant equal to 3.97C, where C is an empirical correlation factor to account for the difference between an equivalent capillary model and real porous media
Hirasaki and Pope [26] Haas and Durst [78] Heemskerk et al. [75]	$\frac{1}{\theta_p} = \dot{\varepsilon} = \frac{v}{d} = \frac{U_w}{(1-\phi S_w)\sqrt{150 K K_r / (\phi S_w)}}$	

Several experimental results [68,79] show that the Deborah number alone is not sufficient to predict the onset of extensional viscosity. As an explanation, Ranjbar et al. [80] stated that the onset of extensional viscosity highly depends on the elastic properties of polymer solutions and relaxation time alone cannot capture viscoelastic properties. Experimental results reported by Garrouch and Gharbi [79] support this idea. They investigated two different polymer solutions (xanthan and HPAM) in Berea and sand-packs. Calculated Deborah numbers for these two completely and inherently different polymer solutions inside sand-packs were (surprisingly) identical. While xanthan consists of rigid, rod-like molecules that do not show extensional viscosity, HPAM consists of flexible and elastic chain-structured molecules.

Zamani et al. [67] numerically studied the effect of porous media on the onset of extensional viscosity by using real images of porous media obtained from digital rock physics. They confirmed that microscopic features of porous media had significant impact on the onset of extensional viscosity. Furthermore, by increasing the aspect ratio and inaccessible pore volume and decreasing the coordination number, extensional viscosity occurred at lower shear rates, in agreement with several experimental results [55,68,81].

Skauge et al. [37] reported that in radial flow, the onset of extensional viscosity occurred at higher shear rates than at typical core flooding. Since radial flow is more representative of real field conditions, results obtained from radial disks should be more accurate as laboratory data for field implementation.

Briefly summarized, at low shear rates where the amplitude of the elastic component is negligible, flow is controlled by shear forces. In contrast, above a critical shear rate, flow is extensional and governed by elastic forces. Therefore, the response of polymer solutions to imposed stress may be expressed as the sum of shear and elastic components:

$$\Delta P = \Delta P_{shear} + \Delta P_{elastic} \tag{26}$$

$$\mu = \mu_{shear} + \mu_{elastic} \tag{27}$$

The viscosity of polymer solutions under shear flow can be described by empirical equations such as the power-law and Carreau models. To describe viscosity under elongational flow, several models have been suggested, and some of them are summarized in Table 4.

Table 4. Proposed models for calculation of elongational viscosity.

Model	Equation	Description
Hirasaki and Pope [26]	$\mu_{el} = \frac{\mu_{sh}}{[1-N_{De}]}$	
Masuda et al. [77]	$\mu_{elas} = \mu_{sh} C_c (N_{De})^{m_c}$	where C_c and m_c are constant and relate to pore geometry
Delshad et al. [61]	$\mu_{el} = \mu_{max}\left[1 - \exp\left(-\left(\lambda_2 \tau_r \dot{\gamma}\right)^{n_2 - 1}\right)\right]$ $\tau_r = \tau_1 + \tau_0 C_p$ $\mu_{max} = \mu_w \left(AP_{11} + AP_{22} \ln C_p\right)$	τ_r is the characteristic relaxation time and can be calculated by dynamic frequency sweep test in the laboratory. Some empirical correlations are also proposed for dependency of different parameters on polymer concentration
Stavland et al. [62]	$\mu_{el} = \left(\lambda_2 \dot{\gamma}\right)^m$ $\lambda_2 = \left\{N_{De}\left(\frac{1-\phi}{\phi}\right)\left(\frac{6\alpha\sqrt{\tau}}{\lambda_1}\right)\right\}^{-1}$	m is a non-zero tuning parameter which is known as the elongation exponent and depends on the molecular weight and demonstrates linear correlation with $[\mu]$ C_p. α in the listed formulation is considered 2.5

2.3. Injectivity

Polymer injectivity is a crucial factor governing the economics of polymer flooding projects and its accurate estimation is a prerequisite in terms of optimizing the upper-limit injection rate [82]. Injection well pressure may increase due to one of the following causes: (1) oil bank formation, (2) in-situ polymer viscosity (especially shear thickening due to viscoelasticity) and (3) different types of retention, which cause permeability reduction.

The highest pressure drops observed during polymer flooding are located in the vicinity of the injection wellbore due to dramatic variations in flow rate. Therefore, it is important to include non-Newtonian effects of polymer solutions to accurately predict polymer injectivity. Although both HPAM and xanthan demonstrate shear thinning behavior at low to moderate shear rates, HPAM exhibits apparent shear thickening above a critical flow rate due to its inherent viscoelastic nature. For field applications, injection rates in the vicinity of the injection well may easily exceed the onset of extensional viscosity, and injectivity will then dramatically decrease. In contrast to HPAM, xanthan shows exclusively shear thinning behavior and will attain its highest value of injectivity in the near-wellbore region.

Injectivity investigations at the lab scale are required before implementing field applications, and effects of polymer solution properties, in-situ rheology, temperature, pH, level of retention and the nature of porous media should be accurately measured [83,84]. Furthermore, if screening criteria for polymer type are disregarded, polymer entrapment in narrow pore throats can have significant effects on its injection rate. The salinity of solutions can also affect polymer solubility, resulting in filter cake formation near injection wells or precipitation of polymer molecules in the reservoir. Inaccurate measurement of in-situ rheology and especially the onset of extensional viscosity may lead to either an underestimation or overestimation of injectivity. In some polymer flooding projects, measured injectivity may differ significantly from the simulation or analytical forecast. These unexpected injectivities may be due to the occurrence of mechanical degradation [82,85,86], induced fractures [87–89], or even inaccurate analytical models for calculating in-situ rheology and predicting extensional viscosity.

3. Radial In-Situ Rheology

Injectivity (I) may be defined as the ratio of volumetric injection rate, Q, to the pressure drop, ΔP, associated with polymer propagation between injection well and producer [1]:

$$I = \frac{Q}{\Delta P} \tag{28}$$

As previously mentioned, formation fracture pressure may constrain the value of volumetric injection rate. Due to its significant effect on project economics, accurate determination of differential pressure, and hence injectivity, at a given injection rate is essential. To achieve this, all factors affecting differential pressure during polymer flooding must be quantified. Darcy's law for radial flow may be expressed in terms of differential pressure as follows:

$$\Delta P = \frac{\mu_{app} Q}{2\pi h k_{e,i}} ln \frac{r_e}{r_w} \tag{29}$$

where μ_{app} is apparent viscosity, h is disk thickness, $k_{e,i}$ is effective permeability to polymer solution, r_e is disk radius and r_w is injection well radius.

In this paper, the ratio of resistance factor (RF) to residual resistance factor (RRF) is used to represent apparent viscosity of polymer solutions propagating through porous media, thus isolating its viscous behavior, i.e.,

$$\mu_{app} = \frac{RF}{RRF} \tag{30}$$

where the resistance factor (RF) represents the pressure increase of polymer relative to brine and the residual resistance factor (RRF) is defined as the ratio of pressure before and after polymer injection (i.e., pressure caused by irreversible permeability reduction induced by retention mechanisms).

Due to their inherent viscoelastic behavior in porous media, synthetic polymers (e.g., HPAM) will exhibit shear-dependent apparent viscosity. Although the common consensus on apparent shear thickening as a phenomenon is accepted, its viscosifying magnitude is still an ongoing topic of debate in scientific communities.

Accurate polymer rheology estimation is a prerequisite for reasonable injectivity estimates due to the proportionality between apparent viscosity and differential pressure. In linear core floods where steady-state pressure conditions exist, polymer flux will remain constant from inlet to outlet, rendering rheology estimation a straightforward task. However, in radial flow, polymer flux is gradually reduced as it propagates from injection well to producer, therefore attaining a range of viscosities rather than one specific value. Since the degree of mechanical degradation generally increases with injection rate, discrepancies in polymer rheology obtained from different injection rates may transpire. Instead of possessing one definite rheology, polymers propagating through radial disks will exhibit both shear-dependent and history-dependent viscosity behavior, thus increasing the complexity of rheology estimation in radial compared to linear models. To date, no correction factor has been suggested to account for this dual nature phenomenon. Even when mechanical degradation is excluded, i.e., when injected and effluent viscosities are approximately equal, this dual nature phenomenon persists, and is suggested to be attributed to non-equilibrium pressure conditions experienced in radial flow and inherent history-dependent nature of polymer molecules.

In addition, synthetic polymers are susceptible to mechanical degradation at high flux, typically in the near-wellbore region, which will impart an irreversible viscosity reduction due to polymer molecule fragmentation. Mechanical degradation induces a pressure drop that improves injectivity. However, since it disrupts the carefully selected viscous properties of the polymer solutions by a non-reversible viscosity decrease, mechanical degradation is not a sought-after phenomenon in polymer flooding. A remediation measure to reduce mechanical degradation is to pre-shear the polymer before injection. Pre-shearing removes the high molecular weight part of the molecular weight distribution, which is believed to be most susceptible to mechanical degradation [6]. Mechanical degradation may also be minimized by shifting to a lower molecular weight polymer. However, this would require higher amounts of polymer to obtain the same concentration, thus potentially influencing polymer project economics.

As mentioned, in radial geometry, high flux causing mechanical degradation occurs principally in the near-wellbore region, as opposed to linear geometry where this high flux persists throughout the entire propagation distance. Therefore, the time that polymer is exposed to high shear is short in radial transient flow pattern, as opposed to that of a steady-state linear core flood, [34]. Based on this time-differing condition between linear and radial flow, it was suggested by Skauge et al. that polymer is degraded to a lesser extent in radial compared to linear flood when injected at the same volumetric flow rate [33].

In summary, there are two principal factors governing injectivity during polymer flooding in linear geometry: (1) viscoelasticity of polymer that induces large injection pressures mainly due to apparent shear thickening behavior at high flux; and (2) mechanical degradation in the near-wellbore region, which causes an entrance pressure drop [1]. In radial disks, two additional factors should be included: (3) non-equilibrium pressure conditions due to kinetic effects; and (4) memory-effects of polymer molecules in non-constant velocity fields.

4. Materials and Methods

Rock: Bentheimer outcrop rock (porosity of ~23%, permeability of about 2.6 Darcy). Based on XRD measurements, Bentheimer consists predominantly of quartz (90.6%) with some feldspar (4.6%), mica (3.2%) and siderite (1.0%).

Polymer: Flopaam 3630S, 30% hydrolyzed, MW = 18 million Da.

Brine: Relatively low salinity with a low content of divalent ions. Brine composition by ions is given in Table 5.

Table 5. Brine ionic composition.

Ion	Concentration (ppm, *w*/*w*)
Na	1741
K	28
Ca	26
Mg	17
SO_4	160
Cl	2687
TDS	4659
Ionic strength	0.082
Hardness	43

Linear core floods: Core data are summarized in Table 6. All experiments were performed at room temperature and pressure.

Radial core floods: Bentheimer disks were prepared by coating with epoxy resin, vacuuming and saturating with brine. One disk was then drained with an extra heavy oil and aged for 3 weeks at 50 °C to a non-water-wet state. The crude had an initial viscosity of about 7000 cP. The extra heavy oil used for drainage and aging, was then exchanged with a flooding oil of 210 cP. Both experiments were performed at room temperature and pressure. Core data are given in Table 7. The pressure ports were located in the injection and production wells and at radii 0.5, 1.0, 1.5, 2.0, 3.0, 4.0 and 5.0 cm for the disk without oil and at radii 1.1, 2.0, and 5.0 cm for the disk containing oil.

The Bentheimer cores show a pore-throat distribution function similar to other outcrop sandstone material, Figure 4. All porous media have local pore-size variation, involving continuous contraction and expansion of pore-scale transport.

Table 6. Core data for linear core floods.

Experiment	Conc.	L (cm)	D (cm)	ϕ (-)	K_{wi} (Darcy)	K_{wf} (Darcy)	RRF (-)	η_i (cP)	η_e (cP)
No oil	500 ppm	9.54	3.77	0.24	2.48	1.35	1.84	6.81	6.62
No oil	1500 ppm	4.89	3.79	0.24	1.99	0.32	6.29	33.76	32.87
With oil, not aged	500 ppm	10.44	3.78	0.23	1.83	0.36	5.08	6.65	6.77
With oil, aged	500 ppm	9.85	3.78	0.23	2.27	0.27	8.41	6.99	5.90

Table 7. Core data for radial core floods.

Experiment	Diameter (cm)	Thickness (cm)	Well Radius (cm)	ϕ (-)	PV (mL)	Soi (frac)	Sorw (frac)	$K_{w,abs}$ (Darcy)	$K_{w,Sorw}$ (Darcy)	K_{wf} (Darcy)
No oil	30.00	2.20	0.15	0.24	373	n.a.	n.a.	2.600	n.a.	0.056
With oil	29.90	2.21	0.30	0.23	352	0.91	0.22	1.551	0.041	0.039

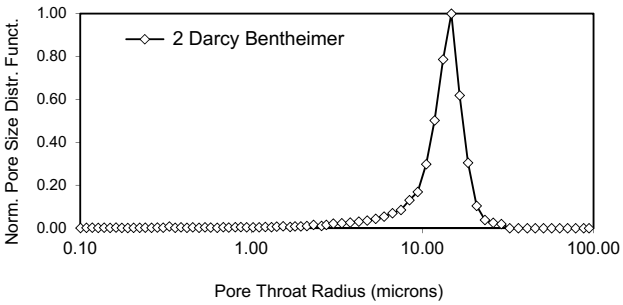

Figure 4. Mercury injection derived pore throat distribution for Bentheimer core material used in the polymer flow experiments.

Simulation: The experimental set-up enabled detailed monitoring of pressure by internal pressure ports located at various distance from the injection well. Differential pressure as function of radial distance was history matched using the STARS simulator, developed by Computer Modeling Group (CMG). The simulation model encompassed a radial grid with 360 sectors, each consisting of 150 grid block cells in radial direction, where the grid block cell size is 1 mm. Porous media permeability (tuning parameter) was obtained by history matching water floods prior to polymer flooding. Local permeability variation improved the history match compared to analytical solution (Darcy's law for radial flow). Permeability data obtained from water floods were used in subsequent polymer floods to isolate the effects of polymer apparent viscosity on differential pressure. In polymer floods, as the permeability obtained from the precursor water flood was held constant, apparent viscosity could be quantitatively investigated as a function of velocity and was used as the tuning parameter to history match differential pressure. The STARS simulation tool can include both shear thinning and thickening behavior of viscoelastic fluids.

Due to the inherent grid averaging calculation method of the simulation tool, the velocity in the first grid block after the injection well was below its analytical value. Because of a rapid velocity decrease with distance in radial models, this phenomenon was addressed by decreasing the injection well radius, thus effectively parallel shifting the position of the first grid block towards the injection well until the correct velocity was attained. This was a necessary step, since the tuning parameter is apparent viscosity as a function of velocity.

5. Polymer In-Situ Rheology in Linear Cores

Four Bentheimer outcrop cores were used to study polymer in-situ rheology in linear systems. Petro-physical properties of core samples as well as properties of polymer solutions are given in Table 6. Two experiments were carried out to examine the effect of polymer concentration on in-situ rheology of the polymer solution. Partially-hydrolyzed Flopaam 3630S at 500 ppm and 1500 ppm was injected into the cores and the in-situ rheology of the polymer solutions was measured. The two concentrations were chosen to give viscosities representative of the upper and lower limit of what would be economically viable for polymer flooding in an oil field. Both concentrations are above the polymer critical overlap concentration, C*. The results are presented in Table 6 and Figure 5. The bulk viscosity of 1500 ppm 3630S is about 34 cP which is about 5 times that of 500 ppm 3630S. Comparing in-situ rheology of 500 ppm and 1500 ppm 3630S shows that the onset and degree of apparent shear thickening behavior are fairly similar for both concentrations. This is in line with observations by Skauge et al. [8] and Clarke et al. [60] that the onset of extensional viscosity is independent of polymer concentration and only depends on polymer molecular weight. It is noted that this is generally only true for $C^* < C < C_{lim}$, where C_{lim} is the economic limit for polymer concentration, typically between 1500 and 2500 ppm. Table 6 and Figure 5 show that the magnitude of resistance factor (RF) and residual resistance factor (RRF) are about 4 and 3 times higher for 1500 ppm compared to 500 ppm, respectively. This implies that polymer injectivity is a function of polymer concentration, and better injectivity is achieved with lower polymer concentrations.

A series of experiments was also performed to study the effect of the presence of residual oil on polymer in-situ rheology. In these experiments, Bentheimer cores at residual oil saturations of about 22% and different initial wettability states were flooded with polymer and the in-situ rheology behavior was compared to that of single-phase polymer injection in absence of residual oil. Prior to polymer injection, the cores containing oil were water flooded to residual oil saturation. At the end of the water flood, the flow rates were increased to generate pressures higher than that expected for the subsequent polymer flood. This was performed in order to avoid oil mobilization during the polymer flood and, indeed, no oil production was observed during the subsequent polymer flood. The results are presented and compared in Figure 6. As this figure shows, the onset of apparent shear thickening is not affected by the presence of residual oil or the wettability state of the cores. However, the slope of apparent shear thickening and magnitude of resistance factor is significantly affected by oil presence in

the cores. That is, although onset of apparent shear thickening is independent of oil presence in porous media and its wettability condition, the results show that the degree of apparent shear thickening is lower when oil is present in the porous media.

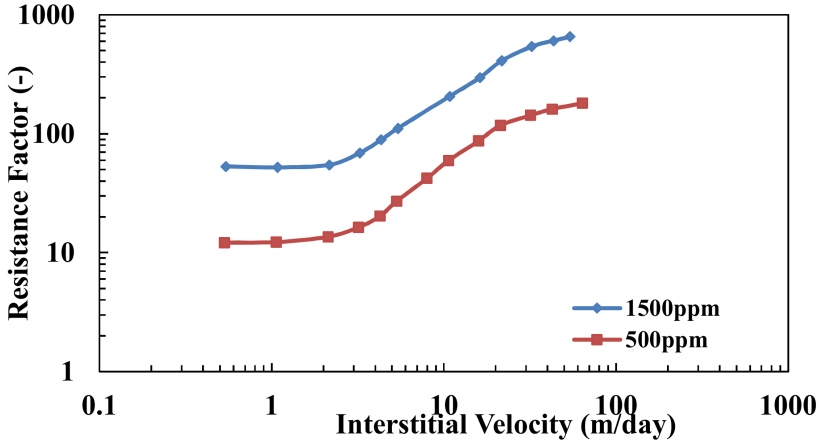

Figure 5. Resistance factor versus interstitial velocity of pre-filtered Flopaam 3630S HPAM polymer dissolved in 1 wt% NaCl brine.

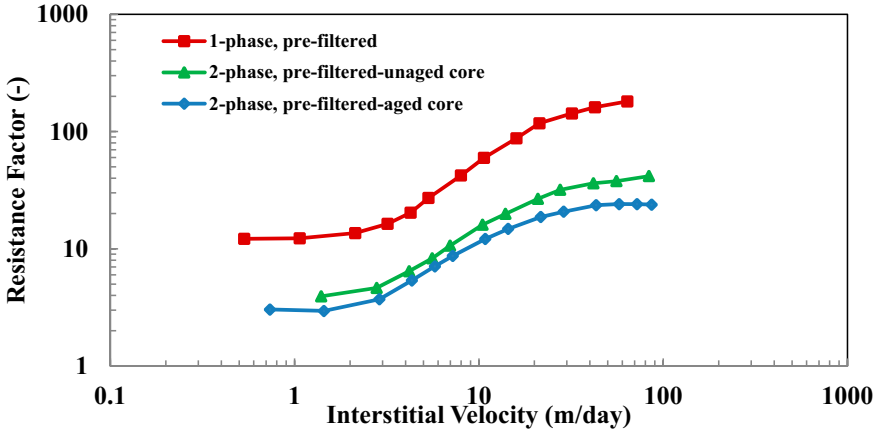

Figure 6. Resistance factor versus interstitial velocity of 500 ppm pre-filtered Flopaam 3630S partially hydrolyzed polyacrylamide (HPAM) polymer dissolved in 1 wt% NaCl brine, single-phase polymer flow and polymer flow at residual oil saturation.

It is important to note that a lower resistance factor in the presence of oil is achieved while porous media is partially occupied by residual oil. Therefore, unlike the single-phase system, in which the pore volume (assuming no inaccessible pore volume) is available for polymer flow, only PV*(1-Sor) is available for polymer flow in two-phase system. This influences and reduces permeability and therefore an even higher resistance factor is expected in the presence of oil. However, the results do not show such an effect, and a lower resistance factor and polymer injectivity is observed with the presence of oil in porous media, which supports the significance of the positive effect of oil on polymer injectivity. The effluent polymer viscosity is reduced by 18% compared to the injected polymer solution

for the single-phase, water-wet case, while there is no reduction in effluent viscosity for the two-phase experiments (water-wet and non-water-wet). Shiran and Skauge [90] studied wettability using the same crude oil for aging and found that intermediate wettability was achieved. The end-point water relative permeability confirms that a similar condition was obtained.

Polymer injection in cores with residual oil results in a lower resistance factor which means better polymer injectivity. Furthermore, the resistance factor in the aged core with the non-water-wet state is lower than the resistance factor in the water-wet core. The lower resistance factor in the presence of oil could be attributed to lower adsorption/retention of polymer molecules on rock surface, as reported by Broseta et al. [10]. The rock surface in the presence of an oil film, and especially in less water-wet conditions is partially covered by crude oil polar components during flooding. Therefore, in comparison to single-phase systems, the rock surface has fewer adsorption sites to adsorb polymer molecules. The analysis of reduced apparent viscosity in the presence of oil, assumes that end-point water relative permeability remains constant for polymer as it does for water. The RRF measured with brine after the polymer injection is assumed constant for all rate variation of polymer flow. Under these assumptions a lower resistance factor and better polymer injectivity is expected.

6. Polymer In-Situ Rheology in Radial Flow

Recently, polymer injectivity was analyzed by matching field injectivity tests [5,6,91,92]. In addition to history matching, modification of equations to incorporate fractures and polymer degradation in the near-wellbore zone were reported. The laboratory experiment simplifies the analysis as additional complications like fractures and strong heterogeneity can be avoided.

In earlier studies of radial flow experiments, Skauge et al. [37] used local pressure taps as a function of radial distance from the injection well to derive in-situ rheology. These experiments demonstrated both shear thinning and strong apparent shear thickening behavior.

Two radial flow experiments were performed on circular Bentheimer sandstone disks of 1.6 and 2.6 D permeability with 30 cm diameter and 2.2 cm thickness, see Table 7. The first experiment was performed on a disk that was drained with crude oil and aged to non-water-wet conditions. The second experiment was performed in the absence of oil on a water-wet disk. For the first experiment, the disk was flooded extensively with brine to reach residual oil saturation, Sorw = 0.22. Bump rates were applied to avoid oil mobilization by viscous forces during the subsequent polymer flood. The polymer flood was performed by first saturating the disk with polymer at a low rate to avoid mechanical degradation due to shearing. Thereafter, rate variations were performed to determine in-situ rheology of the polymer. A brine flush was performed between concentration slugs to remove non-adsorbed polymer.

Concentrations of 800 and 2000 ppm were chosen to represent lower and upper boundaries of the semi-dilute region. The second experiment included the same steps, except for water flooding to Sorw. In this case, the water flood was performed to obtain a pressure reference for the subsequent polymer flood. No oil production was detected during polymer floods.

Differential pressure was measured by internal pressure ports located at different radii from the injection well. The 800-ppm HPAM solution was injected in the presence of residual oil at flow rates of 2.2 and 2.8 mL/min, and in the absence of residual oil at 2.0 and 4.0 mL/min. Differential pressure decay as a function of radial distance from injector is shown in Figure 7. The pressure transition zone from semi-steady-state to steady-state is extended compared to the case without oil. Most notable is the difference in pressure in the injection well. While differential pressures measured from internal pressure ports are higher for the two-phase system (as expected), well injection pressure is significantly lower in the presence of residual oil. Taking the pressure ratio of pressure ports at ~1 cm from injection well as a reference, injection pressure should be 5–6 times higher for the disk with oil, compared to the one without. Instead, the injection pressure is 25% lower. There may be several reasons for this observed result. One reason may be that the presence of oil reduces the effective pore volume, thereby leading to higher flow velocities for the polymer in the near-well region. This would

subsequently lead to higher effective shear forces on the polymer, producing mechanical degradation. If mechanical degradation occurs, it has only a minor effect on the shear viscosity. The shear viscosity is 15.1 mPas for the effluent sample taken at 2.0 mL/min, while it was 16.0 mPas for the injected solution (measured at 22 °C, 10 1/s). However, as discussed in Section 2.2, it is the extensional viscosity that is the determining factor for high pressures in near-well region. Changes in extensional viscosity are intrinsically hard to measure and were not performed here. It is still possible that the increase in shear forces for the case with residual oil lead to a reduction in extensional viscosity but not for the case without oil where the effective pore volume was larger. The two other reasons are related to the wetting state of the porous media. If the oil is located in smaller pores, polymer flow is diverted to larger pores where it flows at higher velocities (higher flux). Since the velocity increase takes place in larger pores, only minor degradation would be expected. A third reason may be that porous media is fractionally oil-wet and that there is a difference in the slip conditions for the water-wet and the oil–wet surfaces. This may reduce effective shear for the oil-wet surfaces leading to reduced mechanical degradation. Although there have been speculations on the "lubricating" effect of oil-wet surfaces, no clear evidence of the effect on apparent viscosity or injectivity for core material have been shown to date. It is not possible to differentiate between the three phenomena based on the pressure data alone.

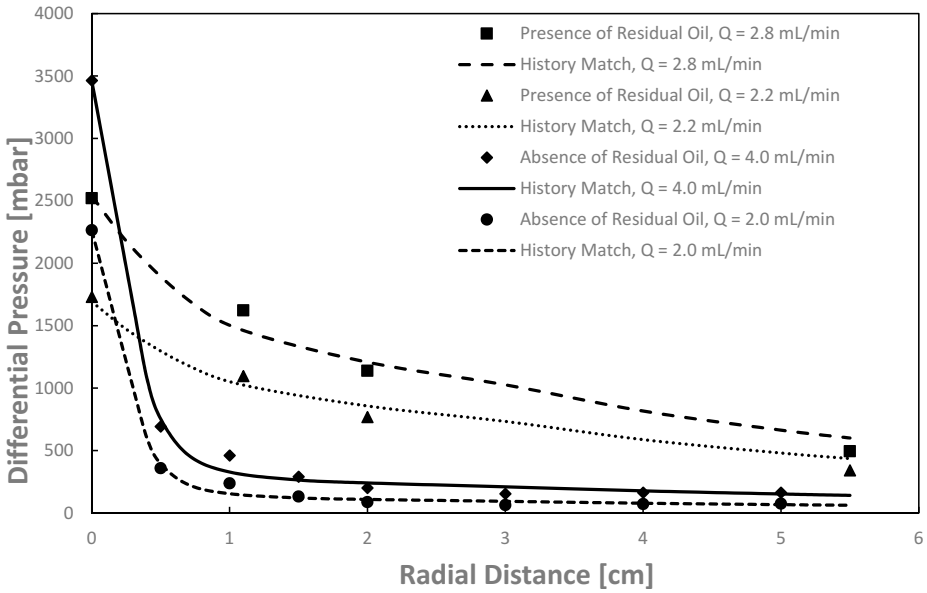

Figure 7. Differential pressure profiles for 800-ppm HPAM floods in the presence and absence of residual oil in radial geometry as a function of distance from injector to producer for four flow rates.

Each of the polymer floods were history matched using STARS (CMG). The measured differential pressures as a function of distance from injection well were used as history match parameters, while polymer apparent viscosity was used as a tuning variable. History matches and polymer rheology from both experiments for 800-ppm HPAM floods are shown in Figures 7 and 8, respectively. It is evident from Figure 8 that the polymer rheology is significantly influenced by the presence of residual oil. In terms of absolute values, the apparent viscosity is between a factor of 5 and 10, and it is higher in the absence, compared to the presence of residual oil. Furthermore, the onset of apparent shear thickening shifts to lower velocities in the presence of residual oil. This occurrence is suggested to result from reduced propagation cross-section caused by the residual oil saturation. When flow

channels in porous media become narrower, the extensional flow regime is reached at a lower flux, and HPAM exhibits viscoelastic behavior at an earlier stage, thus the onset of apparent shear thickening commences at a lower flux. The effect of shifting the onset of apparent shear thickening to a lower flux may be detrimental for injectivity. However, since the apparent shear thickening seems to be much more extensive in the absence of residual oil, the rheology shows that overall injectivity is significantly improved in presence of residual oil.

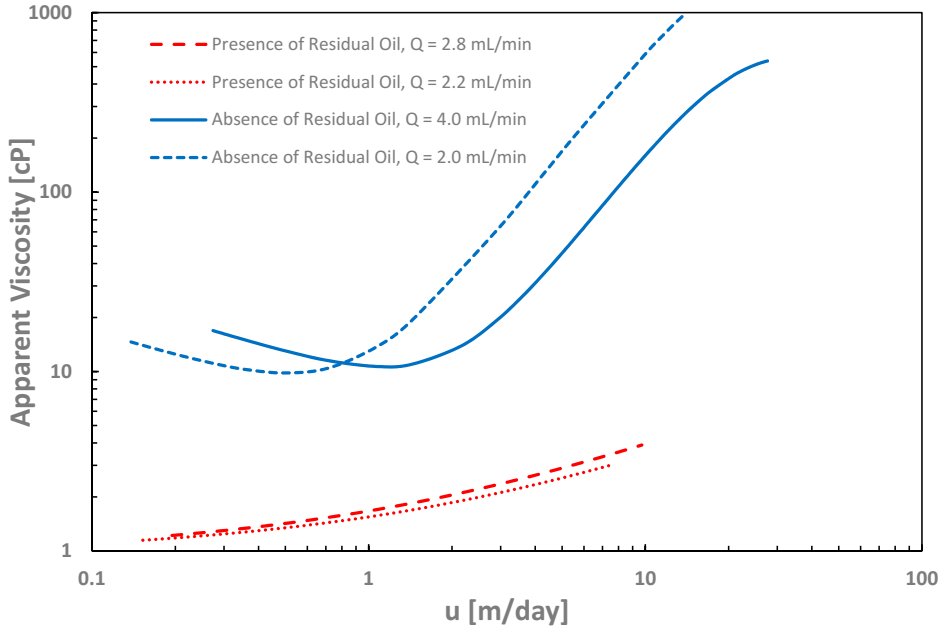

Figure 8. Apparent viscosity from history match of differential pressure for 800 ppm HPAM in presence and absence of residual oil in radial geometry.

History matches and polymer rheology in the presence and absence of residual oil for 2000 ppm floods are shown in Figures 9 and 10, respectively. In order to evaluate the influence of polymer concentration on in-situ rheology, 2000 ppm HPAM was injected in both disks. The differential pressures are shown in Figure 9. In this case, the injection rates were Q = 2.0 and 5.0 mL/min for the disk with no oil, and Q = 1.4 and 1.6 mL/min for the disk with oil. These data show the same trend as for the 800 ppm injection: strong reduction in injection well pressure in the presence of residual oil and extension of the transition zone.

In accordance with the 800 ppm solution, polymer viscosity was significantly higher in the absence compared to presence of residual oil, and ranged between a factor of 6 and 16 in their joint velocity interval, Figure 10. In addition, the 2000 ppm solution also showed a decrease in the onset of apparent shear thickening in the presence of residual oil, consistent with the lower concentration solution investigated. Similar to the 800 ppm solution, apparent shear thickening is observed to be much more extensive in absence of residual oil, thus improved injectivity in the presence of residual oil is further corroborated.

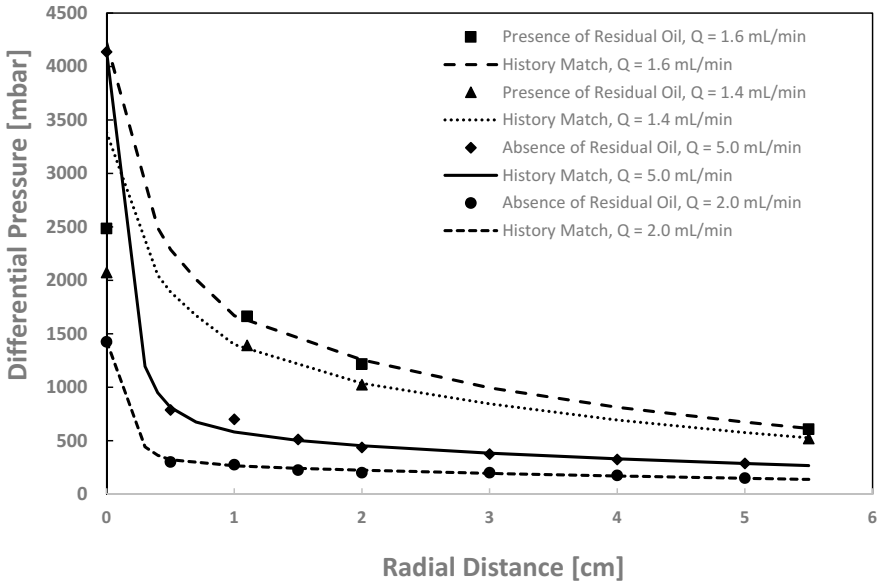

Figure 9. Differential pressure profiles for 2000 ppm 3630S HPAM floods in presence and absence of residual oil in radial geometry as a function of distance from injector to producer for four flow rates.

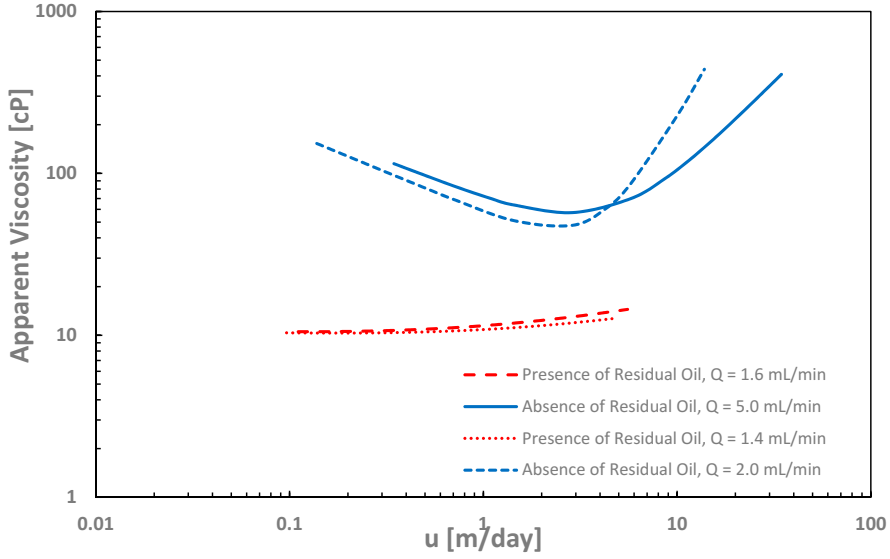

Figure 10. Apparent viscosity from the history match of differential pressure for 2000 ppm 3630S HPAM in the presence and absence of residual oil in radial geometry.

7. Conclusions

A review of polymer flow in a porous medium was presented. The available EOR analytical models we evaluated have limitations in accurately describing flow of polymer at high shear rates, e.g., near injector, and this leads to underestimating or overestimating of polymer injectivity.

The experimental results presented expand our insight into polymer flow in a porous medium. Shear thinning behavior may be present in core floods while bulk rheology is predominant from rheometer measurements. Linear polymer flow experiments are dominated by apparent shear thickening which is not measured in standard rheometers. The extensional viscosity, which is the main cause of the apparent shear thickening behavior, occurs at flow velocities strongly influenced by the porous media.

Linear core floods are commonly used for evaluating polymer in-situ rheology and injectivity, but they suffer from steady-state conditions throughout the core as opposed to the well injection situation where both pressure and shear forces are nonlinear gradients.

In the linear core floods, the onset of apparent shear thickening is independent of polymer concentration, when polymer type, brine composition and porous media are held constant. It is also independent of the presence of oil and wettability for the three cases evaluated here.

Radial flow injections show more complex in-situ rheology. The in-situ rheology shows a much higher degree of apparent shear thickening in the presence of oil. This may be due to restrictions in the pore space available. In the absence of oil, high concentration polymer (2000 ppm) showed shear thinning behavior. The onset of apparent shear thickening was shifted to higher flow velocities. There is a need for further development of numerical models that incorporate memory effects and possible kinetic effects for high polymer flow rates in the near-well region.

Both linear and radial experiments confirm lower apparent viscosity when oil is present in the porous medium. This conclusion is based on the assumption that brine end-point relative permeability is unchanged for polymer injection compared to two-phase flow by water injection. No extra oil was produced during polymer injection and this support the lowering of in-situ polymer viscosity in the presence of oil.

Author Contributions: A.S., B.S.S., and T.S. were responsible for the experimental program and simulation study. N.Z. structured the review contribution, while B.A.-S. and J.G.J. are Ph.D. students working on polymer injectivity, including the experimental study and simulation work. All authors contributed in writing the paper.

Funding: This research received no direct external funding.

Acknowledgments: The authors gratefully acknowledge support from the Norwegian Research Council, Petromaks 2 program. Badar Al-Shakry acknowledge support from, PDO, Petroleum Development Oman. Arne Skauge acknowledge support from Energi Simulations, Canada as the Energi Simulation EOR chair at University of Bergen.

Conflicts of Interest: The authors declare no conflicts of interest.

Nomenclature

A	Cross section area
C	Power-law constant
C_p	Polymer concentration
D_p	Grain size diameter
De	Deborah number
h	Disk thickness
H	Constant, equation 11
k	Constant, equation 18
K_{ei}	Effective permeability to polymer
K	Permeability
L	Length of model
M_w	Polymer molecular weight
N_1	Normal stress difference

n	Ellis, Carreau or power-law constant
P	Pressure
Q	Flow rate
R	Radius
r_e	Disk radius
r_w	Injection well radius
RF	Resistance factor
RRF	Residual resistance factor
R_{eq}	Equivalent radius obtained from Blake-Kozeny model
S_w	Water saturation
T	Temperature
Tr	Trouton ratio
U	Darcy velocity
Wi	Weissenberg number
I	Injectivity
α	Correction factor
β	Constant, equation 10
ω	Angular velocity
$\dot{\varepsilon}$	Stretch rate
ΔP	Pressure drop
$\dot{\gamma}$	Shear rate
$\tau_{1/2}$	Ellis model parameter
$\dot{\gamma}_{eff}$	Effective shear rate
$\dot{\gamma}_{app}$	Apparent shear rate
$\dot{\gamma}_c$	Critical shear rate
λ	Polymer relaxation time
λ_z	Zimm relaxation time
μ	Viscosity
μ_{app}	Apparent viscosity
μ_{eff}	Effective viscosity
μ_0	Upper Newtonian plateau
μ_s	Solvent viscosity
μ_{sh}	Shear rate viscosity
μ_e	Elongational viscosity
μ_∞	Lower Newtonian plateau
ϕ	Porosity
ψ	Tortuosity
θ_f	Characteristic relaxation time of fluid
θ_p	Characteristic time of porous media

References

1. Seright, R.S. The Effects of Mechanical Degradation and Viscoelastic Behavior on Injectivity of Polyacrylamide Solutions. *Soc. Pet. Eng. J.* **1983**, *23*, 475–485. [CrossRef]
2. Shuler, P.J.; Kuehne, D.L.; Uhl, J.T.; Walkup, G.W., Jr. Improving Polymer Injectivity at West Coyote Field, California. *Soc. Pet. Eng. Reserv. Eng.* **1987**, *2*, 271–280. [CrossRef]
3. Southwick, J.G.; Manke, C.W. Molecular Degradation, Injectivity, and Elastic Properties of Polymer Solutions. *Soc. Pet. Eng. Reserv. Eng.* **1988**, *3*, 1193–1201. [CrossRef]
4. Yerramilli, S.S.; Zitha, P.L.J.; Yerramilli, R.C. Novel Insight into Polymer Injectivity for Polymer Flooding. Presented at the SPE European Formation Damage Conference and Exhibition, Noordwijk, The Netherlands, 5–7 June 2013. [CrossRef]
5. Lotfollahi, M.; Farajzadeh, R.; Delshad, M.; Al-Abri, K.; Wassing, B.M.; Mjeni, R.; Awan, K.; Bedrikovetsky, P. Mechanistic Simulation of Polymer Injectivity in Field Tests. Presented at the SPE Enhanced Oil Recovery Conference, Kuala Lumpur, Malaysia, 11–13 August 2015. [CrossRef]
6. Glasbergen, G.; Wever, D.; Keijzer, E.; Farajzadeh, R. Injectivity Loss in Polymer Floods: Causes, Preventions and Mitigations. Presented at the SPE Kuwait Oil & Gas Show and Conference, Mishref, Kuwait, 11–14 October 2015. [CrossRef]

7. Al-Shakry, B.; Shiran, B.S.; Skauge, T.; Skauge, A. Enhanced Oil Recovery by Polymer Flooding: Optimizing Polymer Injectivity. Presented at the SPE Kingdom of Saudi Arabia Technical Symposium and Exhibition, Dammam, Saudi Arabia, 23–26 April 2018.
8. Skauge, T.; Kvilhaug, O.A.; Skauge, A. Influence of Polymer Structural Conformation and Phase Behaviour on In-situ Viscosity. Presented at the 18th European Symposium on Improved Oil Recovery, Dresden, Germany, 14–16 April 2015. [CrossRef]
9. Hughes, D.S.; Teeuw, D.; Cottrell, C.W.; Tollas, J.M. Appraisal of the Use of Polymer Injection To Suppress Aquifer Influx and To Improve Volumetric Sweep in a Viscous Oil Reservoir. *Soc. Pet. Eng.* **1990**, *5*, 33–40. [CrossRef]
10. Broseta, D.; Medjahed, F.; Lecourtier, J.; Robin, M. Polymer Adsorption/Retention in Porous Media: Effects of Core Wettability on Residual Oil. *Soc. Pet. Eng.* **1995**, *3*, 103–112. [CrossRef]
11. Sorbie, K.S. *Polymer-Improved Oil Recovery*; Blackie and Son Ltd.: Glasgow, UK, 1991.
12. Lake, L.W. *Enhanced Oil Recovery*; Prentice Hall: Upper Saddle River, NJ, USA, 1989.
13. Savins, J.G. Non-Newtonian Flow through Porous Media. *Ind. Eng. Chem.* **1969**, *61*, 18–47. [CrossRef]
14. Sadowski, T.J. Non-Newtonian Flow through Porous Media. II. Experimental. *J. Rheol.* **1965**, *9*, 251–271. [CrossRef]
15. Sochi, T. Non-Newtonian flow in porous media. *Polymer* **2010**, *51*, 5007–5023. [CrossRef]
16. Sadowski, T.J.; Bird, R.B. Non-Newtonian Flow through Porous Media. I. *J. Rheol.* **1965**, *9*, 243–250. [CrossRef]
17. Teeuw, D.; Hesselink, F.T. Power-Law Flow And Hydrodynamic Behaviour of Biopolymer Solutions In Porous Media. Presented at the SPE Fifth International Symposium on Oilfield and Geothermal Chemistry, Stanford, CA, USA, 28–30 May 1980. [CrossRef]
18. Cannella, W.J.; Huh, C.; Seright, R.S. Prediction of Xanthan Rheology in Porous Media. Presented at the 63rd Annual Technical Conference and Exhibition of the Society of Petroleum Engineers, Houston, TX, USA, 2–5 October 1988. [CrossRef]
19. Fletcher, A.J.P.; Flew, S.R.G.; Lamb, S.P.; Lund, T.; Bjornestad, E.; Stavland, A.; Gjovikli, N.B. Measurements of Polysaccharide Polymer Properties in Porous Media. Prepared for presentation at the SPE International Symposium on Oilfield Chemistry, Anaheim, CA, USA, 20–22 February 1991. [CrossRef]
20. Sorbie, K.S.; Clifford, P.J.; Jones, E.R.W. The Rheology of Pseudoplastic Fluids in Porous Media Using Network Modeling. *J. Colloid Interface Sci.* **1989**, *130*, 508–534. [CrossRef]
21. Lopez, X.; Valvatne, P.H.; Blunt, M.J. Predictive network modeling of single-phase non-Newtonian flow in porous media. *J. Colloid Interface Sci.* **2003**, *264*, 256–265. [CrossRef]
22. Pearson, J.R.A.; Tardy, P.M.J. Models for flow of non-Newtonian and complex fluids through porous media. *J. Non-Newton. Fluid Mech.* **2002**, *102*, 447–473. [CrossRef]
23. Willhite, G.P.; Uhl, J.T. Correlation of the Flow of Flocon 4800 Biopolymer with Polymer Concentration and Rock Properties in Berea Sandstone. In *Water-Soluble Polymers for Petroleum Recovery*; Springer Publishing: Manhattan, NY, USA, 1988.
24. Bird, R.B.; Stewart, W.E.; Lightfoot, E.N. *Transport Phenomena*; John Wiley and Sons, Inc.: New York, NY, USA, 1960.
25. Christopher, R.H.; Middleman, S. Power-Law Flow through a Packed Tube. *Ind. Eng. Chem. Fundam.* **1965**, *4*, 422–426. [CrossRef]
26. Hirasaki, G.J; Pope, G.A. Analysis of Factors Influencing Mobility and Adsorption in the Flow of Polymer Solution Through Porous Media. *Soc. Pet. Eng. J.* **1974**, *14*, 337–346. [CrossRef]
27. Duda, J.L.; Hong, S.-A.; Klaus, E.E. Flow of Polymer-Solutions in Porous-Media—Inadequacy of the Capillary Model. *Ind. Eng. Chem. Fundam.* **1983**, *22*, 299–305. [CrossRef]
28. Kishbaugh, A.J.; McHugh, A.J. A rheo-optical study of shear-thickening and structure formation in polymer solutions. Part I: Experimental. *Rheol. Acta* **1993**, *32*, 9–24. [CrossRef]
29. Pope, D.P.; Keller, A. Alignment of Macromolecules in Solution by Elongational Flow—Study of Effect of Pure Shear in a 4 Roll Mill. *Colloid Polym. Sci.* **1977**, *255*, 633–643. [CrossRef]
30. Binding, D.M.; Jones, D.M.; Walters, K. The Shear and Extensional Flow Properties of M1. *J. Non-Newton. Fluid Mech.* **1990**, *35*, 121–135. [CrossRef]
31. Gogarty, W.B. Rheological Properties of Pseudoplastic Fluids in Porous Media. *Soc. Pet. Eng. J.* **1967**, *7*, 149–160. [CrossRef]

32. Perrin, C.L.; Tardy, P.M.J.; Sorbie, K.S.; Crawshaw, J.C. Experimental and modeling study of Newtonian and non-Newtonian fluid flow in pore network micromodels. *J. Colloid Interface Sci.* **2006**, *295*, 542–550. [CrossRef] [PubMed]
33. Sochi, T.; Blunt, M.J. Pore-scale network modeling of Ellis and Herschel–Bulkley fluids. *J. Pet. Sci. Eng.* **2008**, *60*, 105–124. [CrossRef]
34. Balhoff, M.T.; Thompson, K.E. A macroscopic model for shear-thinning flow in packed beds based on network modeling. *Chem. Eng. Sci.* **2006**, *61*, 698–719. [CrossRef]
35. Zamani, N.; Bondino, I.; Kaufmann, R.; Skauge, A. Computation of polymer in-situ rheology using direct numerical simulation. *J. Pet. Sci. Eng.* **2017**, *159*, 92–102. [CrossRef]
36. Hejri, S.; Willhite, G.P.; Green, D.W. Development of Correlations to Predict Biopolymer Mobility in Porous Media. *SPE Reserv. Eng.* **1991**, *6*, 91–98. [CrossRef]
37. Skauge, T.; Skauge, A.; Salmo, I.C.; Ormehaug, P.A.; Al-Azri, N.; Wassing, L.M.; Glasbergen, G.; Van Wunnik, J.N.; Masalmeh, S.K. Radial and Linear Polymer Flow—Influence on Injectivity. Prepared for presentation at the SPE Improved Oil Recovery Conference, Tulsa, Oklahoma, 11–13 April 2016. [CrossRef]
38. Faber, T.E. *Fluid Dynamics for Physicists*; Cambridge University Press: Cambridge, UK, 1995.
39. Brown, E.; Jaeger, H.M. The role of dilation and confining stresses in shear thickening of dense suspensions. *J. Rheol.* **2012**, *56*, 875–923. [CrossRef]
40. Choplin, L.; Sabatie, J. Threshold-Type Shear-Thickening in Polymeric Solutions. *Rheol. Acta* **1986**, *25*, 570–579. [CrossRef]
41. Indei, T.; Koga, T.; Tanaka, F. Theory of shear-thickening in transient networks of associating polymer. *Macromol. Rapid Commun.* **2005**, *26*, 701–706. [CrossRef]
42. Odell, J.A.; Müller, A.J.; Keller, A. Non-Newtonian behaviour of hydrolysed polyacrylamide in strong elongational flows: A transient network approach. *Polymer* **1988**, *29*, 1179–1190. [CrossRef]
43. Degennes, P.G. Coil-Stretch Transition of Dilute Flexible Polymers under Ultrahigh Velocity-Gradients. *J. Chem. Phys.* **1974**, *60*, 5030–5042. [CrossRef]
44. Trouton, F.T. On the coefficient of viscous traction and its relation to that of viscosity. *R. Soc.* **1906**, *77*, 426–440. [CrossRef]
45. Edwards, B.J.; Keffer, D.I.; Reneau, C.W. An examination of the shear-thickening behavior of high molecular weight polymers dissolved in low-viscosity newtonian solvents. *J. Appl. Polym. Sci.* **2002**, *85*, 1714–1735. [CrossRef]
46. Hatzignatiou, D.G.; Moradi, H.; Stavland, A. Experimental Investigation of Polymer Flow through Water- and Oil-Wet Berea Sandstone Core Samples. Presented at the EAGE Annual Conference & Exhibition incorporationg SPE Europec, London, UK, 10–13 June 2013. [CrossRef]
47. McKinley, G.H.; Sridhar, T. Filament-stretching rheometry of complex fluids. *Annu. Rev. Fluid Mech.* **2002**, *34*, 375–415. [CrossRef]
48. Fuller, G.G.; Cathey, C.A.; Hubbard, B.; Zebrowski, B.E. Extensional Viscosity Measurements for Low-Viscosity Fluids. *J. Rheol.* **1987**, *31*, 235–249. [CrossRef]
49. Meadows, J.; Williams, P.A.; Kennedy, J.C. Comparison of the Extensional and Shear Viscosity Characteristics of Aqueous Hydroxyethylcellulose Solutions. *Macromolecules* **1995**, *28*, 2683–2692. [CrossRef]
50. Anna, S.L.; McKinley, G.H.; Nguyen, D.A.; Sridhar, T.; Muller, S.J.; Huang, J.; James, J.F. An interlaboratory comparison of measurements from filament-stretching rheometers using common test fluids. *J. Rheol.* **2001**, *45*, 83–114. [CrossRef]
51. Shipman, R.W.G.; Denn, M.M.; Keunings, R. Mechanics of the Falling Plate Extensional Rheometer. *J. Non-Newton. Fluid Mech.* **1991**, *40*, 281–288. [CrossRef]
52. Sridhar, T.; Tirtaatmadja, V.; Nguyen, D.A.; Gupta, R.K. Measurement of Extensional Viscosity of Polymer-Solutions. *J. Non-Newton. Fluid Mech.* **1991**, *40*, 271–280. [CrossRef]
53. Tirtaatmadja, V.; Sridhar, T. A Filament Stretching Device for Measurement of Extensional Viscosity. *J. Rheol.* **1993**, *37*, 1081–1102. [CrossRef]
54. James, D.F.; Chandler, G.M.; Armour, S.J. A Converging Channel Rheometer for the Measurement of Extensional Viscosity. *J. Non-Newton. Fluid Mech.* **1990**, *35*, 421–443. [CrossRef]

55. Chauveteau, G. Moluecular interpretation of several different properties of flow of coiled polymer solutions through porous media in oil recovery conditions. Presented at the 56th Annual Fall Technical Conference and Exhibition of the society of Petroleum Engineers of AIME, San Antonio, TX, USA, 5–7 October 1981. [CrossRef]
56. Lewandowska, K. Comparative studies of rheological properties of polyacrylamide and partially hydrolyzed polyacrylamide solutions. *J. Appl. Polym. Sci.* **2007**, *103*, 2235–2241. [CrossRef]
57. Briscoe, B.; Luckham, P.; Zhu, S.P. Pressure influences upon shear thickening of poly(acrylamide) solutions. *Rheol. Acta* **1999**, *38*, 224–234. [CrossRef]
58. Dupuis, D.; Lewandowski, F.Y.; Steiert, P.; Wolff, C. Shear Thickening and Time-Dependent Phenomena—The Case of Polyacrylamide Solutions. *J. Non-Newton. Fluid Mech.* **1994**, *54*, 11–32. [CrossRef]
59. Jiang, B.; Keffer, D.J.; Edwards, B.J.; Allred, J.N. Modeling shear thickening in dilute polymer solutions: Temperature, concentration, and molecular weight dependencies. *J. Appl. Polym. Sci.* **2003**, *90*, 2997–3011. [CrossRef]
60. Clarke, A.; Howe, A.M.; Mitchell, J.; Staniland, J.; Hawkes, L.A. How Viscoelastic-Polymer Flooding Enhances Displacement Efficiency. *Soc. Pet. Eng. J.* **2016**, *21*, 675–687. [CrossRef]
61. Delshad, M.; Kim, D.H.; Magbagbeola, O.A.; Huh, C.; Pope, G.A.; Tarahhom, F. Mechanistic Interpretation and Utilization of Viscoelastic Behavior of Polymer Solutions for Improved Polymer-Flood Efficiency. Prepared for presentation at the 2008 SPE/DOE Improved Oil Recovery Symposium, Tulsa, OK, USA, 19–23 April 2008. [CrossRef]
62. Stavland., A.; Jonsbråten, H.C.; Lohne, A.; Moen, A.; Giske, N.H. Stavland. A.; Jonsbråten, H.C.; Lohne, A.; Moen, A.; Giske, N.H. Polymer Flooding—Flow Properties in Porous Media Versus Rheological Parameters. Presented at the SPE EUROPEC/EAGE Annual Conference and Exhibition, Barcelona, Spain, 14–17 June 2010. [CrossRef]
63. Aitkadi, A.; Carreau, P.J.; Chauveteau, G. Rheological Properties of Partially Hydrolyzed Polyacrylamide Solutions. *J. Rheol.* **1987**, *31*, 537–561. [CrossRef]
64. Lee, K.; Huh, C.; Sharma, M.M. Impact of Fractures Growth on Well Injectivity and Reservoir Sweep during Waterflood and Chemical EOR Processes. Presented at the SPE Annual Technical Conference and Exhibition, Denver, CO, USA, 30 October–2 November 2011. [CrossRef]
65. Hu, Y.; Wang, S.Q.; Jamieson, A.M. Rheological and Rheooptical Studies of Shear-Thickening Polyacrylamide Solutions. *Macromolecules* **1995**, *28*, 1847–1853. [CrossRef]
66. Cho, Y.H.; Dan, K.S.; Kim, B.C. Effects of dissolution temperature on the rheological properties of polyvinyl alchol solutions in dimethyl sulfoxide. *Korea-Aust. Rheol. J.* **2008**, *20*, 73–77.
67. Zamani, N.; Bondino, I.; Kaufmann, R.; Skauge, A. Effect of porous media properties on the onset of polymer extensional viscosity. *J. Pet. Sci. Eng.* **2015**, *133*, 483–495. [CrossRef]
68. Gupta, R.K.; Sridhar, T. Viscoelastic Effects in Non-Newtonian Flows through Porous-Media. *Rheol. Acta* **1985**, *24*, 148–151. [CrossRef]
69. Smith, F.W. Behavior of Partially Hydrolyzed Polyacrylamide Solutions in Porous Media. *J. Pet. Technol.* **1970**, *22*, 148–156. [CrossRef]
70. Kemblowski, Z.; Dziubinski, M. Resistance to Flow of Molten Polymers through Granular Beds. *Rheol. Acta* **1978**, *17*, 176–187. [CrossRef]
71. Wissler, E.H. Viscoelastic Effects in the Flow of Non-Newtonian Fluids through a Porous Medium. *Ind. Eng. Chem. Fundam.* **1971**, *10*, 411–417. [CrossRef]
72. Vossoughi, S.; Seyer, F.A. Pressure-Drop for Flow of Polymer-Solution in a Model Porous-Medium. *Can. J. Chem. Eng.* **1974**, *52*, 666–669. [CrossRef]
73. Marshall, R.J.; Metzner, A.B. Flow of Viscoelastic Fluids through Porous Media. *Ind. Eng. Chem. Fundam.* **1967**, *6*, 393–400. [CrossRef]
74. Durst, F.; Haas, R.; Interthal, W. Laminar and Turbulent Flows of Dilute Polymer-Solutions—A Physical Model. *Rheol. Acta* **1982**, *21*, 572–577. [CrossRef]
75. Heemskerk, J.; Rosmalen, R.; Janssen-van, R.; Holtslag, R.J.; Teeuw, D. Quantification of Viscoelastic Effects of Polyacrylamide Solutions. Presented at the SPE/DOE Fourth Symposium on Enhanced Oil Recovery, Tulsa, OK, USA, 15–18 April 1984. [CrossRef]

76. Metzner, A.B.; White, J.L.; Denn, M.M. Constitutive equations for viscoelastic fluids for short deformation periods and for rapidly changing flows: Significance of the deborah number. *AIChE J.* **1966**, *12*, 863–866. [CrossRef]
77. Masuda, Y.; Tang, K.-C.; Miyazawa, M.; Tanaka, S. 1D Simulation of Polymer Flooding Including the Viscoelastic Effect of Polymer Solution. *SPE Reverv. Eng.* **1992**, *7*, 247–252. [CrossRef]
78. Haas, R.; Durst, F. Viscoelastic Flow of Dilute Polymer-Solutions in Regularly Packed-Beds. *Rheol. Acta* **1982**, *21*, 566–571. [CrossRef]
79. Garrouch, A.A.; Gharbi, R.C. A Novel Model for Viscoelastic Fluid Flow in Porous Media. Presented at the 2006 SPE Annual Technical Conference and Exhibition, San Antonio, TX, USA, 24–27 September 2006. [CrossRef]
80. Ranjbar, M.; Rupp, J.; Pusch, G.; Meyn, R. Quantification and Optimization of Viscoelastic Effects of Polymer Solutions for Enhanced Oil Recovery. Presented at the SPE/DOE Eight Symposium on Enhanced Oil Recovery, Tulsa, OK, USA, 22–24 April 1992. [CrossRef]
81. Kawale, D.; Marques, E.; Zitha, P.L.J.; Kreutzer, M.T.; Rossen, W.R.; Boukany, P.E. Elastic instabilities during the flow of hydrolyzed polyacrylamide solution in porous media: effect of pore-shape and salt. *Soft Matter* **2017**, *13*, 765–775. [CrossRef] [PubMed]
82. Seright, R.S.; Seheult, J.M.; Talashek, T. Injectivity Characteristics of EOR Polymers. *SPE Reserv. Eval. Eng.* **2009**, *12*, 783–792. [CrossRef]
83. Kulawardana, E.U.; Koh, H.; Kim, D.H.; Liyanage, P.J.; Upamali, K.; Huh, C.; Weerasooriya, U.; Pope, G.A. Rheology and Transport of Improved EOR Polymers under Harsh Reservoir Conditions. Presented at the Eighteenth SPE Improved Oil Recovery Symposium, Tulsa, OK, USA, 14–18 April 2012. [CrossRef]
84. Sharma, A.; Delshad, M.; Huh, C.; Pope, G.A. A Practical Method to Calculate Polymer Viscosity Accurately in Numerical Reservoir Simulators. Presented at the SPE Annual Technical Conference and Exhibition, Denver, CO, USA, 31 October–2 November 2011. [CrossRef]
85. Manichand, R.N.; Moe Soe Let, K.P.; Gil, L.; Quillien, B.; Seright, R.S. Effective Propagation of HPAM Solutions Through the Tambaredjo Reservoir During a Polymer Flood. *SPE Prod. Oper.* **2013**, *28*, 358–368. [CrossRef]
86. Zaitoun, A.; Makakou, P.; Blin, N.; Al-Maamari, R.S.; Al-Hashmi, A.-A.R.; Abdel-Goad, M.; Al-Sharji, H.H. Shear Stability of EOR Polymers. *SPE J.* **2011**, *17*, 335–339. [CrossRef]
87. Suri, A.; Sharma, M.M.; Peters, E. Estimates of Fracture Lengths in an Injection Well by History Matching Bottomhole Pressures and Injection Profile. *SPE Reserv. Eval. Eng.* **2011**, *14*, 405–417. [CrossRef]
88. Zechner, M.; Clemens, T.; Suri, A.; Sharma, M.M. Simulation of Polymer Injection under Fracturing Conditions—A Field Pilot in the Matzen Field, Austria. *SPE Reserv. Eval. Eng.* **2014**, *18*, 236–249. [CrossRef]
89. Van den Hoek, P.; Mahani, H.; Sorop, T.; Brooks, D.; Zwaan, M.; Sen, S.; Shuaili, K.; Saadi, F. Application of Injection Fall-Off Analysis in Polymer flooding. Presented at the 74th EAGE Conference & Exhibition incorporating SPE EUROPEC 2012, Copenhagen, Denmark, 4–7 June 2012. [CrossRef]
90. Shiran, B.S.; Skauge, A. Wettability and Oil Recovery by Polymer and Polymer Particles. Presented at the SPE Asia Pacific Enhanced Oil Recovery Conference, Kuala Lumpur, Malaysia, 11–13 August 2015. [CrossRef]
91. Al-Abri, K.; Al-Mjeni, R.; Al-Bulushi, N.K.; Awan, K.; Al-Azri, N.; Al-Riyami, O.; Al-Rajhi, S.; Teeuwisse, S.; Ghulam, J.; Abu-Shiekha, I.; et al. Reducing Key Uncertainities Prior to a Polymer Injection Trial in a Heavy Oil Reservoir in Oman. Presented at SPE EOR Conference at OGWA, Muscat, Oman, 31 March–2 April 2014. [CrossRef]
92. Li, Z.; Delshad, M. Development of an Analytical Injectivity Model for Non-Newtonian Polymer Solutions. Presented at the SPE Reservoir Simulation Symposium, Woodlands, TX, USA, 18–20 February 2014. [CrossRef]

Graphic design: Communication Division, UiB / Print: Skipnes Kommunikasjon AS

uib.no

ISBN: 9788230867181 (print)
9788230867266 (PDF)